THE UNIVERSITY
of EDINBURGH

Immune modulation in pigs through editing of the RELA locus

Maeve Ballantyne

Thesis presented for the degree of Doctor of Philosophy

University of Edinburgh, March 2017

Contents

List of Figures

List of Tables

Declaration

This thesis and the work presented in it is, unless otherwise stated, my own work. The work presented here has not been submitted for any other degree or professional qualification.

Maeve Ballantyne, March 2017

Acknowledgements

I would like to thank my supervisors Professor Bruce Whitelaw and Dr Simon Lillico for their continued motivation, support and guidance throughout my studies. I would also like to thank all of the other members of the Whitelaw group, especially Claire Neil, Dr Chris Proudfoot, Dr Spring Tan, Dr Rachel Huddart, Alex Brown and Sarah Fletcher, for keeping me sane and providing much needed help and advice during this project.

I am also very grateful to Prof Linda Dixon and her group who welcomed me to the Pirbright Institute and provided me guidance and training to work with African swine fever virus. I would especially like to thank Claire Barber, for her friendship and supervision during my time at Pirbright.

Many thanks to my external supervisor, Dr Alan Mileham, and Genus plc for their practical and financial support for this work.

Finally, to my family and Callum for all of their encouragement, love and support that helped me finish this thesis. Thank you.

Abstract

Livestock animals are an ancient, vital renewable natural resource. Many livestock species have the ability to convert inedible crops and waste food into food fit for human consumption, in the form of meat, eggs and dairy products. As the global demand for high value animal protein is ever increasing, the livestock market continues to play a major role in worldwide economics.

Animal disease has the potential to be a huge burden on the livestock industry, impacting both welfare and production. Major outbreaks of transboundary diseases, such as foot and mouth disease, rinderpest and classical swine disease, have resulted in devastating global economic losses. As a result, scientific research is engaged in lowering this impact by generating effective preventative measures and treatments. One way to reduce livestock disease is to select animals that are genetically resistant, traditionally carried out through selective animal breeding programs; however, this is a time-consuming process and requires that appropriate genetic variation exists within the population. Advances in genome engineering technologies offer us an alternative approach, with the capability to make genetic improvements in livestock within a single generation. It is hypothesised that resilience to a disease, known as African swine fever (ASF), could be genetically engineered into the domestic pig.

ASF is a highly contagious disease of domestic pigs and is a re-emerging global threat to the swine industry. It is a lethal haemorrhagic disease caused by a virus, known as the African swine fever virus (ASFV). At present, there is no vaccine or treatment for ASF, and disease control relies on rapid diagnosis, quarantine and the mass slaughter of animals. Unlike the domestic pig, swine indigenous to Sub-Saharan Africa, such as the warthog, show no clinical signs of disease following infection with ASFV. A comparative study was carried out to identify host genetic variation that could underlie the difference in response to ASFV, with candidate genes selected based on their potential involvement with the viral protein A238L, involved in immune evasion. Functional polymorphisms where identified in the porcine RELA gene, encoding RelA, a subunit of the NF-κB transcription factor family. This evolutionary conserved protein family plays a vital role in mediating inflammatory and immune responses. The specific RELA polymorphisms identified alter potential phosphorylation sites

within the C-terminal transactivation domain of RelA which have been found to modulate NF-κB transcriptional activity *in vitro*. We set out to investigate whether genome editing tools could be employed to engineer the RELA sequence of domestic pigs. Initial attempts targeted the final exon of RELA, producing animals with a truncated RelA protein; modified animals lack the final 60 amino acids of the C-terminal transactivation domain. The aim of this thesis was to genotype and characterise the effects of this RELA modification at a molecular, cellular, morphological and whole organism level. The ultimate goal of this project was to investigate whether this RELA modification altered the domestic pig's response to ASFV *in vitro* and *in vivo*.

Unlike *rela*-/- mice which have an embryonic lethal phenotype, these RELA-edited pigs were born healthy and were fully viable when housed in a typical farm environment. Phenotypic analysis of lymphoid tissues from the RELA-edited pigs demonstrated no significant anatomical or histological changes compared to unmodified counterparts. Pigs homozygous for the RELA mutation had a significantly lower body weight compared to wild-type pigs. Molecular studies of samples from these pigs have shown that the modified RelA has an altered activity; however, the RELA modified pigs do develop the characteristic disease phenotype when challenged with ASFV. Finally, genome editors have been developed to introduce a specific warthog allele into the domestic pig RELA locus, these editors are currently being taken forward to produce a novel pig line.

Lay Summary

Livestock animals are an ancient, vital renewable natural resource. Many livestock species have the ability to convert inedible crops and waste food into food fit for human consumption, in the form of meat, eggs and dairy products. As the global demand for high value animal protein is ever increasing, the livestock market continues to play a major role in worldwide economics.

Animal disease has the potential to be a huge burden on the livestock industry, impacting both welfare and production. Major outbreaks of transboundary diseases, such as foot and mouth disease, rinderpest and classical swine disease, have resulted in devastating global economic losses. As a result, scientific research is engaged in lowering this impact by generating effective preventative measures and treatments. One way to reduce livestock disease is to select animals that are genetically resistant, traditionally carried out through selective animal breeding programs; however, this is a time-consuming process and requires that appropriate genetic variation exists within the population. Advances in genome engineering technologies offer us an alternative approach, with the capability to make genetic improvements in livestock within a single generation. It is hypothesised that resilience to a disease, known as African swine fever (ASF), could be genetically engineered into the domestic pig.

ASF is a highly contagious disease of domestic pigs and is a re-emerging global threat to the swine industry. It is a lethal haemorrhagic disease caused by a virus, known as the African swine fever virus (ASFV). At present, there is no vaccine or treatment for ASF, and disease control relies on rapid diagnosis, quarantine and the mass slaughter of animals. Unlike the domestic pig, swine indigenous to Sub-Saharan Africa, such as the warthog, show no clinical signs of disease following infection with ASFV. A comparative study was carried out to identify host genetic variation that could underlie the difference in response to ASFV, with candidate genes selected based on their potential involvement with the viral protein A238L, involved in immune evasion. Functional polymorphisms where identified in the porcine RELA gene, encoding RelA, a subunit of the NF-κB transcription factor family. This evolutionary conserved protein family plays a vital role in mediating inflammatory and immune responses. The specific RELA polymorphisms identified alter potential phosphorylation sites

within the C-terminal transactivation domain of RelA which have been found to modulate NF-κB transcriptional activity *in vitro*. We set out to investigate whether genome editing tools could be employed to engineer the RELA sequence of domestic pigs. Initial attempts targeted the final exon of RELA, producing animals with a truncated RelA protein; modified animals lack the final 60 amino acids of the C-terminal transactivation domain. The aim of this thesis was to genotype and characterise the effects of this RELA modification at a molecular, cellular, morphological and whole organism level. The ultimate goal of this project was to investigate whether this RELA modification altered the domestic pig's response to ASFV *in vitro* and *in vivo*.

Unlike *rela*-/- mice which have an embryonic lethal phenotype, these RELA-edited pigs were born healthy and were fully viable when housed in a typical farm environment. Phenotypic analysis of lymphoid tissues from the RELA-edited pigs demonstrated no significant anatomical or histological changes compared to unmodified counterparts. Pigs homozygous for the RELA mutation had a significantly lower body weight compared to wild-type pigs. Molecular studies of samples from these pigs have shown that the modified RelA has an altered activity; however, the RELA modified pigs do develop the characteristic disease phenotype when challenged with ASFV. Finally, genome editors have been developed to introduce a specific warthog allele into the domestic pig RELA locus, these editors are currently being taken forward to produce a novel pig line.

List of Abbreviations

Anti-Anti	Antibiotic-Antimycotic
ANK	Ankyrin
A-NHEJ	Alternative non-homologous end joining
ASF	African swine fever
ASFV	African swine fever virus
ATP	Adenosine triphosphate
BSA	Bovine serum albumin
BSL	Biosafety level
Cas9	CRISPR associated protein 9
cDNA	Complementary DNA
C-NHEJ	Classical non-homologous end joining
CKII	Casein kinase II
CBP	CREB binding protein
CRISPR	Clustered regularly interspaced short palindromic repeat
crRNA	CRISPR RNA
CSF-1	Colony stimulating factor 1
DMEM	Dulbecco's modified Eagle's medium
DMSO	Dimethyl sulfoxide
DNA	Deoxyribonucleic acid

DNA-PK	DNA-dependent protein kinase
DNA-PKcs	DNA-dependent protein kinase, catalytic subunit
dNTP	Deoxynucleotides
DSB	Double strand break
dsDNA	Double stranded DNA
DTT	Dithiothreitol
ECL	Enhanced chemiluminescence
EDTA	Ethylenediamine tetra-acetic acid
eIF2α	Translation initiation factor α subunit of eukaryotic initiation factor 2
eGFP	enhanced GFP
ES	Embryonic stem cell
FAO	Food and Agriculture Organization
FACS	Fluorescence-activated cell sorting
FCS	Foetal calf serum
FDA	Food and Drug Administration
FFU	Focus forming units
gDNA	genomic DNA
GE	Genetically engineered
GFP	Green fluorescent protein
GM	Genetically modified
GMO	Genetically modified organism

GM-CSF	Granulocyte/Macrophage-colony stimulating factor
HDR	Homology-directed repair
HR	Homologous recombination
HSC	Haematopoietic stem cell
IFN	Interferon
IκB	inhibitor of kappa B
IKK	I kappa B kinase
IL	Interleukin
iPS	Induced pluripotent stem
kDa	KiloDalton
LB	Luria broth
MGF	Multigene family
MMEJ	Micro-homology-mediated end joining
M.O.I	Multiplicity of infection
mRNA	Messenger RNA
NCLDV	Nucleocytoplasmic large DNA viruses
NEMO	NF-κB essential modulator
NES	Nuclear export signal
NFAT	Nuclear factor of activated T Cells
NF-κB	Nuclear factor kappa-light-chain-enhancer of activated B cells
NHEJ	Non-homologous end joining

NIK	NF-κB inducing kinase
NK cell	Natural killer cell
NLS	Nuclear localisation signal
NMR	Nonsense-mediated decay
OIE	World Organisation for Animal Health
ORF	Open reading frame
PAFs	Porcine adult fibroblasts
PAGE	Polyacrylamide gel electrophoresis
PAM	Protospacer adjacent motif
PAMP	Pathogen-associated molecular patterns
PBMCs	Peripheral blood mononuclear cells
PBS	Phosphate buffered saline
PCR	Polymerase chain reaction
PEFs	Porcine embryonic fibroblasts
PFA	Paraformaldehyde
PIKK	Phosphoinositol-3-kinase-like protein kinase
PNI	Pronuclear injection
qPCR	quantitative real time PCR
RBC	Red blood cell
RFLP	Restriction fragment length polymorphism
RHD	Rel homology domain

RIP1	Receptor interacting protein 1
RNA	Ribonucleic acid
ROS	Reactive oxygen species
RPMI	Roswell Park Memorial Institute medium
RVD	Repeat variable diresidue
SAPO	Specified animal pathogen
SCNT	Somatic cell nuclear transfer
S.D	Standard deviation
S.E.M	Standard error of the mean
sgRNA	Short guide RNA
SNP	Single nucleotide polymorphism
SOB	Super Optimal Broth
SOC	Super Optimal Broth with Catabolite repression
SpCas9	*Streptococcus pyogenes* Cas9
ssDNA	single stranded DNA
ssODN	Single-stranded donor oligonucleotides
TA1	Transactivation domain 1
TA2	Transactivation domain 2
TAD	Transactivation domain
TAK1	Transforming growth factor β-activated kinase 1
TALE	Transcription activator-like effector

TALEN	TALE-nuclease
$TCID_{50}$	Tissue culture infective dose
TCR	T-cell receptor
TLR	Toll-like receptor
TNFα	Tumour necrosis factor alpha
TNFR1	Tumour necrosis factor receptor 1
tracrRNA	trans-activating CRISPR RNA
TRADD	TNFR1 associated death domain protein
TRAF2	TNF receptor associated factor 2
UTR	Untranslated region
UV	Ultraviolet
VF	Viral factory
WBC	White blood cell
WT	Wild-type
ZF	Zinc finger
ZFN	Zinc finger nuclease

Chapter 1 General Introduction

1.1 Global importance of livestock

Farm animals are an important global provider of human livelihoods and source of high quality dietary protein. Many livestock species, such as pig, goat, cattle and chickens, have the ability to convert inedible crops and waste food into food fit for human consumption. Moreover, ruminants often graze on land that is unsuited to arable crops, accounting for ~75% of total agricultural land (Oltjen et al., 1996). Of course, some land utilised currently for livestock could be used for biomass production for energy or to grow crops for human consumption. A major disadvantage of livestock production is the impact it has on climate change, currently representing 14.5% of all human induced CO_2 emissions (Gerber et al., 2013). Despite this, there is an ever-increasing global demand for high value animal protein, driven by a combination of factors, including population growth, rising affluence and increasing levels of urbanisation. Livestock also provides an estimated one billion poor people in developing countries with food security and income (Herrero et al., 2013).

The global population is projected to reach up to 9.2 billion people by 2050. If the current trend for livestock products remains, this is estimated to lead to an increase in demand for livestock products by 70% by 2050 (Robinson, 2014). There is an ever-increasing pressure on the livestock sector to meet these demands, therefore there is particular focus on increasing the sustainability by increasing production efficiencies at animal and herd level to reduce impact on climate change, biodiversity and use of land and water resources.

1.2 Traditional breeding and selection

For centuries humans have bred livestock with the intention of improving desirable qualities in the next generation. Even before a knowledge of genetics, a selective breeding approach was used to improve livestock by selecting parents with a particular desired characteristic. This led to the generation of a wide variety of livestock breeds and animal pedigrees being recorded for individuals. As our awareness of genetics grew, animals breeding programs were developed based on a combination of

quantitative statistics and genetic information derived from pedigrees. Another development in animal breeding was the use of artificial insemination, allowing a single father to parent more offspring. These methods accelerated livestock productivity however led to an increase in inbreeding over time (Daetwyler et al., 2007, Clark et al., 2013). Increased inbreeding rate led to a reduction of genetic variation within a population, often resulting in an increased risk of disease and lower productivity (Croquet et al., 2006, Norberg & Sørensen et al., 2006, Yavarifard et al., 2014, Eteqadi et al., 2015). Currently, many breeding companies use DNA markers to estimate breeding values and selectively breed to maintain genetic diversity alongside genetically improving breeds (Garrick., 2011, Bouquet & Juga., 2013).

1.3 Animal transgenesis

Our ability to manipulate the genomes of cells and organisms has become fundamental to scientific research, aiding our understanding of biology processes and offering potential solutions to problems in human health, biosecurity and climate change. Genetically modified organisms (GMOs) are organisms that have had either a segment of foreign DNA inserted into, or a modification made to, their genomic sequence. *Escherichia coli* transformed with exogenous DNA were the first reported GMOs (Cohen et al, 1972; Jackson et al, 1972). Subsequently, the transfer of genetic material has been carried out in multicellular eukaryotes, including nematodes (Stinchcomb et al., 1985), plants (Bevan et al., 1983), insects (Rubin et al., 1982), fish (Maclean et al., 1987), birds (Bosselman et al., 1989) and mammals, including mice (Jaenisch & Mintz., 1974), sheep (Hammer et al., 1985) pigs (Hammer et al., 1985) and primates (Chan et al., 2001).

In 1981, a technique known as pronuclear injection (PNI) was used to inject DNA into the pronuclei of mouse zygotes to produce transgenic mice with foreign DNA stably incorporated into the genome, which was passed down to progeny through the germline (Gordon & Ruddle., 1981; Brinster et al., 1981). This technique was subsequently used to produce transgenic livestock (Hammer et al., 1985). Initial efforts in transgenic livestock research focussed on producing animal bio-reactors for pharmaceuticals, by transferring genes encoding a significant human bio-medical protein to be expressed and extracted from the biological fluids (e.g. milk or urine) of

the transgenic animal (Simons et al., 1987, Clark et al., 1998). PNI requires a high level of technical expertise for success and its inefficiency of producing founder animals proved very expensive, especially for large mono-zygotic animals. Despite this, the production of many transgenic livestock species has been accomplished through random integration of naked DNA introduced using PNI into single-cell embryos (Lo et al., 1991., Golovan et al., 2001, van Berkel et al., 2002). However, techniques utilising viral vectors and transposons soon came to be the preferred method to generate transgenic animals as this significantly increased gene transfer efficiencies (Chan et al., 2001). These techniques rely on random integration of the transgene into the genome, which can be error-prone and unpredictable. A significant breakthrough was made with the development of gene targeting through homologous recombination (HR), which made precise manipulation of the genome possible.

HR-mediated targeting involves the exchange of nucleotide sequences between two similar or identical DNA molecules. In this way, precise changes can be introduced at a specific site in the genome, permitting the production of gene knock-in and gene knock-out animal models. However, the frequency of HR-mediated targeting in mammalian cells is extremely low. The inefficiency of this method makes it impractical for use in zygotes for the production of transgenic animals. However, by incorporating a selectable marker in the HR construct, and performing HR-mediated targeting and artificial selection *in vitro*, transgenic cells can be selected for embryo production. Furthermore, strategies involving a site-specific recombinase system, known as Cre-Lox recombination, can be utilised to remove undesired marker genes following targeting (Hamilton & Abremski, 1984). This has been demonstrated for the production of transgenic animals using embryonic stem (ES) cells and induced pluripotent stem (iPS) cells (Thomas and Capecchi, 1987, Doetschman et al., 1987, Tong et al., 2010, Okita et al., 2007). Stem cell lines retain the capacity to differentiate into a range of embryonic tissue types in culture. Hence, they can be modified and screened *in vitro* before transferring to an early stage host embryo to contribute to further development. This method generates chimeric founder animals where tissues derived from the *in vitro* modified stem cells will contain the desired modification, which is often present in the germ cells. However, at present this resource only exists for a few species, including mice and rats (and in theory humans).

To date, the robust culture of livestock stem cells is yet to be established, however somatic cell nuclear transfer (SCNT), more commonly referred to as cloning, gives an alternative route to produce transgenic livestock (Wilmut et al, 1997). Utilising the SCNT technique the nucleus of a transgenic cell can be used to reconstitute an enucleated oocyte for embryo production. Gene targeting and screening can be achieved in primary somatic cells in culture, following similar methodologies used in stem cell lines. SCNT has permitted the generation of livestock with HR-targeted genetic modifications (Denning et al., 2001, Yu et al., 2006, Richt et al., 2007). However, the efficiency of producing live animals by SCNT is low and it is technically challenging, few laboratories have acquired the technical expertise required for successful livestock cloning.

The development of a group of tools collectively known as genome editors has been transforming the field of animal genetic modification (for a detailed discussion on Genome editing see Section 1.4). In brief, genome editors are programmable nucleases which can be utilised to induce a double strand break (DSB) at a specific DNA target site. DSBs are known to induce endogenous repair mechanisms which in turn can increase the efficiency of site specific genome modification through two broad mechanisms; non-homologous end joining (NHEJ) or homology dependent repair (HDR). Most often DSBs are repaired by NHEJ, an error-prone process frequently leading to small insertions or deletions, however if a repair template is available the DSB can be repaired by HDR; this mechanism is sought to achieve precise changes at a target site. This technology can be used to introduce site-specific mutations without leaving any other genetic marks on the genome, with the potential to induce modifications that are indistinguishable from naturally occurring mutations. These programmable nucleases have boosted the activity of research in the field of large animal transgenics in part due to the high efficiencies of targeted mutagenesis achieved. The efficiencies are high enough that it is no longer necessary to perform targeting and selection *in vitro* before embryo production. Furthermore, genome editors can even be injected directly into zygotes for efficient production of transgenic animals (Lillico et al., 2013, Proudfoot et al., 2015).

With advances in genotyping and sequencing technologies, livestock companies are successively collecting more and more genomic data. In turn, analysis of allelic sequence variation is leading to an increased understanding of the genetics underlying desirable traits. With current genome editor techniques, it is possible to introduce genetic changes to remove alleles associated with deleterious traits and increase desirable alleles associated with favourable traits. Genetic improvement of livestock via transgenesis has many benefits over traditional selective breeding methods as it permits; 1) the fixation of alleles without any deleterious inbreeding effects 2) the introduction of alleles that are not present in the population 3) the desired genetic change within one generation.

Thus far, genetic engineering in livestock species has been used for the following applications; as bio-reactors for human pharmaceuticals (Liu et al., 2013), for human disease models (Tan et al., 2013), for xenotransplantation (Hauschild et al., 2011; Li et al., 2015) and to improve livestock for agricultural proposes, for example enhanced productivity (Luo et al., 2014, Proudfoot et al., 2015), disease resistance (Liu et al., 2014, Wu et al., 2015, Whitworth et al., 2016, Burkard et al., 2017) or animal welfare (Tan et al., 2013, Carlson et al., 2016).

1.4 Genome engineering

Genome engineering tools, such as the zinc finger nucleases (ZFNs), transcription activator-like effector nucleases (TALENs) and the Clustered regularly interspaced short palindromic repeats (CRISPR)/Cas 9 system, allow us to modify the genomes of living cells and organisms with unprecedented ease and accuracy. Applications utilizing these tools are bringing forward a new era of biological understanding and control.

Advances in sequencing technologies has progressed faster than our understanding of gene functions, and with the increasing availability of whole genome sequences, many genetic differences underling the predisposition to various diseases and traits have been identified. In scientific research, genome engineering tools are often used to the study these differences and investigate gene functions. In addition to research, these tools have been commercially implemented in agriculture, for genetically improving

crops and livestock, and in medicine, for modelling and treating human disease. To date most human therapeutic applications of genome engineering are pre-clinical, however the few that have progressed into clinical trials have thus far shown success; these include genome engineering of T-lymphocytes to protect against HIV and treat cancers (Tebas et al., 2014, Qasim et al., 2015, McGranahan et al., 2016, Cyranoski., 2016).

Genome editors consist of two principle components; 1) a customisable DNA-binding molecule, currently either a protein or RNA, and 2) an endonuclease which relies on the DNA-binding molecule to direct its cleavage specificity. When introduced into a cell, genome editors induce double-strand breaks (DSBs) at their target DNA locus. These breaks, in turn, stimulate the cell's DNA damage response and eventual repair of the DNA. In this way, programmable nucleases rely in part on the cells innate repair mechanisms to generate desired genetic modifications.

Genome engineering tools can also be used for regulating gene expression; in this case the nuclease component is modified or replaced with a domain which acts as a transcriptional activator or repressor or acts to install or remove epigenetic marks (Konermann et al, 2013; Mendenhall et al, 2013; Gilbert et al, 2014; Konermann et al, 2015; Vojta et al, 2016). In this chapter, I will primary discuss the use genome engineering tools to edit the genome via the induction of DSBs.

1.4.1 DNA double strand break (DSB) repair

DSBs, although common, can inflict critical damage to the cell. DSBs as the name suggests, are induced when DNA breaks are generated in both complementary strands of the DNA double helix simultaneously, as a consequence the two broken DNA ends are vulnerable to dissociating from one another, posing a major threat to the genomic integrity of the cell. Despite their potential lethality, DSBs occur frequently in the genome; known causes include reactive oxygen species, endogenous nucleases, ionizing radiation, and programmed genomic rearrangements. The cell has many mechanisms in place to repair such damage. Following the formation of a DSB, there are a number of different pathways that may be utilised by a cell for restoration of its

genome, involving either homology-directed repair (HDR) or non-homologous end joining (NHEJ) at the cut site.

Genome editors are used to generate DSBs at a specific genomic site, subsequent exploitation of the cells innate DSB repair mechanisms allows the creation of desired genetic changes. In order to knock-out or disrupt a gene, the NHEJ repair pathway is ideal as it is error prone, typically introducing small insertions or deletions (indels) at the site of repair. These mutations often lead to a frameshift of an open reading frame, introducing premature stop codons that can result in either degradation of mRNA transcripts following detection by the cells nonsense-mediated decay (NMR) surveillance system or translation termination leading to a truncated protein with reduced or ablated activity. If a precise change is desired to modify a gene of interest, the genome editors are introduced alongside a donor DNA template, which contains the desired changes within a sequence that is homologous to the sequences flanking the DSB, which is incorporated into the genome by the HDR pathway. In addition, DSBs can be used to induce chromosomal rearrangements and delete specific genomic fragments (Figure 1.1).

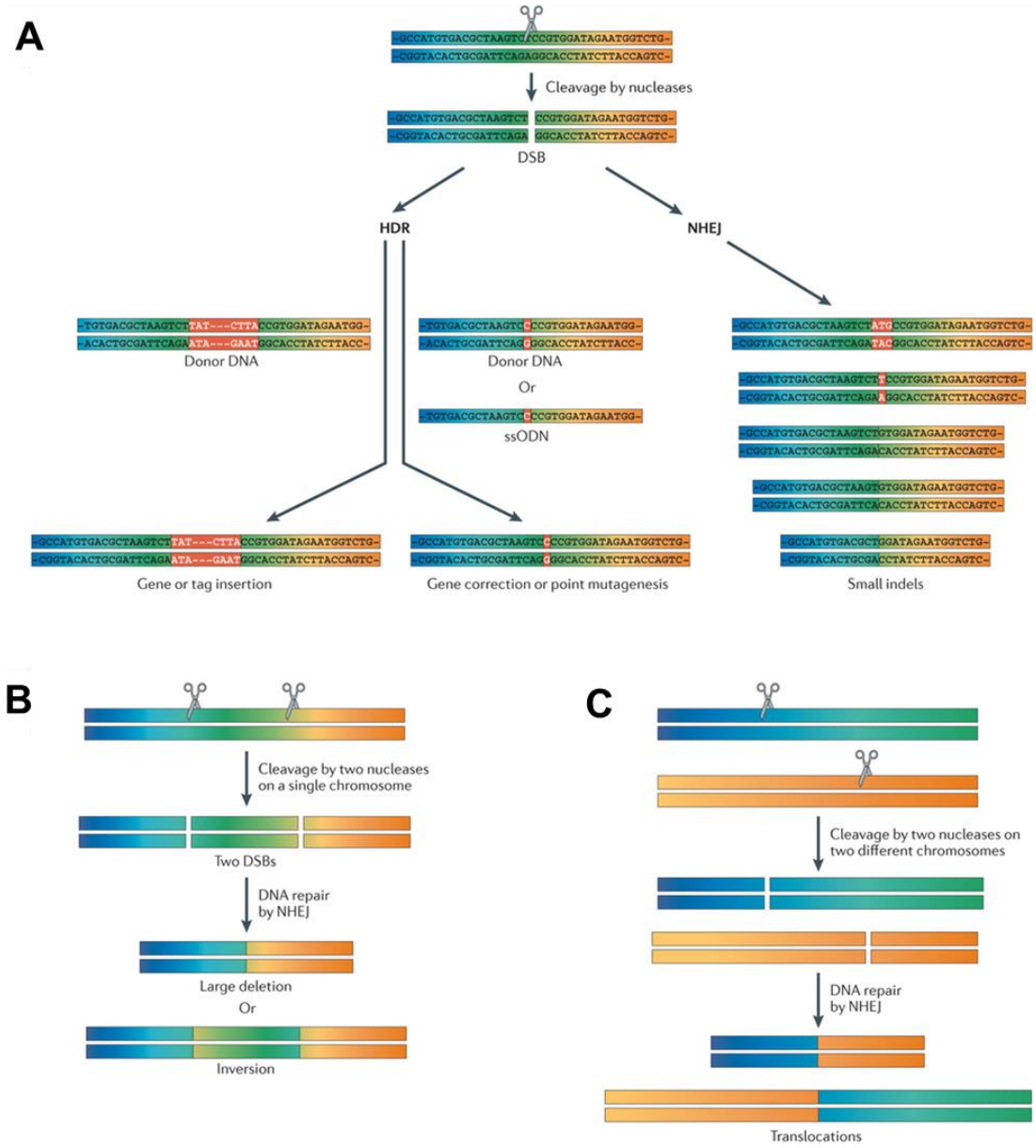

Figure 1.1 Potential applications of genome editors. A) Genome editor induced DSBs can lead to precise changes in the genome if repaired by the HDR pathway using a donor template containing the desired changes (red box) surrounded by sequence homologous to target. DSBs can also be repaired through error prone NHEJ, often leading to small indels. B) Two DSBs can be induced on the same chromosome to generate a large deletion or inversion. C. Two DSBs generated on two different chromosomes can induce chromosomal translocations. Figure reproduced from Kim & Kim, (2014).

Non-homologous end joining

NHEJ is the predominant mechanism for DSB repair in multicellular eukaryotes. NHEJ repair is vital for the development of our immune system as the antibody maturation process relies on repair of programmed DSBs to make DNA rearrangements, known as V(D)J recombination and class switch recombination, in lymphocytes. In short the NHEJ repair mechanism involves modifying the broken DNA ends and making them compatible for re-joining, it is often imprecise and leads in the introduction of small deletions or insertions at the site of damage.

The best understood mechanism of NHEJ is known as the canonical non-homologous end joining (C-NHEJ) pathway. This pathway relies on the Ku70-Ku80 heterodimer, which binds the broken DNA ends forming a ring providing protection from further degradation and recruiting other NHEJ factors required for repair. Early NHEJ repair factors often include DNA-PKcs–Artemis nuclease, DNA polymerases μ and λ, and DNA ligase IV-XX (Lieber et al, 2010). The DNA-PKcs–Artemis nuclease and DNA polymerases μ and λ process the broken DNA ends in preparation for ligation by the DNA ligase IV-XX to re-seal the break. C-NHEJ does have the potential to accurately repair DSBs if the broken ends of the DNA are fully complementary. However, most breaks typically do not possess such complementary ends and the process proceeds with the annealing of short (1-4 nucleotide) homologous sequences resulting in small (1-4bp) insertions or deletions in the repaired sequence (Lieber et al, 2010).

Mechanisms of NHEJ that do not require the Ku70-Ku80 heterodimer have be termed alternative-non-homologous end joining (A-NHEJ) or micro-homology-mediated end joining (MMEJ). The distinguishing feature of MMEJ is the use of 5-25 nucleotide homology sequences, known as micro-homologous sequences (McVey et al, 2008). These sequences anneal with one another and all the additional nucleotides are removed and gaps are filled in, often resulting in longer deletions and insertions compared to the C-NHEJ pathway (McVey et al, 2008). For a detailed review on the mechanisms of the different NHEJ pathways see Lieber et al, 2010.

Homology Directed Repair

HDR is the cells method of repairing DSBs largely error free, for this it requires a homologous DNA template. In multicellular eukaryotes HDR typically occurs only in late S/G2 and M phases of the cell cycle, when sister chromatids are optimally positioned to be used as templates. NHEJ is supressed during late S/G2 stages of the cell cycle promoting the HDR pathway for repair of DSBs (Zhang et al., 2009, Davis el al., 2014). Moreover, the complexity of chromatin structure at the position of the DSB influences the DNA repair pathway choice (Goodarzi et al, 2010).

There are a number of HDR repair mechanisms, however all share a set of core biochemical steps; the first step is termed ‘end resection’ where repair of a DSB is initiated by nucleolytic processing of the 5’-terminal DNA ends. The end resection process commits the repair of the DSB to HDR, as the long 3'-single stranded DNA tails it generates are poor substrates for NHEJ (Symington et al, 2016). The sequence of these 3’-ssDNA tails defines the homologous pairing. Once the 3’-ssDNA tails have been generated they act as a scaffold for the assembly of the RecA (in prokaryotes) or Rad51 (in eukaryotes) proteins into long helical filaments. Combined they form a nucleoprotein filament that promotes the search for complementary sequence, then catalyses the exchange of DNA strands, known as strand invasion. The invading strand is subsequently repaired via extension by polymerases and annealing to the end of the break, forming four-stranded DNA intermediate structures known as Holliday junctions, which are disjoined by either nucleolytic resolution or topological dissolution. The described mechanisms are conserved in most phage, prokaryotic and eukaryotic organisms (Kuzminov et al., 1999, Kreuzer et al., 2000, Seitz et al., 2001, Hever et al., 2010). For a detailed review of the different HDR mechanisms see Kowalczykowski, (2016).

1.4.2 Genome editors

Genome editors are used to induce a DSB in the DNA at a given target locus. Each genome editor consists of two main components; a customisable DNA-binding molecule, which is usually a protein or RNA molecule, and an endonuclease which relies on the DNA-binding molecule for its cleavage specificity. So far such customisable DNA binding molecules have been derived from eukaryotic zinc finger proteins (ZFs), prokaryotic TALE (transcription activator-like effectors) proteins and the prokaryotic derived CRISPR (clustered regularly interspaced short palindromic repeat)/Cas9 (CRISPR-associated protein 9 nuclease) system. Each will be discussed here in order of discovery.

Zinc Fingers (ZFs)

Zinc Finger (ZF) domains were first described as the DNA-binding motif in transcription factor TFIIIA from the African clawed frog (*Xenopus laevis*) (Miller et al., 1985). This motif comprised of nine repeating units, of approximately 30 amino acids length, each unit was folded around a zinc ion forming individual protein structures which bound to the DNA, these structures were thought to resemble fingers, hence their name, Zinc Fingers (Klug et al., 1987). ZF domains have since been identified as a common DNA binding domain of eukaryotic transcription factors and the rules underlying their DNA recognition have been uncovered leading to the creation of 'programmable' synthetic DNA binding motifs.

The Cys_2His_2 class of ZF domains is one of the largest families found in eukaryotes and recognise a diverse set of DNA sequences. A single Cys_2His_2 zinc finger unit is composed of a two-stranded antiparallel β-sheet, containing a loop made by two cysteine residues, and an alpha helix containing two histidine residues. The two distinct secondary structures are held together by a small hydrophobic core. The zinc ion is contained within this core, coordinated by the conserved cysteine and histidine residues (Neuhaus et al., 1992; Nakaseko et al., 1992; Figure 1.2.A). The crystal structure of a zinc finger domain bound to its DNA target, revealed that each zinc finger unit recognizes three successive bases, with key contacts typically made through

3 or 4 amino acids located within the alpha helix (Pavletich et al., 1991, Elrod-Erickson., 1998). Adjacent zinc finger units are joined together by flexible linkers allowing the recognition of varying lengths of DNA sequences (Neuhaus et al., 1992).

The Cys_2His_2 class of ZF motifs were identified as an attractive candidate for designing customisable DNA-binding proteins due to the following factors; DNA recognition is made principally via individual amino acids to an individual DNA base, each finger unit can have different triplet specificities, single fingers act as independent modules and can be linked together to give specific recognition of longer DNA target sequences.

FokI nuclease

FokI bacterial type II restriction endonuclease, was first discovered in *Flavobacterium okeanokoites* (Li et al, 1992). In its natural form, it comprises of an N-terminal DNA binding domain which recognises 5'-GGATG-3' sequences and a C-terminal non-specific DNA cleavage domain (Hiroyuki and Susumu, 1981; Li et al, 1992). When FokI dimerises, the cleavage domain becomes active and cleaves the target DNA 9 base pairs downstream of the recognition site (Wah et al, 1998).

It was first reported in 1994, that the FokI non-specific DNA nuclease domain could be fused to an alternative DNA binding domain, enabling the creation of a hybrid restriction enzyme (Kim and Chandrasegara, 1994). This discovery was key for the development of both ZFNs and TALENs. The FokI endonuclease domain has been modified for optimal use in these genome editor systems, a number of point mutations were introduced to increase the cutting efficiency and specificity of the editors. A commonly used modified FokI has been dubbed 'Sharky', it contains two point mutations, S418P and K441E, which confer an increase in activity when compared to wild-type FokI of up to 15-fold (Guoetal, 2010).

Zinc finger nucleases (ZFNs)

The customisable ZF domains were fused to the FokI endonuclease to create ZFNs, one of the first representatives of a new generation of tools termed 'genome editors'. A pair of ZFNs are required for a DSB to occur as the FokI nuclease domain must dimerise for it to cleave the DNA (Bitinaite et al., 1998; Smith et al., 2000). To bring

together the two FokI nuclease domains, ZFNs are designed to bind opposite sides of the DNA target in an inverted position, separated by 5-7 nucleotides (Figure 1.2.B). Once both ZFNs have bound their DNA target, the Fok1 nuclease can dimerise and induce a DSB. This requirement for a pair of ZFNs increases the length of recognition sequence thereby increasing the accuracy and reducing the probability of cutting at non-target sites. In principle, a pair of ZFNs, each composed on three zinc fingers will recognise a sequence of 18 nucleotides which is sufficient specificity for targeting a single site in a genome.

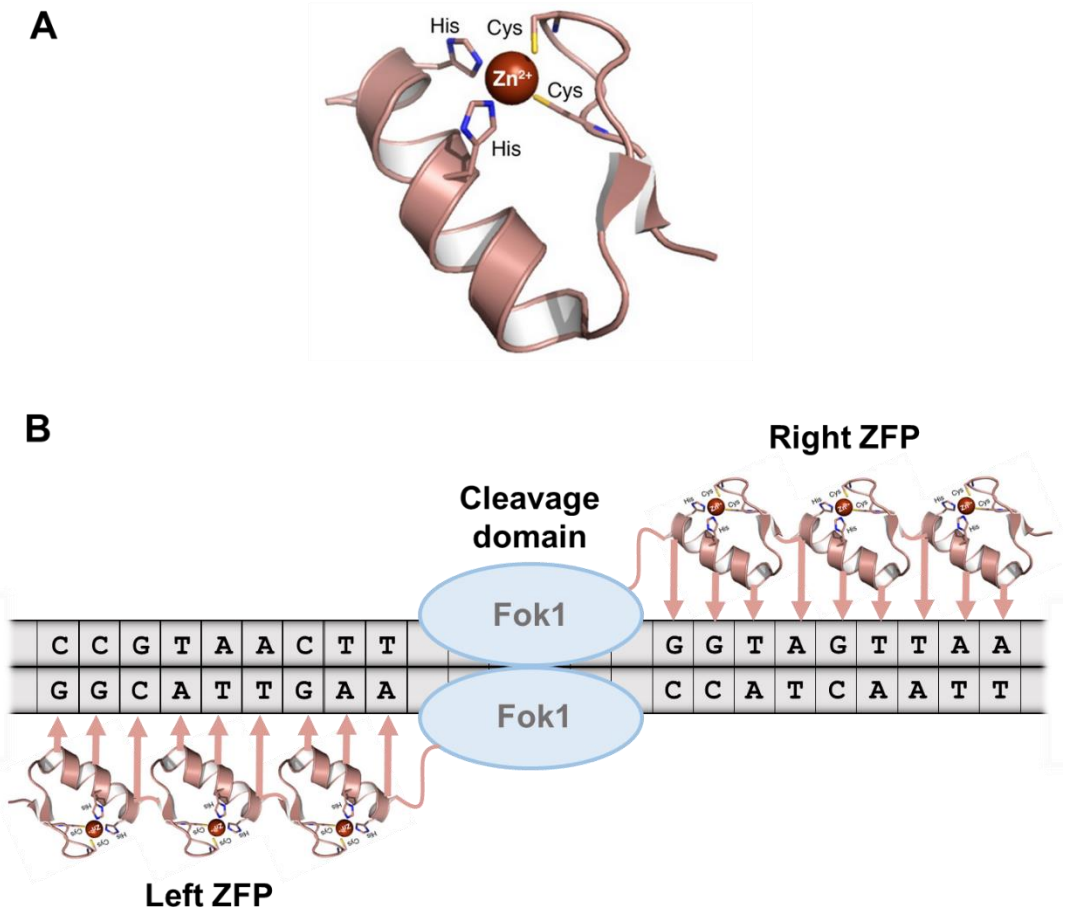

Figure 1.2 ZFNs. A) Single zinc finger structure B) Schematic diagram of ZFN pair bound to DNA. Each ZF domain interacts with three nucleotides. The two FokI endonucleases are required to dimerise before induction of a double strand break in the DNA. Figure adapted from Urnov et al, (2010).

Synthetic zinc finger domains have been produced that recognise all possible 5'-GNN-3', 5'-ANN-3', 5'-CNN-3' DNA triplets, where N represents any base (Segal et al., 1999; Dreier et al., 2000; Dreier et al., 2001). However currently only a few ZFs have been developed to recognise 5'-TNN-3' DNA triplets (Dreier et al., 2005).

ZFN pairs have been designed and successfully used for modifying the genomes of various different species including drosophila (Bibikova et al., 2002), silkworm (Morton et al., 2006), zebrafish (Meng et al., 2008), mouse (Meyer et al., 2010), pig (Hauschild et al., 2011), cow (Liu et al., 2014), sheep (Zhang et al, 2014) and human (Porteus and Baltimore, 2003). Despite this widespread success of ZFN targeting, this technology has many limitations. Initially, it was thought that each zinc finger module could be linked together to gain the desired specificity, however production of ZFNs in this way lead to high failure rates likely due to context dependent behaviour i.e. the ZF DNA-binding efficacy fluctuated depending on the neighbouring ZF module (Ramirez et al., 2008). The interactions between ZF units has complicated the design process however a number of context-sensitive selection approaches exist to efficiently generate active ZFNs (Maeder et al. 2008). These strategies involve the construction of large randomised zinc finger libraries followed by selection to identify ZF combinations that work well together. Constructing ZFNs requires specialised expertise and is often labour intensive. Researchers that choose to use ZFNs, often purchase them from commercial biotechnology companies which can be expensive (Scott, 2005).

Transcription Activator-Like Effectors (TALEs)

Transcription activator-like effectors (TALEs) are proteins which originate from bacteria belonging to the *Xanthomonas* family, which infect plants (Bonas et al, 1989). Naturally occurring TALE proteins are virulence factors secreted by the proteobacteria, they are injected into plant cells where they enter the nucleus and bind specific DNA promoter sequences to activate transcription of host genes. In susceptible plants, TALEs manipulate host gene expression to benefit bacterial virulence. Each TALE protein consists of a DNA-binding motif flanked by an N-terminal domain, which is required for bacterial secretion, and a C-terminal domain

which is required for activating transcription of host genes and for nuclear localisation (Römer et al., 2007).

The DNA binding motif is often referred to as the central repeat domain, it consists of repeating units of 33-35 amino acids. Each TALE repeating unit is identical with the exception of two amino acids at positions 12 and 13, known as the repeat variable di-residues (RVDs). These RVDs define each unit's binding specificity for a single base pair in the target DNA (Moscou et al., 2009). Structural studies of TALE DNA-binding domains bound to their DNA target sites revealed that each repeating unit is composed of two α-helices linked by a short loop containing the RVDs. Each unit forms a superhelical structure around the DNA with the RVDs positioned in the major groove, residue 12 is involved in stabilising this contact and residue 13 makes the base-specific contacts (Deng et al., 2012; Mak et al., 2012). The number of the TALE repeating units is typically 13-28, the RVDs they contain determines the length and nucleotide composition of the target sequence each TALE recognises. Common RVDs include amino acids NI, HD, NG and NN, which recognise A, C, T and G/A bases respectively (Bosh et al, 2009). This simple DNA recognition pattern and modular nature of TALEs makes them ideal for the generation of designer DNA binding domains for use in genome editors.

Transcription Activator-Like Effector Nucleases (TALENs)

In 2010, transcription activator-like effector nucleases (TALENs) brought about a new generation of 'customable' DNA-binding proteins (Christian et al., 2010). TALENs contain the FokI endonuclease domain, engineered in ZFN development, fused to the DNA binding motif of the TALEs adapted to recognise a specific DNA target. TALENs, like ZFNs, are employed in pairs to allow dimerization of the FokI endonuclease domains (Figure 1.3).

TALENs have been successfully used in a wide-range different species, including rice (Li et al, 2012), drosophila (Liu et al., 2012), zebrafish (Huang et al, 2011), frog (Lei et al., 2012), mouse (Wefers et al., 2013), rat (Tesson et al., 2011), pig and cattle (Carlson et al., 2012), to induce targeted DNA modification. Comparative *in vitro* studies between TALENs and ZFNs targeting the same locus have revealed that both have similar mutagenesis efficiencies, although TALENs have been reported to have

lower cytotoxicity effects (Mussolino et al., 2014; Dreyer et al., 2015). TALENs have grown in popularity due to their relative ease in design and assembly compared with ZFNs. TALEs have a simple 1:1 interaction between a RVD code and a single nucleotide, compared to ZFs where multiple ZFs can bind a given nucleotide triplet. Furthermore, unlike ZFs, individual TALE repeats are largely independent of their neighbouring units, giving TALENs greater flexibility in their DNA recognition sequence (Cermak et al., 2011). However, TALENs aren't without their limitations; genes encoding for TALENs are typically three times the size of those which encode corresponding ZFNs, often reducing the efficiency of vector delivery into cells *in vitro* (Holkers et al., 2013). Moreover, the generation of TALENs that contain a large number of repeating units can be challenging due to recombination stimulated by the high sequence homologies of each TALE unit (Briggs et al., 2012).

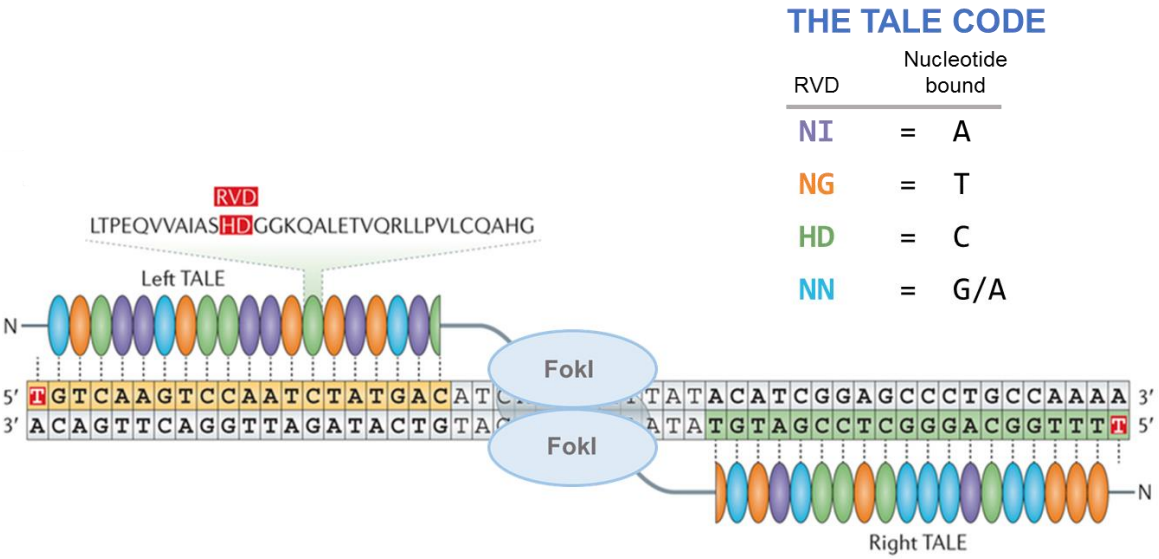

Figure 1.3 TALENs bound to target DNA site. Each TALEN consists of the TALE DNA binding domain and a FokI nuclease domain. The TALE DNA binding domain is composed of TALE repeat units, shown as coloured ovals, each specifies for the binding of a single nucleotide, which is defined by two residues known as its hypervariable RVD motif. The amino acid sequence of a single TALE repeat is expanded with the two hypervariable residues highlighted in red. The TALE code is displayed in the table showing which RVD motifs target which base. Once the two TALENs bind the Fok1 nuclease can cleave the DNA target site. Diagram adapted from Kim & Kim, (2014).

CRISPRs and CRISPR associated (Cas) proteins

Clustered regularly interspaced palindromic repeats, more often referred to as CRISPRs, are part of an adaptive defence mechanism that protects bacteria against invading DNA viruses and plasmids. CRISPRs first described in the genome of *E.coli* as a repetitive series of palindromic sequences interspersed by short 'spacer' sequences (Ishino et al., 1987, Nakata et al., 1989). CRISPRs have since been discovered in a range of bacteria and archaea species (Mojica et al., 2000). It was observed that the 'spacer' sequences in the array were of pathogenic bacteriophage or plasmid origins, which lead to the identification of CRISPRs as part of a prokaryotic immune response (Bolotin et al., 2005, Mojica et al., 2005, Pourcel et al., 2005). This heritable adaptive immunity is achieved in three following steps; 1) short sequences of invading nucleic acid are inserted into the CRISPR locus in the form of a 'spacer', 2) the CRISPR locus is transcribed and processed into small CRISPR RNAs (crRNAs), 3) mature crRNAs associate with the CRISPR associated (Cas) proteins and direct them their complementary sequences which the Cas proteins cleave (Barrangou & Marraffini., 2014).

Three broad CRISPR-Cas system types have been described, each utilising a distinct molecular mechanism to achieve DNA recognition and cleavage (Makarova et al., 2011). The type I and III systems use a complex consisting of multiple Cas proteins to process crRNAs and cleave target DNA. By contrast, the type II system only requires a single large Cas protein, for RNA-guided recognition and cleavage of foreign DNA. This feature of the type II systems has proved extremely useful for the development of the CRISPR-Cas9 system as a tool for genome engineering (Gasiunas et al., 2012).

CRISPR-Cas system

The CRISPR-Cas9 editor system is the latest of the customisable genome editor approaches, and is currently the most widely used system for genome editing due to its efficiency and ease of use. The CRISPR-Cas9 editors consist of two molecules; a 'programmable' guide RNA molecule that recognises the target site via Watson-Crick base pairing; and the Cas9 endonuclease, which induces a double strand break in the DNA target.

There are many different CRISPR-Cas systems described from varies prokaryotic species, however, currently the most widely used genome editor is the CRISPR-Cas9 system adapted from *Streptococcus pyogenes* (Jinek et al., 2012). In the *S. pyogenes* system, an active CRISPR-Cas9 complex consists of three molecules; the *S. pyogenes* Cas9 (SpCas9) endonuclease, for DNA cleavage, the crRNA, for recognition of target DNA, and a trans-activating-crRNA (tracrRNA) that hybridises with the crRNA and facilitates in Cas9 binding. For genome engineering purposes, a chimeric RNA molecule is often used, known as single guide RNA (sgRNA), where the 3' end of the crRNA is fused to the 5' end of the tracrRNA, retaining critical features for Cas9 binding and target recognition (Jinek et al., 2012). The target DNA sequence is specified by a 20nt sequence located in the crRNA portion of the sgRNA (Figure 1.4).

A requirement for Cas9 cleavage is that the target DNA must have a protospacer adjacent motif (PAM) sequence adjacent to the crRNA-target. The PAM sequence is important in its natural system as it prevents autoimmunity as 'spacer' sequences within the CRISPR locus lack the adjacent PAM sequence required for Cas9 cleavage. Cas9 proteins isolated for various prokaryotic species contain differing PAM site requirements, however in the case of SpCas9 this is a 5'-NGG-3', where N is any nucleotide (Sander & Joung., 2014).

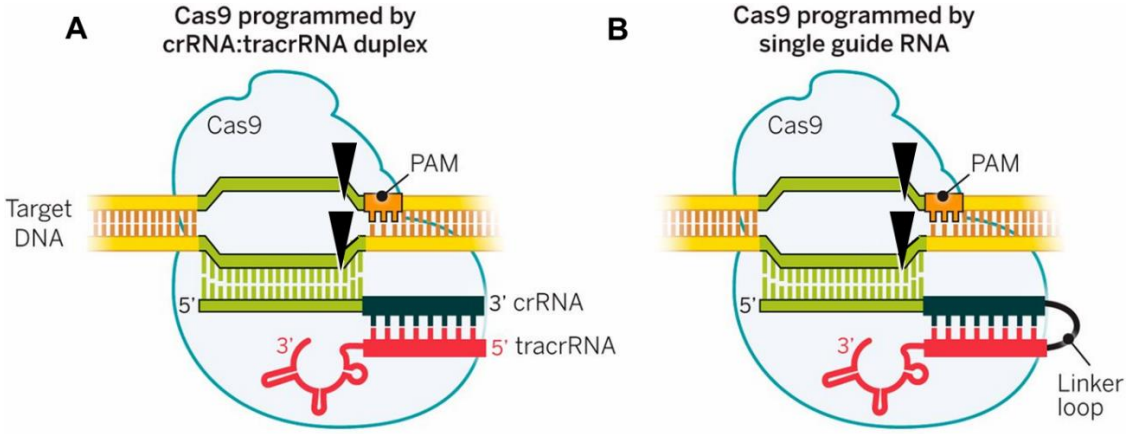

Figure 1.4 *S. pyogenes* Cas9-CRISPR complexes bound to target DNA. A) structure of Cas9 complexed in native form with dual-RNAs (tracrRNA & crRNA) bound to target DNA B) structure of Cas9 complexed with synthetic sgRNA and target DNA. The black triangles indicate the site of Cas9-induced cleavage of target DNA. Figure adapted from Doudna & Charpentier., (2014).

The CRISPR-Cas9 system has proven to be simple and efficient, relying only on the design of a 20 nucleotide section of the synthetic sgRNA to direct the DSB induced by Cas9. Unlike the ZFN and TALEN systems, the protein component of the CRISPR-Cas9 system, the Cas9, is constant, eliminating the need for protein design and construction. One constrain in designing CRISPRs is the requirement of the PAM site, however a different species of Cas9 can be utilised if there are no SpCas9 PAM sites in the desired sequence. Furthermore, SpCas9 has recently been adapted to have novel PAM specificities, allowing more choice of targetable sequences (Kleinstiver et al., 2015, Anders et al., 2016). The SpCas9 protein has also been modified to increase its DNA specificity and therefore reduce off-target effects by altering the amino acids involved in non-specific contact with the DNA (Kleinstiver et al., 2016).

1.5 Global importance of domestic swine

The species *Sus scrofa* encompasses all domestic pigs, including wild boar, and forms part of the Suidae family of the Cetartiodactyla order, which originate around 20 million years ago (Frantz et al., 2015). Phylogeny analysis of *S.scrofa* revealed that different populations diverged over a million years ago (Figure 1.5). The domestication of *S.scrofa* began approximately 9-10 thousand years ago in two independent locations, in Europe and in China, which has resulted in the many modern European and Chinese varieties we have today (Groenen., 2016).

Domestic pigs are an important source of human dietary protein in many countries, particularly where the production of beef cattle is difficult. Pigs efficiently convert human food waste and by-products into high quality protein. The demand for pork has been rising as a result in differing consumption patterns of nations where incomes are increasing in developing countries with fast growing economies. Together with poultry, the pig sector is the fastest growing livestock sub-sector, supplying the world with over a 100 million tonnes of animal protein annually (FAOstats, 2016). Pig production is a global industry, with exception of regions where there are religious and cultural reservations on the consumption of pork. Small scale pig production is also an important source of livelihoods for many farmers in the developing countries

(http://pigtrop.cirad.fr/). To keep up with the rising global demand, pig breeding companies are investing in novel technologies alongside animal husbandry techniques to increase production efficiencies.

The domestic pig is also a valuable model for biomedical research, due to its biological, physiological and anatomical similarities to humans (Vodicka et al., 2005, Aigner et al., 2010, Schomberg et al., 2016).

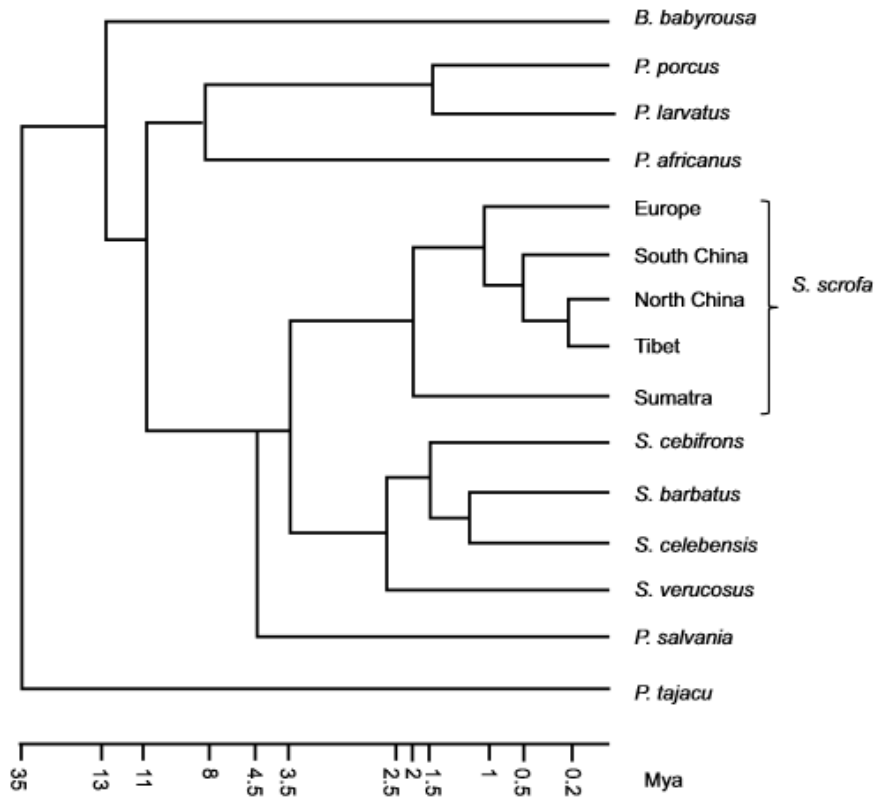

Figure 1.5 Schematic diagram of phylogeny of Suidae family. Reproduced from Groenen, 2016. The phylogenetic tree is based on studies carried on whole-genome sequence data of 11 species of Suidae.

1.6 Diseases of domestic swine

Animal disease is a huge burden on the livestock industry, impacting on both welfare and production. Disease arises due to a variety of pathogenic agents, including bacteria, viruses, fungi, worms, nematodes and prions. Diseases of swine that are classified as 'List A' by the World Organisation for Animal Health include foot and mouth disease, swine vesicular disease, vesicular stomatitis, rinderpest, classical swine fever and African swine fever (Table 1.1). These diseases are on the highest risk category as they have the potential to spread across the world, i.e. they are transboundary diseases. Moreover, all are viral diseases. The majority of high threat transboundary diseases are often viral, unlikely coincidental, as viruses have extremely high mutation rates leading to rapid adaption to various environments.

Diseases of swine often have a significant socio-economic impact in affected countries. Scientific research in effective preventative measures and treatments is fundamental to lowering this impact. Diseases of swine are often controlled by the following; biosecurity methods, improved husbandry, vaccination, the use of drugs and mass culls. A combination of these approaches is often required for the successful management of a disease. An alternative approach to tackle pig diseases is through their genetics. This can be carried out through selective breeding programs however, this is a time-consuming process and requires that appropriate genetic variation both exists and can be located within the population. Advances in genome engineering technologies offer us an alternative approach, with the capability to make genetic modifications in pigs within a single generation. Recently, a genome editing approach has been used to generate pigs that are resistant to viral infection with porcine reproductive and respiratory syndrome virus by disrupting a gene involved in viral entry (Whitworth et al., 2016, Burkard et al., 2017).

Disease	Infectious agent	OIE class
African swine fever	Virus (Asfarviridae, *Asfivirus*)	A
Atrophic rhinitis of swine	Bacterium (Pasteurellaceae, *Pasteurella multocida*)	B
Classical swine fever	Virus (Flaviviridae, *Pestivirus*)	A
Enterovirus encephalomyelitis	Virus (Picornaviridae, *Teschovirus*)	B
Foot and mouth disease	Virus (Picornaviridae, *Aphthovirus*)	A
Porcine brucellosis	Bacterium (Brucellaceae, *Brucella suis*)	B
Porcine cysticercosis	Worm (Taeniidae, *Taenia solium*)	B
Porcine reproductive and respiratory syndrome	Virus (Arteriviridae, *Arterivirus*)	B
Rinderpest	Virus (Paramyxoviridae, *Morbillivirus*)	A
Transmissible gastroenteritis	Virus (Alphacoronavirus, *Alphacoronavirus 1*)	B
Swine vesicular disease	Virus (Picornaviridae, *Enterovirus*)	A
Vesicular stomatitis	Virus (Rhabdoviridae, *Vesiculovirus*)	A

Table 1.1 Diseases of swine listed by the World Organisation for Animal Health (OIE). Class A represents the highest category of infectious pathogen.

1.7 African swine ever

African swine fever (ASF) is a highly contagious disease of domestic and feral pigs. African swine fever virus (ASFV), a DNA arbovirus, is the causative agent of ASF. Upon infection with highly virulent isolates of ASFV, domestic pigs develop an acute haemorrhagic fever and die within 10-14 days of infection. ASF has a huge socio-economic impact in affected countries and its current spread is increasing its risk to global pig production.

1.7.1 Distribution and epidemiology

ASF was first reported in Kenya in 1909 and close proximity with warthogs was implicated as a likely source of infection (Montgomery., 1921). It has since been reported all over the African continent and is considered endemic to Sub-Saharan Africa. The disease was confined to Africa until 1957 when an outbreak was reported in Portugal, thought to have been introduced by the importation of contaminated pork products in airline waste (Manso Ribeiro et al., 1961). This outbreak was effectively eradicated through the slaughter of herds, however new outbreaks were reported again in Portugal in 1960. From these initial outbreaks the disease spread throughout the Iberian Peninsula (Spain and Portugal), where it remained endemic until eradication in the mid-1990s. During this time ASF outbreaks were also reported in Holland, France, Belgium, Madeira, Sardinia, Malta, Italy, Cuba, Dominican Republic, Haiti and Brazil. In most jurisdictions it has been eradicated by the mass slaughter of animals, with the exception of Sardinia (Costard et al., 2009). Eradication programs in Sardinia are unsuccessful likely due to infected wild boar populations which contribute to the spread to free ranging domestic pigs (Mur et al., 2016). In a Spanish outbreak, a species of soft tick, *Ornithodoros erraticus,* was discovered to be a reservoir and vector of ASFV (Diaz Montilla et al., 1966). Subsequently, other tick vectors of the *Ornithodoros* genus where identified as reservoirs and vectors of ASFV in Africa (Plowright et al., 1969). However, the spread of disease to unaffected areas is most often due to the feeding of contaminated pork products to domestic pigs, brought in from aeroplanes and boats. Once infection is established in herds, the disease is disseminated through infected pigs and contaminated pork products. Within the last 20 years, ASFV has become more prevalent in the African continent, spreading to

countries not previously affected such as Côte d′Ivoire (1996), Nigeria (1997), Togo (1997), Ghana (1999), Burkina Faso (2003), Chad (2010) and to islands on the coast of the continent, Madagascar (1998) and Mauritius (2007). In 2007, ASFV was re-introduced into the European continent, first reported in Georgia following rapid spread into surrounding countries, including Armenia (2007), the Russian Federation (2007), and Azerbaijan (2008). The disease has since spread to Armenia (2010) Ukraine (2012), Belarus (2013), Estonia (2014), Latvia (2014), Lithuania (2014), Poland (2014), Moldova (2016). This European spread in still not under control with new outbreaks occurring regularly in affected countries (OIE, November 2016).

This recent spread and increasing incidence of ASF means that it now affects more countries than ever before in the history of the disease. A contributing factor to this may be globalization; as the movement of people, animals and products increases so does the potential for introducing pathogens to new territories. Despite intensive research towards development of ASFV vaccines, to date no effective vaccine or antiviral drugs exists (Zakaryan & Revilla, 2016). Current management of ASF consists of strict biosecurity methods, rapid diagnostics and the mass slaughter of animals. Culling as a method for eradication of disease was successful in the previously ASF affected European countries. However, the more recent European spread of ASF is further complicated by the prevalence of ASFV in the wild boar population, contributing to the spread of the disease.

1.7.2 Sylvatic cycle

In Africa, ASFV is maintained in a sylvatic cycle between natural hosts, wild swine including the common warthog (*Phacochoerus africanus*), bushpigs species (*Potomochorus larvatus* and *Potomochorus porus*), and soft ticks of the *Ornithodoros* genus (Heuschele & Coggins., 1969, Plowright et al., 1969, Plowright et al., 1981, Thomson et al., 1980, Thomson et al., 1985, De Tray et al., 1957, Anderson et al., 1998). There has also been one report of ASFV isolation in a giant forest hog, although their role in the maintenance of ASF is considered insignificant (*Hylochoerus meinertzhageni*; Heuschele & Coggins., 1965, Penrith et al., 2007). In natural hosts, the virus causes a persistent but clinically inapparent infection, thus they act as reservoirs (De Tray et al., 1957, Plowright et al., 1981). Out of the three genera of

African wild suid, the role in the maintenance of ASF is best described in the warthogs of the genus *Phacochoerus*. Moreover, the warthogs are more widespread and numerous compared to both the bushpigs and giant forest hog, ranging across most of sub-Saharan Africa (Jori & Bastos., 2009). Evidence for the bushpigs and giant forest hog role in the maintenance of ASF in Africa is generally lacking (Jori et al., 2007). The role of warthogs in maintaining ASFV in sub-Saharan Africa is thought to be essential to the disease persistence, making eradication of the disease extremely difficult in this continent.

Direct viral transmission between warthogs or from infected adult warthogs to domestic pigs is not thought to occur (Plowright et al., 1981). Maintenance of ASFV is dependent on the sylvatic cycle involving warthogs and soft bodied ticks of the *Ornithodoros* genus (Figure 1.6). The *Ornithodoros porcinus* species is the most abundantly studied for its involvement in this sylvatic cycle (Jori et al., 2013). This species often lives in warthog burrows and feeds on the suid inhabitants. Once infected, juvenile warthogs transiently develop a sufficient viremia to infect subsequent feeding ticks, with infectious period typically lasting 2-3 weeks (Thomson et al., 1985). The virus circulating in the sylvatic cycle can be transmitted to domestic pigs through infected ticks (Plowright et al., 1981). The levels of virus in adult warthogs is insufficient for viral transmission to feeding ticks or other warthogs (Jori & Bastos., 2009). The *O. porcinus* soft tick species can transmit ASFV through transstadial (from one life stage to the next; Hess et al., 1989), transovarial (from parent to offspring; Plowright et al., 1970) and sexual transmission (from male to female; Plowright et al., 1974). The *O. porcinus* ticks are long-lived, and viral infection has been demonstrated to persist for several years (Hess et al., 1989). A study of ASFV infection rates on warthogs living in eastern and southern Africa found that over 80% of the population are infected in areas where these *Ornithodoros spp.* of tick are present (Plowright et al., 1994).

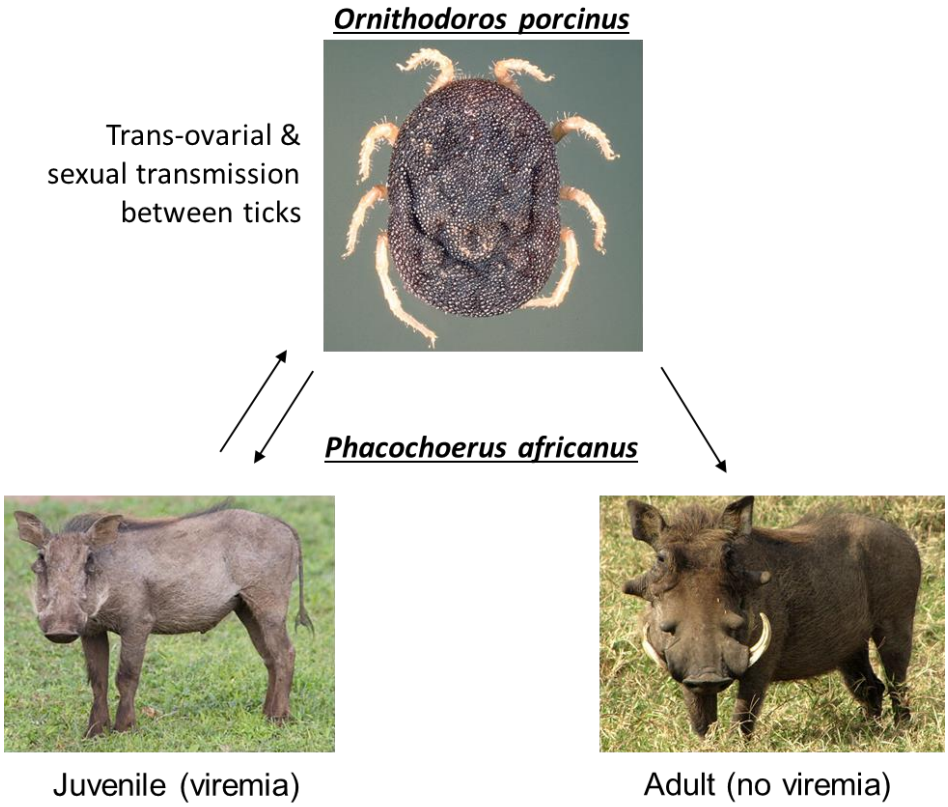

Figure 1.6 Warthog-Tick Sylvatic cycle. ASFV transmission pathways between the soft bodied tick, *Ornithodoros porcinus*, and the common warthog, *Phacochoerus africanus* are indicated with arrows.

1.7.3 African swine fever virus

African swine fever virus is a large, enveloped, icosahedral, double stranded DNA (dsDNA) virus. ASFV is morphologically similar to some Iridoviruses, those which are enveloped and have an icosahedral nucleocapsid, but has a genome organisation and replication mechanism more similar to the Poxviruses. ASFV was deemed significantly different to both of these viral families to warrant classification as a novel virus family, th*e Asfarviridae* family of the genus *Asfivirus* of which it is the sole member. All of these viral families belong to a superfamily known as nucleocytoplasmic large DNA viruses (NCLDV) which also includes the Phycodnaviries and Mimivirus, all of which are proposed to share a common ancestor (Iyer et al., 2001; Raoult et al., 2004; Iver et al., 2006). Members of the NCLDV predominantly replicate in the cytoplasm and their viral replication cycle is typically independent of host replication or transcriptional factors (Dixon., 2005). ASFV is the only known DNA arbovirus (virus transmitted by arthropods).

Each ASFV virion contains a nucleoprotein core structure containing the DNA, surrounded by an internal layer of core protein (inner core shell; Figure 1.7) This core structure is enclosed in an internal lipid bilayer (inner membrane) derived from the endoplasmic reticulum (Cobbold et al., 2001) and an outer icosahedral capsid (Andrés et al., 1998; Carrascosa et al., 1984). An external lipid envelope (outer envelope) is added to the virion on exiting the cell via budding through the plasma membrane (Breese, 1966; Carrascosa et al., 1984).

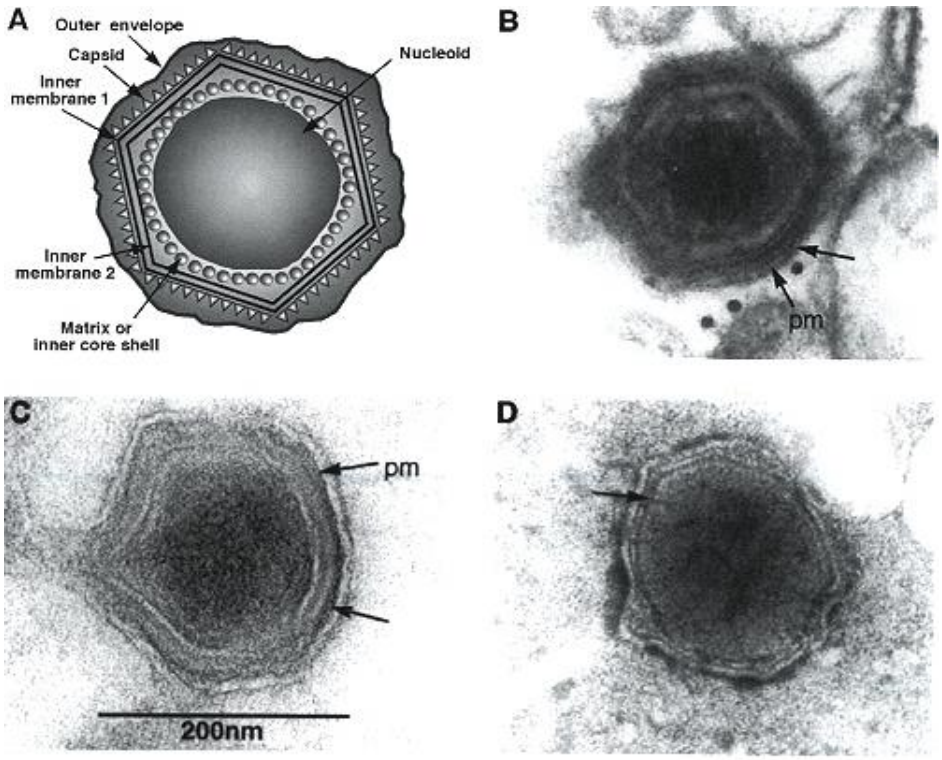

Figure 1.7 African swine fever virus morphology. A) Schematic diagram of ASFV virion section indicating the inner membranes, outer envelope, capsid and nucleoid core. B) Thin section, C) cyrosection and D) negative contrast electron micrograph of ASFV particles. Figure reproduced from Dixon et al., (2003).

The genome of ASFV is 170-190 kbp in length and contains between 151 and 167 open reading frames (ORFs) depending on the virus isolate (Yáñez et al., 1995 Chapman et al., 2008, de Villiers et al., 2010). The genome is a single molecule of linear dsDNA containing inverted and complementary end sequences that form covalently closed hairpin loops at either end (Gonzalez et al., 1986). To date, the complete genome sequences of 14 ASFV isolates have been determined (de Villiers et al., 2010, Dixon et al., 2013, Bishop et al., 2015). Most of the variation between isolates is present with the terminal end regions of the genome which contain five multigene families (MGFs), these are sets of paralogous genes which present in multiple copies per genome (Yáñez et al., 1995). The copy number of these genes varies considerably between isolates, which largely accounts for differences in genome length and gene number between isolates (Dixon et al., 2013). The function of these genes is currently not fully understood; however, some are known to play a role in determining host range and virulence (Zsak et al., 2001, Burrage et al., 2004, Afonso

et al., 2004, Golding et al., 2016). A total of 22 ASFV genotypes have been defined based on comparison of a part of the B646L gene sequence, which encodes the main capsid protein vp72 (Dixon et al., 2013). Complete sequencing of ASFV genomes has only been completed for 8 of these 22 genotypes.

ASFV replicates mainly in cells derived from the monocyte/macrophage lineage and exhibits a predominantly cytoplasmic replication cycle. ASFV has been identified to enter a range of species and cells *in vitro*, but then does not lead to effective viral production in most circumstances (Alcamí et al., 1989, Alcamí et al., 1990, Carrascosa et al., 1999). The virus enters swine macrophages by either receptor-mediated endocytosis, although the receptor(s) are currently unknown, or through macropinocytosis (a non-selective uptake mechanism; Alcami et al., 1990, Hernáez et al., 2016). Once inside the cell, the virions are recruited to the host endosomal compartment by various proteins and lipids before the virion inner membrane is exposed and fuses to host endosomal membrane in a pH-dependent process, releasing the nucleoprotein core into the cytosol (Hernáez et al., 2016). Early viral gene expression occurs in the cytosol, using several viral enzymes carried in the viral core (Carrascosa et al., 1986). ASFV assembly and replication takes place within perinuclear viral factories (VFs), which share similarities with aggresomes, which are formed in a cell as a result of misfolded proteins (Heath et al., 2001, Muñoz-Moreno et al., 2015). Following viral assembly, mature virions are transported from VFs to the cellular membrane via microtubules and released through budding (Jouvenet et al., 2004, Jouvenet et al., 2006)

1.7.4 ASFV infection in domestic pigs

The ability of ASFV to infect and replicate in cells of the monocyte/macrophage lineage is considered to play a critical role in the pathogenesis of this disease. Macrophages are key cells involved in activating and co-ordinating the innate and adaptive immune response to infection. The dysregulation of gene transcription in ASFV infected macrophages has been demonstrated by many studies and has been implicated in causation of disease pathogenesis (Powell et al., 1996, Gomez del Moral et al., 1999). ASFV also infects other cell types during later stages of infection, including endothelial cells, fibroblasts and reticular cells (Carrasco et al., 1997;

Gomez-Villamandos et al., 1997). However, this is not thought to play a central role in disease pathology as it occurs after characteristic symptoms of ASFV have been observed.

The clinical symptoms of ASF vary considerably depending on the virus isolate, host species, dose and route of exposure. In domestic pigs the disease is characterised into 4 forms: peracute, acute, subacute and chronic (Boinas et al., 2004, Hess., 1981; Wardley et al., 1983). Symptoms range from 100 % mortality within a few days of infection before clinical signs are detected (peracute), to chronic infections where pigs exhibit few signs of illness. Pigs infected with moderately virulent isolates of ASFV can recover from infection, but remain persistently infected, providing a potential reservoir of virus in domestic herds. Virus has been isolated from the lymph nodes of recovered animals up to 48 days post-infection (Oura et al., 1998) and viral DNA has been detected in peripheral blood mononuclear cells (PBMCs) at greater than 500 days post-infection by a PCR assay (Carrillo et al., 1994). Clinical effects of acute form ASF is characterised by multiple haemorrhages, lymphopenia associated with intense destruction of lymphoid tissue and disseminated intravascular coagulation, leading to death within a few days as a result of shock.

A characteristic of the disease pathogenesis is extensive apoptosis of uninfected lymphocytes surrounding ASFV infected macrophages in the lymphoid tissue (Oura et al., 1998). The mechanisms involved in ASFV induced lymphocyte apoptosis have not been defined, but are thought to involve the release of proinflammatory cytokines, such as TNFα and IL-1β from infected monocytes/macrophages. An increase in the macrophages expressing proinflammatory cytokines TNFα, IL-1 and IL-6 was observed nearby lymphocytes undergoing apoptosis (Salguero et al., 2002; Salguero et al., 2005). Lymphopenia is wide-spread, observed in the peripheral blood, lymph nodes and spleen of pigs infected with highly virulent strains (Zakaryan et al., 2015) T cell apoptosis has been shown to precede that of B cells in pigs infected with the virulent isolate Malawi LIL 20/1 (Oura et al., 1998).

Factors secreted from ASFV infected macrophages have also been associated with increased vascular permeability and the stimulation of bystander uninfected endothelial cells, leading to haemorrhage (Carrasco et al., 1997). An increase in the

levels of TNFα has been shown to coincide with ASFV disease pathology (Carrasco et al., 2002, Gomez del Moral et al., 1999, Salguero et al., 2002), and is thought to make a significant contribution to some of the major clinical manifestations of acute ASF. In addition to providing signals involved in the induction of apoptosis, TNF-α induces vasodilation, an increase in vascular permeability and activation of the vascular endothelium (Mantovani et al., 1997). These contribute to damage to the vascular endothelial cells and result in haemorrhage.

Protection against ASFV is not fully understood and no current vaccine exists. Although ASFV infection induces production of neutralizing antibodies against some virion proteins (Ruiz-Gonzalvo et al., 1986; Zsak et al., 1993; Gomez-Puertas et al., 1996), this protection is not enough to effectively counter viral challenge (Neilan et al., 2004). Cellular immunity plays an important role in protection against ASFV infection, with CD8+ cytotoxic T lymphocytes and natural killer (NK) cells playing an important role in the destruction of virus infected cells (Leitão et al., 2001, Oura et al., 2005). Cross-protection has been also demonstrated by challenging infected animals with homologous isolates, (Mebus & Dardiri, 1980, Ruiz-Gonzalvo et al., 1986, Leitão et al., 2001, Boinas et al., 2004, King et al., 2011). It is thought that these animals develop sufficient adaptive immunity with ASFV-specific cytotoxic T-cells, as experimental depletion of the CD8+ T-cells removes this immunity (Oura et al., 2005). Most recently, attenuated viruses produced experimentally via the deletion of genomic region encoding MGF360 and MGF530 genes can provide approaching 100% protection from subsequent challenge with pathogenic homologous isolates (O'Donnell et al., 2015, Reis et al., 2016).

1.7.5 ASFV infection in natural swine hosts

In persistently infected adult warthogs, no detectable viremia is displayed in peripheral blood and the virus is restricted to lymphoid tissues (Heuschele & Coggins 1965, Plowright et al., 1969, Thomson et al., 1980, Anderson et al., 1998). Neonate warthogs are infected by feeding ticks in burrows that they inhabit, these young warthogs develop a viremia which is infectious to ticks for up to 3 weeks (Thomson et al., 1985, Anderson et al., 1998, Kleiboeker & Scoles., 2001). Direct transmission from warthog to domestic pig has not been reported. However infected bushpigs are able to transmit

virus to domestic pigs when kept in an adjacent pen (Anderson et al., 1998). In bushpigs, ASFV infected adult bushpigs develop high level of viremia post-infection, sufficient for infecting feeding ticks, however after for 8 months no virus can be detected even within lymph tissues (Anderson et al., 1998).

1.7.6 Modulation of host defences by ASFV proteins

As intracellular obligate "parasites", viruses depend on the host cell for survival. The co-evolution of viruses and their hosts often leads to the development of a complex anti-viral host immune response in an arms race with the diverse viral mutational variants that circumvent and indeed exploit the hosts immune response. ASFV encodes between 150-167 proteins, some of which are known to modulate host immune responses (Table 1.2; Dixon et al., 2004, Tulman et al., 2009).

Inhibition of host cell apoptosis by ASFV

One host cell strategy to prevent viral replication is to trigger apoptosis of infected cells. ASFV induces apoptosis in both infected macrophages *in vitro* and *in vivo* and in non-infected lymphocytes *in vivo* (Oura et al., 1998, Portugal et al., 2009). Apoptosis is triggered in host cells after viral DNA replication, allowing sufficient time for completion of the replication cycle (Reis et al., 2017). Subsequent apoptosis of the host cell could be beneficial for the virus, as it may lead to the recruitment of additional macrophages to the infection site to clear apoptotic debris.

Four ASFV proteins are known to interact with the host apoptosis pathways, namely A224L, A179L and EP153R, which inhibit this pathway, and E183L which can activate it. Each of these proteins are expressed at different times during the ASFV infection and target different members of the host apoptosis pathway. A224L is an inhibitor of apoptosis (IAP) homologue, which inhibits capase-3 and is expressed late in ASF infection (Nogal et al., 2001). Deletion of this gene from a virulent ASFV isolate does not affect its virulence in domestic pigs however it may be more important in natural host infections (Reis et al., 2017). A179L, is an anti-apoptotic Bcl-2 homologue and is expressed throughout ASFV infection (Neilan et al., 1993, Brun et al., 1996). A179L also interacts with a component of autophagy, suggesting a broader role of this protein in modulating host cell responses (Banjara et al., 2017). EP153R is another anti-apoptotic viral protein, although the mechanism of which it inhibits

apoptosis is not yet known (Hurtado et al., 2004). E183L is a pro-apoptotic ASFV gene, encoding structural protein p54 which induces apoptosis by activation of caspase-3 through a mechanism that is dependent on interaction with dynein (a family of cytoskeletal motor proteins), which is also essential for viral replication (Hernaez et al., 2004).

Inhibition of host immune response by ASFV

ASFV encodes many proteins known to regulate host transcription of cytokines, chemokines, interferons (IFNs), adhesion proteins and other immunoregulatory proteins. Important viral genes for immune regulation include I329L, A238L and multigene families 360 (MGF360) and MGF530.

The multigene family 360 (MGF360) and MGF530 genes are known to be involved in inhibiting induction of IFNs in host cell (Afonso et al., 2004, Golding et al., 2016). However, the mechanistic roles of the encoding proteins have yet to be discovered. It has recently been discovered that deletion of these multigene families can attenuate several highly virulent isolates in the domestic pig, demonstrating that IFNs play a crucial role in the severity of ASF pathogenesis (O'Donnell et al., 2015, Reis et al., 2016). Moreover, in the soft-tick vector, deletion of these genes severely reduces viral replication (Burrage et al., 2004). Another viral protein known to inhibit the host interferon response is I329L, a viral Toll-like receptor (TLR) homologue. This viral protein acts as an inhibitor of toll-like receptor (TLR) 3 reducing transcription of genes downstream of this receptor, including NF-κB (an immunoregulatory factor) and IRF3 (an interferon regulatory factor; de Oliveira et al., 2011).

Many viral pathogens have evolved to manipulate the NF-κB pathway in order to evade host immune response, influence host cell cycle and enhance viral replication (Hiscott et al, 2001). The NF-κB signalling pathway (described in Section 1.8) regulates transcription of a diverse range of genes including cytokines, chemokines, IFNs, cell adhesion molecules, anti-apoptotic genes and other immunoregulatory proteins (Ghosh et al., 1998). Another ASFV protein known to inhibit NF-κB is A238L (Powell et al., 1996; Revilla et al., 1998; Tait et al., 2000). A238L has also been shown to regulate transcription factor Nuclear Factor of Activated T Cells (NFAT), which regulates expression of immunoregulatory genes including cytokines and cell-surface

receptors (Rao et al., 1997, Miskin et al., 1998). A238L inhibits activation of these pathways through inhibition of PKC-theta-mediated p300 transactivation (Granja et al., 2006, Granja et al., 2008, Granja et al., 2009). p300 along with CREB binding protein (CBP) are transcriptional co-activators that play a key role in recruiting and assembly of transcription enhancer complexes to specific promotor regions of immunoregulatory genes. The deletion of A238L does not impact on viral replication *in vitro* and does not reduce viral virulence in the domestic pig *in vivo* (Neilan et al., 1997). However, A238L is highly conserved between different ASFV field isolates indicating that it may have an important role in the replicative cycle of ASFV in one or more of its natural hosts (Neilan et al., 1997).

Viral protein CD2v has a role in immunoregulation as it was found to inhibit *in vitro* lymphocyte proliferation (Borca et al., 1998). CD2v is known to be involved in haemaglutination and mediating the attachment of virus to the surface of erythrocytes via an interaction with a ligand expressed on these cells (Borca et al., 1998). CD2v is present on the viral particles, facilitating viral dissemination. In *in vivo* infections with CD2v deleted ASFV, domestic pigs show a delay in onset of clinical signs and viremia (Borca et al, 1998). Interestingly, deletion of CD2v was also shown to reduce viral replication in the soft-tick vector (Rowlands et al., 2009).

Another ASFV protein known to regulate the host cells response is DP71L. DP71L appears to counteract a common anti-viral response, which is to shut down protein synthesis within a cell. Under numerous cell stresses, phosphorylation of translation initiation factor α subunit of eukaryotic initiation factor 2 (eIF2α) occurs, which triggers shut down of protein synthesis. The DP71L protein indirectly induces dephosphorylation of eIF2α (Zhang et al., 2010).

Host antiviral pathway	Effect of ASFV infection	ASFV modulatory proteins	Phenotype of gene deletion mutants
Type I IFN induction	Inhibition by virulent isolates	MGF360 and MGF505/530 I329L	Non-essential. Gene deletions attenuate *in vivo* Non-essential
Type I IFN responses	Inhibition by virulent isolates	MGF360 and MGF505/530	
Apoptosis	Inhibition at early times and induction at late times by high- and low-virulence isolates	Inhibitors: A179L, A224L, EP153R Activators: E183L	Non-essential. A224L and EP153 do not reduce virulence Essential structural protein
Shut-off of host protein synthesis	Inhibition by high- and low-virulence isolates	Inhibitors: DP71L and unknown others	Non-essential. Effect on virulence dependent on isolate
Stress responses	Activation of ATF6	DP71L and unknown others	
Host transcription factor, e.g., NFAT, NF-κB	Inhibition of activation	A238L	Non-essential, deletion does not reduce virulence
Autophagy	Unknown	Inhibitor: A179L	
Lymphocyte activation	Inhibition	CD2v (EP402Rp)	Non-essential. Effect on virus dissemination and virulence dependent on isolate

Table 1.2. ASFV proteins known to host antiviral pathways. Table reproduced from Reis et al., (2017).

1.8 African swine fever and variation in porcine RELA

The difference in host suid species response to ASFV infection suggests a causal genetic difference between the porcine breeds. In the Palgrave et al (2011) study a candidate gene approach was employed to identify genes underlying differences in response to ASFV infection. Candidate genes were selected through association with ASF viral protein A238L. Functional variation between the warthog RELA and domestic pig RELA was hypothesised to underlie the dramatic difference in response to ASFV infection in these two species (Palgrave et al., 2011). RELA encodes for the RelA protein, a member of the NF-κB transcription factor family. The NF-κB transcription factors play a vital role in upregulating immune and inflammatory responses, including many of the pro-inflammatory cytokines indicated in ASF pathology (Zhang et al., 2006, Gomez del Moral et al., 1999, Gomez-Villamandos et al., 2013).

Many viral pathogens have evolved to manipulate the NF-κB pathway in order to evade host immune response, control host cell cycle and enhance viral replication (Hiscott et al, 2001). Genetic variations in the porcine RELA locus have been associated with varied responses to infectious diseases such as porcine reproductive and respiratory syndrome (PRRS) and classical swine fever (CSF; Li et al, 2011).

The RelA NF-κB subunit was identified to have three amino acids changes between warthog and domestic pig (Figure 1.8). Initial *in vitro* characterisation of the RelA pig and warthog protein variants revealed that domestic pig RelA had a higher activity than the warthog RelA. *In vitro* reporter studies of the RelA variants containing each of the three single amino acid changes –, T448A, S485P and S531P –, revealed that the S531P mutation contributed the majority of these functional differences (Palgrave et al, 2011). In the human RelA the serine at 529 (equivalent of pig S531) is a phosphorylation site, which once phosphorylated by CKII (casein kinase II) has enhanced transactivation potential (Wang et al, 2000).

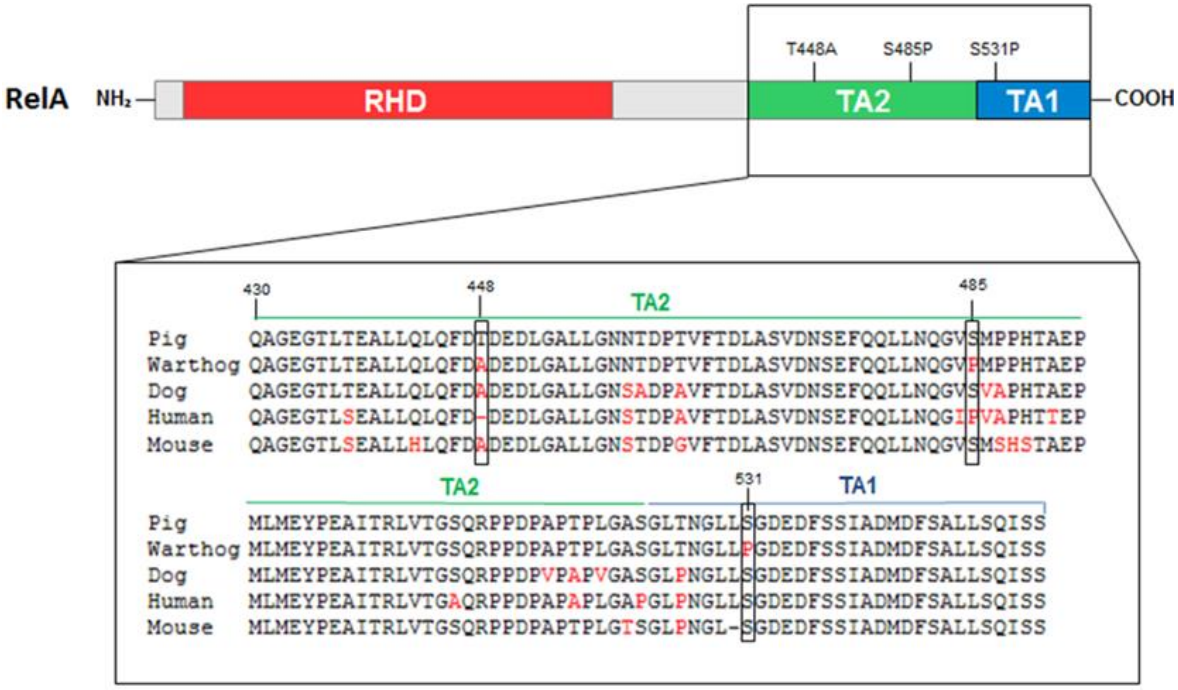

Figure 1.8 Evolutionary conserved transactivation domain of NF-κB subunit RelA. The RelA transactivation domain is subdivided into two regions, TA1 and TA2 (described later). Diagram displays primary protein sequence of RelA transactivation domain of domestic pig, warthog, dog, human and mouse. The sites of variations between the warthog and domestic pig are boxed. All amino acid variations from domestic pig RelA are highlighted in red.

1.9 Nuclear factor kappa B (NF-κB)

Nuclear Factor kappa B (NF-κB) is the collective term for the NF-κB family of transcription factors. First discovered in 1986 as a DNA-binding factor that bound to a specific enhancer element within the gene encoding immunoglobulin kappa light chain gene in mature B cells, it later became clear that NF-κB was widespread amongst most cell types and regulated a plethora of genetic targets (Sen & Baltimore., 1986). NF-κB regulates transcription by binding approximately 10 bp DNA motifs, known as κB sites, present in the promoters or enhancers of many genes and is induced by large array of stimuli, including bacterial and viral products, various cytokines, ionizing radiation and reactive oxygen species (ROS). Active NF-κB is known to regulate gene expression at over 150 target loci with important roles in the immune, inflammatory, proliferative, stress and apoptotic cellular responses (Pahl., 1999). Due to their role in regulating a large number cellular and organismal processes, the NF-κB proteins are amongst the most abundantly studied transcription factor families. In addition,

aberrant NF-κB activation is a characteristic many human diseases; including, cancers (Nakshatri et al., 1997, Dejarden et al., 1999, Pacifico & Leonardi., 2006, Jost & Ruland., 2007), autoimmune diseases (Schreiber et al., 1998, Okamoto., 2006, Mc Guire et al., 2013), premature aging syndromes (Osorio et al, 2012), septic shock (Liu & Malik., 2006), neurodegenerative diseases (Mogi et al., 2007, Mattson et al., 2001) and heart disease (Valen et al., 2001). There is intense study into unravelling the molecular mechanisms behind the NF-κB responses in order to discover targets with therapeutic potential for these diseases.

The NF-κB transcription factors are evolutionary conserved and have representative members in a wide range of species, including both vertebrates and invertebrates. Homologs of NF-κB proteins, inhibitors of NF-κB proteins (IκB) and IκB kinases (IKK) have been identified in invertebrates such as Drosophila (Han & Ip., 1999), Cnidarians (sea anemones, corals and hydra; Sullivan et al., 2007, Meyer et al., 2009, Lange et al., 2011), Poriferans (sponges; Gauthier & Degnan 2008) and even the single-celled eukaryote *Capsaspora owczarzaki* (Sebé-Pedrós et al., 2011). The presence of NF-κB in *C.owczarzaki* places its origin into a group known as the Opisthokonta, which are thought to have existed for around 1000 million years (Chernikova et al., 2011).

1.9.1 The NF-κB protein family

In mammals, the NF-κB family consists of five structurally related proteins; RelA (p65), c-Rel, RelB, p105/p50 (NF-κB1) and p100/p52 (NF-κB2; Figure 1.9). All five NF-κB proteins contain a highly conserved Rel Homology domain (RHD) at their N-terminus, which contains the residues responsible for mediating DNA binding, nuclear localisation, interaction with inhibitory proteins (the IκBs) and dimerization. All NF-κB proteins can form homo- or hetero- dimers, except from RelB which can only form heterodimers, to generate a NF-κB transcription factor. Heterodimer NF-κB complexes and formed through combinations of either p50 or p52 with either RelA, c-Rel or RelB. Each NF-κB dimer targets a distinct, but overlapping, collection of κB site sequences, in some cases resulting in the regulation of a specific set of genes (Perkins & Gilmore, 2006) Among the five NF-κB proteins, three monomers, RelA, RelB and C-Rel, contain a C-terminal transactivation domain (TAD), which is essential for

transcriptional activity. The other two family members, p100 and p105, serve as precursor proteins for active NF-κB subunits, p52 and p50 respectively. These precursor proteins have a long C-terminal domain containing multiple copies of ankyrin (ANK) repeats, which act to inhibit NF-κB. The ANK repeat residues are present in all NF-κB inhibitors (IκB) and function primarily by masking the nuclear localisation signal (NLS). Both p100, and p105 are processed by partial degradation by the proteasome removing the C-terminal ANK repeat residues to form the active NF-κB monomers (Fan & Maniatis., 1991, Lin et al., 1998, Moorthy et al., 2006, Senftleben et al., 2001). These p52 and p50 subunits lack the TAD thus can only activate transcription when dimerized with any TAD containing NF-κB protein. Homodimers of the p52 and p50 subunits bind target κB sites but are transcriptionally inactive, thus act as competitive repressors of NF-κB target genes (Bohuslav et al., 1998, Zhong et al., 2002).

Although the NF-κB subunits are ubiquitously expressed, they are regulated in a cell type and stimulus dependent manner, resulting in a diverse range of NF-κB signalling outcomes. Moreover, there is potential for many different dimer combinations. However, the most abundant NF-κB complex present in most cells is the RelA-p50 heterodimer. As a consequence, the term NF-κB is commonly used to refer specifically to the RelA-p50 heterodimer.

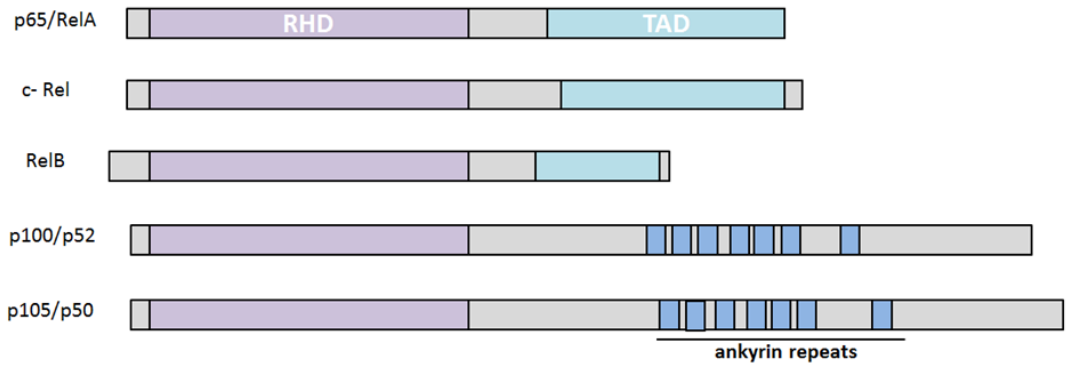

Figure 1.9 Mammalian NF-κB family members. All proteins share the N-terminal Rel homology domain (RHD) which is responsible for DNA binding, dimerization, nuclear localisation and interactions with NF-κB inhibitors. The three Rel proteins contain one or several transactivation domains (TAD) at their C-terminus end. The ankyrin repeats residues are inhibitory to NF-κB activation as they bind the RHD and inhibit nuclear localisation. Ankyrin repeats are present in all IκB proteins. Figure adapted from Hayden & Ghosh, (2004).

1.9.2 The IκB protein family

In resting cells, the NF-κB exists in an inactive state in the cytoplasm primarily regulated by its interaction with inhibitory IκB proteins. The IκB proteins are characterised by the presence of ANK repeats, which interact with the RHD present in the NF-κB dimers. At present nine members of IκB protein family have been identified, which can be categorised into three mains groups 1) NF-κB protein precursors IκBs, p105 (IκBγ) and p100 (IκBσ), 2) cytoplasmic/typical IκBs, IκBα, IκBβ and IκBε, and 3) nuclear/atypical IκBs, IκBζ, Bcl-3, IκBη and IκBNS. These inhibitors are regulated slightly differently, with precursors and cytoplasmic IκBs being controlled by post-translation modification whereas nuclear IκBs are scarcely present in unstimulated cells and are regulated by induced transcription (Hinz et al., 2012). Furthermore, each of the IκB proteins have differing affinities for specific NF-κB dimers and are often expressed in a tissue-dependent manner (Zabel et al., 1990, Thompson et al., 1995, Li et al., 1997, Whiteside et al., 1997, Sedwick and Smerdon., 1999., Hoffman et al, 2002).

IκBα

The best characterised and founding member of the IκB family is IκBα, which has a role in the canonical NF-κB pathway. IκBα primarily interacts with the NF-κB RelA-p50 heterodimer, binding the RHD domains of the RelA-p50 to block the DNA binding ability of NF-κB (Trelle et al., 2016). The NF-κB-IκBα complex has been found to shuttle continuously between the cytoplasm and nucleus, with the equilibrium state strongly based towards the cytoplasm in resting cells due to a stronger nuclear export signal of the IκBα protein (Huang et al., 2000, Johnson et al., 1999, Tam et al., 2000). Newly translated IκBα has been shown to translocate into the nucleus to bind deacetylated RelA-p50 dimers and shuttle them back to the cytoplasm, terminating TNFα induced NF-κB activation (Arenzana-Seisdedos et al., 1997, Chen et al., 2001, Huang & Miyamoto., 2001). This ability of IκBα to directly bind NF-κB dimers that are either free or bound to DNA allows for efficient inhibition of NF-κB-dependent transcription. Interactions between each IκB protein and NF-κB are different; for

example when IκBβ binds a NF-κB dimer, the complex is retained in the cytoplasm (Huang & Miyamoto., 2001, Malek et al., 2001).

1.9.3 NF-κB pathways

In unstimulated cells, the NF-κB transcription factor complex is retained in the cytoplasm by a cytoplasmic or precursor IκB protein. NF-κB activation mechanisms can be broadly characterised into two different pathways termed the 'canonical' and 'noncanonical' pathways. Which pathway is activated depends on the extracellular stimuli and the receptors engaged. Each pathway leads to a distinct pattern of NF-κB dimer activation and thus downstream NF-κB transcription responses.

Canonical pathway

The canonical pathway, also known as the classical pathway, relies on the degradation of the cytoplasmic IκBs (Figure 1.10). Degradation of these IκBs releases bound NF-κB dimers, allowing their translocation to the nucleus where they bind and regulate NF-κB target genes. The canonical signalling pathway is known for its quick NF-κB response to stimuli, as no *de novo* protein synthesis is required. This rapid NF-κB response is a critical requirement of the immune system. Canonical activation of NF-κB occurs in response to a diverse array of stimuli, including a wide variety of cytokines (including TNFα and IL-1), pathogen-associated molecular patterns (PAMPs), mitogens, growth factors, hormones and physical and oxidative stresses.

A well characterized example of canonical signalling is the transduction cascade induced by the cytokine TNFα leading to nuclear translocation of the most abundant NF-κB dimer RelA-p50. TNFα binds as a trimer to TNF receptor 1 (TNFR1) inducing trimerization of the TNFR1 subunits which in turn recruits and activates TNFR1 associated death domain protein (TRADD), TNF receptor associated factor 2 (TRAF2) and a kinase, receptor interacting protein 1(RIP1; Hsu et al., 1996). TRAF2 subsequently ubiquitinates itself and RIP1, resulting in the recruitment and activation of the IκB kinase (IKK) complex (Hsu et al., 1996, Devin et al., 2000, Sebban et al., 2006., Wu et al., 2006). The IKK complex is composed of three subunits: two catalytic subunits IKKα and IKKβ; and a regulatory subunit IKKγ/NEMO (NF-κB essential modulator). Polyubiquitinated RIP1 can bind additional proteins, including IKKγ and

Transforming growth factor β-activated kinase 1 (TAK1) to activate the IKK. The IKK kinases are activated by phosphorylation by either the multimerizing of IKKγ which permits trans-autophosphorylation or by kinase TAK1 (Iwai., 2012., Adhikari et al., 2007). Activation of the IKK complex triggers the IKKβ subunit to phosphorylate IκBs at two conserved serine residues targeting them for subsequent ubiquitination and degradation via the proteasome (DiDonato et al., 1997, Li et al., 1999, Krappman & Scheidereit., 2005). The IKK complex preferentially phosphorylates the IkBα protein as directed by the IKKγ subunit (Schröfelbauer et al., 2012). Following its release from IκB, the NF-κB relocates to the nucleus where it binds κB DNA elements to initiate a transcriptional response.

Most canonical signalling leads to the activation of predominant NF-κB RelA-p50 dimer. RelA activation is thought to be synonymous with canonical signalling, however this is not always the case, as cytosolic IκBs (IκBα and IκBβ) can also associate with other NF-κB hetero- and homo- dimers containing either RelA or C-Rel (Malek et al., 2001). Moreover, in dendritic cells RelB-p50 dimers were found bound to IκBα, thus canonical signalling activates RelB transcriptional control in this cell type (Shih et al., 2012). NF-κB induces expression of cytokines such as TNFα and IL-1β (Collart et al., 1990, Ziegler-Heitbrock et al., 1993, Hiscott et al., 1993), as well as some anti-apoptotic genes (Stehlik et al., 1998) and genes involved in innate immunity such as the growth factor, granulocyte/macrophage-colony stimulating factor (GM-CSF; Schreck & Baeuerle., 1990). NF-κB also upregulates genes encoding other NF-κB subunits, including p100/p52 (Lombardi et al., 1995), p105/p50 (Ten et al., 1992), RelB (Bren et al., 2001) and C-rel (Hannink & Temin et al., 1990) and IκB proteins, IκBα (Sun et al., 2003) and IκBε (Tian et al., 2005).

Negative feedback loop

NF-κB activation is transient, with mechanisms in place to prevent aberrant NF-κB activation as this can be associated with chronic inflammation and malignancies (Karin & Greten., 2005). IκBα is transcriptionally upregulated by NF-κB and is the primary contributor to a self-regulating negative feedback loop that terminates signalling (Hoffman et al., 2002). Upon transcriptional induction and synthesis, IκBα enters the nucleus, binds and inhibits RelA-p50 dimers bound to DNA. This aids in the IκBα-

RelA-p50 complex dissociating from the DNA, and translocates back to the cytoplasm (Arenzana-Seisdedos et al., 1997). Due to the delay between proteasomal degradation and resynthesis of IκBα, even transient cytokine exposures lead to NF-kB activation for approximately one hour (Werner et al., 2008). It is worth noting that free IκBα is an intrinsically unstable protein with a half-life of 10 minutes or less when unbound to NF-κB (Mathes et al., 2008). This rapid degradation is regulated by a C-terminal PEST region on IκBα which is masked when bound to NF-κB, thus stabilising the IκBα protein (Huxford et al., 1998, Phelps et al., 2000., Mathes et al., 2008).

Alternative negative feedback mechanisms regulate the other IκBs; IκBε (Kearns et al., 2006) and IκBσ (p100; Shih et al., 2009). Slow transcriptional induction and protein synthesis of IκBσ, leads to its role in repressing persistent NF-κB signalling (Shih et al., 2009). Another NF-κB-induced negative feedback regulator is A20 (also known as TNFα-induced protein 3; TNFAIP3), a zinc finger protein, well-known to be anti-inflammatory, NF-κB inhibitory and anti-apoptotic. It consists of two domains, an ovarian tumour domain with deubiquitinase activity and a zinc finger domain which mediates its ubiquitin ligase and binding activity. The A20 protein interacts with ubiquitin enzyme complexes to deubiquitinate RIP1 and TRAF2 and other components of the TNFR1 signalling complex, restricting their ability to activate NF-κB. While the long half-life of the A20 protein renders its impact on the negative feedback loop of NF-κB to have low immediate impact, it does make the NF-κB pathway less sensitive to subsequent inductions (Werner et al., 2008).

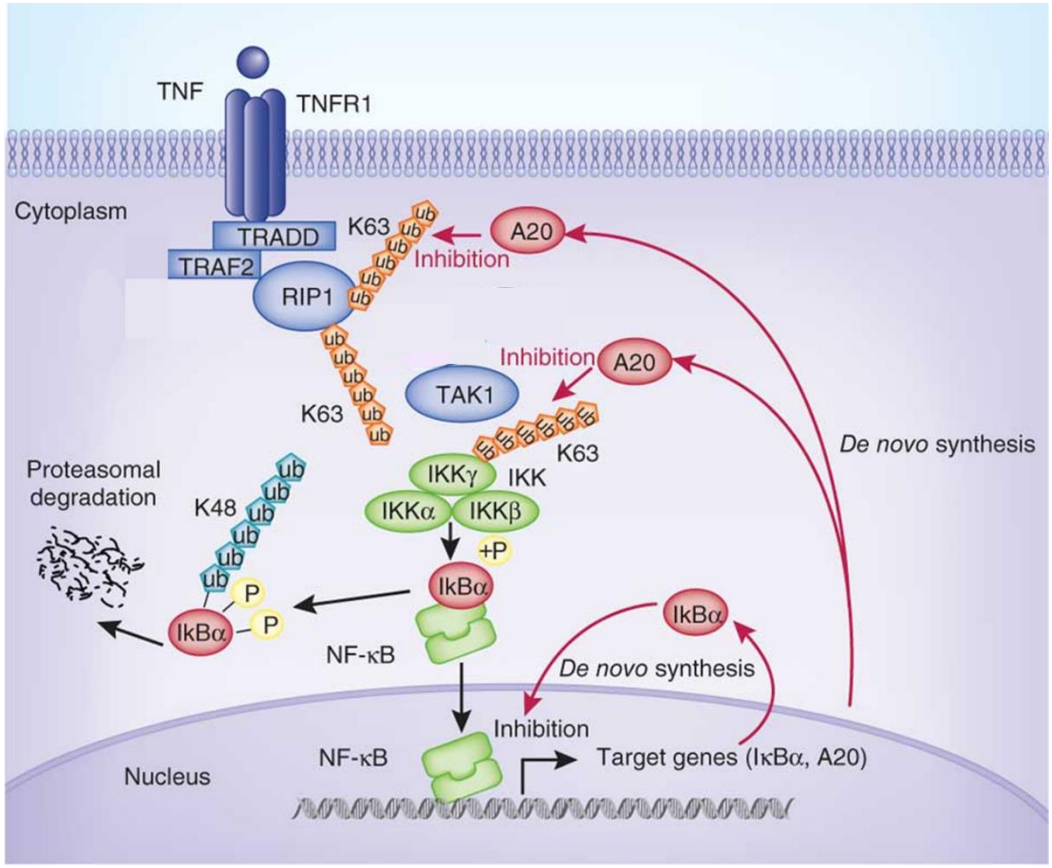

Figure:1.10 The canonical NF-κB pathway activated by TNF. Figure adapted from Ruland., (2011).

Non-canonical pathway

A second pathway, the non-canonical or 'alternative' NF-κB pathway, was first discovered in a study on the processing of precursor NF-κB protein p100 (Xiao et al., 2001). This pathway activates RelB-p52 NF-κB dimer using a mechanism which is dependent of the processing of p100 instead of degradation of the cytoplasmic IκBs (Figure 1.11). As previously mentioned, p100 acts as a IκB protein until proteolytically processed to create p52 (see Section 1.9.1-2). The p100 protein preferentially binds to the RelB subunit, inhibiting its translocation to the nucleus (Solan et al., 2002). Thus, processing of p100 to p52 typically leads to the nuclear translocation of the RelB-p52 dimer. The non-canonical NF-κB pathway is known to regulate a distinct set of genes with important roles in lymphoid organ development, B-cell survival and maturation and bone metabolism (Bonizzi et al., 2004, Dejardin., 2006). The non-canonical pathway is induced by a more restricted group of ligands in comparison to the vast array that can induce the canonical pathway. Non-canonical inducers include the B cell-activating factor, CD40 and lymphotoxin β which target a specific set of receptors.

A central component of this pathway is the NF-κB inducing kinase (NIK) which activates a downstream kinase, IKKα, which in turn phosphorylates p100 leading to its processing to p52 (Heusch et al., 1999, Xiao et al, 2001). Unlike the canonical pathway, the noncanonical pathway is independent of the IKKβ and IKKγ subunits and has slower and more persistence NF-κB activation kinetics, than the canonical pathway (Sun., 2011). This delayed NF-κB activation is partly caused by its requirement of *de novo* protein synthesis of the NIK protein, as levels of NIK are extremely low in unstimulated cells (Liao et al., 2004, Sun., 2011). As with the canonical pathway, the non-canonical pathway is regulated by a negative feedback loop, although this is not as tightly controlled as the canonical loop, thus allowing a more persistent activation. Upon activation of IKKα dimer by NIK, the IKKα dimer in turn phosphorylates NIK, thereby targeting it for proteolysis and preventing accumulating levels of NIK; such accumulation is associated with lymphoid malignancies (Razani et al., 2010). Processing of p100 to p52 is tightly controlled by activation of the non-canonical pathway whereas processing of p105 to p50 is constitutive.

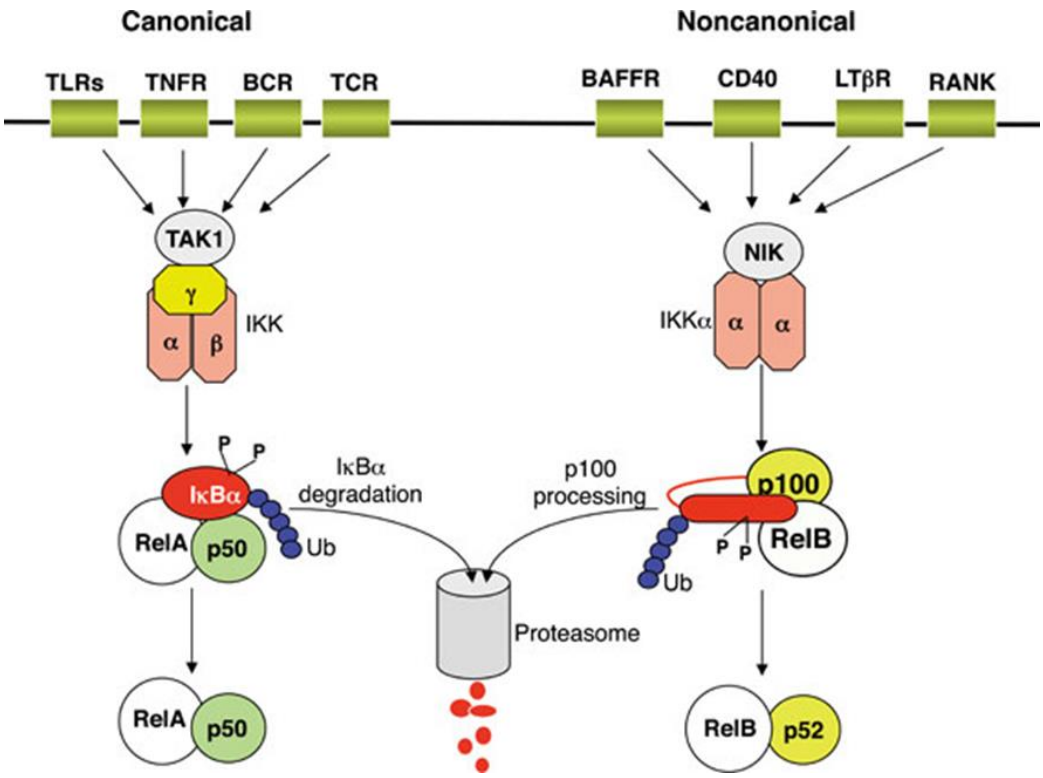

Figure 1.11 Differences between the canonical and non-canonical NF-κB pathways. Figure reproduced from Sun., 2011.

Most NF-κB inducers act through the canonical and non-canonical pathways. However, alternative pathways have been discovered that are independent of the IKK subunits and instead are activated by other kinases such as casein kinase II (CK2) (Kato et al, 2003; Schoonbroodt et al, 2000). These include pathways induced by cellular stresses such as hypoxia and UV exposure.

Mice deficient of one or more of the NF-κB family members have been generated revealing redundant and non-redundant roles of these proteins in cell survival, haematopoietic regulation, control of innate and adaptive immune responses and the development of secondary lymphoid organs (Table 1.3).

Knockout(s)	Phenotype	Reference(s)
rela	Embryonic lethal (E14); liver apoptosis; sensitivity to TNF	Beg & Baltimore, 1996
nfkb1	General Immune defects; abnormal B-cell response	Sha et al., 1995
c-rel	Impaired lymphocyte activation	Kontgen et al., 1995
relb	Defects in adaptive and innate immunity	Burkley et al., 1995, Weih er al., 1995
nfkb2	Abnormal spleen and lymph node architecture; defective T-cell reponse	Caamano et al., 1998, Franzoso et al, 1998
nfkb1, relb	Lethal 3-4 weeks post-natal; increased organ inflammation	Weih et al., 1997
nfkb1, rela	Embryonic lethal (E12)	Horwitz et al., 1997
nfkb1, c-rel	Decreased humoral immunity	Pohl et al., 2002
nfkb1, nfkb2	Reduced growth; bone defects; B-cell defects	Franzozo et al., 1997, Iotsova et al., 1997
ikba	Early neonatal lethal; inflammatory dermatitis and granulocytosis	Beg et al., 1995b, Klement et al., 1996
ikbe	Reduction in CDD44- and CD25+ T-cells	Memet et al., 1999
IKKa	Early neonatal lethal; skin defects	Hu et al., 1999, Takeda et al., 1999
IKKb	Embryonic lethal (E12-14); liver apoptosis; sensitivity to TNF	Li et al., 1999a, Li et al., 1999b, Tanaka et al., 1999
IKKg (NEMO)	Embryonic lethal; liver apoptosis; sensitivity to TNF	Rudolph et al., 2000, Makris et al., 2000
IKKa/IKKb	Embryonic lethal; liver apoptosis; sensitivity to TNF; neural defects	Li et al., 2000

Table 1.3 Mouse NF-κB knockouts.

1.9.4 The RelA protein

Of the five NF-κB members RelA is the most extensively studied due to its abundance and strong transcriptional activation potential (Schmitz, 1991). As previously mentioned the RelA/p50 dimer represents the most common NF-κB complex in most cells, with RelA contributing the TAD and thereby all of the transactivation function.

Mice that lack RelA die at around day 14.5 of gestation as a result of liver degeneration (Beg et al, 1995). When these mice were crossed with knockouts of either TNFα or TNFR1 the liver degeneration phenotype was rescued (Doi et al 1999; Alcamo et al, 2001). This revealed the crucial role that RelA plays in protecting cells from TNFα induced apoptosis. However, these double deficient mice displayed a compromised immune system with a high susceptibility to bacterial and viral infections, and none survived beyond 5 weeks after birth (Doi et al 1999; Alcamo et al, 2001). The TNFR1/RelA deficient mice were shown to completely lack lymph nodes and Peyer's patches, and displayed a disorganised spleen microarchitecture suggesting that NF-κB is a key mediator for secondary lymphoid organ development (Alcamo et al, 2002).

Alternative animal models have been generated in an attempt to understand RelA's function in the immune system. In order to study RelA's role in lymphocytes, Doi et al (1997) transplanted foetal *rela*$^{-/-}$ liver cells into irradiated SCID mice. These animals display impaired T and B cell functions and proliferation (Doi et al, 1997). A conditional mouse knockout of RelA in haematopoietic stem cells (HSCs) was generated; depletion of RelA resulted in altered gene expression and defects in hematopoiesis, leading to altered blood cell compositions (Stein & Baldwin, 2013). These discoveries show that RelA is necessary for normal differentiation, proliferation and function of cells that mediate immune response.

RelA is known to undergo many post-translational modifications such as phosphorylation, acetylation and methylation; these have been shown to alter NF-κB transcriptional activity and nuclear translocation and can contribute to target gene specificity (Huang et al, 2010). The majority of the posttranslational modification sites in RelA are present within the N-terminal RHD and the C-terminal transactivation domains.

Rel-Homology Domain (RHD)

The RHD is present in all NF-κB proteins and is essential for dimer formation, nuclear localisation, IκB association and DNA binding. The RHD is present at the amino-terminus of RelA and is approximately 300 amino acids in length. It exhibits high homology with RHDs of other NF-κB family members and is also conserved across species. The crystal structure of human RelA's RHD bound to DNA and IκB proteins have been determined (Huxford, 1998). The structure of the RHD is composed of two immunoglobulin-like domains connected by a flexible linker of 10 amino acids. The first immunoglobulin-like domain is located at the immediate N-terminal 180 amino acids and mediates all specific DNA-base contacts. The second is approximately 100 amino acids in length and mediates dimerization between NF-κB subunits. The flexible linker allows structural changes between the closed conformation required for binding inhibitory IκB proteins and open conformation to mediate DNA binding.

Post-translation modifications of RelA are known to alter its structural qualities to either weaken or enhance binding to NF-κB co-factors (Huang et al, 2010). Several post-translational modifications have been characterized in the RHD, including phosphorylation, acetylation and methylation. For example, the phosphorylation of S276 on human RelA by PKAc or MSK1 results in an increase in the transcriptional activity of NF-κB by enhancing binding of p300/CBP (Zhong et al, 1998, Reber et al, 2009). Other modifications can decrease transcriptional activity, such as acetylation of human RelA at K122 and K123 by p300/CBP or PCAF, which reduces affinity for κB enhancer sites (Kiernan et al, 2003). Many other sites of post-translational modification have been identified in RelA, most of which are conserved throughout mammalian species.

Transactivation domain (TAD)

The presence of the TAD in the NF-κB complex is necessary for the induction of target gene expression. Conservation of these domains between members of the NF-κB family is lower than observed for the RHD, although the RelA TAD is conserved across species (Figure 1.2). In RelA the TAD is divided into two transactivation domains, TA1 and TA2. TA1 (porcine residues 523-553) is located C-terminal to TA2 (porcine residues 430-523). Activity of RelA is regulated through a number of

phosphorylation sites. Unlike the RHD, the TAD does not contain lysine (Lys, K) residues, indicating that it is not directly influenced by lysine specific modifications such as acetylation, methylation and ubiquitination, SUMOylation or succinylation (O'Shea & Perkins., 2008). Previous studies on the TAD indicate that there is some redundancy between TA1 and TA2 (Schmitz et al, 1995).

TA1 (human 521-551) is an acidic domain that forms an alpha-helical conformation (Schmitz, 1995). Two phosphorylation sites, S529 and S536, have been identified to play a key role in transactivation activity of the TA1 domain (pig S531 and S538 respectively). S529 is phosphorylated by CKII and has been shown to enhance transcriptional activity (Wang et al, 2000). S536 has been reported to be phosphorylated by multiple kinases, including IKKε, IKKβ, IKKα, NAK and RSK1 and also enhances the transactivation activity of RelA (Vermeulen et al., 2003, Viatour et al., 2005). There are also another five possible phosphorylation sites within TA1 which could further regulate its activity (O'Shea & Perkins., 2008).

TA2 (human 428-521) is the larger of the two domains and has been found to contain a region of homology with the TA1 domain (458-483). Human RelA contains three proven phosphorylation sites, S435, S468 and T505. Phosphorylation of either S435 or T505 has a negative effect on the transcriptional activity (Perkins., 2006, Msaki et al., 2011). S468 has been reported to be phosphorylated by kinases GSK3β, IKKε and IKKβ, and has either an enhancing or repressing effect on transcriptional activity, depending on the cell context (Holger et al., 2004, Mattioli et al., 2006, Wang et al., 2012). There are eight other possible phosphorylation sites within TA2 which are currently being investigated for their consequences on NF-κB transcription (O'Shea & Perkins., 2008).

These conserved phosphorylation sites are likely to mediate interactions with co-transcription regulators and basal transcription machinery. Around 30 proteins have been identified to directly interact between the RelA TAD; including TATA-binding proteins, transcription factor IIB and p300 (O'Shea & Perkins, 2008).

1.10 Hypothesis

RelA is a member of the NF-κB family of transcription factors, which play an essential role in regulating the mammalian immune and inflammatory response. This protein is highly conserved throughout mammalian species. Amino acids changes identified between the warthog and the domestic pig have been proposed to confer an altered activity of the NF-κB transcription factor to specific stimuli (Palgrave et al, 2011). It has been hypothesised that the warthog variant of RELA has the potential to underlie the warthog's apparent tolerance to ASFV infection. In order to test this hypothesis, genetic engineering tools have been employed to convert the *Sus scrofa* RELA sequence to that of its warthog counterpart. As a first step to test the validity of a genetic engineering approach, reagents were constructed to target *S.scrofa* RELA. These were injected into pig zygotes for the production of RELA-edited animals.

1.11 Thesis objectives

1. To genotype and characterise porcine RELA genome edited animals at the molecular, cellular and morphological level

2. To determine whether the porcine RELA editing events impact on the response to ASFV infection *in vitro* and *in vivo*

3. To develop and effectively use genome editors to exchange a warthog 'ASF tolerance' RELA polymorphism into the domestic pig for the production of live transgenic swine.

Chapter 2 Materials and Methods

2.1 DNA techniques

2.1.1 Genomic DNA extraction

Ear notching of piglets a few days after birth was routinely carried out by farm staff for identification purposes. To genotype piglets, the ear tissue removed during this procedure was collected into a falcon tube transferred to the laboratory for genomic DNA (gDNA) extraction. The ear tissue was cut into a 2-3 mm^3 piece with a scalpel before using the DNeasy blood and tissue kit (Qiagen) to extract the gDNA following the manufacturer's protocol.

2.1.2 Polymerase chain reaction (PCR)

Unless stated otherwise, PCR reactions were carried out using Phusion® High-Fidelity PCR Master Mix (BioLabs). The reactions were set-up on ice and transferred to a T Professional thermocycler (Biometra) when the block and lid had preheated to 80-96°C. A 50 µl PCR reaction mixture contained 25 µl of 2X Phusion High Fidelity (containing 3 mM $MgCl_2$, 400 µM of each dNTP plus 1 unit of Phusion DNA polymerase), 10 µl of 5X Fi-RED loading dye (see Section 2.12.1), 1.25 µl of each 10 µM stock primer (forward and reverse), 50-150 ng of genomic DNA template, and made up to final volume of 50 µl with nuclease-free water. The PCR program consisted of the following steps; initial denaturation step at 98°C for 30 secs, 35 cycles of 98°C for 20 secs, an optimised annealing temperature (shown in Section 2.11.1) for 20 secs, 72°C for 30 secs, followed by a final elongation step of 72°C for 30 secs and then held at 10°C. If required samples were stored at -20°C prior to use.

2.1.3 Agarose gel electrophoresis

Agarose gels were made by dissolving UltraPure agarose (Life Technologies) in 1X TAE buffer (see Section 2.12.1). Different percentages of agarose gels were used depending on the size-range of samples being resolved. For example, to make a 1% agarose gel, 1 g of agarose was added to 100 ml of TAE and the mixture was heated in a microwave to fully dissolve the agarose in solution. Once the gel mixture had cooled 10 µl of 10X SYBR™ Safe DNA stain (Thermo Scientific) was added before

pouring the gel. The DNA samples were loaded alongside 5 µl of GeneRuler DNA Ladder Mix (Thermo Scientific), for both DNA length and mass approximations. These were separated by running gels at a voltage between 1-10 V/cm, depending on the requirement, and bands were visualized and imaged on UV Transilluminator Gel Dock.

2.1.4 Purification of DNA from agarose gels and PCR reactions and agarose gels

To extract DNA fragments from agarose gels, the desired bands were visualised under a UV light source and excised from the gel with a scalpel. DNA from gel slices and PCR reactions were purified using the illustra GFX PCR DNA and Gel Band Purification Kit (GE Healthcare Life Sciences). Purification was carried out according to the manufacturer's protocol; PCR reactions were mixed thoroughly with 500 µl of Capture buffer type 3 and then loaded directly into a GFX column. Gel slices were incubated with 500 µl of Capture buffer type 3 at 60°C until the agarose had completely dissolved, approximately 15-30 minutes, before loading onto the GFX column. Once loaded onto the GFX column the samples were centrifuged, washed once with 500 µl of Wash type buffer 1, and then incubated in 30 µl of Elution buffer type 4 for 1 minute before centrifugation to elute the DNA from the column into a new DNase free collection tube. All centrifugation steps were carried out at 16,000 x g for 1 minute.

2.1.5 Nucleic acid quantification

The concentration of DNA samples was routinely estimated using the Nanodrop™ 1000 spectrophotometer (Thermo Scientific) and ND-1000 software. Prior to measuring the DNA samples, the Nanodrop was initialised with 1.5 µl of deionized water and then a blank measurement was taken using the 1.5 µl of the buffer that the DNA was suspended in. To use the Nanodrop spectrophotometer, 1.5 µl of solution was pipetted onto the receiving fiber sensor on the lower pedestal, before lowering the upper pedestal arm bringing the source fiber sensor into contact with the liquid sample, a spectral measurement was then taken. Once each measurement was completed the loaded sample was wiped from both pedestals using a lint-free cloth. The ND-1000 software calculates the concentration of DNA displayed in ng/µl (one OD260 unit =

50 ng/µl of dsDNA). It also displays the 260/280 and 260/230 absorbance ratios for each sample, which was used to assess the purity of DNA. A 260/280 ratio of ~1.8 is considered "pure" for DNA and an acceptable range for the 260/230 ratio is around 1.8-2.2. RNA samples were also quantified using the Nanodrop™ 1000 spectrophotometer (Thermo Scientific) in the same manner. The ND-1000 software calculates the concentration of RNA displayed in ng/µl (one OD260 unit = 40 ng/µl of RNA).

2.1.6 DNA sequencing

4.5-10 ng of purified PCR product (see Section 2.1.4) was sent to Edinburgh Genomics in 5 µl of deionized water with 1 µl of 6.4 µM primer solution for Sanger sequencing. Edinburgh Genomics performed Big Dye reactions using the BigDye v3.1 Terminator Cycle Sequencing Kit (Thermo Fisher Scientific), which were then column purified, dried in a vacuum concentrator, resuspended in Hi-Di Formamide (Applied Biosystems) and denatured before running capillary analysis on the 3730X DNA Analyser (Applied Biosystems). The sequencing data was received from Edinburgh Genomics in .ftv file format. The traces were initially analysed using freeware program, FinchTV (Geospiza). If further analysis was required Lasgergene software was employed.

2.2 Techniques involving E.coli

2.2.1 Preparation of chemically competent *E.coli*

Top10 *E.coli* cultures where streaked onto LB agar plates, containing 12.5 µg/ml Streptomycin, and incubated at 37°C overnight. The next day a single colony was used to inoculate 20 ml of SOC (see Section 2.12.1), containing 12.5 µg/ml Streptomycin, in a 250 ml conical flask and incubated at 37°C overnight with shaking. 1 ml of the overnight culture was used to inoculate 100 ml of SOB (containing 12.5 µg/ml Streptomycin) in a 1 litre conical flask. The culture was incubated at 37°C for ~2-3 hours, until a cell density of ~4-7x10^7 cells/ml was reached (equivalent to OD600 of 0.45). The culture was divided into two 50 ml tubes and the cells were pelleted by centrifugation at 6,000 x g for 10 minutes at 4°C. The supernatant was discarded and the cells were resuspended gently in 33 ml of ice cold RF1 (see Section 2.12.1) using

a 25ml serological pipette and incubated on ice for 20 minutes. The cells were pelleted again at 6,000 x g for 10 minutes at 4°C, supernatant discarded, and resuspended gently in 8 ml of RF2 (see Section 2.12.1) and incubated on ice for 20 minutes. Competent bacteria were then distributed into 50 µl aliquots in pre-chilled tubes before snap freezing on dry ice and storing at -80°C until use.

2.2.2 Transformation of competent *E.coli*

Aliquots of Top10 chemically competent *E.coli* cells were thawed on ice prior to use. 50 µl of Top10 competent *E.coli* cells were gently mixed with 3 µl (1-10 ng) of DNA, and incubated on ice for 10 minutes, followed by heat shocking the mixture at 42°C for 45 seconds, then immediately returning to ice for 5 minutes. 125 µl of SOB medium was then added to each transformation before incubation at 37°C in shaking incubator for 1 hour. 50 µl of each culture was pipetted onto agar plates containing Carbenicillin (50 µg/ml) and spread using 10-20 sterile glass beads (3mm in diameter) per plate. The beads were removed and plates were incubated overnight at 37°C. The next day plates were removed from 37°C incubator and stored at 4°C until analysis of the colonies was carried out.

2.2.3 Small scale preparation of plasmid DNA

The QIAprep Plasmid Spin Miniprep kit (Qiagen) was used to extract up to 20 µg of plasmid DNA and was used for all small scale preparations following the manufactures guidelines. All centrifugation steps were carried out at 16,000 x g unless stated otherwise.

Single bacterial colonies were inoculated into 5ml of LB medium (see Section 2.12.1) supplemented with Carbenicillin (50µg/ml) and incubated at 37°C with shaking overnight. 1.5 ml of the overnight culture was transferred to a 1.5 ml tube and spun at 6800 x g for 3 minutes to pellet bacteria. After the supernatant was discarded, the bacterial pellet was resuspended in 250 µl of buffer P1 and then lysed in 250 µl of buffer P2 for no longer than 5 minutes. The cellular debris and genomic DNA was precipitated with the addition of 350 µl of buffer N3 and then pelleted by centrifugation for 10 minutes. The supernatant was collected and transferred into a QIAprep spin column and centrifuged for 30 seconds. Flow through was discarded and the column

was washed with 750 µl of buffer PE, with the flow-through again discarded. The centrifugation step was then repeated for 1 minute to remove any residual wash buffer. Each column was then transferred into a new 1.5 ml DNase free tube. 30-50 µl of EB buffer was added to each column followed by incubation at room temperature for 1 minute. Plasmid was eluted with a final centrifugation step for 1 minute. The plasmid DNA was quantified using the Nanodrop (see Section 2.1.5) and stored at -20°C for future use.

2.2.4 Large scale preparation of plasmid DNA

The EndoFree Plasmid Maxi kit (Qiagen) was used to extract up to 500 µg of plasmid DNA for large scale preparations of plasmids following the manufactures guidelines. All incubation steps were carried out at 37°C with shaking unless otherwise stated.

Single colonies were inoculated into 5 ml of LB medium supplemented with Carbenicillin (50 µg/ml) and incubated for 6-8 hours. After initial incubation, the 5 ml culture was transferred into a 500 ml conical flask containing 100 ml of LB (supplemented with Carbenicillin (50 µg/ml)) and incubated overnight. To harvest bacteria, 50 ml of overnight culture was transferred into a 50 ml falcon tube and centrifuged at 6000 x g for 15 minutes at 4°C. The supernatant was discarded and the cell pellet was left to air-dry by inverting the open tube onto blue cloth until all of the medium had drained. The bacterial pellet was resuspended thoroughly in 10 ml of Buffer P1 (containing RNase A) by vortexing. The cells were lysed with the addition of 10 ml of Buffer P2 and gently mixed by inverting the tube 4-6 times followed by an incubation at room temperature for no longer than 5 minutes. The lysis step was terminated with the addition of 10 ml of chilled Buffer P3 and immediate mixing by inverting the tube 4–6 times. The lysate was transferred into the QIAfilter Cartridge and incubated at room temperature for 10 minutes after which it was passed through the QIAfilter cartridge using the supplied plunger. To remove endotoxins, 2.5 ml of Buffer ER was added to the filtered lysate before inverting the tube 10 times and incubating on ice for 30 minutes. The lysate was loaded into an equilibrated QIAGEN-tip 500 column (column equilibrated by flowing 10 ml of Buffer QBT through the column) and allowed to flow through. The column was washed twice with 30 ml of Buffer QC and then the DNA was eluted in 15 ml of Buffer QN into an endo-toxin

free tube. The DNA was precipitated with the addition of 10.5 ml of isopropanol and pelleted at 5,000 x g for 1 hours at 4°C. The supernatant was discarded and the DNA pellet was subsequently washed with 5 ml of endotoxin-free 70% ethanol and centrifuged step was repeated at 5,000 x g for 1 hour at 4°C. The pellet was air-dried for 5-10 minutes at room temperature, and resuspended in 200 µl of endotoxin-free Buffer TE. Plasmids were quantified using the Nanodrop (see Section 2.1.3) and stored at -20˚C until use.

2.3 Animals

2.3.1 Pigs

All pigs in this project are Landrace/Large White crosses. Founder animals in this line are described in Lillico et al, 2013. The procedures and experiments on all animals were carried out under approved UK Home Office License regulations. This animal line was maintained through natural matings, all carried out at The Large Animal Unit, Roslin Institute, University of Edinburgh.

2.3.2 Blood sampling and analysis

Blood samples were collected by jugular venepuncture into BD Vacutainer® Heparin coated tubes, this procedure was conducted by appropriately licensed large animal staff. Blood was collected for the isolation peripheral blood mononuclear cells (PBMCs; see Section 2.4.1) and for routine blood count analysis. Approximately 1ml of blood from each animal was sent to the R(D)SVS Clinical Pathology Laboratory, University of Edinburgh, for blood count analysis. Total differential white blood cell (WBC) counts of samples were measured on the Siemens Advia 2010 analyser within two hours after blood collection.

2.3.3 Tissue processing

All pigs were sedated with Ketamine (Vetalar) and Azaperone (Stresnil) before being euthanised via injection of a lethal dose of Pentoject (Animalcare). Tissues were excised from euthanised animals and cross sectioned using a scalpel into pieces no larger than ~1 cm^3 before placing into 10 % neutral buffered formalin. Samples were left in fixative overnight at room temperature before moving to 4°C. These were

subsequently sent to the R(D)SVS pathology department to carry out histology. Tissues were placed in histology cages and then processed for wax embedding using Shadon™ Pathcentre tissue processor (Thermo Fisher Scientific) following the protocol:

Reagent	Incubation time
70% Ethanol	1 hour
95% Ethanol	1 hour
Absolute ethanol	1 hour
Absolute ethanol	1 hour
Absolute ethanol	1 hour
Absolute ethanol	1 hour
50% Absolute ethanol 50% Xylene	1 hour
Xylene	1 hour
Xylene	1 hour
Wax	1 hour
Wax	1 hour
Wax	1 hour
Wax	1 hour

After processing, the samples were embedded in paraffin wax blocks and stored at 4°C prior to sectioning. A microtome was used to cut 5 μm sections which were mounted onto poly-L-lysine slides. Slides were dried overnight at 37°C before incubating at 62°C for 25 minutes, to melt away any excess wax before staining with H&E. Staining was carried out using the Gemini AS Automated Slide Stainer (Thermo Fisher Scientific) following the protocol below:

Reagent	Incubation time
Xylene	2 minutes
Xylene	2 minutes
Xylene	2 minutes
Absolute ethanol	2 minutes
Absolute ethanol	2 minute
Absolute ethanol	2 minute
Running water wash	2 minutes
Harris haematoxylin	18 minutes
Running water wash	1 minute
Running water wash	1 minute
Acid alcohol	10 seconds
Running water wash	2 minutes
Scott's tap water substitute	2 minutes
Running water wash	2 minutes
Eosin	30 seconds
Running water wash	4 minutes
Absolute ethanol	1 minute
Absolute ethanol	2 minutes
Absolute ethanol	2 minutes
Xylene	2 minutes
Xylene	2 minutes
Xylene	1 minute

Finally, the slides were mounted with Histomount (Thermo Fisher Scientific) and a glass coverslip was place on top. Details of the solutions used during histology can be found in Section 2.12.4.

2.3.4 Bone marrow smear

To collect bone marrow smears from euthanised pigs the back left femur was excised and cut open with a surgical saw. The bone marrow was removed from the femur and spread across a microscopy slide. These were immediately taken to the R(D)SVS pathology department who carried out Giemsa staining. Once stained, a differential cell count was performed by Prof Elspeth Milne, R(D)SVS pathology unit, University of Edinburgh.

2.4 Primary cell isolation and culture

2.4.1 Porcine PBMC isolation

Peripheral blood mononuclear cells (PBMCs) were isolated from whole blood (see Section 2.3.2 for collection details). The blood was transferred into a tissue culture hood before diluting 1:1 with PBS. The diluted blood was layered on top of 20 ml of Lymphoprep™ (Axis-Shield) in a 50 ml falcon tube before centrifugation for 30 minutes at 700 x g in a swinging-bucket rotor with no brake. As the vast majority of PBMCs have a lower density than the Lymphoprep™ medium (which has a density of 1.077 g/ml) these cells form a distinct layer at the sample/medium interface after centrifugation, this layer is termed the buffy coat (Figure 2.1). The erythrocytes and the polynuclear blood cells (granulocytes) sediment through the medium as their density is higher than the Lymphoprep™. The buffy coat was carefully removed using a 20 ml serological pipette and transferred into a new 50 ml falcon tube which was topped up to 50 ml with PBS before centrifugation at 350 x g for 10 minutes. The supernatant was discarded before washing the cell pellet with PBS and spinning at 100 x g for 10 minutes to remove any contaminating platelets, this step was repeated twice. If any erythrocytes were visible in the cell pellet they were lysed by resuspending the pellet in 5 ml of RBC lysis buffer (see Section 2.12.3) for 2 minutes before washing twice with PBS.

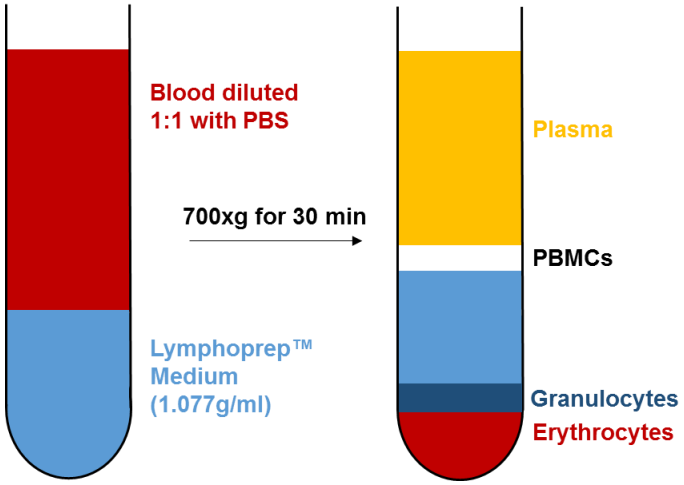

Figure 2.1 Density gradient centrifugation used to isolate PBMCs from whole blood.

2.4.2 Porcine fibroblast isolation

Porcine adult fibroblasts, PAFs, were isolated from the ear tissue of adult pigs and porcine embryonic fibroblasts, PEFs, were isolated from 60-day old pig foetuses.

Preparation of porcine adult tissue:

For isolation of PAFs, an ear from a euthanised pig was scrubbed thoroughly with Povidone-iodine solution and rinsed with PBS before removing the top half of the ear by cutting with a sterile blade. The ear was transported from the farm to the laboratory in a container in containing PBS with 2X Antibiotic-Antimycotic (Gibco) on ice. To clean the ear, it was repeatedly scrubbed with Povidone-iodine solution outside the tissue culture hood and rinsed with PBS. Once cleaned thoroughly, the hair was removed from the ear with a sterile scalpel before scrubbing for a final time with Povidone-iodine solution using a fresh sterile brush and then rinsing three times with PBS. The ear was transferred into a tissue culture hood onto a sterile round glass dish. The skin was removed from both sides of the ear with forceps and a sterile scalpel and cut into ~4 cm^2 pieces of tissue, these were placed in 50 ml tubes containing chilled PBS with 2X Anti-Anti (Gibco) and kept on ice until further processing.

Preparation of porcine embryonic tissue:

For the recovery of porcine embryos, a pregnant sow was euthanized 60 days after serving. The abdominal cavity of the pregnant sow was opened and the uterus removed. The foetuses were excised from the uterus directly into a container containing chilled PBS using a fresh sterile blade. Each embryo was kept at 4°C until further processing. Once transferred into a tissue culture hood the foetus was rinsed three times in PBS, before decapitation and evisceration.

Further processing of both adult and embryonic tissue:

In the tissue culture hood, both adult and embryonic preparations were placed on a sterile petri dish and minced finely (into 1 mm^3 pieces) using two sterile scalpels in a scissoring motion. The minced tissue was then placed into a T-75 cm^2 flask with 10 ml of digestion medium (containing collagenase, 2X for adult tissues and 1X for embryonic, see Section 2.12.3 for all medium components). The minced tissue was then dispersed using a 10 ml serological pipette to break up any clumps of tissue before

incubation for 16 hours at 37˚C with 5 % $C0_2$ without agitation. The cells were then harvested by transferring all of the overnight digestion into a 50 ml falcon tube. To separate large residual clusters of tissue from cells the mixture was thoroughly dispersed by pipetting up and down at least 10 times before letting the mixture settle for 30-60 seconds. The supernatant, containing cell suspension, was then transferred into new 50 ml falcon tube. The large residual tissue that had settled at the bottom of the falcon tube was discarded. To pellet cells, the suspension was first topped up to a total volume of 50 ml with PBS and then centrifuged at 200 x g for 5 minutes. The supernatant was discarded and the cell pellet was resuspended in 25 ml of outgrowth media (see Section 2.12.3 for all medium components) and plated in a T-175 cm^2 flask. When the cells approached 100 % confluency (usually between one and two days) these cells were split 1:2 (see Section 2.4.5) and cultured until they reached 95 % confluency when they were frozen down (see Section 2.4.3) for future use. Six vials of cells were frozen per T-175 cm^2 flask.

2.4.3 Freezing porcine fibroblasts

To cryopreserve fibroblast cells, the medium was removed from the culture vessel and the cells were rinsed with PBS. To dissociate the cells from the culture vessel an appropriate volume of TrypLE™ Express (Thermo Scientific) was added to cover the bottom of the culture vessel (e.g. 3 ml for a T-75 cm^2 flask), and incubated at 37°C for 3-5 minutes after which an appropriate volume of pre-warmed culture medium was added to quench the TrypLE™ Express (e.g. 10 ml for a T-75 cm^2 flask). The cell mixture was then transferred into a 50 ml falcon tube and centrifuged at 300 x g for 5 minutes. The supernatant was discarded and the cell pellet was resuspended in the appropriate volume of freezing medium (see Section 2.12.3). 1 ml of the freezing mixture was then aliquoted into a pre-labelled 1.5 ml tubes, these were first stored in an isopropanol freezing container at -80°C overnight which allows a slow and constant decrease in the temperature before transferring to a -150°C freezer for long-term storage.

2.4.4 Thawing porcine fibroblasts

Frozen cells were thawed quickly in a 37°C water bath, and then transferred to 10 ml of fibroblast medium (see Section 2.12.3) and centrifuged for 5 minutes at 300 x g. The cell pellets were then resuspended in appropriate volume of medium for the culture vessel and grown as standard in a humidified 37°C incubator with 5 % CO_2.

2.4.5 Porcine fibroblast cell maintenance

When cells reached ~95 % confluency they were split 1:2. To split fibroblasts grown in a T-75 cm^2 flask, the cell medium was discarded and the attached fibroblast cells were washed with 10 ml of PBS. To dissociate the cells from the culture vessel, 3 ml of TrypLE™ Express (Thermo Scientific) was added to cover the surface of the flask which was then incubated at 37°C for 3-5 minutes. The flask was viewed under a light microscope to ensure complete cell detachment before the addition of 10 ml of pre-warmed media to quench the TrypLE™ Express. The cells suspension was transferred into a 50 ml tube and pelleted by centrifugation at 300 x g for 5 minutes. The cell pellet was resuspended in 16 ml of medium which was divided between two T-75cm^2 flasks. All fibroblast cultures were grown in a humidified 37°C incubator with 5 % CO_2.

2.4.6 Porcine bone marrow cell isolation

Macrophages were collected from pigs to perform *in vitro* infection studies with ASFV. To harvest macrophages, bone marrow cells were flushed from the ribs of euthanised pigs. Five posterior ribs from each side of the pig were removed and transferred into a sterile bag on ice. The ribs were individually transferred into the tissue culture hood for processing. A sterile blade was used to remove as much muscle as possible from the bones which were then washed in 70 % ethanol and then rinsed in PBS. The ends of each rib were cut off with bone cutters and a bone marrow biopsy/aspiration needle (Cardinal Health, USA) is screwed into one extremity of the rib. The bone was flushed with 20 ml RPMI media containing 5 mM of EDTA (in order to prevent possible clumping) into a sterile culture dish. The media was then transferred into a 50 ml falcon tube for centrifugation for 10 minutes at 400 x g to pellet the cells. Red blood cells present in the pellet were lysed by resuspending the pellet in 5 ml of red blood cell lysis buffer and incubating at room temperature for 5

minutes. The cell solution was then brought up to 50 ml with PBS and centrifuged again at 400 x g for 10 minutes. The cells were resuspended in 5 ml of RPMI medium and counted using a haemocytometer (see Section 2.4.10). The cells were then cryopreserved for future use (see Section 2.4.7).

2.4.7 Freezing porcine bone marrow cells

Bone marrow cells were cryopreserved at a concentration of 10^8 cells per vial. The cells were pelleted by centrifugation at 400 x g for 10 minutes and then resuspended in a volume of FCS, subsequently an equal volume of freezing medium was added. The freezing medium comprised 80 % FCS and 20 % DMSO. To retain good viability of cells, the freezing medium was added slowly in a dropwise manner with a 1 ml pipettor while gently agitating the mixture. The final freezing cell suspension mix, which then comprised 90 % FSC and 10 % DMSO, was transferred into pre-labelled vials in 1 ml aliquots. The vials were stored in an isopropanol freezing box at -80°C overnight and then transferred to a -150°C freezer for long term storage.

2.4.8 Thawing porcine bone marrow cells

Cryopreserved bone marrow cells were transferred from -150°C freezer to dry ice and subsequently thawed quickly in a 37°C water bath. The thawed cell solution was then transferred into an empty 50 ml tube before slowly adding 20 ml of RPMI medium drop by drop. This method reduces the chances of cell shock due to sudden changes in DMSO concentration and thus increases cell viability. The cells were pelleted by centrifugation at 300 x g for 10 minutes and cells were resuspended in an appropriate volume of RPMI media for the culture vessel.

2.4.9 Culturing bone marrow cells to derive macrophages

Bone marrow cells where cultured with human recombinant CSF-1 to promote the maturation of monocytes into macrophages. $1x10^8$ bone marrow cells were plated in a non-tissue culture treated 10 cm dish with final concentration of 10^4 U/ml (100 ng/ml) of human recombinant CSF-1 (rhCSF1; a gift from Chiron, Emeryville, CA). The cells were initially cultured for five days without agitation at 37˚C with 5 % CO_2 after which the matured macrophages had adhered to the surface of the dish. To split the

macrophage cells, media was removed and 5 ml of PBS was added with a serological pipette to rinse the plate removing all cells other than the adherent macrophages. After the initial PBS wash was discarded, 5 ml of fresh PBS was vigorously added to the dish using an 18-gauge blunt needle and 10 ml syringe. The action of vigorously pushing the PBS in and out of the syringe was repeated 10 times to forcibly detach the macrophages from the dish. The cell suspension was transferred to a falcon tube before repeating this process with the addition of another 5 ml of fresh PBS. The final 10 ml of cell suspension was centrifuged at 400 x g for 10 minutes before resuspending the cell pellet in an appropriate volume of cell culture media for re-plating. All macrophage cultures were grown in a humidified 37°C incubator with 5 % CO_2.

2.4.10 Counting cells using a haemocytometer

A cover slip was placed on the haemocytometer and 10 µl of cell suspension was carefully added at the side of the glass coverslip, which enters the chamber by capillary attraction. The average number of cells were counted using a light microscope as indicated below. The haemocytometer is divided to several squares; since each square is equal to a volume of 0.1 mm^3 (10^{-4} cm^3), and 1 ml is equal to 1 cm^3, the total cell number per 1 ml solution can then be determined using the following equation:

Cells/ml = (Average count per square) x 10^4 (chamber conversion factor)

Total cells = (cells/ml) x (original volume of solution)

2.5 Protein techniques

2.5.1 Preparation of whole cell extracts

Whole cell protein extracts were prepared in cell lysis buffer containing RIPA buffer (Sigma) plus cOmplete™, Mini, EDTA-free protease inhibitor cocktail tablet (Roche) and PhosSTOP phosphatase inhibitor cocktail tablet (Roche; see Section 2.12.2). Both protease and phosphatase inhibitor tablets were dissolved in deionized water to a 10X stock solution and added to the RIPA buffer immediately before use. Prior to cell lysis a fully confluent T-75 cm^2 flask (containing approximately 5 x 10^6 PAF cells) was rinsed twice with chilled PBS. After rinsing, the cells were lysed directly in the flask

with the addition of 1 ml of lysis buffer, followed by incubation on ice for 5 minutes, swirling the flask occasionally to ensure uniform spreading of lysis buffer. The lysate was collected by scraping the flask surface with a cell scraper and pipetting into a fresh 1.5 ml tube. To pellet the cellular debris, the lysate was centrifuged at 14,000 x g for 15 minutes at 4°C. The supernatant was distributed into 20 µl into aliquots, flash-frozen on dry ice and stored at -80°C until use.

2.5.2 Subcellular Fractionation

Fibroblast cultures were incubated with and without recombinant porcine TNFα (ThermoScientific), at a final concentration of 10 ng/ml, for 30 minutes prior to harvesting and fractionation using NE-PER nuclear and cytoplasmic protein extraction reagents (Thermo Scientific), CER I, CER II and NER, following the manufacturer's guidelines. All the following incubation steps were carried out on ice and centrifugation at 4°C.

Cells were first harvested from one T-75 cm^2 flask using TrypLE™ (see Section 2.4.5) and centrifuged at 500 x g for 5 minutes. The cell pellet was resuspended in 1 ml of chilled PBS and then transferred into a 1.5 ml tube before centrifugation at 500 x g for 5 minutes. The supernatant was removed using a pipettor and the cell pellet allowed to air dry. 200 µl of ice-cold CER I was added to the cell pellet which was resuspended by vortexing for 15 seconds. Samples were incubated for 10 minutes before adding 11 µl of ice-cold CER II and vortexing vigorously for 5 seconds. Following a 1-minute incubation, samples were vortexed for another 5 seconds. To isolate the cytoplasmic fraction, samples were centrifuged for 5 minutes at 16,000 x g after which the supernatant was transferred to a clean pre-chilled labelled tube. Cytoplasmic lysates were flash-frozen on dry ice in 20 µl aliquots, to avoid more than one freeze-thaw cycle, before transferring to -80°C for long term storage. To extract proteins from the nuclei the insoluble pellet was resuspended in 100 µl of ice cold NER and vortexed vigorously for 15 seconds, the samples were then placed on ice and vortexed for 15 seconds at 10 minute intervals for a total of 40 minutes. Following incubation and vortexing steps, the nuclear samples were centrifuged at 16,000 x g for 10 minutes, after which the supernatant was immediately transferred into a pre-chilled tube before dispensing in 10 µl aliquots which were flash-frozen on dry ice before storing at -80°C.

2.5.3 Quantifying protein concentration

The Bradford method was used to determine the total protein concentration of lysates directly before running western blots. The Bradford method was first described in Bradford et al, 1976, and involves the binding of Coomassie Brilliant Blue G-250 dye to lysine, histidine and arginine residues in proteins.

In a 96-well plate, 200 µl of Quickstart Bradford Dye Reagent (Biorad) is dispensed to all protein sample wells. 5 µl of each of seven Pierce™ pre-diluted BSA protein standards (125, 250, 500, 750, 1000, 1500 & 2000 µg/ml, Thermo Scientific), were added in duplicate to wells containing Bradford Dye. 2 µl of each cell lysate (thawed on ice) were added in duplicate to wells containing Bradford Dye. Two wells were kept with only Bradford Dye Reagent for a blank reading. Any air bubbles present were burst using a hypodermic needle dipped in EtOH. The absorbance at 595nm was then measured using the Biotek Synergy HT plate reader and Gen5 software. Once absorbency readings were obtained, the protein concentrations were determined from the BSA protein standard curve using Excel software.

2.5.4 Gel electrophoresis of proteins

Polyacrylamide gel electrophoresis (PAGE) was used to separate proteins based on their size under denaturing conditions. Protein lysates where thawed on ice (previously stored at -80°C). Once thawed a Bradford assay was performed to estimate protein concentration (see Section 2.5.3). To prepare samples for PAGE the required quantity of protein was aliquoted and the volume adjusted to 10 µl with the lysis buffer. The protein samples were subsequently denatured by the addition of 10 µl of 2X Novex® Tris-Glycine SDS Sample Buffer and incubating at 96˚C for 3 minutes. The denatured samples were immediately loaded onto pre-cast Novex® 10% Tris-Glycine polyacrylamide gels in the XCell*SureLock*™ Mini-Cell filled with 1X Novex® Tris-Glycine SDS Running Buffer. The samples were electrophoresed at 125 V for 90 minutes. All Novex products mentioned were manufactured by Invitrogen.

2.5.5 Western blotting

Proteins were transferred from the polyacrylamide gel onto a nitrocellulose membrane by electrophoretic blotting in wet conditions. A sandwich of sponge, filter paper, gel, membrane, filter paper and sponge was made up immersed in 1X Tris-Glycine transfer buffer (set up shown in Figure 2.2). This sandwich was stacked together tightly in a Bio-Rad transfer cassette to ensure no bubbles formed between the gel and the membrane. The cassette was correctly orientated into a Bio-Rad electrophoresis tank with the membrane side closest to the anode, thus the negatively charged proteins would migrate from the gel towards the positive electrode and become bound by the membrane. An ice pack was placed into the tank before filling with 1X Tris-Glycine buffer. Transfer was carried out at a constant current of 100 V for 1 hour.

Figure 2.2. Diagram of wet transfer set up for western blotting

Following transfer, the membrane was removed from the cassette and stained with Ponceau S (see Section 2.5.6). In order to block non-specific binding sites, the membrane was incubated in blocking buffer (5 % semi-skimmed milk, 0.01 % Tween-20 in PBS) for 1 hour at room temperature. Membranes were incubated overnight at 4°C in the appropriate primary antibody diluted to optimal concentration (Table 2.4) in blocking buffer. The next day, membranes were washed five times in PBS-T on an orbital shaker for a minimum of 5 minutes. Once washed, a secondary HRP-conjugated antibody (either rabbit or mouse, depending on the primary antibody used) was diluted 1:1000 in blocking buffer and incubated on the membrane for 1 hour at room temperature. After another five washes in PBS-T, the antibody was detected using chemiluminescence. The membranes were placed on a sheet of glass and incubated with Pierce™ enhanced chemiluminescence (ECL) western blotting substrate (solution 1 and solution 2 were mixed together immediately before use at 1:1 ratio) for

2 minutes. The membranes on glass were then covered with cling film and placed into cassettes and taken to a dark room where they were exposed to X-ray film (Hyperfilm™, GE Healthcare) for the required time and developed using an X-ograph developer (X-ograph).

2.5.6 Total protein stain of nitrocellulose membranes

Total protein was visualised on the nitrocellulose membranes with Ponceau S. The membrane was fully submerged in Ponceau S staining solution (see Section 2.12.2) for approximately 5 minutes before rinsing the membrane with deionised water. The total protein stained membrane was imaged using the white light settings on the gel dock imager. The Ponceau S stain was then removed completely by washing the membrane several times with PBS.

2.5.7 Immunocytochemistry (ICC)

Fibroblast monolayers were grown on round (12mm diameter) glass coverslips in a well of a 24-well plate. Fibroblasts were plated at 5 x 10^4 cells per well and cultured overnight at 37°C with 5 % CO_2 in a humidified incubator. The next day, the cells were ~70-80 % confluent and were treated with or without a 5 minute 'pulse' of recombinant porcine TNFα (Thermo Scientific) and fixed at a specified time-point post treatment. To treat cells, the media was removed and replaced with 0.5 ml of media supplemented with recombinant porcine TNFα (10 ng/ml) and incubated at 37°C for 5 minutes. Immediately after the incubation period the TNFα media was aspirated before washing the cells three times with 1ml of fresh media. Finally, 0.5 ml of media (without TNFα) was added to the cells for the remaining time in culture at 37°C. Once the desired time-point was reached post-TNFα stimulation, the cells were rinsed with PBS before fixing for 20 minutes in 4 % Paraformaldehyde (PFA) at room temperature. To permeabilise the cells, 100 µl of 0.1 % Triton X-100 was added to each well and incubated for 10 minutes at room temperature. Cells were then washed three times with 1 ml PBS before incubating with 500 µl of blocking buffer (1 % BSA, PBS) for 1 hour at room temperature. The primary antibody was diluted in blocking buffer and incubated on the coverslips for 1 hour at room temperature. The primary antibody was subsequently washed off by rinsing three times in 1 ml of PBS. The appropriate Alexa Fluor

conjugated secondary antibody was incubated on the coverslips for 1 hour at room temperature before washing with three rinses of 1 ml of PBS. To prepare slides, 15 µl of ProLong® Gold Antifade Mountant with DAPI (Molecular Probes™) was dispensed onto a microscopy slide before carefully placing a coverslip (cells side down) onto the mountant and pressed gently to ensure the coverslip was flat against the slide. The slides where left to dry overnight in the dark and then transferred to 4°C in the dark until analysis. Slides were stored for no longer than 1 week before viewing and imaging using the inverted Zeiss LSM 710 confocal microscope.

2.6 ASFV and cell culture

All of the following work with African Swine Fever Virus (ASFV) was carried out within the SAPO4 restricted area of The Pirbright Institute, Surrey.

2.6.1 Virus isolates

Initial stocks of both virulent isolate, Benin 97/1, and non-pathogenic isolate, OURT 88/3, were provided by Dr David Chapman, Pirbright. The Benin 97/1 isolate was first isolated from samples submitted during an ASFV outbreak of domestic pigs in West Africa in 1997 and the OURT 88/3 isolate was first isolated from *Ornithodoros erraticus* ticks from a pig farm in Portugal in 1988 (as described in Chapman et al., 2008).

2.6.2 Titration of ASFV by Immunofluorescence

To titrate viral stocks, matured porcine bone marrow cells were infected with viral stock dilutions. Bone marrow cells were extracted from a 6-week old piglet (see Section 2.4.6) and plated out on a 96-well plate at 1 x 10^6 cells per well and incubated for 4 days in a humidified incubator at 37°C with 5 % CO_2. After the initial incubation period of 4 days, 10-fold serial dilutions of the viral stock, from 10^{-1} to 10^{-8}, were set up in culture medium on a 96-well plate with each dilution performed in triplicate. The media was removed from the 96-well plate containing the bone marrow cells using a multi-channel pipette and replaced with 100 µl of each virus dilution. The cells were then incubated with the virus for three days in a humidified 37°C incubator with 5 % CO_2. After incubation, the supernatant was removed, the cells washed once with 200

µl PBS and then fixed by submerging the plate in 4 % PFA for 1 hour. The cells were then washed in PBS three times before adding 0.2 % Triton X-100 (in PBS) for 5 minutes at room temperature and washed again three times with PBS. The primary antibody, anti-vp72 (see Section 2.11.2), was diluted in PBS and 50 µl dispensed into each well. Following a 1 hour incubation period with the primary antibody at room temperature the cells were washed three times with PBS. 50 µl of anti-mouse 488 Alexa Fluor was then added to each well and incubated in the dark for 1 hour. The cells where then washed three times in PBS before viewing under an inverted UV microscope. The lowest virus dilution to contain a positive cell was recorded and used to calculate the $TCID_{50}$ (median tissue culture infective dose) using the Spearman and Kärber algorithm as described in Hierholzer & Killington, 1996. The $TCID_{50}$ equals approximately 0.69 FFU (focus forming units).

2.6.3 Production of virus stocks

T-175 cm^2 flasks, each containing 40 ml of resuspended porcine bone marrow cells (BMCs) at a concentration of 10^7 cells/ml, were cultured in RPMI medium containing 10 % porcine serum with an ASFV isolate (see Section 2.6.1) at a multiplicity of infection (M.O.I) of 5. The flasks were incubated at 37°C, 5 % CO^2 for three days before the virus was harvested. To harvest the virus, the cells were removed from the surface of the flask by scraping and the media was transferred into a 50 ml tube. To pellet cellular debris, the mixture was centrifuged at 2000 x g for 20 minutes. The supernatant containing virus was collected stored at 4°C until use.

2.6.4 Virus preparation

The virus stocks were partially purified for *in vitro* ASFV infections to remove any cellular contaminants. Firstly, the viral stocks were centrifuged at 6000 x g at 4°C for 10 minutes to pellet cellular debris. The supernatant was then loaded into each sterilised centrifuge tube and weighed in the buckets for Beckman SW 32Ti centrifuge rotor. Once balanced, the virions were pelleted at 170,000 x g for 1 hour at 4°C. The supernatant was discarded and the viral pellet was resuspended in 2 ml of PBS before passing through a 0.8 µM syringe filter to remove any large debris. Once filtered the sample was diluted to a final volume of 20 ml with PBS and then concentrated using

a centrifugation spin column with 100 kDa molecular weight cut off (Vivaspin® 20 concentrator). The 20 ml sample was loaded into the Vivaspin® 20 column in a swing-out rotor at 6000 x g for 1 hour at 4°C. The sample was brought up to 20 ml again with fresh PBS and this process was repeated three times. On the final 6000 x g centrifugation step the volume was left to reduce to 1-2 ml in the Vivaspin column which was aliquoted as the concentrated virus stock.

2.7 RNA techniques

2.7.1 RNA extraction from mammalian cells

RNA was isolated from cells using TRIzol® Reagent (Life Technologies), following the manufacturer's instructions. All centrifugation steps were carried out at 12,000 x g for 15 minutes at 4˚C unless otherwise stated.

Cells for RNA extraction were grown in monolayer cultures in 6-well plates until ~80 % confluent. Cells were washed with chilled PBS before lysing directly in the plate by adding 1 ml of TRIzol reagent per well. The TRIzol cell lysate was mixed in the well by pipetting up and down several times before transferring into a pre-labelled RNase free 1.5 ml tube and incubated at room temperature for 5 minutes. 200 µl (0.2 volumes) of chloroform was added to the lysate before vortexing on the highest setting for ~15 seconds and then incubating on ice for 10 minutes. After incubation, the samples were centrifuged to separate the mixture into organic phase and aqueous phase. The aqueous top layer (~400 µl), containing the RNA, was then transferred into a new RNase free 1.5 ml tube containing 500 µl of isopropanol and mixed via pipetting. Following incubation at room temperature for 10 minutes, the samples were centrifuged to pellet precipitated RNA, the supernatant was discarded. The RNA pellet was washed with 500 µl of nuclease-free 85% ethanol and the samples centrifuged. The supernatant was removed carefully with a pipettor and the RNA pellet was left to air dry for 5-10 minutes before resuspension in 20 µl of nuclease free water. The concentration of RNA was then quantified using the Nanodrop (see Section 2.1.5). RNA samples were transferred to -80°C for storage.

2.7.2 cDNA synthesis

Before cDNA synthesis, RNA was treated with DNase to remove any contaminating DNA. The TURBO DNase kit (Life Technologies) was used following the manufactures guidelines. 2-5 µg of RNA was added to 5 µl 10X TURBO DNase buffer, 5 µl of DNase I buffer, 1 µl of DNase I and nuclease free water to a volume of 50 µl. After an incubation at 37°C for 20 minutes, 5.5 µl of DNase inactivation reagent was added and the reaction incubated at room temperature for 5 minutes mixing occasionally. The samples were subsequently centrifuged at 10,000 x g for 1.5 minutes before transferring the supernatant containing RNA into a new RNase free tube. The Nanodrop was used to measure RNA concentration (see Section 2.1.5).

cDNA synthesis was carried out using the SuperScriptTM III First-Strand Synthesis System (Invitrogen), the manufacturer's guidelines were followed. 1 µg of RNA was added to 1 µl of 50 µM oligo (dt), 1 µl of 10 mM dNTP mix and made up to a final volume of 10 µl in nuclease-free water. The reaction was incubated at 65°C for 5 minutes and then placed on ice for a 1-5 minutes. The cDNA synthesis mastermix was prepared adding each component in the following order, for one reaction; 2 µl of 10X RT buffer, 4 µl of 25 mM MgCl2, 2 µl of 0.1 M DTT, 1 µl of RNaseOUT (40 U/µl) and 1 µl of SuperScript III RT (200 U/µl). 10 µl of cDNA mastermix was added to the 10 µl RNA/primer mixture before incubating at 50°C for 50 minutes. The reactions were terminated by heating at 85°C for 5 minutes. After cooling the samples on ice, 1µl of RNase H (2 U/µl) was added and incubated at 37°C for 20 minutes. The cDNA was stored at either -20°C or -80°C until use.

2.7.3 Quantitative PCR

In order to compare gene expression between control samples and samples containing RELA mutants, quantitative real time PCR (qPCR) was used. All of the following procedures were carried out on ice unless otherwise stated.

All cDNA samples were diluted 1:20 before performing qPCR. Each reaction contained the following components; 12.5 µl of Platinum® SYBR® Green qPCR SuperMix-UDG (Invitrogen), 0.1 µl of ROX reference dye, 2 µl of each 5 µM primer, 5 µl of diluted cDNA sample plus nuclease free water to a final volume of 25 µl. A

master-mix was made up, containing all components except the cDNA sample, and 20µl was pipetted into each well of a 96-well Thermo fast PCR plate before adding 5 µl of each cDNA sample. A no reverse-transcriptase control (see Section 2.7.2) and a no cDNA template control (5 µl of nuclease-free water) were also included for each primer set. The plates were sealed with strip caps and centrifuged for 1 minute at 6000 x g before the plate was read on an Mx3005P qPCR machine. Set-up and analysis was performed using the MxPro software (Stratagene). The qPCR programme was as follows; 50°C for 2 minutes; 95°C for 2 minutes; then 40 cycles of 95°C for 15 seconds, 60°C for 1 minute; then 95°C for 1 minute, 60°C for 30 seconds, 95°C for 30 seconds. The gene expression was normalised to appropriate porcine reference genes (details stated in experimental description) and the comparative Ct (cycle threshold) ΔΔCt method used to quantify relative gene expression using the formula: Fold Change = $2^{-\Delta(\Delta Ct)}$, where ΔCt = Ct (target) – Ct (reference) and Δ(ΔCt) = ΔCt, (treatment) – ΔCt (control).

2.8 CRISPR construction and validation

2.8.1 Short guide RNA (sgRNA) oligonucleotide design

Short guide RNAs (sgRNAs) were designed to cut close to the codon encoding S531 of *Sus scrofa* RELA for the targeted HDR-mediated exchange from domestic pig to warthog sequence, S531P. All guides were designed based on the requirements of the CRISPR-Cas system derived from *Streptococcus pyogenes*; these include that a target 20-nt sequence is immediately followed with 5'-NGG protospacer adjacent motif (PAM). The PAM sequence is essential in preceding the 20-nt genomic target DNA locus however is not included as part of the sgRNA sequence itself.

There are a variety of online tools available for designing suitable sgRNAs, these use algorithms which rank candidate guides based on predictions of on-target cutting efficiencies and potential off-target sites. The online design tools used for the design of the RELA sgRNAs included; CCTop (CRISPR/Cas9 target online predictor (Stemmer et al, 2015)), which ranks all candidate sgRNA target sites according to their off-target quality and Cas-Designer (Park et al, 2015) which ranks guides based on predictions of maximal on-target knockout efficiency and low off-target effects. Four

sgRNAs were selected based on the list rankings generated for the design tools and that had the closest proximity to the target codon.

2.8.2 Preparation and cloning of short guide RNA (sgRNA) oligonucleotides into pSpCas9(BB)-2A-GFP (PX458)

Oligonucleotides (oligos) containing the sgRNA sequences were cloned into pSpCas9(BB)-2A-GFP (PX458; Feng Zhang Lab; Addgene ID 48138) according to published methods (Ran et al, 2013). This plasmid expresses the Cas9 from *S.pyogenes* with a 2A-GFP fusion and contains the human U6 (hU6) promoter to drive expression of the sgRNA (see vector map in Appendix A). The hU6 promoter requires a purine (usually guanine) to be directly adjacent to it to initiate transcription, thus an extra guanine (G) was added to the 5' end of the selected guide if necessary. Oligos were ordered from IDT with the addition of BbsI overhangs to clone the guide sequence into the plasmid in the correct orientation (Figure 2.3).

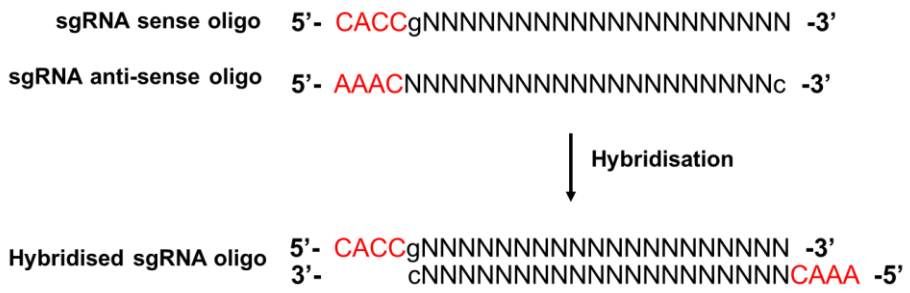

Figure 2.3 sgRNA oligonucleotide design for cloning into PX458. N respresents any nucleotide. Additional BbsI overhangs are shown in red and hU6 promoter guanine requirement shown in lower case.

Lyophilised oligonucleotides were resuspended in nuclease-free TE buffer to a final concentration of 100 µM. To prepare sgRNA oligos for cloning they were annealed in the following reaction; 0.5 µl of sgRNA sense oligo (100 µM), 0.5 µl sgRNA anti-sense (100 µM), 0.5 µl 10X NEB Buffer 2 and nuclease free water to a total volume of 5 µl in a PCR strip tube. The oligos where annealed in a thermocycler at 37°C for 30 minutes, 95°C for 5 minutes, ramping down to 25°C at 5°C min¯1. The annealed oligos were diluted 1:100 in TE before cloning into PX458.

To clone the sgRNA oligos into PX458 a ligation reaction was prepared; 0.5 µl of PX458 (100 ng/µl), 0.5 µl of diluted annealed oligo, 1 µl of 10X Tango buffer (Thermo

Scientific), 0.5 µl of DDT (10 mM), 0.5 µl of ATP (10 mM), 0.5 µl of FastDigest BbsI (Thermo Scientific), 0.25 µl of T7 ligase and nuclease free water to a final volume of 10 µl. The ligation reactions where incubated in a thermocycler running the following program; 6 cycles of; 35°C for 5 minutes; 21°C for 5 minutes. The ligation reaction was then treated with plasmid-safe nuclease to digest any remaining linearized DNA. For plasmid-safe treatment the following components were added to the ligation reaction (10 µl); 2 µl of 10X plasmid safe buffer, 2 µl of ATP (10 mM), 1 µl of plasmid safe nuclease and nuclease-free water to give a final reaction volume of 20 µl. The plasmid-safe reactions were incubated in a thermocycler at 37°C for 30 minutes followed by 70°C for 30 minutes. 2 µl of the plasmid-safe treated plasmid (2.5 ng/µl) was transformed into Top10 competent cells (see Section 2.2.2). Colonies were picked the next day for bacterial PCR (see Section 2.8.3) and maxi-prep cultures (see Section 2.2.4).

2.8.3 Bacterial PCR

A PCR was performed directly from bacterial colonies to check that ligated oligonucleotides had been successfully cloned into PX458. Three colonies were selected from each transformation plate to initiate mini-cultures and perform bacterial PCRs. Each colony was picked with a sterile pipette tip and spotted onto the bottom of a PCR tube for bacterial PCR and subsequently used to inoculate 125 µl SOB (mini-culture). The mini-culture was incubated in a 37°C shaking incubator during which the bacteria PCR was carried out. The following reagents where added to the bacterial PCR tube; 0.5 µl of primer oSL35 (20 mM) which binds PX458 sequence downstream of the oligo insert, 0.5 µl of the appropriate sgRNA sense oligo (20 mM), 12.5 µl of 2X DreamTaq Green DNA polymerase (Thermo Scientific) and nuclease free water to give a total reaction volume of 25 µl. The reactions were placed in a thermocycler with the following PCR program: 95°C for 60 seconds; 35 cycles of 95°C for 30 seconds, 50°C for 30 seconds and 72°C for 30 seconds; 72°C for 5 minutes; before being held at 10°C after completion of the program. The presence of insert was confirmed by resolving 5 µl of this PCR product on a 1 % agarose gel (see Section 2.1.3). Once successful cloning was confirmed one of the positive bacterial cultures was selected to continue to maxi-prep culture (see Section 2.2.4).

CRISPR preparation	Oligo sequences (5'→3')
sgRNA sense oligo #1	CACCgACCAACGGTCTCCTCTCGG
sgRNA antisense oligo #1	AAACCCGAGAGGAGACCGTTGGTc
sgRNA sense oligo #2	CACCGCTCACCAACGGTCTCCTCt
sgRNA antisense oligo #2	AAACAGAGGAGACCGTTGGTGAGC
sgRNA sense oligo #3	CACCGAAGTCTTCGTCCCCCGAG
sgRNA antisense oligo #3	AAACCTCGGGGGACGAAGACTTC
sgRNA sense oligo #4	CACCgCACCAACGGTCTCCTCTCG
sgRNA antisense oligo #4	AAACCGAGAGGAGACCGTTGGTGc
oSL35	GTCAATAGGGGGCGTACTTG

Table 2.1 CRISPR oligonucleotides used in preparation for cloning into plasmid PX458. Bbs1 overhang sequence is highlighted red and additional bases are shown in lowercase.

2.8.4 HDR template oligonucleotides design

Custom single strand oligodeoxynucleotides (ssODNs) were designed to be homologous to the target site with the exception of the desired codon change (encoding S531P) and silent single nucleotide change to interrupt the PAM sequence. The introduction of the S531P SNP also introduced a XmaI restriction site that can be utilised during subsequent RFLP analysis. Four different ssODNs were ordered from IDT; these included sense and anti-sense versions of a 70-mer and 120-mer containing the described nucleotide changes (Table 2.2).

ssODNs	Oligo sequences (5'→3')
antisense 70mer	CTGGGGGCCTCTGGGCTCACCAACGGTCTCCTCCCGGGAGACGAAG ACTTCTCCTCCATTGCGGACATGG
sense 70mer	CCATGTCCGCAATGGAGGAGAAGTCTTCGTCTCCCGGGAGGAGACC GTTGGTGAGCCCAGAGGCCCCCAG
antisense 127mer	CCCCTGGGGGCCTCTGGGCTCACCAACGGTCTCCTCCCGGGAGACG AAGACTTCTCCTCCATTGCGGACATGGACTTCTCAGCCCTTCTGAGTC AGATCAGCTCCTAAAGGGCTGACACCTGCTCTG
sense 127mer	CAGAGCAGGTGTCAGCCCTTTAGGAGCTGATCTGACTCAGAAGGGCT GAGAAGTCCATGTCCGCAATGGAGGAGAAGTCTTCGTCTCCCGGGAG GAGACCGTTGGTGAGCCCAGAGGCCCCCAGGGG

Table 2.2 single strand oligodeoxynucleotides (ssODNs) used as donor templates to introduce the S531P codon change. Nucleotide changes from wild-type sequence are coloured red and resulting Xma1 restriction site is underlined.

2.8.5 Transfections

Low passage porcine embryonic fibroblasts (PEFs; see Section 2.4.2) were used to test CRISPRs and HDR templates. CRISPR/Cas9 plasmids and HDR templates were delivered into cells using the Neon transfection system (Life Technologies) with 100 µl reaction tips. PEFs were thawed (see Section 2.4.4) and maintained until ~95 % confluent and were subsequently spilt 1:2 and harvested (see Section 2.4.5) for transfection the next day, when they reached ~70-80 % confluent. The PEFs were washed in PBS and counted using a haemocytometer (see Section 2.4.10) prior to resuspending in buffer R at 6 x 10^6 cells/ml. 2 µl of CRISPR/Cas9 plasmid DNA (1 µg/µl) with or without 2 µl of 100 µM HDR ssODNs was added to 6 x 10^5 resuspended cells to make up each transfection mixture. To transfect the cells, each mixture was electroporated using the following parameters: 1800 V; 1 pulse with 20 ms width. After transfection the cells were split into two wells of a 6-well plate containing DMEM medium with 10 % FBS and expanded for 48 hours in a humidified 37°C incubator with 5 % CO_2. After incubation, the PEFs were harvested and resuspended in 200 µl of PBS for sorting with the FACS Aria machine (BD Biosciences) using the FACSDiva software (BD Biosciences). The PX458 expresses Cas9 linked to eGFP, therefore, to positively select transfected cells, they were sorted based on their GFP fluorescence into a 1.5 ml nuclease-free tube for analysis. Sorted cells were lysed for

PCR amplification and analysis of target locus with T7 assay and/or Xma1 digestion (see Section 2.8.7).

2.8.6 Lysing cells for PCR

Cells were lysed at a density of ~5000 cells per 1 µl of PCR compatible lysis buffer (1X). Cells were washed once in PBS prior to addition of PCR compatible lysis buffer (see Section 2.12.1). To completely lyse cells, samples were incubated in a thermocycler at 55°C for 55 minutes before 95°C for 15 minutes and then held at 10°C. 2 µl of each lysate was used for a 25 µl PCR reaction (see Section 2.1.2) using PCR primers for RELA (see Section 2.11.1) that span a 308 bp region (on WT sequence) spanning the sgRNA target locus.

2.8.7 T7 assay and RFLP analysis

T7 endonuclease I (NEB) was used to detect on-target CRISPR/Cas9 events due to its ability to detect and cleave miss-matched DNA. After PCR amplification on DNA from transfected cells, 2 µl from each PCR was run on a 1 % agarose gel to estimate DNA concentrations. 200 ng of PCR product from each PCR reaction was denatured and reannealed in a thermo cycler program to allow the formation of heteroduplex DNA. The denature and reanneal program was as follows; 95°C for 10 minutes; then decreasing the temperature to 85°C at a rate of -2°C/sec; 85°C for 1 minute; decreasing the temperature to 75°C at a rate of 0.3°C/sec; 75°C for 1 minute, decreasing the temperature to 65°C at a rate of 0.3°C/sec; 65°C for 1 minute, decreasing the temperature to 55°C at a rate of 0.3°C/sec; 55°C for 1 minute decreasing the temperature to 45°C at a rate of 0.3°C/sec; 45°C for 1 minute decreasing the temperature to 35°C at a rate of 0.3°C/sec; 35°C for 1 minute, decreasing the temperature to 25°C at a rate of 0.3°C/sec; 25°C for 1 minute, decreasing the temperature to 4°C at a rate of 0.3°C/sec; 4°C hold. After reannealing, 1 µl of T7 endonuclease was added to each tube, mixed well and incubated at 37°C for 15 minutes. Immediately after incubation, the reactions were resolved on a 2 % agarose gel. The resulting cleaved and full-length PCR products were visualized and imaged using a UV Transilluminator Gel Dock. Image J software was used to analyse the cutting efficiency (as described in Guschin et al, 2010).

HDR was detected restriction fragment length polymorphism (RFLP) analysis with XmaI (NEB). 200 ng of the PCR reaction (described in Section 2.4.6) was used in a restriction digest containing 1 µl of XmaI, 2 µl of 10X CutSmart® buffer (NEB) and nuclease free water to a final volume of 20 µl. Reactions were incubated at 37°C for 1 hour before resolving on a 2 % agarose gel.

2.8.8 Microinjection of porcine embyros

Preparation and transfer of embryos was carried out as described in Lillico et al (2013) by the staff at The Large Animal Unit, Dryden Farm, Roslin Institute. All embryo microinjections were carried out by Dr Simon Lillico.

2.8.9 *In vitro* analysis of embyros

Embryos were cultured for 6-8 days post-injection for *in vitro* analysis, which was carried out by Claire Neil. All embryos that reached blastocyst stage in culture were collected and transferred individually to PCR tubes and stored at -20°C for future analysis. Embryos were lysed for PCR amplification (see Section 2.1.2). To digest an embryo, 10 µl of embryo digestion buffer (see Section 2.12.1) was added to the PCR tube and then incubated at 55°C overnight before heating at 95°C for an additional 10 minutes. 5 µl of the digested embryo product was used per 25 µl PCR reaction (see Section 2.1.2). The PCR product was then prepared for sequencing (see Section 2.1.6) and analysis of sequence data was carried out on Lasergene Software (DNASTAR).

2.9 Statistical Analysis

Data was analysed using Student t-test. All of the results presented display the mean and error bars represent the standard error of the mean (S.E.M). Analysis was performed using Microsoft Excel. A probability (p) value of less than 0.05 was considered statistically significant.

2.10 Computer software and online resources

Online sgRNA design tools included CCTop (CRISPR/Cas9 target online predictor) and Cas-Designer:

http://crispr.cos.uni-heidelberg.de/
http://www.rgenome.net/cas-designer/

All primer design was carried out NCBI primer BLAST tool:

http://www.ncbi.nlm.nih.gov/tools/primer-blast/

BLAST searches were performed using NCBI databases:

http://blast.ncbi.nlm.nih.gov/Blast.cgi

DNASTAR Lasergene 9 core suite was used for sequence analysis and alignments.

2.11 Reagents

2.11.1 PCR primers

PCR	Primer sequences (5'→3')	Annealing Temperature	Product Size	Notes
RELA	F: GCAATAACACTGACCCGACCGTG	62°C	308bp	Product size for WT RELA sequence
	R: GCAGGTGTCAGCCCTTTAGGAGCT			
qRT-PCR	**Primer sequences (5'→3')**	**Annealing Temperature**	**Product Size**	**References**
B2M	F: ACTTTTCACACCGCTCCAGT	60°C	180bp	Cinar et al, 2012
	R: CGGATGGAACCCAGATACAT			
CCL2	F: CTTGCCCAGCCAGATGCAAT		78bp	
	R: CCGCTGCATCGAGATCTTCTT			
CSF2	F: GCGGCTGTGATGAATGAAACC		94bp	
	R: GCTTGTACAGGTTCAGGCGA			
CXCL2	F: GAAGTTTGTCTCAACCCCGC		79bp	
	R: ATCAGTTGGCACTGCTCTTGT			
CXCL8	F: AGCCCGTGTCAACATGACTT		86bp	
	R: GAACTGCAGCCTCACAGAGA			
CXCL10	F: GAAAGCAATTAGCAAAGAAAGGTCT		90bp	
	R: TCTCCGGCCCATCCTTATCA			
GAPDH	F: ACTCACTCTTCTACCTTTGATGCT		100bp	Erkens et al, 2006
	R: TGTTGCTGTAGCCAAATTCA			
IFNA	F: GGAGATCGTCAGGGCAGAAG		67bp	
	R: CCTGAGTCTGTCTTGCAGGT			
IKBA	F: GAGACTCGTTCCTGCACTTG		74bp	
	R: CTTCACTTGGCGGACCACTT			
IL12	F: CCAAATCTCAGCCAAGGTTACAT		118bp	Gil et al, 2007
	R: TAGAACCTAATTGCAGGACACAGATG			
IL1B1	F: GAAGAAGAGCCCATCATCCTTGA		54bp	
	R: GGCATCACAGACAAAGTCATCA			
IL6	F: GCCCACCAGGAACGAAAGAG		78bp	
	R: CTGAAGGCGCTTGTGGAGA			
NFKB1	F: CACTGAAGCCATTGACGTGAT		143bp	
	R: CATCCCGGAGCTCGTCTATTT			
NFKB2	F: TGGTAGCTGGAAAGGTGTCG		105bp	
	R: TGTTTCCCCGGAGTTTCAGG			
PPIA	F: ACGGGTCCTGGCATCTTG		68bp	Gil et al, 2007
	R: AAATGAAAAACTGGGAACCGTTT			
RBL4	F: AGGAGGCTGTTCTGCTTCTG		185bp	Cinar et al, 2012
	R: TCCAGGGATGTTTCTGAAGG			
REL	F: CTGTGGCAGGATTGTGGAGT		116bp	
	R: ACTGCACCATGAGAAAACAAGT			
RELA	F: CAGAAAGAGGACATCGAGGTGTA		72bp	
	R: TCGGCTTGTGAAAAGGAGC			
RELB	F: CCCGGCACAGCTTTAACAAC		92bp	
	R: GTCGATGCCCAGCTGAATCT			
TNF	F: GGCCCAAGGACTCAGATCAT		82bp	
	R: CTGTCCCTCGGCTTTGACAT			
TNFAIP3	F: AAAACGAATGGGGACGGGAA		79bp	
	R: GCACCAAGTCTGTGTCCTGA			
VCAM	F: ACGTGTGCGAGGGAGTTAAT		75bp	
	R: CCCTGGGAGCAACTTGAACA			

Table 2.3 All PCR primers used in this thesis.

2.11.2 Antibodies

			Dilution (1 / x)	
Primary Antibodies	**Supplier**	**Species**	**ICC**	**WB**
α-Tubulin	Thermo Scientific (62204)	Mouse	*	20000
C-Rel	Santa Cruz (sc-70)	Rabbit	*	500
IkB-α	Abcam (ab32518)	Rabbit	*	1000
Lamin A+C	Abcam (ab8984)	Mouse	*	500
p50/p105	Santa Cruz (sc-114)	Rabbit	*	500
RelA (C-terminal)	Santa Cruz (sc-372)	Rabbit	*	500
RelA (N-terminal)	Santa Cruz (sc-8008)	Mouse	250	500
RelB	Abcam (ab180127)	Rabbit	*	1000
vp-72	IAH (4H3) (Cobbold et al. 1996)	Mouse	5	*
Seconadry Antibodies	**Supplier**	**Recognises**	**ICC**	**WB**
Alexa Fluor 488	Life Technologies (A-11001)	Mouse	500	*
Alexa Fluor 596	Life Technologies (A-11012)	Rabbit	500	*
Mouse Immunoglobulins HRP	Dako (P0447)	Mouse	*	1000
Rabbit Immunoglobulins HRP	Dako (P0446)	Rabbit	*	1000

Table 2.4 Antibodies used in this thesis for immunocytochemistry (ICC) and western blots (WB).

2.12 Buffers and solutions

2.12.1 DNA techniques

Luria-Bertani (LB) Broth: 1 % (w/v) Bacto Tryptone, 0.5 % (w/v) Bacto Yeast Extract and 125 mM NaCl made up with deionised water, this solution was then autoclaved on liquid cycle for 20 minutes at 15 psi before use.

LB Agar: 1 % (w/v) Bacto Tryptone, 0.5 % (w/v) Bacto Yeast Extract, 125 mM NaCl and 1.5 % sugars plus 15 g/L of agar made up with deionised H_2O, this solution was then autoclaved as mentioned above.

Super Optimal Broth (SOB) medium: 2 % (w/v) Bacto Tryptone, 0.5 % (w/v) Bacto Yeast Extract, 10 mM NaCl, 2.5 mM KCl, 10 mM MgCl2, 5 mM MgSO4 made up in distilled water, the solution was then autoclaved as previously mentioned.

Super Optimal Broth with Catabolite repression (SOC) medium: 2 % (w/v) Bacto Tryptone, 0.5 % (w/v) Bacto Yeast Extract, 10 mM NaCl, 2.5 mM KCl, 10 mM $MgCl_2$, 10 mM $MgSO_4$, 20 mM glucose was made up in distilled water, the solution was autoclaved before the addition of glucose. The glucose was filter sterilized by passing a 1M solution through a 0.2 µM filter before use.

Tris-acetate-EDTA TAE (50X) Buffer: For 1 litre of 50X TAE stock solution, 242 g of Tris, 57.1 ml glacial acetic acid, and 100 ml of 0.5 M EDTA (pH 8.0) solution was made up to final volume of 1 litre with deionised water. This stock solution is diluted 50:1 with deionised water to make a 1X working solution (40 mM Tris, 20 mM acetic acid, and 1 mM EDTA)

Tris-EDTA (TE) Buffer: 10 mM Tris hydrochloride, 1 mM EDTA made up in deionised H_2O.

5X PCR compatible loading buffer (5X Fi-RED): 10 % (v/v) Ficoll-400, trace of cresol red dye made up in nuclease-free water in sterile conditions, the solution was filtered through 0.22 μM filter before use.

RF1: 100 mM RbCl, 50 mM $MnCl_2$, 30 mM potassium acetate, 10 mM $CaCl_2$, 15 % (w/v) glycerol, made up in deionised water and adjusted to pH 5.8 with acetic acid, this solution was filter sterilized with 0.22 μM filter and stored at 4°C until use.

RF2: 10 mM MOPS, 10 mM RbCl, 75 mM CaCl2, 15 % (w/v) glycerol, made up deionised water and adjusted to pH 6.8 with 100 mM NaOH, this solution was filter sterilized with 0.22 μM filter and stored at 4°C until use.

PCR compatible lysis buffer (1X): 10 mM Tris-Cl pH 8.0, 2 mM EDTA, 0.45 % (v/v) Triton-X-100, 0.45 % (v/v) Tween-20 and 200 μg/ml Proteinase K made up in nuclease-free water. The solution without Proteinase K was kept at room temperature and Proteinase K was added immediately before use.

Embyro digestion buffer (1X): 50 mM KCl, 10 mM TrisHCl (pH 8.3), 2.5 mM $MgCl_2$, 0.1 mg/ml gelatine, 0.45 % (v/v) NP-40, 0.45 % Tween-20 and 200 μg/ml of Proteinase K made up in nuclease-free water. The solution without Proteinase K was kept at room temperature and Proteinase K was added immediately before use.

2.12.2 Protein techniques

RIPA cell lysis buffer: 1X RIPA buffer (150 mM NaCl, 1.0 % IGEPAL® CA-630, 0.5 % sodium deoxycholate, 0.1 % SDS, 50 mM Tris, pH 8.0) (Sigma) was kept at 4°C. One PhosSTOP inhibitor cocktail tablet (Roche) and one cOmplete™ mini

EDTA-free protease inhibitor cocktail tablet (Roche) were dissolved in 20 ml of RIPA buffer (Sigma) immediately before use.

Protein Sample buffer: 2X Novex® Tris-Glycine SDS Sample Buffer (ThermoFisher Scientific) was used to diluted with protein samples to prepare them for loading on the gel.

1X Western Running Buffer: 25X Novex® Tris-Glycine Transfer Buffer (ThermoFisher Scientific) was diluted 1:25 with deionised water to give working stock solution.

Ponceau S stain: 0.1 % Ponceau S dye (w/v), 5 % acetic acid (v/v) made up in deionised water.

Tris-Glycine transfer buffer: 25 M Tris, 19 mM glycine, 20 % (v/v) methanol made up in deionised water.

Dulbecco's Phosphate Buffered Saline (PBS): 137 mM NaCl, 10 mM Na_2HPO_4, 2.7 mM KCl, 1.8 mM KH_2PO_4 made up in deionised water and adjusted to pH 7.4 using 1 M HCl.

PBS Tween (PBS-T): 0.05 % (v/v) Tween-20 made up in PBS.

Western blocking buffer: 5 % (w/v) Marvel milk powder made up in PBS-T.

4 % Paraformaldehyde (PFA): 4 % formaldehyde powder (w/v) made up in PBS and adjusted to pH 6.9 using 1 M HCl. To make this solution all steps were carried out in a ventilated hood. Formaldehyde powder was added to PBS in a glass beaker which is heated on hot plate to 60°C and the mixture was stirred with a magnetic stirrer. 1 M of NaOH was added in a dropwise manner to raise pH until PFA was fully dissolved and solution goes clear. Once the solution had cooled, the pH was adjusted if required with 1M HCl and filtered through a 0.45 μm filter membrane to remove any particulate matter. The PFA solution was then aliquoted and stored at -20°C for future use.

Immunocytochemistry blocking buffer: 1 % (w/v) bovine serum albumin (BSA) made up in PBS-T.

2.12.3 Cell culture

100X Antibiotic-Antimycotic (Anti-Anti): Gibco product containing 10,000 units/ml of penicillin, 10,000 µg/ml of streptomycin, and 25 µg/ml of Fungizone™

Porcine Adult Fibroblast (PAF) digestion media: Collagenase type I 0.5 % (w/v; Gibco), 0.2 % (v/v) 100X Anti-Anti, 50 µg/ml Gentamycin (Gibco) made up in DMEM containing high glucose, GlutaMAX™ Supplement and pyruvate (Gibco).

Porcine Embryonic Fibroblast (PEF) digestion media: Collagenase type I 0.25 % (w/v; Gibco), 0.1 % (v/v) 100X Anti-Anti made up in DMEM containing high glucose, GlutaMAX™ Supplement and pyruvate (Gibco).

Porcine Fibroblast outgrowth media: 20 % (v/v) FCS (Gibco), 0.1 % (v/v) 100X Anti-Anti made up in DMEM containing high glucose, GlutaMAX™ Supplement and pyruvate (Gibco).

Complete medium for Fibroblast cultures: 10 % (v/v) FCS (Gibco), 10 units/ml penicillin, 10 µg/ml streptomycin made up in DMEM containing high glucose, GlutaMAX™ Supplement and pyruvate (Gibco).

Complete medium for Macrophage cultures: 10 % (v/v) low-endotoxin FCS (gift from Hume group) supplemented with 10^4 units/ml human recombinant CSF-1 (rhCSF1; a gift from Chiron, Emeryville, CA) made up in RPMI 1640 Medium containing GlutaMAX™ Supplement and HEPES (Gibco).

Red Blood Cell Lysis Buffer (RBC-LB): 10 mM $KHCO_3$, 150 mM NH_4Cl, 0.1 mM EDTA pH8 dissolved in deionised water and filtered through 0.22 µM filter before use.

Embyromax buffer: 10 mM Tris-HCL, pH7.5, 0.1mM EDTA dissolved in nuclease-free water, autoclaved and filtered through 0.22 Mm filter before use.

2.12.4 Histology

Eosin Stock solution: To make up 1 litre of Eosin Stock solution; 10 g of Eosin Y CI 45380 (Sigma) was dissolved in 800 ml of Ethanol with 2.5 ml of 1 % Phoxine B (CI number 45410, Acid Red 92) made up to 1 litre with deionised water.

Eosin working solution: For working Eosin solution, 100 ml of stock solution was added to 200 ml of 70% Ethanol, 1.5ml of Glacial acetic acid and mix thoroughly.

Haematoxylin: Harris haematoxylin (Leica Biosystems)

Scott's tap water substitute: To make up 2 litres of Scott's tap water substitute, 7 g of $NaHCO_3$ and 40 g of $MgSO_4$ was diluted in 2 litres of deionised water.

Acid alcohol: To make Acid alcohol, 5 ml of Hydrochloric acid was added to 995 ml of 70 % Ethanol and diluted in 1:1 with deionised water before use.

Chapter 3 The characterisation of gene editing in porcine RELA

3.1 Introduction

As discussed in Chapter 1, it has been proposed that polymorphisms in porcine RELA have the potential to underlie resilience to African swine fever (ASF; Palgrave et al., 2013). ASF is a highly contagious disease of domestic and feral pigs, caused by infection with African swine fever virus (ASFV). Infection with virulent ASFV isolates results in a rapid onset haemorrhagic fever and death within 5-10 days in the domestic pig. The infected macrophages produce high levels of pro-inflammatory cytokines which is thought to initate the course of the disease (Gomez-Villamandos et al., 1995; Sierra et al., 1996, Salguero et al., 2005; Blome et al., 2013). Characteristics of ASF include lymphocyte and lymphoid tissue depletion, severe disruptions to blood clotting process, and lastly heamarhagic lesions predomainantly in the lymph nodes, kidneys and heart. In contrast with domestic pigs, African wild suid hosts, the bushpig and warthog, show no apparent signs of diease when infected with ASFV (Thomson et al., 1980, Oura et al., 1998). Functional variation between the warthog RELA and domestic pig RELA is hypothesised to underlie the dramatic difference in response to ASFV infection in these two species (Palgrave et al., 2011). RELA encodes for the RelA protein, a member of the NF-κB transcription factor family. The NF-κB transcription factors play a vital role in upregulating immune and inflammatory responses, including many of the pro-inflammatory cytokines indicated in ASF pathology (Zhang et al., 2006, Gomez del Moral et al., 1999, Gomez-Villamandos et al., 2013). This RELA variation was found to alter the NF-κB transcription activity levels *in vitro*; with reduced transcriptional levels for warthog RELA compared to domestic pig RELA (Palgrave et al., 2011).

To test this hypothesis genome editors were developed to target proximal to the identified polymorphic region within porcine RELA (Lillico et al., 2013). This region encodes for the C-terminal transactivation domain (TAD), which is essential for initiating transcription of target genes (Schmitz & Baeuerle., 1991). The developed TALEN editors were directly injected into pig zygotes for the production of RELA-edited animals. At the start of my involvement in this project, the first piglets were

being born from this procedure. The main objective of this chapter was to define the outcome of the genome editing. After initial genotyping was completed, specific RELA-editing events were selected for further characterisation, carried out in cells before phenotyping of animals. These experiments will be detailed in the following section.

3.1.1 Aims

The main aims of this chapter are:

i) To genotype TALEN founder animals and coordinate the breeding of RELA-edited pigs to produce cohorts for further study

ii) To investigate the impact of the RELA trunc mutation on NF-κB signalling in primary fibroblasts

iii) To determine whether RELA trunc pigs display a phenotype, regarding their general physiology, with focus on the lymphoid tissues.

3.2 Results

3.2.1 Genotyping and maintaining RELA-edited pigs

3.2.1.1 RELA editing events identified in founder animals

As part of a collaboration with Recombinetics Inc. TALENs were designed to cut between bases 1458 and 1505 bp of the porcine RELA cDNA (NCBI reference sequence: NM_001114281A; Lillico et al., 2013). At the start of this research project, live piglets were born resulting from zygotes injected with mRNA encoding these TALENs. To identify targeted editing events in these piglets, firstly genomic DNA was extracted from ear biopsy tissue, and a 300 bp sequence flanking the TALEN target site was PCR amplified for direct sequencing (Figure 3.1). The reverse primer was used for DNA sequencing as it provides a longer read sequence before the TALEN target site compared to using the forward primer. In the resulting sequence chromatograms, multiple traces were evident in 5 out of the 41 live piglets, indicating the presence of editing events (Figure 3.2). These five RELA-edited animals are the first live born pigs resulting from genome edited zygotes. A single trace of wild-type RELA sequence was present in the other 36 animals, signifying the absence of editing events. Sequencing chromatograms from two animals, pig 16 and 33, consisted of several overlapping traces indicating multiple events, confirmed by sequencing of cloned PCR products. Three independent editing events were identified in each of these animals. Such genetic mosaicism occurs when gene editing takes place after the zygote has undergone cell division. Two traces of similar signal intensities are displayed both pigs 26 and 34, suggesting that editing occurred only at the one-cell stage. The sequence chromatogram from pig 30 also displays two traces, however, the 4 bp deletion trace appears at a lower intensity compared to the 111 bp deletion trace. This is likely a consequence of the PCR favouring the smaller amplicon size of the large deletion product. In total, eight editing events were identified in the five RELA-edited animals, two of which caused in-frame mutations and six of which caused a frameshift mutation; these frameshifts all resulted in the introduction of premature stop codons (Figure 3.3.d).

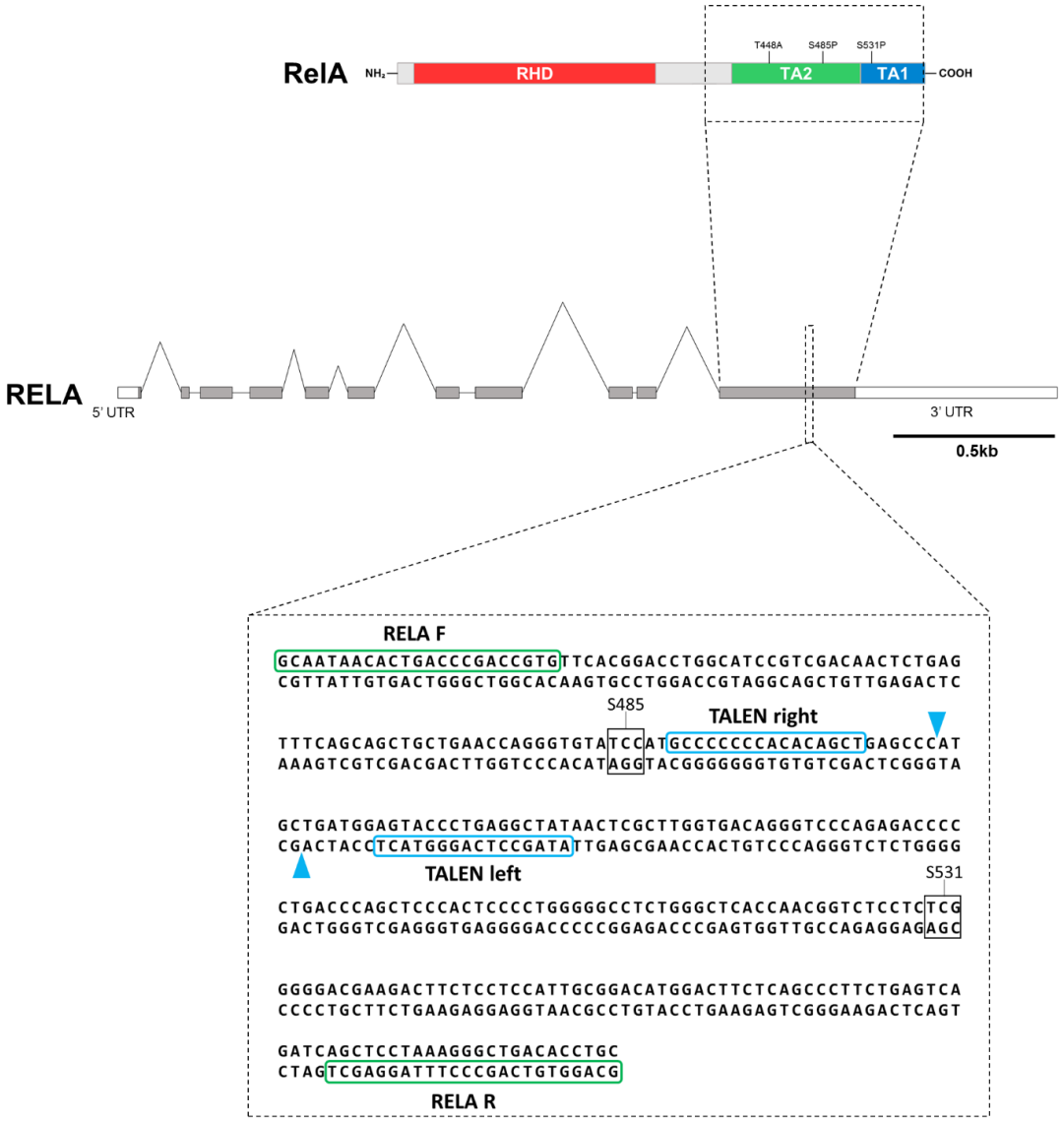

Figure 3.1 Positions of TALEN binding sites and PCR primers on porcine RELA. Schematic diagram showing RelA protein domains, highlighting the protein region that is encoded by the final exon of porcine RELA gene. The porcine RELA gene contains 11 exons that produce a 2.53 kb mRNA transcript. The target region in the final exon is highlighted, and the domestic pig DNA sequence is displayed in the lower panel. Each TALEN binding site is circled with blue and RELA primer sequences circled in green. The predicted TALEN cut sites are indicated with the blue arrows. Codons which encode for the amino acid differences identified between the warthog and the domestic pig RelA are outlined in black.

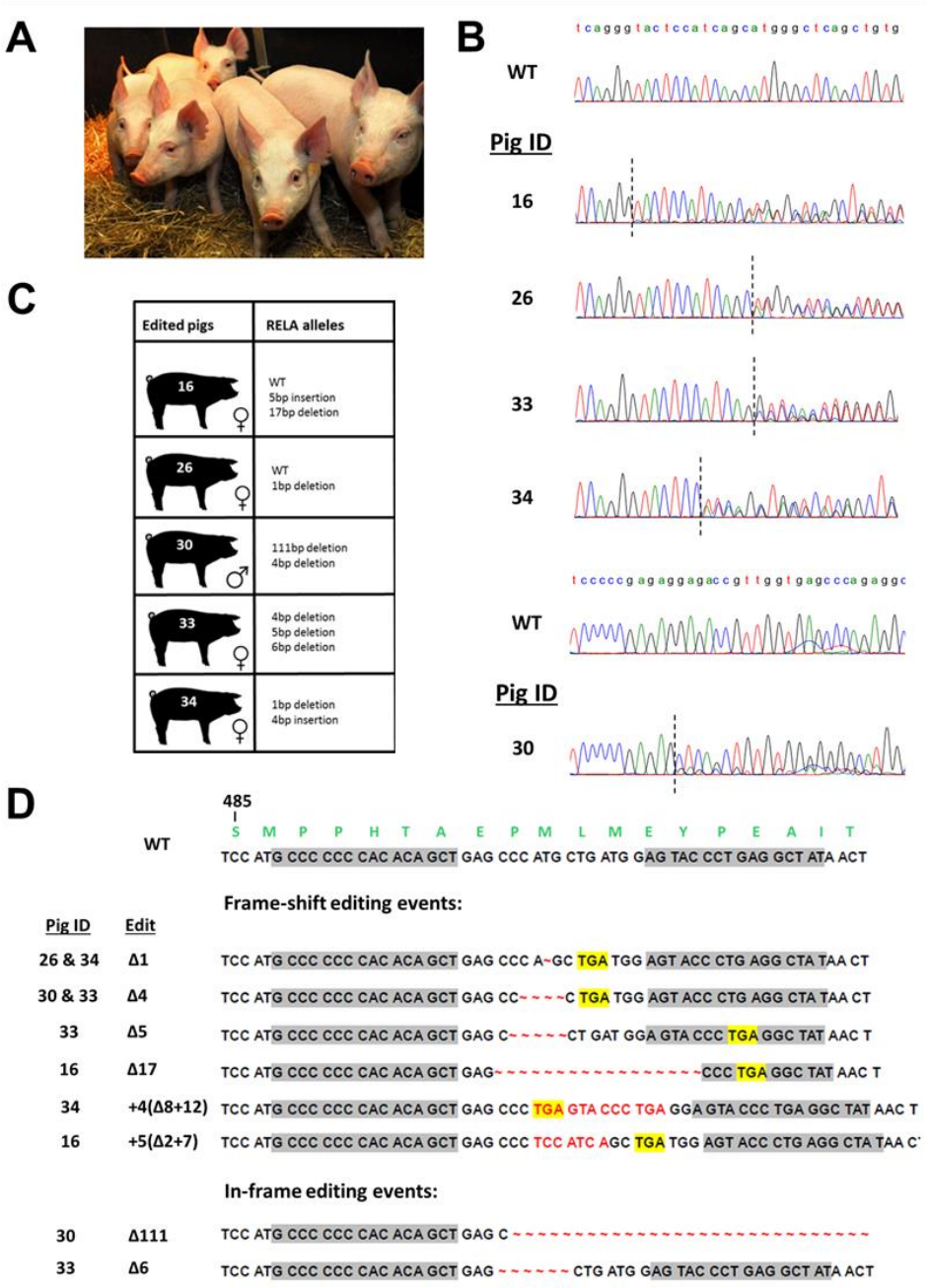

Figure 3.2 Identification of RELA-editing events in founder animals. A) Image of the five RELA-edited piglets B) Sequence chromatograms for a wild-type control and the five RELA-edited animals. The dashed line shows where the sequence diverges from the wild-type sequence, indicating gene editing. Due to the large deletion identified in pig 30, sequence displayed is further downstream than the other edited pigs C) Table displaying the RELA-edited pigs and their corresponding RELA editing events D) All TALEN editing events identified from sequence analysis in the ear biopsy of the five RELA-edited founder animals. The WT control sequence is shown in the top panel with encoding amino acids in green above. TALEN DNA binding sites are highlighted in grey. The edited sequences contain base changes shown in red and in the case of the frame-shift mutations, a premature stop codon, which is highlighted in yellow. Note that sequences shown in B are the results of sequencing using the RELA reverse primer and are the reverse complement of sequences shown in D.

3.2.1.2 Impact of RELA editing on encoding protein sequence

The majority of the indels in the RELA locus cause a frameshift, which in turn generates a premature stop codon. As the RELA gene editing occurs within the final exon, the resulting mRNA transcripts were anticipated to evade the nonsense mediated mRNA decay surveillance and therefore yield a truncated RelA protein.

The genotypes of all five RELA-edited animals and the predicted changes to the encoding protein are shown in figure 3.4. All of the edited pigs contain at least one indel in their coding sequence causing a frameshift event, resulting in the loss of the C-terminal 60 amino acids of wild-type RelA. However, the premature stop codon is not always present at same position in the coding sequence resulting in variety of truncated RelA proteins. Two editing events, the 4 bp deletion and the 4 bp insertion, present in pigs 30, 33 and 34, introduce at stop codon seamlessly at the cut site. These are predicted to result in a RelA protein that lacks the C-terminal 60 residues. The final 60 amino acids encode for the C-terminal region of the TAD encompassing the entire TA1 domain. Editing events that are in-frame include a 111 bp deletion and 6 bp deletion, identified in pig 30 and 33 respectively, result in a RelA protein lacking 60 amino acids in this C-terminal TAD.

To confirm the expression of RELA protein with a truncated C-terminus in these animals, cells were harvested for western blot analysis. Peripheral blood mononuclear cells (PBMCs) were isolated from the blood of each edited animal and one wild-type control. Subsequently, the PBMCs were counted and equal numbers prepared for whole cell lysis. 20 μg of each protein lysate was run per well on an SDS-page and probed with antibody recognising the N-terminal region of RelA, allowing detection of both truncated and wild-type RelA. As expected full length RelA (553 aa, 65 kDa) was detected in the wild-type control and in pigs 26 and 16, both of which maintain a WT allele (Figure 3.3.B). Additional products from the truncated alleles were detected in samples from all five edited pigs (lower bands).

Pig 34 is of particular interest as the genotyping and western blot results have revealed that both of its RELA alleles encode a truncated protein missing the final 60 amino acids at the C-terminal end. As discussed in Chapter 1, *rela*-/- mice have an embryonic lethal phenotype, whereas all the RELA-edited pigs were born healthy and were fully

viable when housed in typical farm environment, suggesting that the truncated RelA protein retains significant functionality despite lacking a highly-conserved domain. Initial studies were carried out on pig 34 and 26, as they provide a bi-allelic and a heterozygote model to investigate the impact of the truncated RelA on NF-κB functionality (Figure 3.4).

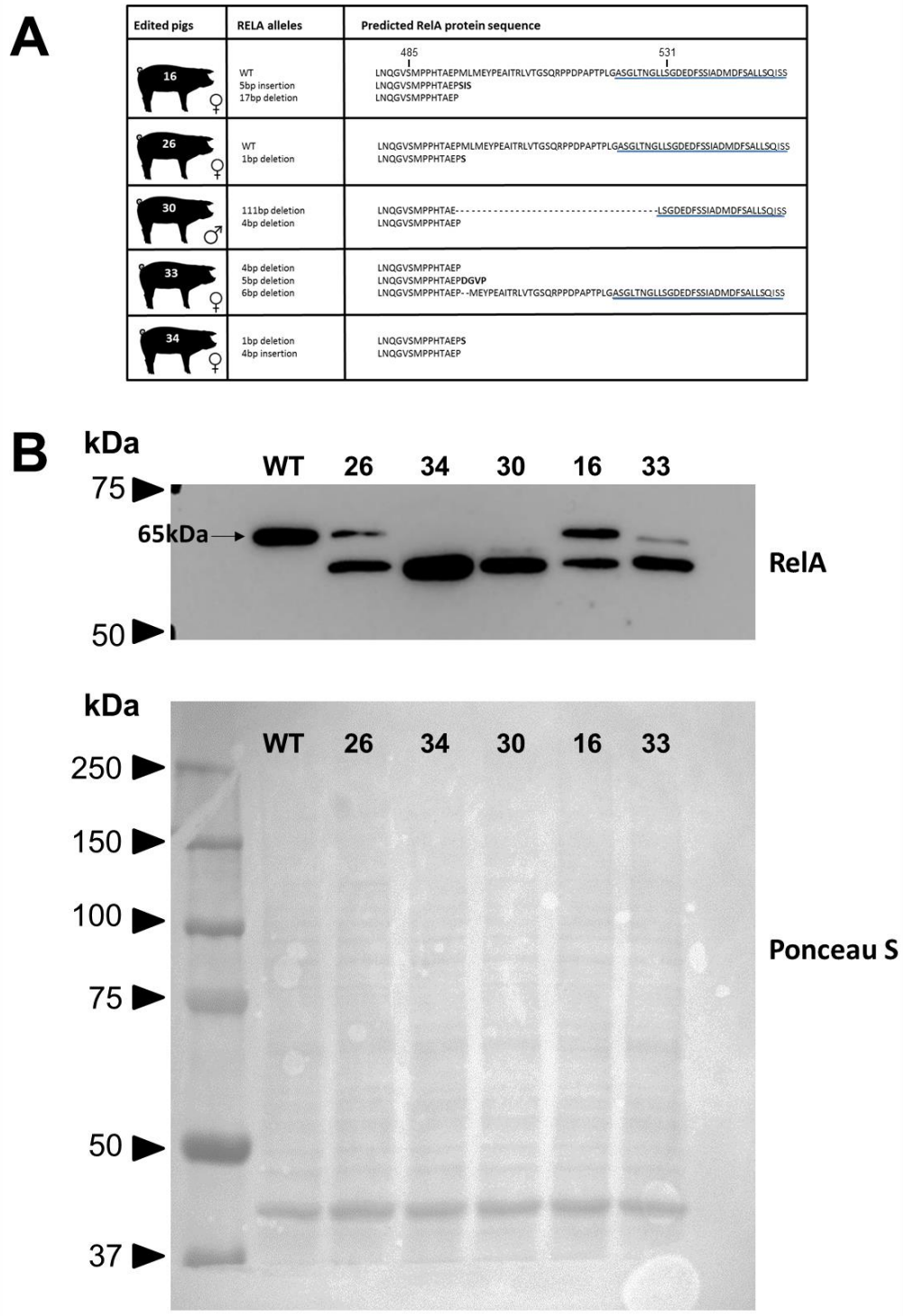

Figure 3.3 Consequences of RELA-editing to the encoding protein in founder animals. A) Table detailing the genotypes of the five RELA-edited pigs and the subsequent changes to the amino acid sequence of RelA. Additional nonsense amino acids are shown in bold, and the polymorphic residues of interest are indicated (S485P and S531P). The TA1 domain is underlined in blue B) Western blot analysis of PBMCs isolated from wild-type control and the five RELA-edited animals. The blot was probed with an antibody recognising the N-terminus of RelA. Before probing the membrane it was stained with Ponceau S to estimate loading.

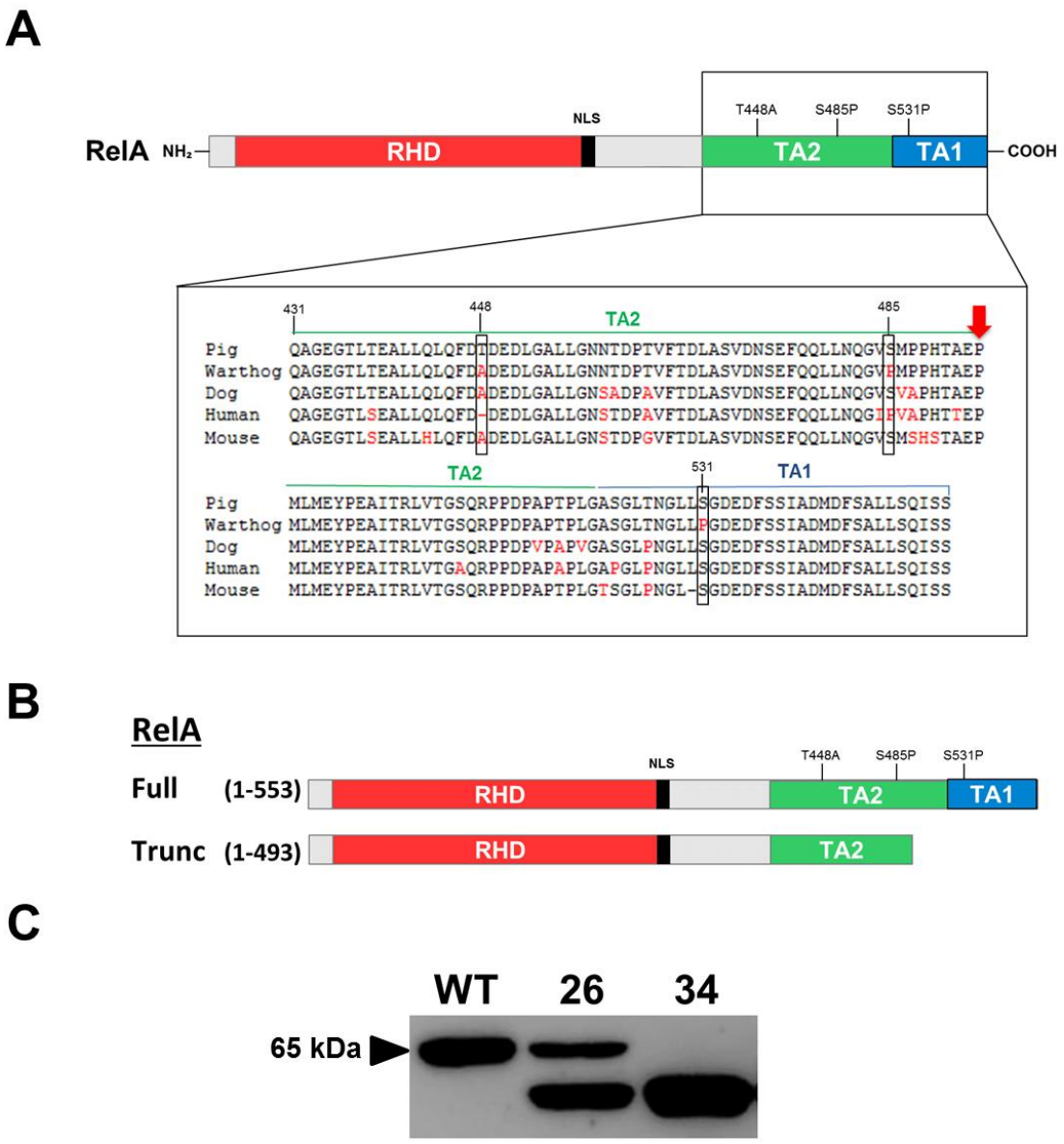

Figure 3.4 The RelA truncation mutant. A) Schematic diagram of RelA protein. The protein sequence of the RelA transactivation domain of the domestic pig (*Sus scrofa*), warthog (*Phacochoerus africanus*), dog (*Canis lupus familiaris*), human (*Homo sapiens*) and mouse (*Mus musculus*) is displayed in panel below. The three polymorphic residues of interest are indicated (T448A, S485P and S531P). The red arrow shows the final amino acid of the RelA truncation mutant. B) Schematic diagram of both full length and the truncated RelA identified within RELA-edited pigs 26 & 34. C) Western blot analysis of PBMCs isolated from wild-type control and RELA-edited pigs 26 & 34, probed with antibody that recognises the N-terminus of RelA. The full-length RelA protein is identifiable as expected at 65 kDa and the truncated RelA protein is identified at approximately 58 kDa.

3.2.1.3 Breeding RELA-edited animals for the production of 2 generations of animals

Once sexually mature, the RELA-edited animals 26, 30 & 34 were selected for a breeding program to generate more animals for this study. Pigs 26 and 30 were mated together to produce a cohort of animals bi-allelic for the RelA truncation for analysis. Pigs 30 & 34 were also bred against unrelated wild-type controls, to produce heterozygous animals. Six female heterozygote F1 offspring were subsequently bred against F1 male heterozygotes to produce the second generation (F2) of animals. Only F1 animals heterozygous for the 4 bp deletion or the 4 bp insertion, derived from founder pigs 30 and 34 respectfully, were selected for breeding (Figure 3.5). These edited-RELA alleles encode for the same truncated RelA protein product, missing the final 60 amino acids of wild-type porcine RelA. In all subsequent sections, the results displayed are from analysis of the F2 animals unless stated otherwise, these are collectively referred to as, homozygote or heterozygote for RELA trunc.

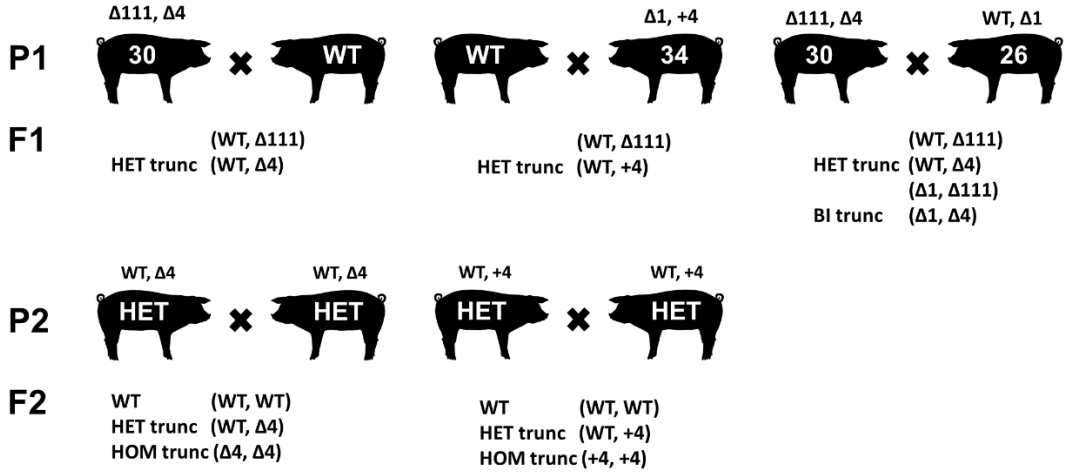

Figure 3.5. Breeding stragey for RELA trunc pigs.

3.2.1.4 Novel genotyping strategy for 2nd generation piglets

A more rapid genotyping strategy was sought for the 2nd gereration of piglets. The highest mortality rate of live-born piglets is observed within the first four days after birth (Marchant et al., 2000). Rapid screening would inform us of the genotype before necessary culls or deaths of young piglets, so we could restrict sampling or further treatment to only those animals of the desired genotypes. All previous screening of piglets was carried out by sequencing PCR products; this takes 3-4 days from acquisition of tissue biopsy to generation of sequence data. A novel genotyping

strategy was designed omitting the requirement for sequencing and instead utilising the CRISPR/Cas9 gene editing system. The customisable component of the CRISPR/Cas9 system, the sgRNA, was designed to identify each of the three parental RELA-alleles (wild-type, 4 bp deletion and the 4 bp insertion) of the second generation. These sgRNAs combined with the Cas9 protein, were intended to be used in an *in vitro* cleavage assay on the RELA PCR product to report on the likely genotype (Figure 3.6.a-b).

In total, four sgRNAs were designed, one to target each of the three individual RELA-alleles, and a fourth intended to identify both the WT and Δ4 alleles. This overlapping sgRNA could be useful for detecting the WT allele in animals known not to contain the Δ4 as a result of breeding design background.

Firstly, to examine if the designed sgRNAs efficiently targeted the intended RELA-allele, a cell transfection assay was carried out. The sgRNA sequence was cloned into plasmid PX458 downstream of a U6 promoter, followed by a CAG driven Cas9-2A-GFP (for detailed description see Section 2.8.2). Each of the CRISPR/Cas9 plasmids were individually transfected into wild-type porcine embryonic fibroblasts (PEFs) using the neon electroporation system. The transfected cells were cultured for 48 hours before extracting genomic DNA for analysis. The RELA PCR was carried out on the genomic DNA to amplify the 308bp region spanning the CRISPR target site. Following a denature/anneal cycle a T7 endonuclease assay was performed on the PCR product to detect mismatches at the target site (Figure 3.6.c). As expected, T7 endonuclease activity was observed in both WT CRISPRs signifying successful editing of WT fibroblasts and not detected in the Δ4 and +4 specific CRISPR transfections (i.e. the target site was absent from WT cells).

After confirming the WT guides activity in cells, we aimed to test these in an *in vitro* cleavage assay. For this assay sgRNA, Cas9 protein and a DNA template are required. PCR amplification of the sgRNA segment from appropriate plasmids using a forward primer designed to contain the T7 promoter was used to produce a template molecule for *in vitro* sgRNA synthesis, carried out as described in Section 2.8.5. 400 ng *in vitro* synthesised WT sgRNA were pre-incubated with 2 μg of Cas9 protein (NEB) in Cas9 Nuclease Reaction Buffer (NEB) for 10 minutes at 21°C to pre-complex sgRNA with

Cas9 protein prior to addition of a DNA template. For the *in vitro* cleavage assay, 200 ng of wild-type RELA PCR product was added to the pre-complexed Cas9/sgRNA solution and incubated for 1 hour at 37°C. The reaction was then resolved on a 1% agarose gel. The resulting gel indicates that the DNA failed to migrate from the well and into the gel. A denaturation step of 72°C post incubations in an attempt to resolve the issue, but no improvement was observed (Figure 3.6.d). All variations on the mixture of components were tried to determine why the DNA did not migrate from the well of this assay, (Figure 3.6.d). The results suggest that a non-specific interaction between the DNA template resulted in this unexpected outcome, although I was unable to find any similar reports in the literature. As a result, this genotyping strategy was abandoned, and direct sequencing was used to confirm the RELA genotypes of each animal.

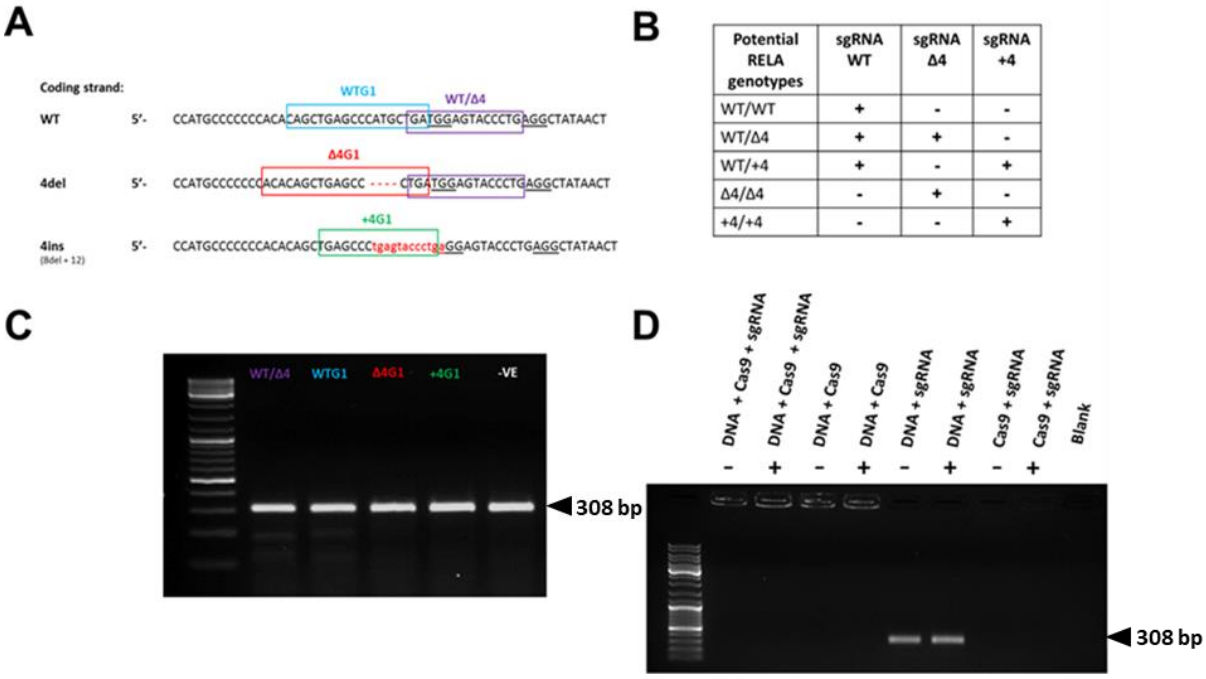

Figure 3.6 Novel genotyping strategy for second generation of animals utilising the CRISPR/Cas9 system. A) The sgRNA target binding sites shown for detection of wild-type or specific RELA-edited allele, with possible PAM sites underlined. Changes from wild-type sequence are shown in red. B) Table displays the possible genotypes of the second generation of piglets and how the sgRNA cutting pattern could decipher the genotype of individual piglets born. C) Gel image of the T7 endonuclease assay conducted on transfected wild-type fibroblasts. D) Gel image of *in vitro* cleavage assay with (+) or without (-) post-denaturation step.

3.2.2 Investigating the impact of truncated porcine RelA on NF-κB signalling in pig fibroblasts

To explore the impact the truncated RelA protein has on the NF-κB pathway fibroblast cells were isolated from wild-type pigs, heterozygote and homozygote RELA trunc pigs. Primary fibroblasts are cells which constitute connective tissue, maintaining structural support of tissues through the production extracellular matrix and collagen. Fibroblasts were chosen as they are sensitive to induction by many cytokines and they are dependent on the RelA subunit to drive the transcription of the majority of NF-κB target genes (Essen et al., 2009, Ouaaz et al., 1999).

Porcine adult fibroblasts (PAFs) where extracted from skin tissue from the ear of individual euthanised pigs and cryopreserved as a fibroblast line labelled with the pig ID and genotype for future use (for methodology see Section 2.4.2). Initial tissue dissociation resulted in the isolation of additional cell types from skin biopsy, such as keratinocytes. While fibroblasts and keratinocytes both adhere to the cell culture vessel, both can be clearly distinguished based on their characteristic morphology and growth patterns. Fibroblasts have elongated, spindle-like bodies and grow aligned and in bundles once confluent, whereas keratinocytes have a polygonal shape and grow in distinct patches. While the presence of serum in the culture media favours growth of fibroblasts, some keratinocyte colonies are usually observered (Shipley et al., 1989). Fortunately we found that the majority of keratinocytes remain adhered to the culture vessel after cell dissociation of fibroblasts cultures using light trypsinisation (Figure 3.7). Thus, all cultures were passaged at least twice to allow for relatively pure fibroblast culture before experimentation. The presence of keratinocytes could not be visually detected in these later cultures.

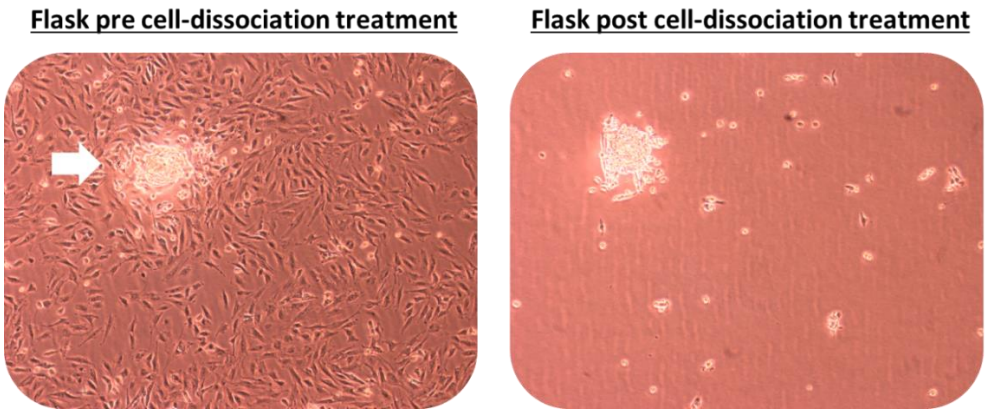

Figure 3.7 Fibroblasts culture pre- and post- cell dissociation treatment. Growth of keratinocyte cells is indicated with the white arrow. The surrounding elongated fibroblast cells are dissociated by the treatment with trypsin.

To induce the NF-κB pathway in the fibroblast cultures, the cells were treated with recombinant porcine TNFα, a well-known activator of the canonical pathway typically involving the RelA-p50 heterodimer (for details on the canonical pathway see Section 1.9.2). Fibroblasts were stimulated with a 5 minute 'pulse' of TNFα (10 ng/ml), and subsquently washed three times with fresh media before culturing for the remaining time, to emulate pulsatile pro-inflammatory signals received *in vivo* (Ashall et al., 2009). The TNFα pulse treatment also permits the investigation into the impact of the truncated RelA on the NF-κB negative feedback loop.

3.2.2.1 Impact on RELA-dependent gene expression

To investigate the impact of the truncation on RelA's transcriptional activity, gene expression analysis was performed on five well-known RelA-dependent target genes in unstimulated and TNFα stimulated fibroblasts. Wild-type control, heterozygous and homozygous RELA trunc fibroblast cell lines were each plated at the same seeding density in four wells. Three wells were treated with TNFα and the other was left as an uninduced control. After the specified time in culture post-TNFα stimulation (i.e. 30, 60 or 120 minutes) the fibroblasts were collected and RNA purified to make cDNA (see Section 2.7.1-2). The level of RelA gene expression was analysed by qRT-PCR (see Section 2.7.3). The expression level was normalised to the mean of Glyceraldehyde 3-phosphate dehydrogenase (GAPDH) and Beta-2-Microglobulin (B2M) expression and the expression levels were calculated relative to the uninduced control for each fibroblast line.

After three independent NF-κB inductions, the homozygous fibroblasts showed significantly lower induced expression of all five RelA-dependent genes compared to wild-type fibroblasts at 30 minutes post-TNFα (Figure 3.8). The heterozygous fibroblasts showed significantly reduced expression in two of the five RelA-dependent target genes, CSF2 and TNF, compared to wild-type at 30 minutes post-TNFα. At 60 minutes post-TNFα a significant reduction of induced gene expression was only identified in IKBA and TNFAIP3 in homozygous fibroblasts. In contrast, a significant increased expression was identified in three out of the five RelA-dependent genes, CSF2, IKBA and TNF, at 120 minutes post-TNFα induction. The overall trend of the gene panel was a retarded upregulation in response to induction in homozygous fibroblasts compared to wild-type cells at 30 and 60 minutes' post-induction. However this later reverted, as at 120 minutes post-induction the relative transcript levels were higher in homozygote cells compared to control cells. These results show that the expression of all five RelA-dependent genes in response to TNFα was altered in cells lacking full-length RelA.

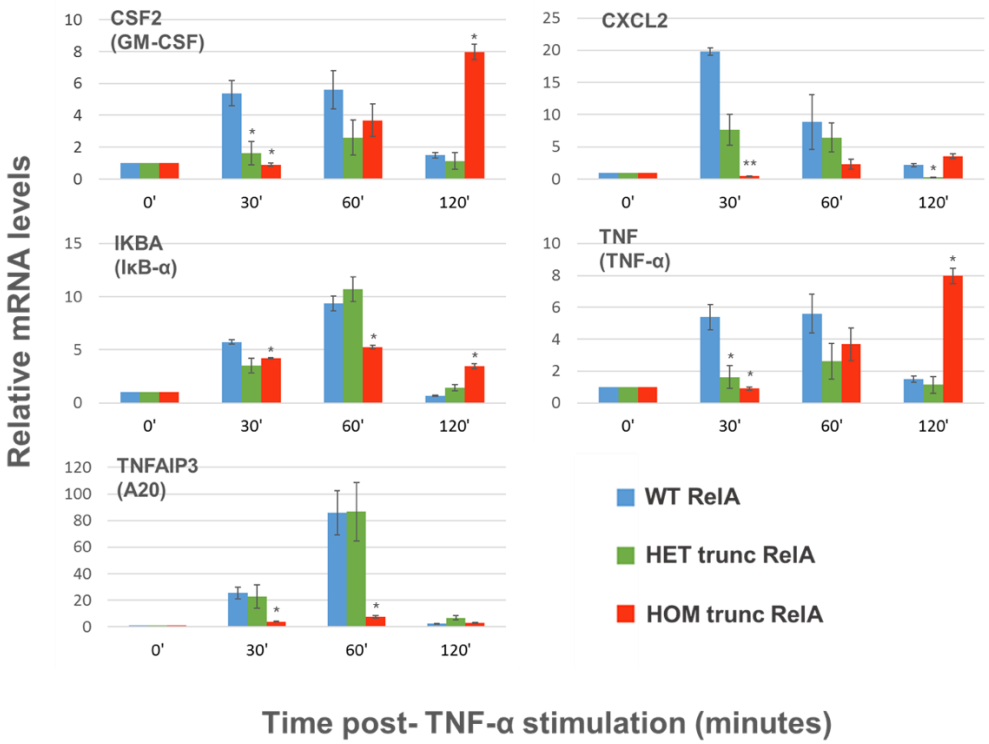

Figure 3.8 Gene expression analysis of RelA-dependent target genes. qRT-PCR analysis of RelA-dependent target genes, CSF2, CXCL2, IKBA, TNF & TNFAIP3 in fibroblasts containing wild-type and truncated RelA induced with TNFα pulse (10 ng/ml). Relative expression was calculated by normalising to the corresponding uninduced fibroblasts. Significant difference was calculated between the wild-type controls and RelA-edited at each specific time post-TNFα using a Student's paired t-test. Significant difference is indicated with black symbol *($p<0.05$) or **($p<0.001$). Error bars represent the standard error of the mean (S.E.M.) from the three independent inductions.

3.2.2.2 Truncated RelA interrupts the NF-κB negative feedback loop

The qRT-PCR analysis revealed that the induced expression of IKBA (IκBα) and TNFAIP3 (A20), which regulate the NF-κB negative feedback loop, were significantly reduced in cells homozygous for the RelA trunc mutation (for details on the NF-κB negative feedback loop see Section 1.9.4.2). IκBα is the key inhibitor of NF-κB and is responsible for the rapid switch off of the NF-κB pathway in TNFα stimulated fibroblasts (Hoffman et al., 2002;). For this reason, the impact of truncated RelA on the negative NF-κB feedback loop was selected for further investigation.

Upon induction with TNFα IκBα is rapidly degraded in a variety of cell types, including fibroblasts (Baldwin., 1996). Furthermore, the upregulation of IκBα by NF-κB allows for the rapid turn off of NF-κB signalling, as IκBα promotes the return of

NF-κB from the nucleus back to the cytoplasm (Sun et al., 1993, Arenzana-Seisdedos et al., 1997). To confirm that the delayed expression of IKBA resulted in the same effect on IκBα protein levels in fibroblasts post-TNFα stimulation, cells were assayed by western blot. Fibroblast cells from wild-type control, heterozygous and homozygous truncated cell lines were each plated into eight wells at the same seeding density. After 24 hours in culture, seven wells were treated with TNFα and the final well was left as an uninduced control. After a specified time in culture post-TNFα stimulation (i.e. 30, 90, 120, 150, 180 or 210 minutes), the fibroblasts were lysed for analysis by western blotting (see Section 2.5.5). 30 μg of each protein lysate was run per well on an SDS-page and probed with antibodies recognising IκBα and α-tubulin (Figure 3.9.a). The level of IκBα was normalised to the α-tubulin level for that sample using densitometric analysis (Figure 3.9.b). The data revealed a delayed response in the rate at which IκBα returned to basal levels in both the heterozygous and the homozygous RELA trunc fibroblasts; as expected this phenomenon was more pronounced in the homozygous fibroblasts. Another noticeable difference was observed in the basal levels of IκBα which were noticeably lower (42.1%) in the homozygous cells when compared to the wild-type control fibroblasts.

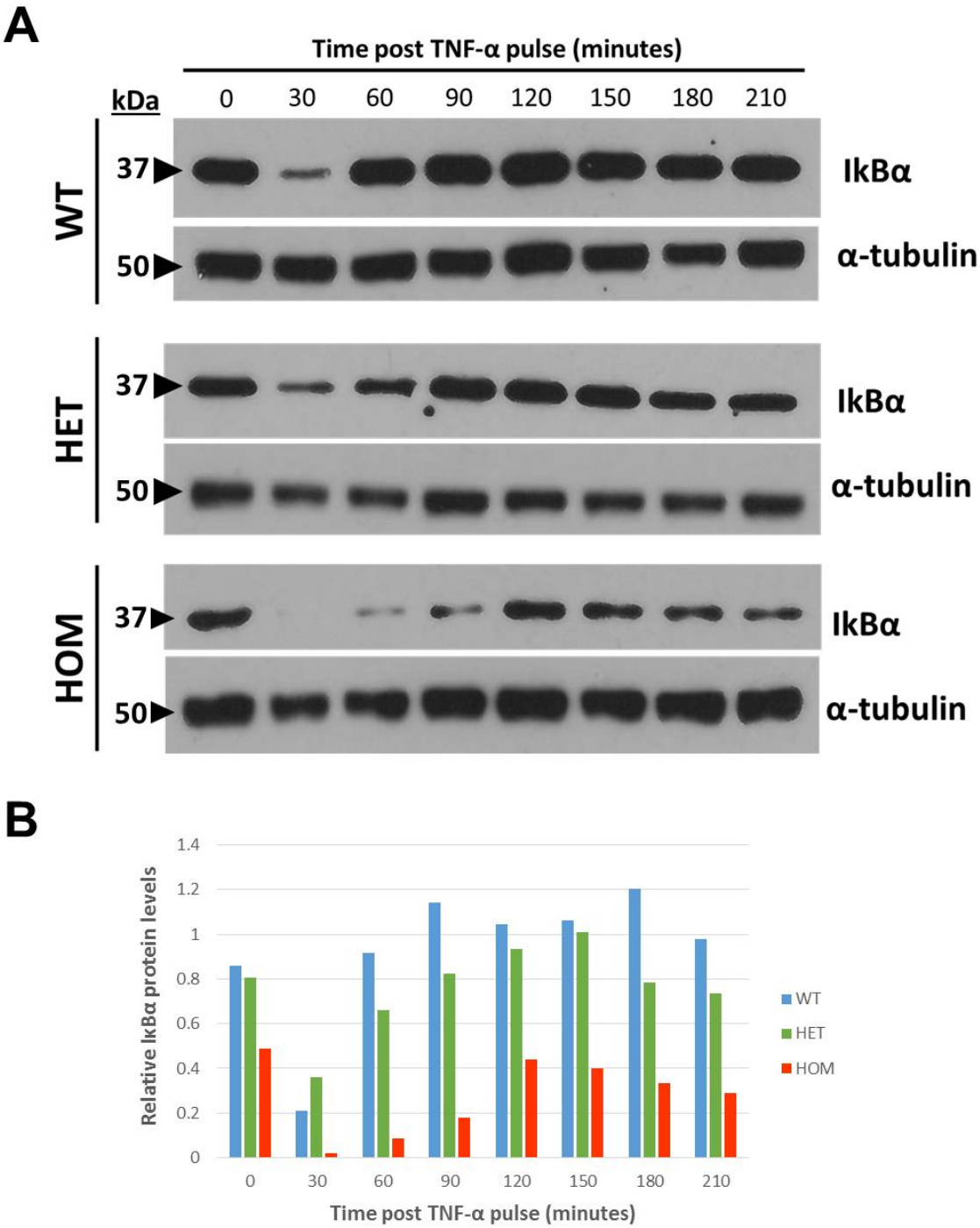

Figure 3.9 Levels of IκBα in RELA trunc fibroblasts over-time after NF-κB stimulation with TNFα. A) Western blot analysis of cells after TNFα treatment with wild-type control cells run in parallel. 30 μg of whole protein lysate was loaded per lane and the blots were probed with an antibody recognising IκBα and α-tubulin B) Levels of IκBα normalised to the α-tubulin level for each sample, performed through densitometric analysis.

3.2.2.3 Nuclear translocation kinetics altered in RELA trunc cells

Due to the delayed restoration of IκBα levels following TNFα induction in homozygous RELA trunc cells, it was reasoned that the truncated RelA protein may occupy the nucleus for an extended time. To test this hypothesis, the nuclear translocation of truncated RelA was investigated using immunocytochemistry and western blotting.

The nuclear translocation of RelA in wild-type, heterozygous and homozygous RELA trunc fibroblast cells was visualised using immunofluoresecent confocal microscopy techniques. Wild-type, heterozygous and homozygous RELA trunc fibroblast lines were each plated into eight wells at the same seeding density, seven were treated with TNFα and the final well left as an uninduced control. After a specified culture period post-TNFα stimulation (i.e. 15, 30, 45, 60, 90, 105 or 120 minutes), the fibroblasts were fixed in preparation for staining (see Section 2.5.7). RelA was stained with an Alexa Fluor® 488 conjugated antibody and nuclei were stained with DAPI (see Section 2.5.7). Digital images were taken on the Inverted Zeiss LSM 710 confocal microscope. Imaged cells were selected based on DAPI staining to identify areas of nearly confluent cells to maximise the number of cells analysed. Sequential scanning was used to create separate images for both DAPI (excitation - 405 nm laser) and Alexa Fluor® 488 (excitation - 488 nm laser).

The experiment was repeated on three independent occasions. In each experiment, wild-type RelA became highly concentrated in the nucleus by 30 minutes post-TNFα treatment. In contrast, translocation to the nucleus in homozygous RELA trunc fibroblasts was significantly reduced, with most RelA remaining in the cytoplasm (Figure 3.10). This result was unexpected and was investigated further using nuclear and cytoplasmic fractionation followed by western blotting. Results from the western blotting analysis were in agreement with the immunohistochemistry results, demonstrating wild-type RelA to be present to a greater extent in the nucleus compared to the truncated RelA 30 minutes post-TNFα treatment (Figure 3.12.c-d). Unexpectedly, the nucelar loading control, Lamin A/C, results did not coincide with the total loading indicated by Ponceau S total protein membrane stain (Figure 3.12.b-c). Lamins are structural components of the nuclear lamina, a matrix of proteins

underlying the inner nuclear membrane which is thought to be involved in nuclear stability, chromatin structure and gene expression (Schreiber & Kennedy., 2013).The LMNA gene is has not been identified previously as a NF-κB target gene, however, Lamin A/C deficient cells have been reported to have impaired NF-κB signalling (Lammerding et al., 2004).

It was previously hypothesised that the delay in restoration of IκBα levels would, in turn, delay the translocation of RelA from the nucleus back to the cytoplasm. At 60 minutes post-TNFα stimulation, wild-type RelA was observed to have translocated from the nucleus back to the cytoplasm, although there was imperfect synchronisation between cells by 60 minutes post-TNFα stimulation (Figure 3.11). By 105 and 120 minutes post-TNFα stimulation, wild-type RelA had translocated back to the cytoplasm in all cells, appearing no different to unstimulated cells. In contrast, the truncated RelA in homozygous fibroblasts did not fully translocate out of the nucleus by the final time-point assayed at 120 minutes post-TNFα stimulation, although the percentage of nuclear RelA had reduced relative to the 30 minute time-point.

Quantitation of digital images at 0, 30 and 120 minutes' post-stimulation of wild-type and homozygous cells was carried out, to assess the impact of truncated RelA on nuclear translocation, following the method described by Noursadeghi et al., 2008. Five images from each genotype at each time-point were analysed using the Image J software. A median filter (3x3 pixel radius) was applied to remove background noise, then the nuclear and cytoplasmic regions of the cells were defined using binary image masks. The images were then converted to binary masks using Image J's Automatic threshold function using the Isodata algorithm (*Ridler & Calvard.,*1978). The DAPI mask was used to define the nuclear RelA and the cytoplasmic RelA was defined by subtracting the DAPI mask from the RelA mask using the image calculator function. Cells that were on the outer edge of the image were omitted from analysis. Fluorescent intensities from the remaining regions of entire cells were quantified from each image and data was exported to Excel to calculate the nuclear:cytoplasmic ratio of RelA. The ratio of nuclear:cytoplasmic RelA was used as a relative measure of RelA nuclear translocation. The results show that at 30 minutes post-TNFα stimulation the nuclear:cytoplasmic ratio of RelA was significantly lower in homozygous fibroblasts

compared to wild-type controls (p=0.00002; Figure 3.13). Furthermore, at 120 minutes post-TNFα, the nuclear:cytoplasmic ratio of RelA was significantly higher in homozygous fibroblasts compared to wild-type controls (p=0.034) This quantitative analysis supports previously findings that truncated RelA does not translocate into the nucleus at the same extent after TNFα stimulation compared to wild-type RelA. Moreover, as expected from findings of delayed IκBα production by homozygous RELA trunc fibroblasts, the truncated RelA remains within the nucleus for an extended time compared to wild-type RelA.

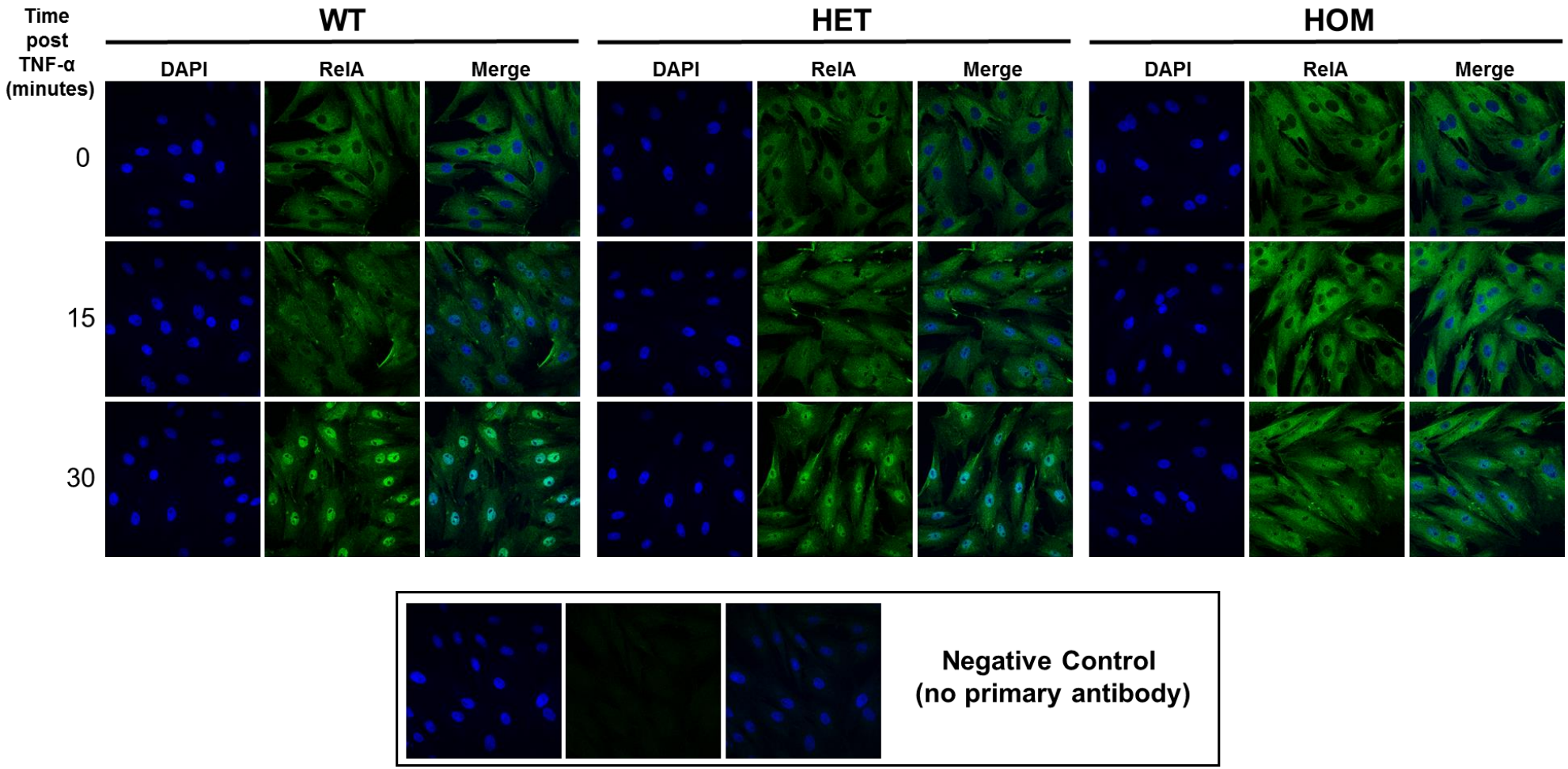

Figure 3.10 Effect of RELA trunc on TNFα stimulated nuclear translocation. Fibroblasts were treated with TNFα and fixed at the indicated time-points. The cells were subsequently stained using an antibody which recognises the N-terminus of RelA and a nuclear stain (DAPI)and analysed using confocal microscopy. These images represent one of three replicate experiments.

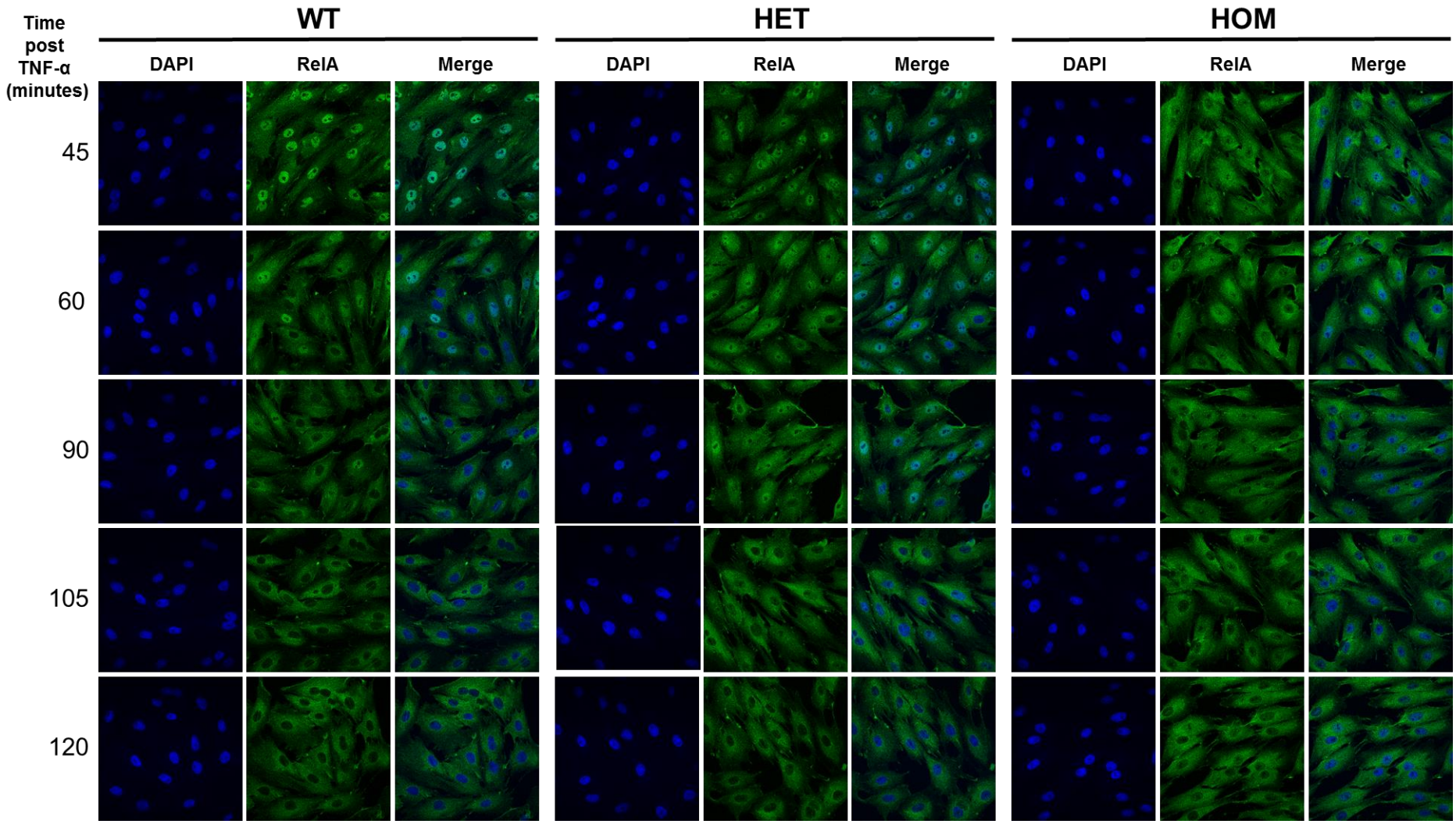

Figure 3.11 Effect of RELA on translocation back out of the nucleus. Fibroblasts were treated with TNFα and fixed at the indicated time-points. The cells were subsequently stained using an antibody which recognises the N-terminus of RelA and a nuclear stain (DAPI) and analysed using confocal microscopy. These images represent one of three replicate experiments

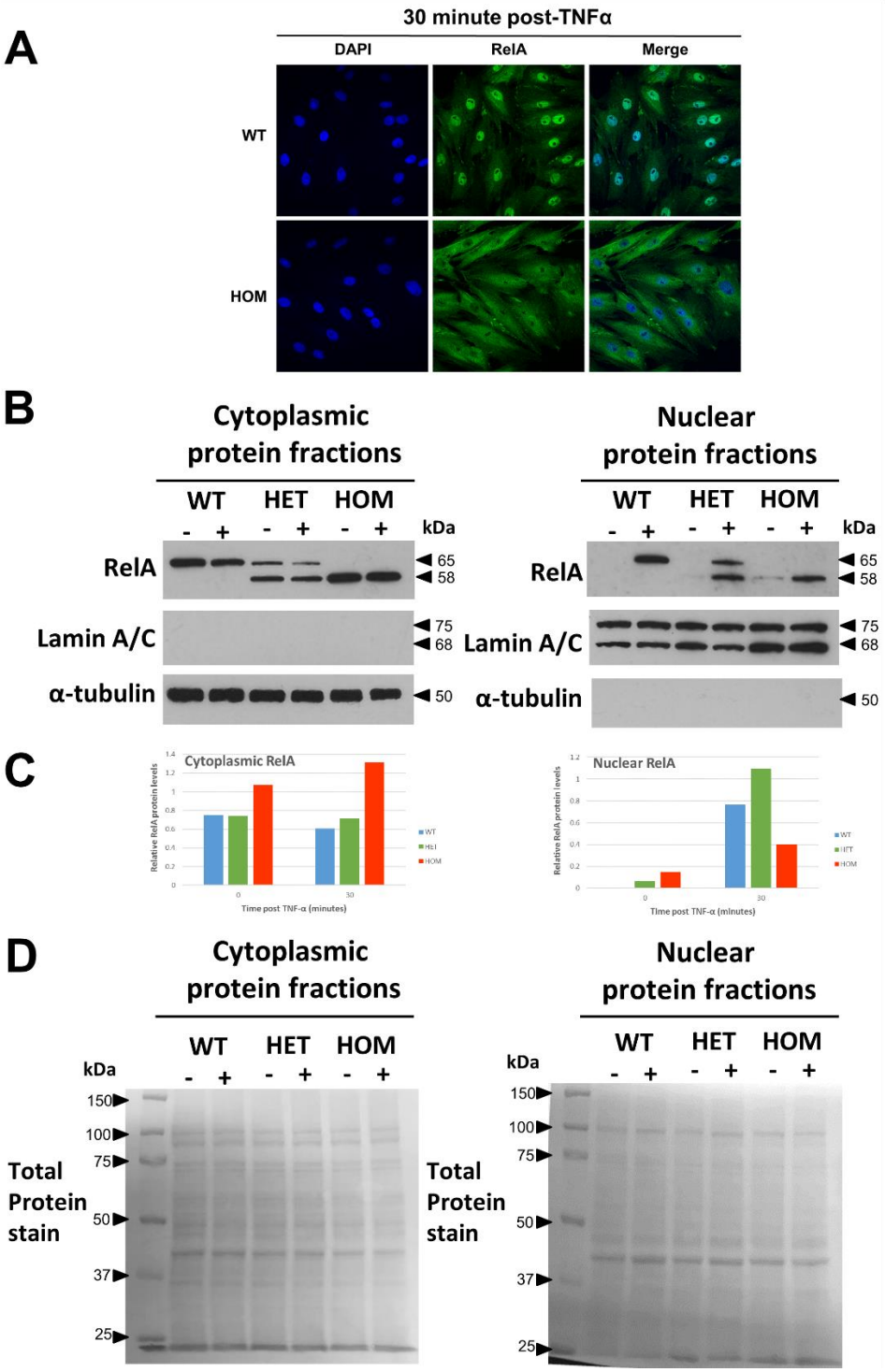

Figure 3.12 Effect of RELA trunc on TNFα stimulated nuclear translocation. A) Fibroblast cells were stimulated with a TNFα pulse and fixed 30 minutes later for staining, then analysed using confocal microscopy. B) Protein loading was assessed by Ponceau S staining of the transfer membrane prior to western blot to estimate loading C) The cytoplasmic and nuclear extracts were analysed for RelA by western blot. D) Levels of RelA were calculated using densitometric analysis normalised to the loading controls for each sample and are displayed graphically. α-tubulin was used as a loading control for cytoplasmic extracts and LaminA/C was used as the loading control for nuclear extracts.

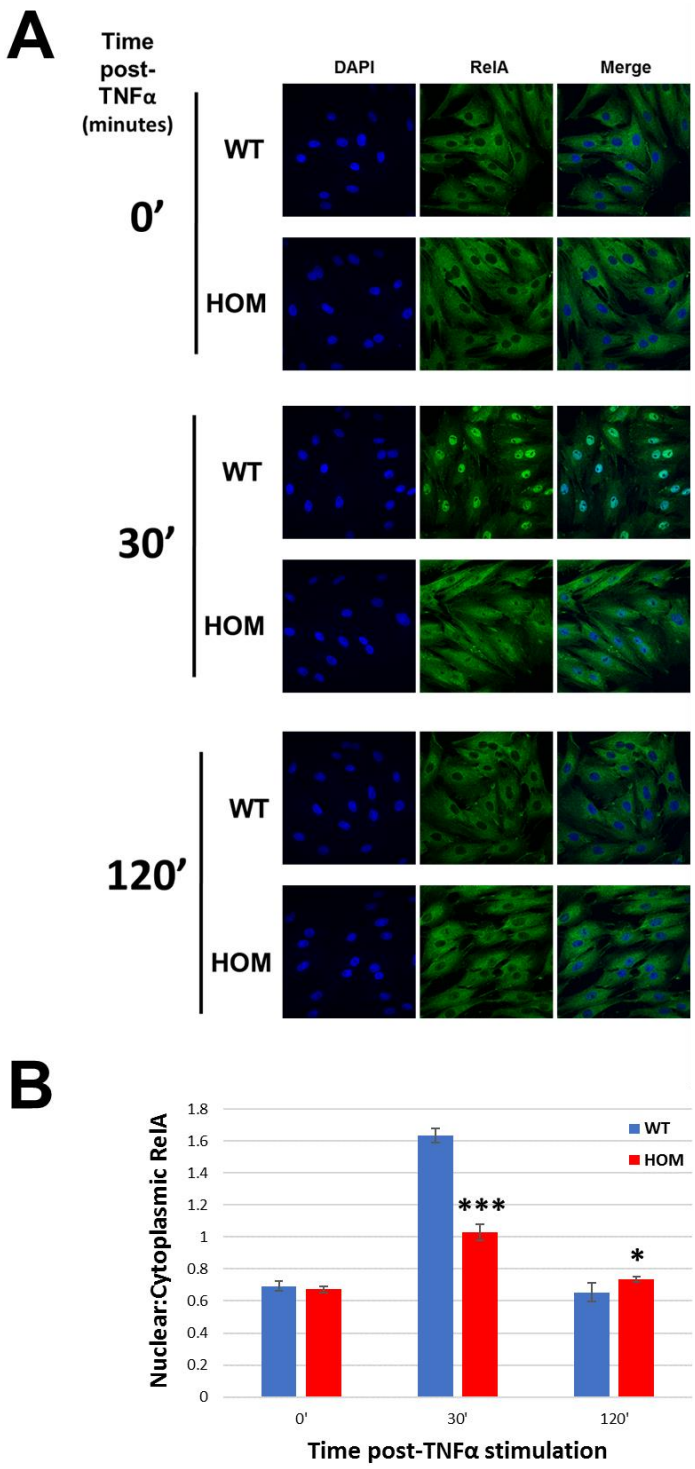

Figure 3.13 Quantitative analysis of RelA nuclear translocation. A) Immunofluorencence staining of RelA in fibroblasts treated with TNFα and fixed at the indicated time-points B) Quantification of nuclear:cytoplasmic ratios of RelA staining. Significance was calculated between wild-type controls and RELA trunc homozygous at the indicated time-points using a Student's paired t-test. Significant difference is indicated with black symbol *($p<0.05$) or ***($p<0.0001$). Error bars represent the standard deviation (S.D) from analysis of the five separate images for each genotype.

3.2.2.4 The impact of the RelA truncation on the production of other NF-κB members in fibroblasts after induction with TNFα

Finally, I investigated the impact the truncated RelA has on the production of other NF-κB protein members. In humans, the RelA-p50 heterodimer regulates expression of NF-κB subunit members REL (C-Rel; Hannink et al., 1990, Grumont et al., 1993), RELB (RelB; Bren et al., 2001), NFKB1 (p105/p50; Lombardi et al., 1995) and NFKB2 (p100/p55; Ten et al., 1992, Cogswell et al., 1993). The regulatory interaction between RelA and other NF-κB members likely plays an important role in the nature of the NF-κB response in terms of the duration and type of NF-κB activity in induced cells. Since the regulation of several RelA-dependent NF-κB target genes were found to be altered by the RELA trunc mutation, I reason that the altered activity of truncated RelA would consequently impact on the expression of the other NF-κB family members after induction (see Section 3.2.2.1). To investigate this potential impact of truncated RelA on the expression of NF-κB family members, qRT-PCR analysis was performed on wild-type control and RELA trunc fibroblasts induced with TNFα.

Wild-type RELA control, heterozygous and homozygous RELA trunc fibroblast cell lines were each plated into four wells at the same seeding density, three were treated with TNFα and the other was left as an uninduced control. After the specified time in culture post-TNFα treatment (i.e. 30, 60 or 120 minutes), the fibroblasts were collected, and RNA purified to make cDNA (see Section 2.7.12). The fibroblast cDNA used in this experiment were the same samples used to investigate the expression of RelA-dependent genes (Figure 3.8). The transcript levels of genes RELA, REL, RELB, NFKB1 and NFKB2 were assayed using qRT-PCR. The expression level for each gene was normalised to the mean expression of GAPDH and B2M, and the changes in expression calculated relative to the uninduced control for each fibroblast line.

After TNFα induction in wild-type fibroblasts, the expression level of RELA remained relatively unchanged whereas those of the NF-κB target genes, REL, RELB, NFKB1 and NFKB2 were upregulated as predicted. In heterozygous and homozygous RELA trunc fibroblasts, the induced levels of NFKB1, NFKB2 and RelB were significantly lower compared to wild-type fibroblasts at a minimum of one time-point post-TNFα treatment (Figure 3.14). The RELB expression remained lower at the later time of 120

minutes after induction in RELA trunc fibroblasts compared to wild-type. However, there was no significant difference between wild-type and RELA trunc fibroblasts at the later, 120 minute, time-point in the levels of NFKB1 and NFKB2 post-TNFα treatment. These results show that the RelA truncation impacts on the induced expression of at least three of the NF-κB subunits, RELB, NFKB1 and NFKB1, in fibroblasts induced with TNFα.

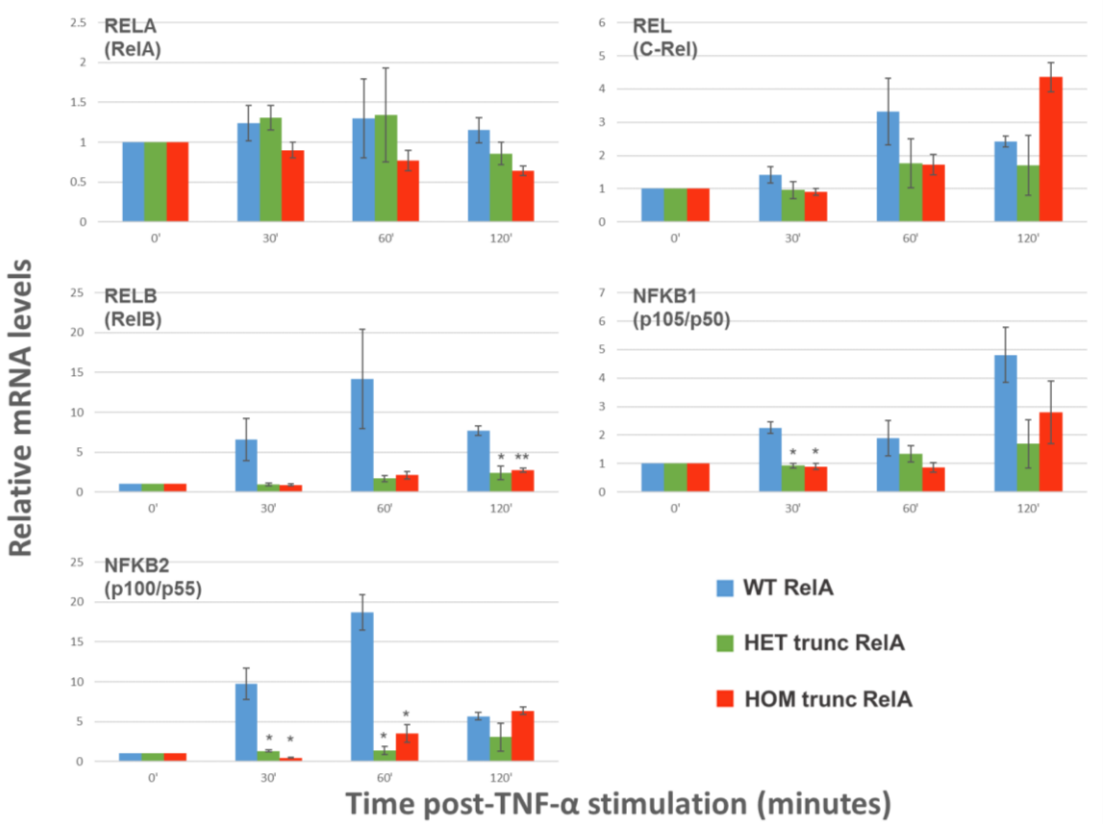

Figure 3.14 Gene expression analysis of NF-κB subunits genes in response to TNFα stimulation. qRT-PCR analysis of genes, RELA, REL, RELB, NFKB1 & NFKB2, in fibroblasts containing wild-type and truncated RelA induced with TNFα pulse (10 ng/ml). Relative expression was calculated by normalising to the corresponding uninduced fibroblasts. Significant difference was calculated between the wild-type controls and RelA-edited at each specific time post-TNFα using a Student's paired t-test. Significant difference is indicated with black symbol *($p<0.05$) or **($p<0.001$). Error bars represent the S.E.M from the three independent inductions.

To determine if the observed differences in the mRNA levels in RELA trunc fibroblasts translate to a similar difference in NF-κB protein levels, western blot analysis was carried out. Four flasks of homozygous and wild-type RELA fibroblast cell lines were prepared. After 24 hours in culture, three flasks were treated with TNFα

and the final kept as an uninduced control for each fibroblast cell line. After the stated time post-TNFα treatment the cells were lysed in the flask and collected for further processing (see Section 2.5.1). 20 μg of each protein lysate, estimated using the Bradford assay, was used for western blot analysis. Antibodies that recognise human p105/p50, C-Rel and RelA were successfully used to detect their porcine equivalents. Unfortunately, the antibodies used for the detection of porcine RelB and p100/p55 were unsuccessful (data not shown). The level of each NF-κB protein was normalised to the level of α-tubulin in that sample using densitometric analysis (Figure 3.15.b). A noticeable difference was the decline in the levels of the p50 subunit at 60 and 120 minutes post-TNFα treatment in the homozygote cell line when compared to the control. A delay in the expression of NFKB1 is observed in homozygote RELA fibroblasts compared to wild-type. However, there is no apparent decline in the level of pre-processed p50, known as the p105 subunit, after induction with TNFα in homozygous fibroblasts.

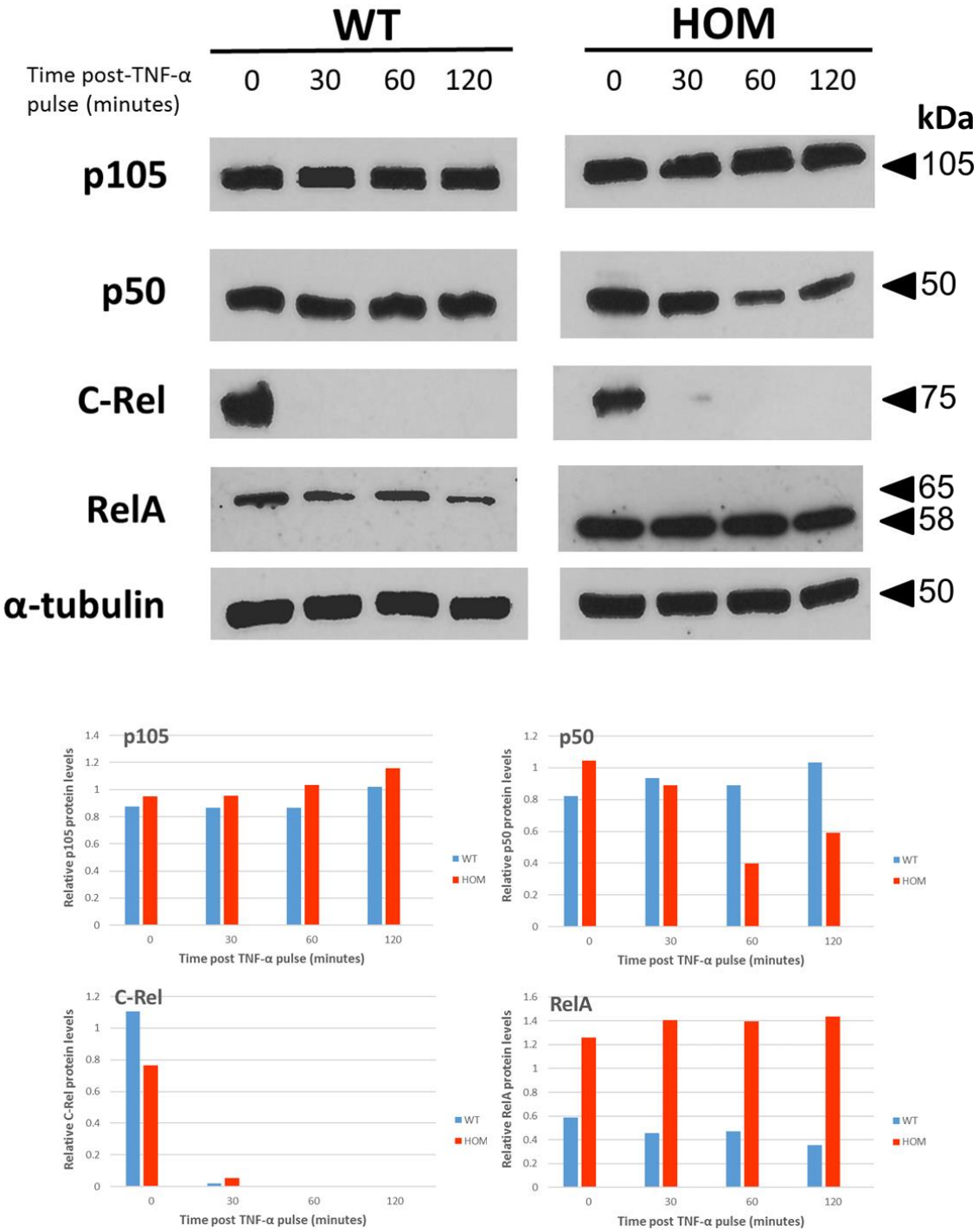

Figure 3.15 The levels of p105, p50, C-Rel and RelA proteins in RELA trunc fibroblasts over-time after NF-κB stimulation with TNFα. A) Western blot analysis of cells after TNFα treatment with wild-type control cells run in parallel. 20 µg of whole protein lysate was loaded per lane and the blots were probed with antibodies that recognise p50/p105, C-Rel, RelA. and α-tubulin. B) Levels of each NF-κB protein was normalised to the α-tubulin level for each sample, performed through densitometric analysis.

3.2.3 Characterisation of RELA trunc pigs

As the RELA trunc pigs are a novel animal model, an overall pathological examination of the 1st generation of animals was completed alongside pathologist Dr Pip Beard. A full-post-mortem was performed on 5 animals of each genotype, wild-type, heterozygous and bi-allelic for the RELA trunc mutations, at 18-20 weeks old. All animals were euthanised by lethal injection. Tissues and organs were excised and examined at the necropsies and a range of tissues were collected in fixative to allow future analyses (see Appendix B). Additionally, tissues were snap frozen to allow subsequent DNA, RNA or protein analysis.

No organs or tissues displayed any macroscopic evidence of pathological alternations that could be attributable to the genetic modification of RELA. For this study, preliminary analysis was carried out on the spleen, bone marrow and a number of lymph nodes including mandibular, ventral superficial cervical, mediastinal, mesenteric and popliteal. Prior to fixing, samples of the spleen were excised from a defined anatomical location, cross-sections from the lower right side. The lymph nodes were dissected free of fat before cross-sectioning and fixing. The bone marrow was removed from the upper left femur, one sample was preserved in fixative and another used to produce a fresh smear that was Giemsa stained the same day.

3.2.3.1 Impact of RelA truncation on development of secondary lymphoid organs

As mentioned in chapter 1, RelA plays an important role in the development of secondary lymphoid organs and in hematopoiesis (Alcamo et al., 2002, Stein & Baldwin., 2013). Mice lacking RelA die at embryonic day 15 due to TNFR1-signaled hepatocyte apoptosis (Begg et al., 1995, Begg et al., 1996). Targeted disruption of TNFR1 rescues the RelA deficient mice, however the immune system of these animals is severely compromised and most die of bacterial infection within 3 weeks after birth (Alcamo et al., 2001). Furthermore, RelA/TNFR1 deficient mice have severely disorganised splenic microarchitecture and lack all lymph nodes and Peyer's patches (Alcamo et al., 2002).

To examine the microanatomy of the spleen and lymph nodes of RELA trunc animals, these samples were excised and fixed for wax embedding, sectioning and H&E

staining (see Section 2.3.3 for details). The resulting sections of spleen and lymph nodes were examined blindly by pathologist, Dr Pip Beard.

All the lymph nodes examined displayed the described typical porcine anatomical features. Like dolphins, elephants and rhinoceroses, pigs have lymph nodes that are described as structurally inverted compared to most other mammals, as the medulla is often located peripheral of the cortex (Binns., 1982, Bowes & Kenny., 1986). The cortex is densely populated by lymphocytes whereas the medulla is less cellular, thus less heavily stained in H&E stained sections. Therefore, to allow a more in depth examination of the lymph nodes, scores were assigned in the following three categories; 1) an estimate of the percentage of the lymph node cross section which consisted of cortical tissue 2) whether the lymphoid nodules were distinctly demarcated from the surrounding parenchyma, and 3) whether there were abundant apoptotic cells in the lymphoid nodule (characterised by shrunken, hyperchromatic nuclei). When the resulting scores were analysed, high variability was observed across individual lymph nodes and no significant difference was found in any of the scoring categories (see Appendix C).

The porcine spleen is similar to other species, consisting of two main components, the red pulp and the white pulp, which can clearly be identified through staining with H&E due to their difference in architecture, cellular composition and vascular organisation. Spleen sections were blind examined by Dr Pip Beard and any abnormalities in morphology were recorded. Notes were taken on the observations of the red and white pulp, including the germinal centres, marginal zones and peri-arteriolar sheaths. In all animals analysed there was a variable amount of congestion in the red pulp, most likely caused by the barbiturate euthanasia. Other noticeable changes were identified in one heterozygote, which showed slightly reduced cellularity in germinal centres, one bi-allelic which displayed prominent germinal centres, and another bi-allelic which had relatively increased amounts of white pulp. A repeat of this analysis was completed un-blinded, however no consistent change was identified in the spleen sections of the RELA-edited animals (Figure 3.16).

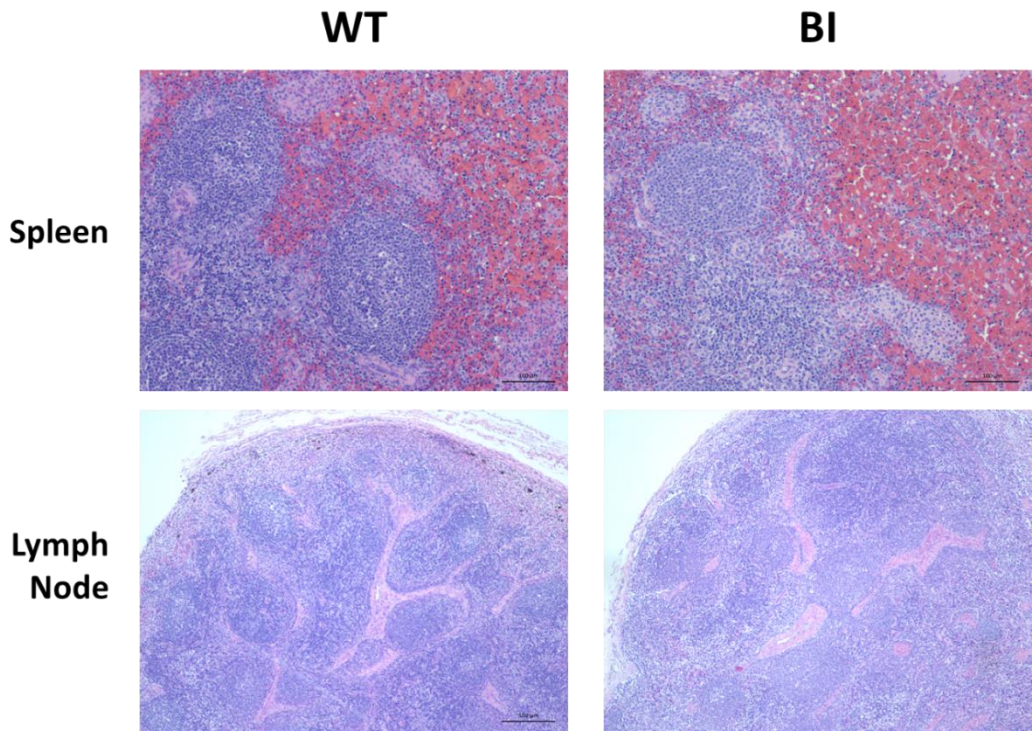

Figure 3.16 H&E staining of spleen and lymph node. The H&E staining of the spleen and submandibular lymph node from wild-type (WT) and bi-allelic (BI) RELA truncated pigs are displayed.

3.2.3.2 Impact of RelA truncation on bone marrow composition

Mice which lack RelA in the hematopoietic compartment have defects in hematopoietic stem cell differentiation and extramedullary haematopoiesis (Stein & Baldwin., 2013). To investigate the impact of truncated RelA on these processes, differential cell counts on both the bone marrow and the peripheral blood were performed on wild-type, and heterozygous and homozygous RELA trunc pigs.

Bone marrow smears and biopsies were all analysed blind by pathologist Prof Elspeth Milne. Most normal differentiated hematopoietic cells types can be identified on bone marrow smears stained by the Giemsa method based on morphology; these include, granulocytes, erythroid cells, megakaryocytes, monocytes, macrophages, mast cells, lymphocytes, plasma cells and bone forming cells. The smear samples taken from the heterozygotes were too thin for adequate analysis thus were omitted from this study. No significance difference in the differential cell counts were observed between the wild-type and homozygous RELA trunc pigs (Figure 3.17). However, mild megakaryocyte hyperplasia and was found in all five bone marrow biopsies and megakaryocyte dysplasia was observed in two of the homozygous RELA trunc pigs.

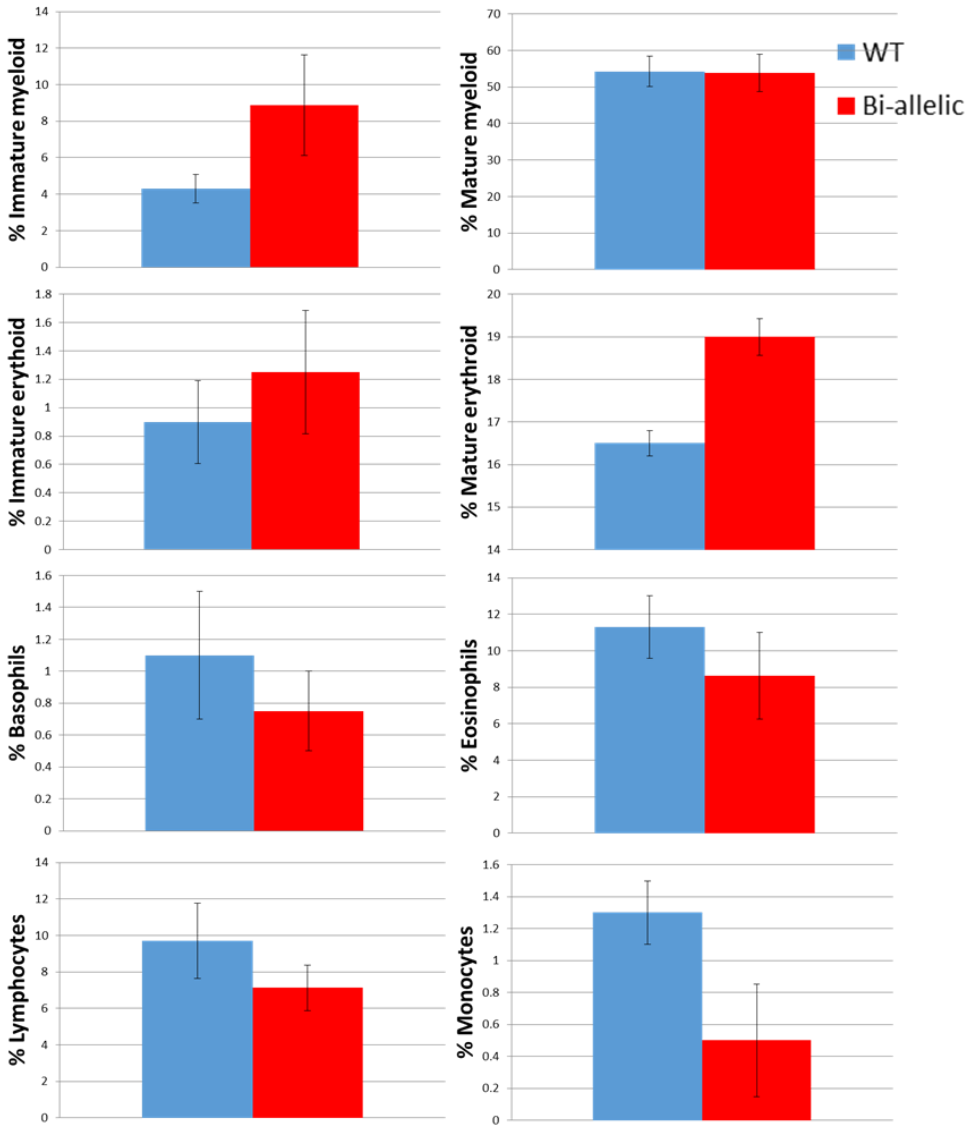

Figure 3.17. Differential cell counts of bone marrow smears from wild-type and F1 bi-allelic RELA trunc pigs. No significant difference was identified between wild-type controls (n=5) and RELA trunc homozygous (n=5) calculated using a Student's paired t-test.

3.2.3.3 The impact of RELA truncation on overall pig weight

Prior to euthanasia the pigs were weighed to calculate drug dosages at which point it was noted that the weights of the bi-allelic pigs were often lower than that of wild-type and heterozygote pigs of the same age. Thus, the weights of the 2nd generation of piglets were recorded at birth, 4 weeks and 8 weeks of age. Homozygous RELA trunc pigs were confirmed to have a significantly reduced body weight compared to wild-type controls at all birth (p=0.004), 4 weeks (p=0.009) and 8 weeks old (p=0.004; Figure 3.18). Moreover, the calculated average daily weight gain for homozygous RELA trunc pigs was significantly lower compared to wild-type controls (p=0.002).

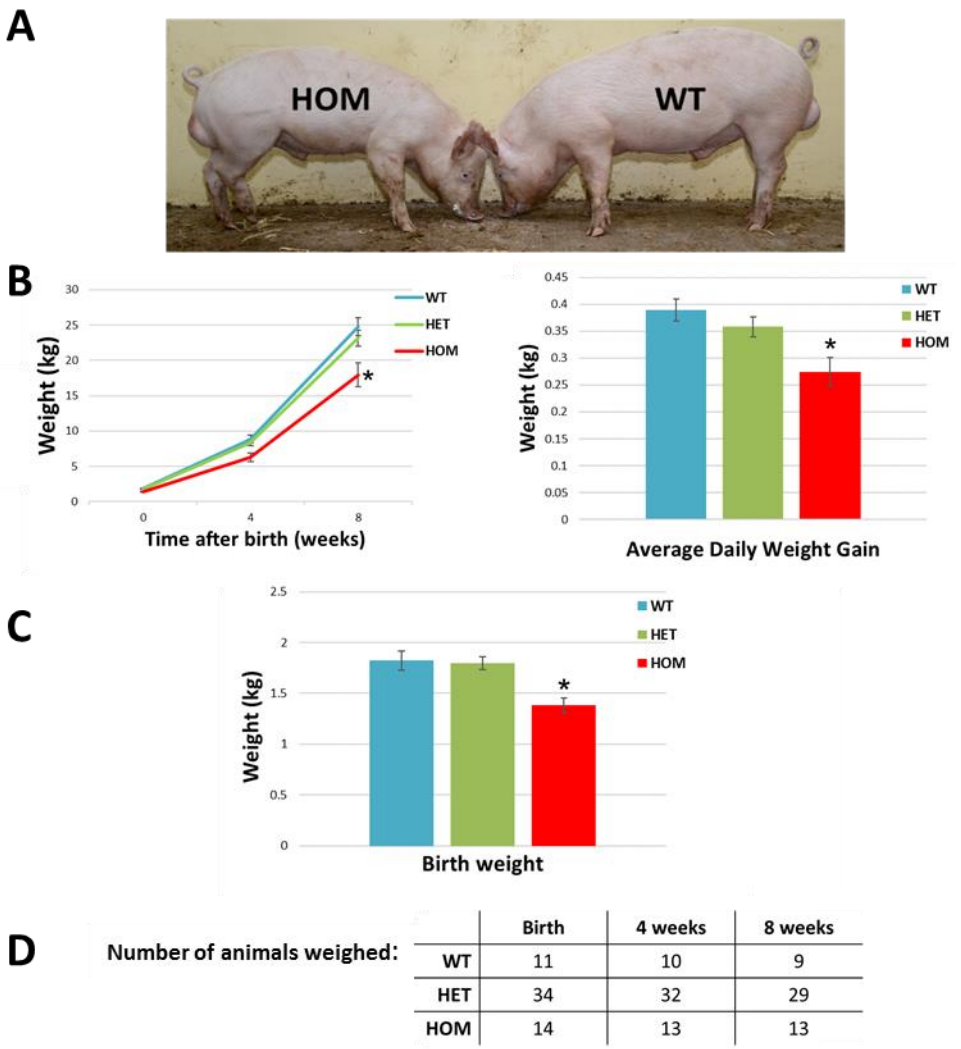

Number of animals weighed:	Birth	4 weeks	8 weeks
WT	11	10	9
HET	34	32	29
HOM	14	13	13

Figure 3.18. Body weight comparison of wild-type and heterozygous and homozygous RELA trunc pigs. A) Image displaying two boar siblings, one homozygous for the RELA trunc mutation and one wild-type. B) Graphs displaying the reduced weight gain of homozygous RELA trunc compared to wild-type pigs C) Bar chart displaying reduced birth weight of homozygous RELA trunc compared to wild-type D) Table displaying the numbers of animals weighed at each time-point. Significant difference was calculated between the wild-type controls and RELA-edited pigs at each time-point using a Student's paired t-test. Significant difference is indicated with black symbol *($p<0.05$).

3.3 Discussion

In this Chapter, genotyping and subsequent characterisation was carried out on the first genome edited pigs born from direct injection of editor mRNAs into zygotes. Five live piglets were identified to contain targeted editing events in their RELA locus. Two of these editing events resulted in frame-shift mutations and the introduction of a premature stop codon proximal to the target site, resulting in a RELA gene predicted to encode a RelA protein that lacks the final 60 amino acids of wild-type RelA. These founder animals were subsequently bred to produce a larger cohort for further characterisation.

3.3.1 Truncated RelA

The RelA truncation mutant was predicted to lack the 60 amino acids of the C-terminal region of the transactivation domain which encompasses the entire TA1 and part of the TA2, and Western blot analysis confirmed that a truncated protein was produced. This deleted region is conserved between mammalian species (O'Shea & Perkin., 2008). Early deletion studies of RelA, performed using *in vitro* reporter systems, found that the TA1 region mediates the majority of RelA's transcriptional activity in a variety of cell types (Schmitz & Baeuerle., 1991). In a study by Mukherjee et al., (2013) the final 60 amino acids of the RelA transactivation domain were shown to mediate RelAs binding to the TAZ1 domain of the transcriptional co-activators creb binding protein (CBP) and p300. RelA's interaction with CBP/p300 promotes the assembly of basal transcriptional machinery on the transcription start site, and is essential for the transcription of these RelA-dependent genes (Gerritsen et al., 1997, Merika et al., 1998, Mukherjee et al., 2013). RelA also makes contact with the KIX domain of CBP/p300, an interaction which requires the phosphorylation of a highly conserved serine, S276, in the RHD of RelA (Zhong et al., 1998). Mutant mice containing an alanine instead of a serine at position 276 (S276A) are embryonic lethal, displaying a variety of phenotypes including aberrant eye development (Dong et al., 2008). The final 60 amino acids of wild-type RelA also harbours several conserved phosphorylation sites including T505, S529 and S536. Phosphorylated T505 represses RelAs transactivation at some target genes by promoting association with HDAC1 (Campbell et al., 2006). Phosphorylated S529 and S536 increases RelA transctivation,

although the functional mechanism is not currently known. These sites are phosphorylated in response to many inflammatory stimuli including TNFα (Vermeulen et al., 2003, Viatour et al., 2005). There are six other possible phosphorylation sites in the truncated region which could further mediate regulation of RelA's activity.

Given the high degree of cross-species conservation of this gene, coupled with the known biological function of the protein, it was surprising that there was no obvious phenotypic difference in pigs homozygous or bi-allelic for truncated RelA. These pigs were born healthy and were fully viable when housed in a typical farm environment. This is in dramatic contrast with *rela*-/- mice, which have an embryonic lethal phenotype, implying that the truncated RelA retains significant functionality.

It is worth noting that western blotting analysis consistently demonstrated that the truncated RelA protein was present in cells at higher levels compared to full-length wild-type RelA. Direct quantitative comparison of these proteins is confounded by the molecular weight difference, as this could impact on the efficiency of protein migration through the polyacrylamide gel during transfer to the membrane. However, higher relative levels of truncated RelA were also observed compared to wild-type, lending support to the above observation. This could be investigated further with an ELISA. Moreover, mutation of single phosphorylation sites within the missing domain in truncated RelA are known to decrease the ubiquitination and thus increase the stability of the protein (Milanovic et al., 2014).

3.3.2 Interpreting the impact on NF-κB signalling pathway

To investigate the impact of altered RELA *in vitro,* TNFα*,* a potent inducer of NF-κB, was used to stimulate fibroblasts isolated from skin biopsies. The transcriptional activity of RelA was assessed by quantifying the expression of several RelA-dependent genes. In a previous study by Mukherjee et al., (2013) the final 60 amino acids region of mouse RelA was found to be essential for the upregulation of a gene encoding IκBα, however my analysis shows this is not the case. Rather, we demonstrate a delay in upregulation of IKBA (encoding IκBα) along with several of the other RelA-dependent genes examined, suggesting that in pig the truncated RelA

has a delayed transcriptional activation. The previous study was performed in immortalised mouse *rela*$^{-/-}$ fibroblasts reconstituted with retroviral vectors containing the mouse *rela* truncation mutants, thus the difference in our results could reflect varied requirements for the same sequence between species, altered response of immortailsed vs primary cells, or copy number variation/ position effects associated with the lentiviral delivery route. In our analysis, higher expression of RelA-dependent genes was identified at later time-points post induction, suggesting that while initial induction was delayed, this morphed into a prolonged activation of truncated RelA. This would fit with a model whereby delayed transcriptional upregulation of IKBA resulted in retarded production of IκBα and subsequent deferred termination of NF-κB activity (Fagerlund et al., 2015).

Using a nuclear translocation assay we discovered that following TNFα stimulation truncated RelA translocated into the nucleus at a similar time to the wild-type protein, but that in contrast to the full-length protein much of the truncated RelA remained in the cytoplasm throughout the timecourse of this experiment. Thus, the lower transcriptional activity of the truncated form may in part be due to its reduced nuclear translocation. This work provides the first evidence that this C-terminal region of RelA is important in promoting nuclear accumulation. Previous studies into the kinetics of NF-κB showed that oscillations of this transcription factor from the cytosol to the nucleus are mirrored by changes in S536 phosphorylation, suggesting dephosphorylation of S536 occurs in the nucleus (Nelson et al., 2004). Mutation of S536 resulted in nuclear translocation of the same kinetics as observed for wild-type, however the level of nuclear accumulation was not compared in this study (Sasaki et al., 2005). Interestingly, phosphorylated S536 RelA has been reported not to associate with IκBα and is predominantly found in the cytoplasm (Sasaki et al., 2005). It is possible that the phosphorylation sites, missing in our RelA truncation mutant, are involved in regulating nuclear translocation. In accordance with study the by Mukherjee et al. (2013) we also observe a prolonged nuclear residence time of truncated RelA, indicating an impaired negative feedback loop.

My gene expression analysis revealed delayed induction of two known regulators of the NF-κB negative feedback loop; IκBα and A20. IκBα is the key inhibitor of NF-κB

activity, retaining NF-κB in the cytoplasm until triggered by an appropriate cellular stimulant; IκBα is then transiently degraded and then subsequently upregulated by newly-active NF-κB (Arenzana-Seisdedos et al., 1997, Chen et al., 2001, Huang & Miyamoto., 2001). Western analysis of the IκBα protein post-TNFα stimulation confirmed the delayed expression levels observed during quantitative analysis of transcript levels. This delay is a likely cause of the prolonged nuclear residence of truncated RelA, leading to the observed higher induced expression levels of RelA-dependent genes at later time-points. The upregulation of negative feedback regulator A20 was also severely impaired in cells homozygous for truncated RelA. A20 negatively regulates NF-κB by inhibiting RIP1 K63-linked polyubiquitination which terminates further downstream activation of NF-κB (Shembade & Harhaj., 2012). This renders the NF-κB pathway less sensitive to subsequent inductions. Mice deficient in A20 develop uncontrolled and spontaneous multi-organ inflammation (Lee et al., 2000).

RelA is known to regulate numerous other components of the NF-κB pathway such as TRAF2, REL, NFKBIA, NFKBIE, NFKBIZ, NFKB1, NFKB2, RELB. As a consequence, the altered RelA activity of the truncated protein will likely have had an influence on the basal cellular levels of a range of proteins prior to experimental induction with TNFα. Lower basal levels of both IκBα and C-Rel proteins were identified in fibroblasts homozygous for the RelA truncation compared to wild-type. Furthermore, the induced expression of NF-κB subunits, NFKB1(p105/p50), NFKB2 (p100/p55), RELB (RelB), was significantly reduced in homozygous RelA trunc cells.

In conclusion, I have identified that the RelA truncation does alter NF-κB signalling, although clear understanding of the mechanisms was confounded by the complexity of the NF-κB signalling pathway and downstream biological networks.

3.3.3 Interpretation of the phenotypic analysis of RELA-edited animals

Gross phenotypic analysis of individuals revealed no gross defects associated with the modified animals. RelA is known to play an important role in the development of secondary lymphoid organs and in hematopoiesis (Alcamo et al., 2002, Stein & Baldwin., 2013). However, analysis of individuals revealed no defects in the lymphoid

organs. As this analysis was limited to gross histology, it is possible that the RelA truncation may have resulted in more subtle changes in cell distribution in these organs, which could be further investigated by immunohistological methods. Overall, the RelA-edited animals displayed no apparent anatomical defects associated with the modification and surprisingly are healthy living in normal farmyard conditions. In recording the weights of our pig cohorts, I unexpectedly found the pigs homozygous for the RelA truncation had significantly lower body weights compared to wild-type controls. Aberrant NF-κB activation has previously been linked to metabolic diseases such as obesitity and type 2 diabeties and identified as a regulator of cell signalling pathways which mediate glycolysis and respiration (Tornatore et al., 2012). Thus, the lower weight phenotype could be the result of the altered NF-κB activity within these animals.

Chapter 4 African Swine Fever virus (ASFV) challenge of RELA edited pigs

4.1 Introduction

African swine fever virus (ASFV) is the causative agent of African swine fever (ASF), a highly contagious lethal disease of domestic pigs. To date, no effective vaccines or treatments are available. Thus, disease control relies on strict biosecurity, rapid diagnosis and the mass slaughter and appropriate disposal of all animals on infected sites. Consequently, ASF causes significant economic losses in affected countries. The disease is endemic to countries of sub-Saharan African and in 2007 was introduced to Georgia in the Caucasus and disseminated into Russia and countries of Eastern Europe where it remains prevalent. The increasing global movement of goods and people combined with increased transboundary spread of ASFV poses a major threat to pig production worldwide.

ASFV infection of domestic pigs often results in an acute haemorrhagic disease causing death within 5-14 days. Infection with ASFV is thought to influence and/or compromise the immune response of domestic pigs. The virus predominantly infects immune cells of the myeloid lineage, especially monocytes and macrophages, which are thought to play a major role in the viral dissemination and persistence (Sierra et al., 1991, Sánchez-Cordón et al., 2008). Macrophages are mature tissue differentiated monocytes, which accumulate in the spleen, lymph nodes, lung, liver sinusoids, connective tissue, serous fluids and skin. These cells play a critical part in the immune system by detecting pathogen-associated molecular patterns through various pattern recognition receptors, triggering immune responses, secreting cytokines and chemokines, presenting antigens and clearing pathogens by phagocytosis. Upon infection, ASFV encodes for a number of viral proteins involved in host immune evasion; these include the NF-κB and NFAT inhibitor A238L, and the apoptosis inhibitors A179L and A224L (Neilan et al., 1997, Miskin et al., 2000, Granja et al., 2006., Brun et al., 1996, Revilla et al., 1997, Nogel et al., 2001). The anti-apoptotic proteins were identified in virulent isolates, and allow for infected cells to survive and spread the virus throughout the body (Dixon et al., 2013). Virulent strains of ASFV induce elevated production of pro-inflammatory cytokines, such as TNFα and IL-1, in

infected macrophages which has been speculated to play an important role in initiating the disease pathogenesis (Gómez del Moral et al., 1999, Gil et al., 2008). A characteristic of ASF pathogenesis is the widespread apoptosis of lymphocytes leading to lymphopenia, which likely impacts on the immune response to ASFV. Other characteristics of ASF include apoptosis of arteriolar and capillary endothelial cells, and disseminated intravascular coagulation, both of which eventually lead to multiple organ failure and shock.

In contrast to domestic pigs, ASFV causes an unapparent persistent infection in swine indigenous to Sub-Saharan African, such as the warthog and bushpig. As discussed in Chapter 1, the genetic variation identified between domestic pig RELA and warthog RELA has been hypothesised to underlie the difference in their responses to ASFV infection (Palgrave et al., 2013). To test this hypothesis genome editors were used to target this variable region of porcine RELA in the domestic pig. TALEN reagents were utilised in porcine embryos to produce live pigs with various edits in their RELA gene (Lillico et al., 2013). The previous results chapter (Chapter 3) discusses the genotyping and characterisation of the RELA-edited animals born from this procedure. Several of the RELA editing events led to a truncated RelA protein product missing 60 amino acids of the highly conserved C-terminal transactivation domain (TAD). These editing events have been termed RELA trunc. Pigs heterozygous or homozygous for the RELA trunc edit are healthy and viable under normal husbandry conditions, however the NF-κB signalling pathway was found to be altered (described in Chapter 3). It has been proposed previously that a reduced transcriptional response of warthog RelA compared to domestic pig RelA may underlie tolerance to ASFV infection (Palgrave et al., 2011). The RELA trunc edited pigs were identified to have a delay in upregulation of RelA-target genes *in vitro* following TNFα stimulation, it was hypothesised that these animals would display an altered response to ASFV infection. There are two main objectives for the experiments described in this chapter. The first objective was to determine whether the porcine RELA-editing impacts on the cytokine response to ASFV infection *in vitro* and *in vivo* and the second objective was to evaluate the impact of RELA-editing on the clinical outcome and mortality of animals infected with a high virulence ASFV isolate.

4.1.1 Aims

The main aims of this chapter are:

iv) To investigate the impact of RELA trunc on the upregulation of ASF-associated cytokines in ASFV infected macrophages *in vitro.*

v) To investigate the impact of RELA trunc on the outcome of infection with the highly virulent ASFV isolate Benin 97/1 *in vivo*.

4.2 Results

4.2.1 *In vitro* ASFV challenge

To investigate the impact of the RELA trunc genotype on the cytokine response to ASFV infection, macrophages derived from wild-type, heterozygous and homozygous RELA trunc animals were infected with ASFV *in vitro* for analysis of cytokine production during infection. Quantitative real-time PCR (qRT-PCR) was utilised to examine the cytokine gene expression response and production of secreted pro-inflammatory cytokines were examined using enzyme-linked immunosorbent assays (ELISAs). All laboratory work with ASFV was carried out at the SAPO CL4 (Specified Animal Pathogens Order Containment Level 4) biocontainment facility at the Pirbright Institute, Surrey.

Bone marrow cells were isolated from the ribs of 16-week old pigs, 5 animals from each RELA genotype (i.e. wild-type, heterozygous and homozygous RELA trunc; see Section 2.4.6). After extraction, the cells were immediately cryopreserved and stored at -80°C until transportation to the Pirbright Institute. At the Pirbright Institute, high virulence isolate Benin 97/1 and the low virulence isolate OURT 88/3 were propagated in pig bone marrow macrophages (see Section 2.6.3). These isolates were selected as both are members of the same virus genotype, Genotype 1 (Chapman et al., 2008). The virus was harvested and concentrated by a centrifugal method, described in Section 2.6.4. An indirect immunofluorescence assay, which detects viral protein 72, was used to titrate each virus by limiting dilution (see Section 2.6.2). Prior to infection with ASFV, the cryopreserved bone marrow cells isolated from RELA-edited and control pigs were thawed and cultured on non-tissue culture treated dishes with human recombinant CSF-1, to stimulate maturation of monocytes into macrophages. The adherent cell populations isolated from each animal were harvested and subsequently plated at a density $1.25 \times 10^5/cm^2$ in eight wells of a 12-well plate (see Section 2.4.7-9). Macrophages were infected at a multiplicity of infection (M.O.I) of 5 with Benin 97/1 in two wells and OUR T88/3 for another two wells. Two uninfected wells were continually stimulated with 1 μg/ml of lipopolysaccharide (LPS; Sigma) and the final two wells were left as uninduced i.e. without the addition of virus or LPS. At 4 and 8 hours after infection or stimulation the cell supernatant was collected and stored at -

80°C, for ELISA analysis. After removal of the cell supernatant the adherent macrophages were washed with PBS and lysed with the Trizol (Invitrogen) which was then collected and stored at 80°C, for RNA extraction. The extracted RNA was reverse transcribed into cDNA then heat-inactivated in a water bath at 56°C for two hours before transferring to the Roslin Institute for RT-qPCR analysis (see Section 2.7.1).

Cytokine expression during *in vitro* ASFV infection

To date, few studies have revealed the effects of ASFV infection on the cytokine responses of macrophages *in vitro* (Gil et al., 2003, Zhang et al., 2006, Gil et al., 2008, Fishbourne et al., 2013a Franzoni et al., 2017). Others have studied the cytokine response in peripheral blood of infected animals (Fishbourne et al., 2013b, Zakaryan et al., 2015). A panel of 10 of these cytokine genes, found to be differentially expressed after infection with ASFV and known to be directly regulated by NF-κB, were selected for qRT-PCR analysis (Collart et al., 1990, Hiscott et al., 1993, Libermann & Baltimore., 1990, Kunsch & Rosen, 1993, Murphy et al., 1995, Schreck & Baeuerle., 1990, Hiscott et al., 1989, Hein et al., 1997, Ueda et al., 1997, Burke et al., 2014). These include proinflammatory cytokines (TNF, IL1B, IL6, IL8), immunoregulatory cytokine (IL12p40), colony stimulating factor (CSF2), interferon alpha (IFNA) and chemokines (CXCL10, CCL2, CXCL2). Two time-points, 4 hours and 8 hours, were selected to analyse the early cytokine response of ASFV-infected wild-type and RELA-trunc mutant macrophages. These time-points were chosen as they occur after viral entry and viral protein synthesis but prior to any apparent ASFV-induced cell death (Zhang et al., 2006). The expression level of each gene was normalised to the mean of cyclophilin A (PPIA) and beta-2-microglobulin (B2M) expression and the expression levels were calculated relative to the uninduced control for each macrophage line. These genes were selected for normalisation as their expression was found to remain stable under induction with LPS in porcine macrophages and are not anticipated to fluctuate during ASFV infection (Cinar et al., 2012).

Both homozygous and heterozygous RELA trunc macrophages showed a significantly lower induced expression of the pro-inflammatory cytokine TNFα (~1-fold increase) at 4 hours' post infection with virulent isolate Benin 97/1 compared to wild-type macrophages (~9-fold increase). Similarly, this difference was observed after 4 hours

with LPS stimulation (Figure 4.1). However, the induced expression of pro-inflammatory cytokine IL1B was significantly higher in homozygote macrophages (~5-fold increase) compared to wild-type macrophages (no significant change from uninduced) at 4 hours' post infection with Benin 97/1. Moreover, the induced expression of chemokines, CXCL10, CCL2 and CXCL2 was significantly higher in homozygous RELA trunc macrophages (~1-fold, ~1-fold & ~6-fold increase) compared to wild-type controls (no significant change from uninduced) at 4 hours' post infection with Benin 97/1. This significant induction of CXCL10 and CXCL2 expression was also observed at 4 hours' post-infection with non-pathogenic isolate OURT 88/3. A significantly higher expression was also observed in IL12p40 at 4 hours' post-infection (~2-fold increase) with both ASFV isolates compared to wild-type (no significant change from uninduced). No statistically significant difference in IL6, IL8, CSF2 and IFNA responses were observed in macrophages infected with either viral isolate or LPS stimulated. These results show that at the early time-point of 4 hours post-infection (PI), when the virus has entered cells and initiated synthesis of early viral proteins, the cytokine response of macrophages contain RELA trunc editing is altered. However, no significance difference was identified at the later time-point of 8 hours PI.

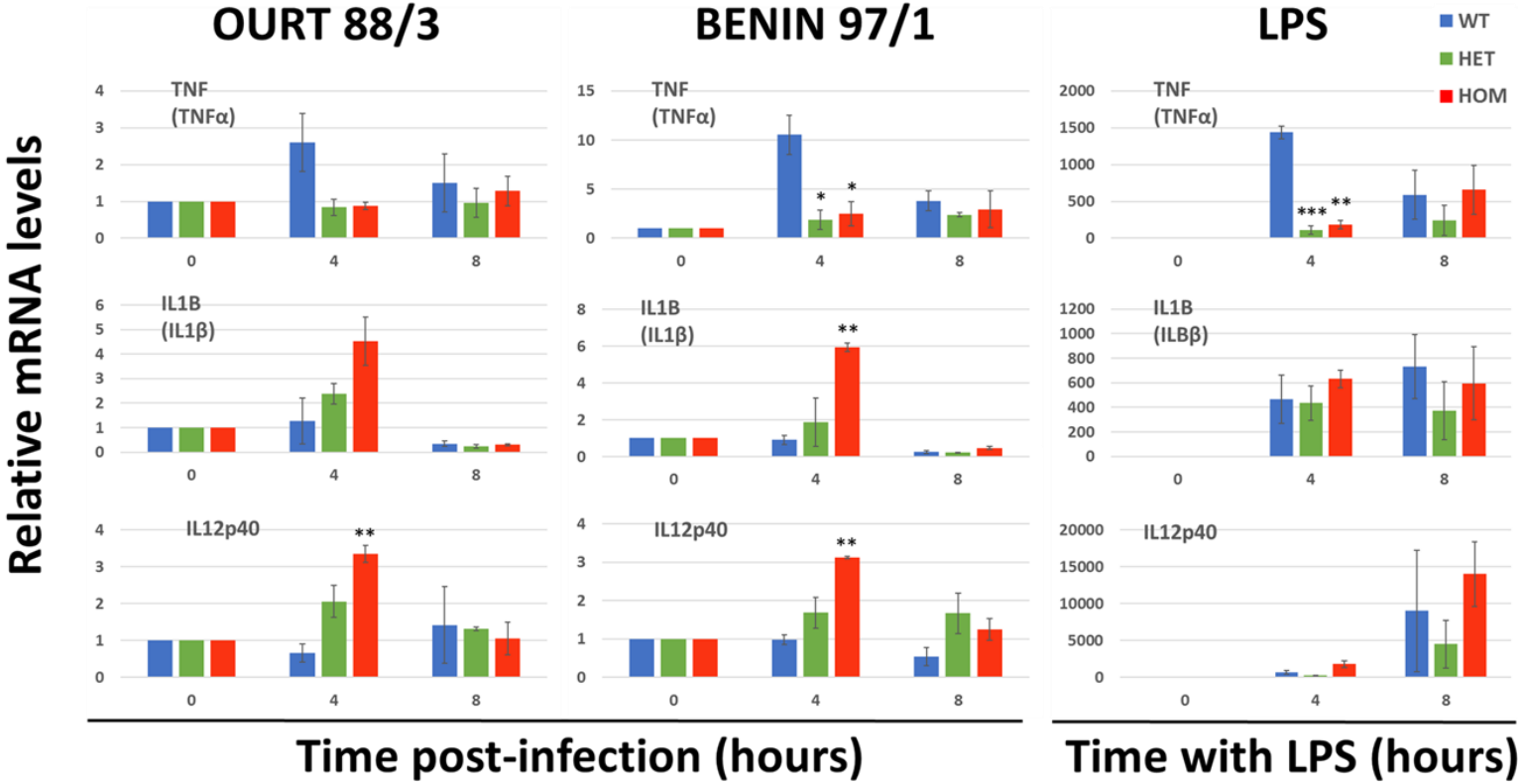

Figure 4.1 Gene expression analysis of ASFV-associated cytokine genes. qRT-PCR analysis of ASF-associated cytokine genes, TNF, IL1B and IL12p40, in macrophages containing wild-type and truncated RelA infected with pathogenic (Benin 97/1) or non-pathogenic (OURT 88/3) ASFV isolate or continuous stimulation with LPS (1 μg/ml). Relative expression was calculated by normalising to the corresponding uninduced macrophages. Significant difference was calculated between the wild-type controls (n=5) and RelA-edited (heterozygous (n=3) and homozygous (n=3)) at each time post-infection or stimulation using a Student's paired t-test. Significant difference is indicated with black symbol *($p<0.05$) or **($p<0.001$) or ***($p<0.0001$). Error bars represent the S.E.M.

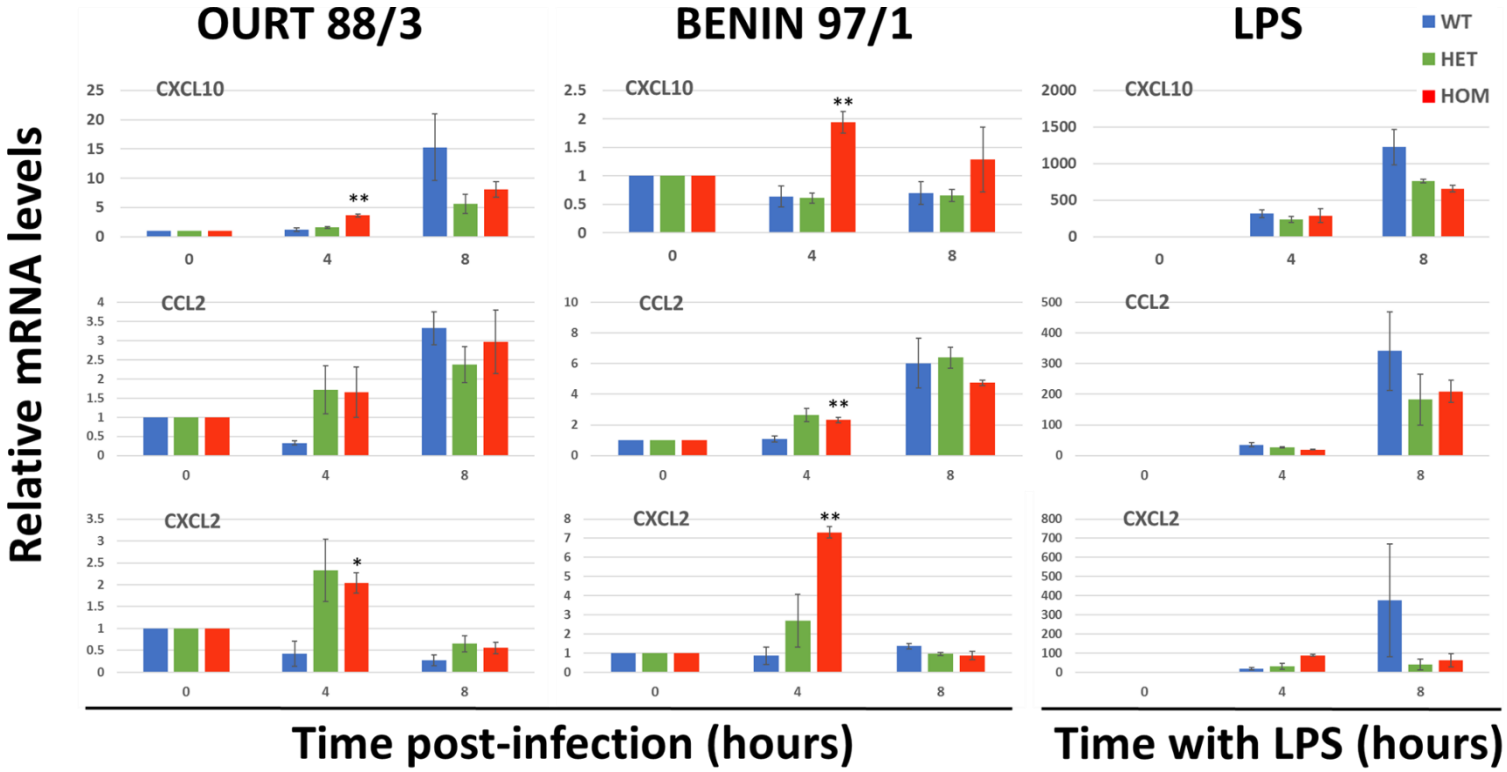

Figure 4.2 Gene expression analysis of ASFV-associated chemokine genes. qRT-PCR analysis of ASF-associated chemokine genes, CXCL10, CCL2 and CXCL2, in macrophages containing wild-type and truncated RelA infected with pathogenic (Benin 97/1) or non-pathogenic (OURT 88/3) ASFV isolate or continuous stimulation with LPS (1 μg/ml). Relative expression was calculated by normalising to the corresponding uninduced macrophages. Significant difference was calculated between the wild-type controls (n=5) and RelA-edited (heterozygous (n=3) and homozygous (n=3)) at each time post-infection or stimulation using a Student's paired t-test. Significant difference is indicated with black symbol *($p<0.05$) or **($p<0.001$) or ***($p<0.0001$). Error bars represent the S.E.M.

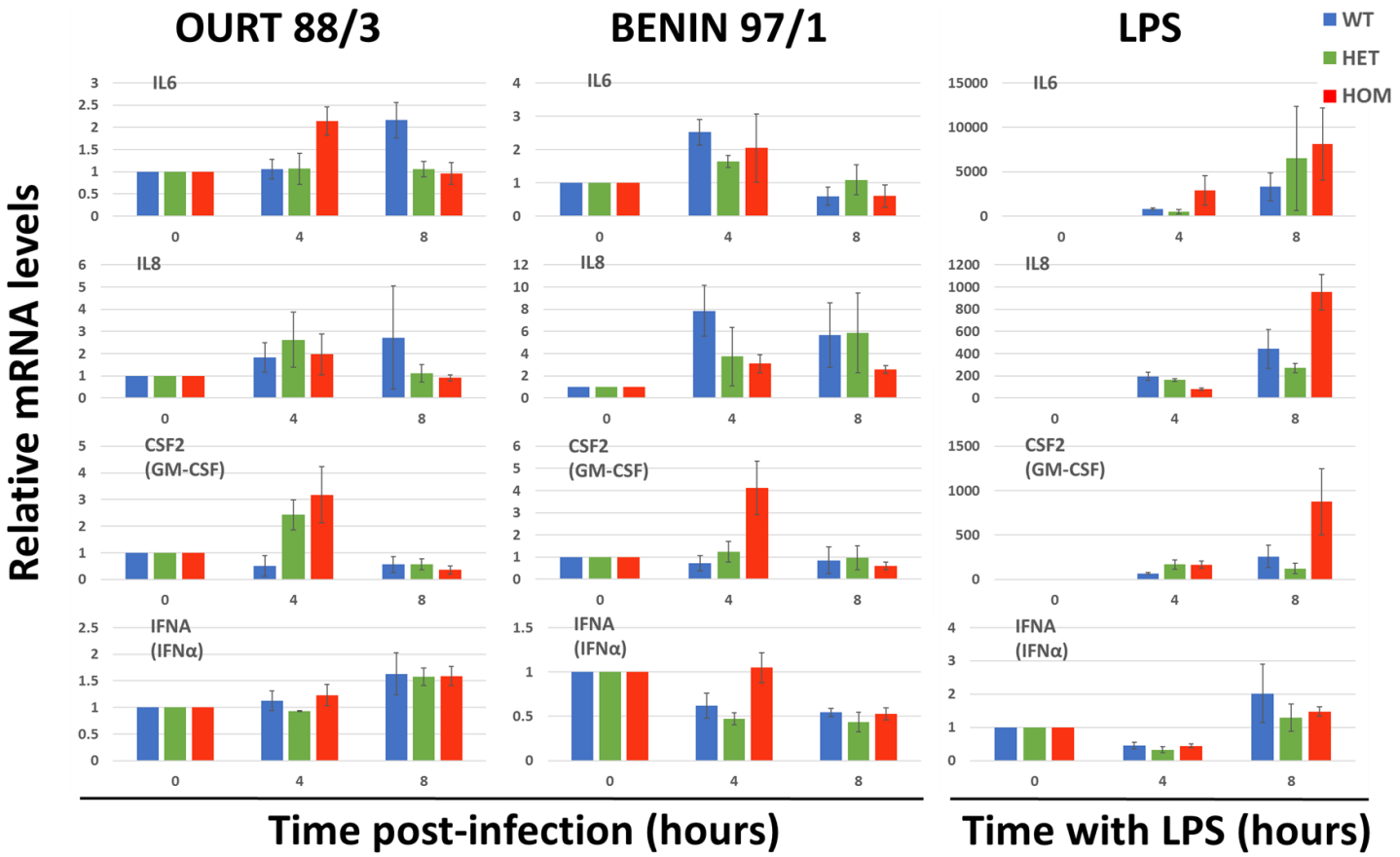

Figure 4.3 Gene expression analysis of ASFV-associated cytokine genes. qRT-PCR analysis of ASF-associated cytokine genes, IL6, IL6, CSF2 and IFNA, in macrophages containing wild-type and truncated RelA infected with pathogenic (Benin 97/1) or non-pathogenic (OURT 88/3) ASFV isolate or continuous stimulation with LPS (1 μg/ml). Relative expression was calculated by normalising to the corresponding uninduced macrophages. Significant difference was calculated between the wild-type controls (n=5) and RelA-edited (heterozygous (n=3) and homozygous (n=3)) at each time post-infection or stimulation using a Student's paired t-test. No significant difference was identified. Error bars represent the S.E.M.

Analysis of TNFα and IL-1β secretion

To investigate changes to levels of secreted cytokines *in vitro* following ASFV infection, ELISA assays were employed to measure the levels of two pro-inflammatory cytokines, TNFα and IL-1β. These cytokines are of particular interest as both have been speculated to play a major role in the pathogenesis of ASF (Gómez del Moral et al., 1999, Carrasco et al., 2002). Furthermore, the RELA trunc homozygous macrophages were shown to have altered induced expression of both TNFα and IL-1β after infection with highly virulent isolate, Benin 91/1 (Figure 4.1). To determine if the observed differences in mRNA levels translated to a similar difference in secreted protein levels, ELISA analysis was carried out. The supernatants from the experiment described previously were collected for analysis. Before ELISA analysis the supernatants were thawed and left to equilibrate to room temperature. ELISA immunoassay kits were used, following manufactures instructions, to detect porcine TNFα and IL-1β protein levels in the supernatants. Results revealed no significant difference in levels of TNFα in medium from RELA-edited macrophages compared to wild-type at any time-point (Figure 4.4), thus these results do not follow the predicted profile based on the mRNA transcript analysis (Figure 4.1). However, a significant increase in the level of IL-1β was observed in both heterozygous and homozygous samples compared to wild-type at 8 hours' post-infection with Benin 97/1. This result correlates with the finding previously that IL-1β transcripts are induced higher in RELA-edited macrophages after infection with Benin 97/1 (Figure 4.1).

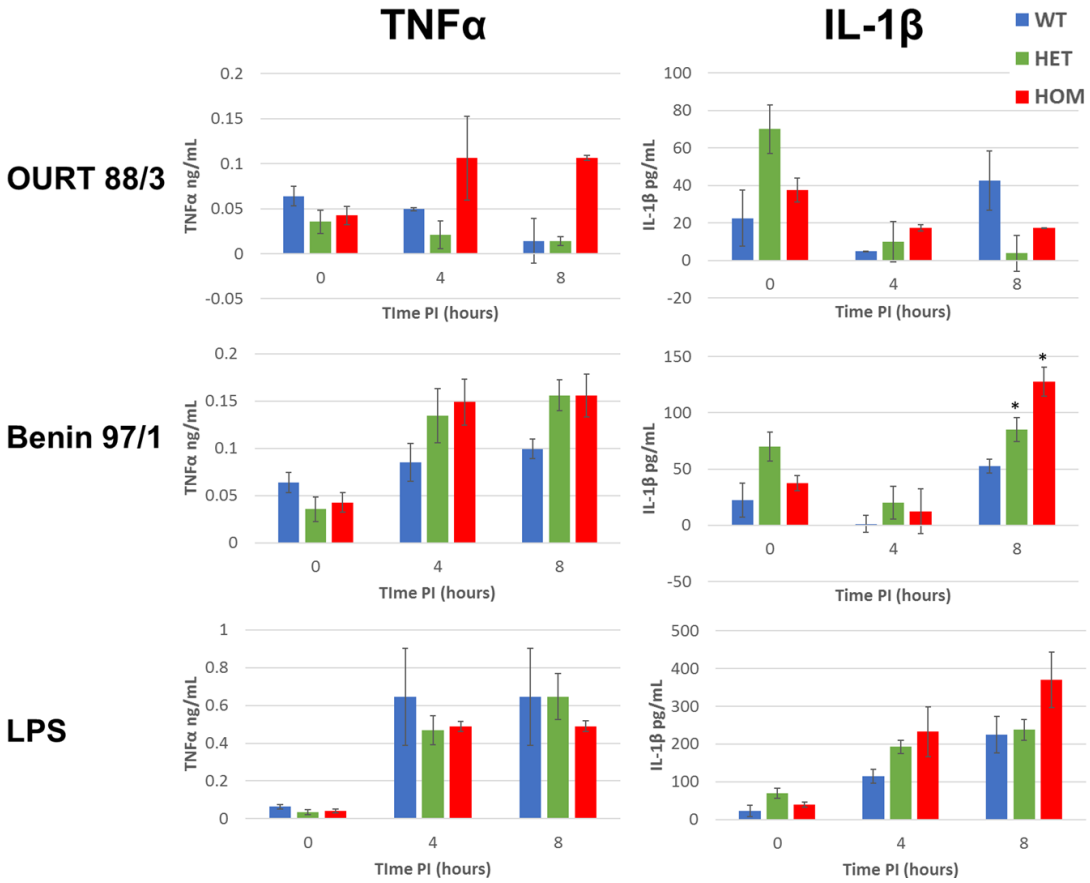

Figure 4.4 Levels of pro-inflammatory cytokines TNFα and IL-1β secreted by ASFV infected cells. A) ELISA analysis of ASF-associated cytokines TNFα and IL-1β in macrophages containing wild-type and truncated RelA infected with pathogenic (Benin 97/1) or non-pathogenic (OURT 88/3) ASFV isolate or continuous stimulation with LPS (1 μg/ml). Significant difference was calculated between the wild-type controls (n=5) and RelA-edited (heterozygous (n=3) and homozygous (n=3)) at each time post-infection or stimulation using a Student's paired t-test. Significant difference is indicated with black symbol *($p<0.05$). Error bars represent the S.E.M from five individual macrophage lines.

4.2.2 *In vivo* ASFV challenge

To determine the differences in immune and pathogenic responses between control pigs and the RELA trunc edited pigs a live animal challenge was carried out with 8 wild-type controls, 8 heterozygous and 8 homozygous for the RELA trunc edit. These animals were born and housed at the Roslin Institute's animal facility until 8 weeks of age before transporting to biosafety level 3 (BSL3) animal biocontainment facilities at the Pirbright Institute. Ear tags were assigned to each pig before transporting and the Pirbright animal caretakers and researchers were blind to the genotype of each pig. At the Pirbright animal facility, the pigs were housed 6 per room in a total of 4 rooms. Each room was to contain 2 pigs from each cohort. The animals were acclimatised to this new environment for 4 days before initiation of the pilot ASFV challenge study. The Pirbright Animal Welfare and Ethical Review Committee requested a pilot study be carried out with 2 animals from each cohort (i.e. 2 controls, 2 heterozygous and 2 homozygous for the RELA trunc edit) to ensure clinical signs of RELA-edited pigs were not more severe than control pigs before proceeding with full experiment. However, due to a misinterpreted ear tag identification number (#9 was selected instead of #6) the pilot study consisted of 2 controls, 3 heterozygotes and one homozygote. All animals were infected via intramuscular injection with 1ml containing 10^4 HAD_{50} of high virulence ASFV isolate Benin 97/1.

Throughout the experiment clinical signs and rectal temperatures were monitored twice daily. A clinical sign score was assigned based on pig's temperature, appetite, recumbency, and any skin haemorrhages, joint swelling, laboured breathing, ocular discharge, diarrhoea or vomiting (see Appendix D for clinical scoring guidelines). Animals were to be terminated when symptoms had reached a clinical score of ≥6 or they displayed the following; a fever above 40.5°C at the beginning of the third consecutive day and/or not eating for a second consecutive day. Animals were terminated by injection of a lethal dose of pentobarbital and necropsies were carried out by or under the supervision of Dr Pedro Sanchez-Cordon.

Clinical signs

After infection with Benin 97/1, all pilot experimental animals displayed a change in behaviour from alert and bright on day 0 to lethargic and depressed at day 3 PI. Moreover, an increase in temperature and clinical signs (including loss of appetite, lethargy and recumbency) was observed in all pigs at day 3 PI. Overall, no substantial difference in clinical signs was identified between RELA-edited and control pigs. However, the homozygous pig displayed a lower temperature at day 3 PI compared to the others (see Figure 4.5). The pilot study was terminated at day 4 PI, although moderate severe end-point had not been met; all animals displayed inappetence, fever and recumbency. The clinical signs of the RELA-edited pigs in the pilot study appeared to be less severe than the control pigs, although significance was lacking due to sample size. As the disease in the edited animals was no more severe than controls we proceeded with the full experiment by infecting all remaining pigs with Benin 97/1.

The remaining cohort included 6 wild-type controls, 5 heterozygous and 7 homozygous animals. These pigs were infected intramuscularly with 1 ml containing 10^4 HAD_{50} of high virulence ASFV isolate Benin 97/1 as in the pilot study. At day 3 PI, all animals had an increased rectal temperature. With exception of a single control animal which appeared lethargic no other clinical signs were apparent. At day 4 PI, all animals displayed varying levels of recumbency and loss of appetite. One homozygous animal (ID #17) displayed a second consecutive day of fever above 40.5°C and erythema (redness of the skin) on left ear, and was euthanised for necropsy at day 4 PI before reaching the moderate severe end-point. The remaining animals did not display clinical signs severe enough to reach the moderate severe end-point at day 4 PI. On the morning of day 5 PI, one control (ID #13) and one homozygous pig (ID #11) were found dead in their pens. The remaining live pigs had all stopped eating and displayed a fever and varying levels of recumbency. Only one homozygote pig (ID #12) met the moderate severe endpoint on day 5 PI, however, due to the sudden deaths of the two animals, the decision was made to terminate the experiment so all pigs were euthanised and necropsies were performed. Unfortunately, another homozygote pig (ID #23) died before euthanasia in the morning of day 5 PI. The sudden deaths of these animals were not anticipated but as the group contained both control and RELA trunc animals it is unlikely to have been caused by the RELA trunc genotype.

Collated data from both the pilot and main experiment show the mean temperatures increased from 39°C on day 0 to approximately 41.0°C on day 4 PI for all genotypes (see Figure 4.5). There was no statistically significant difference between the three RELA genotypes on any day post infection ($p>0.3$). Overall, there was no observable difference in clinical signs between control and RELA-edited pigs.

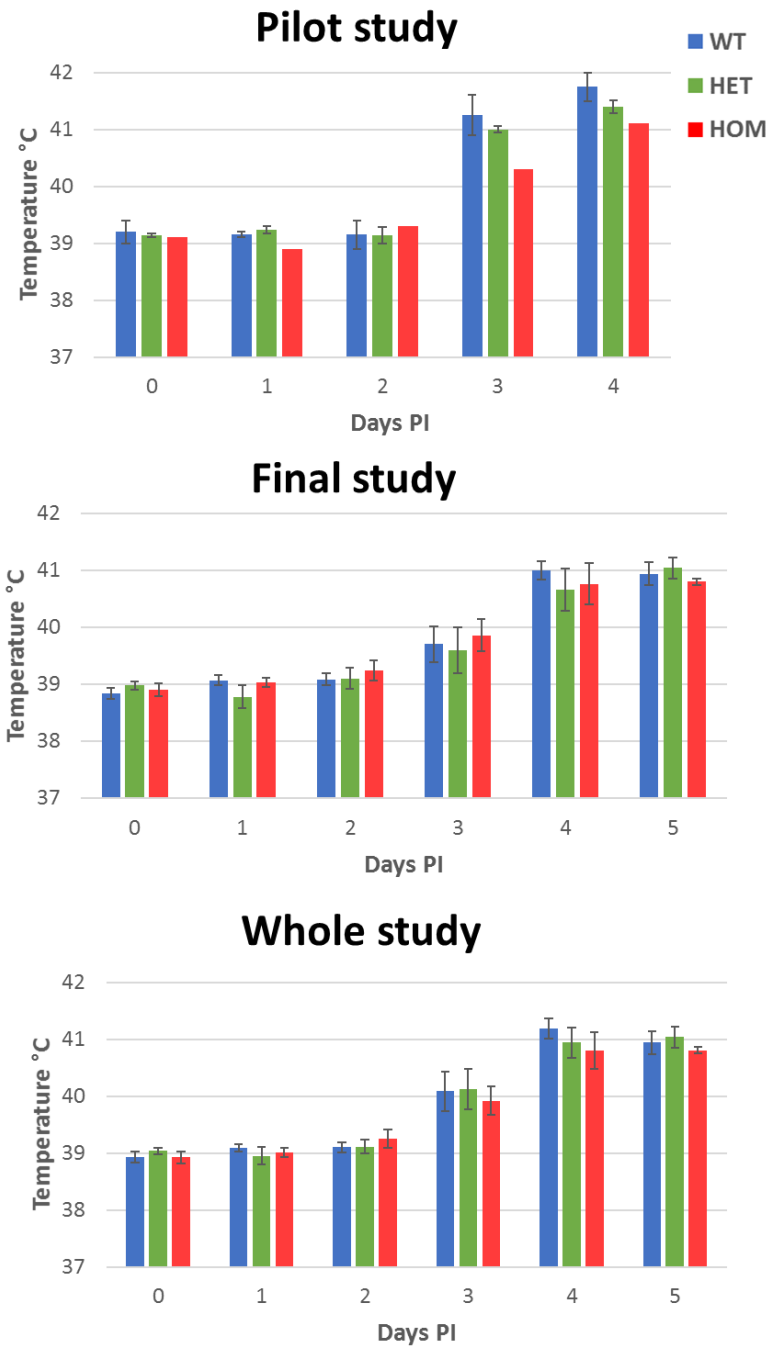

Figure 4.5 Rectal temperatures of wild-type (WT) and knockout (KO) pigs infected with high virulence ASFV isolate, Benin 97/1. A students t-test analysis showed no significant difference between temperatures of WT and RELA-edited pigs on any day ($p>0.3$). Error bars represent means with standard deviations.

Pathology

Necropsies were performed on all animals. Macrolesion scoring was carried out during each post-mortem under the supervision of veterinary pathologist Dr Pedro Sanchez-Cordon. Details of the macrolession scoring system can be found in the Appendix E. Necropsies of pilot study animals revealed the presence of gross lesions characteristic of acute forms of ASF such as hydropericardium, ascites, retroperitoneal edema, hemorrhagic lymphadenitis (gastrohepatic and renal lymph nodes being the most severely affected), hyperemic splenomegaly as well as petechiae in lungs, gallbladder and kidneys (cortex and medulla). In necropsies of the main study animals, many of the pigs displayed more severe macroscopic lesions, also characteristic of acute ASF, such as cyanotic and haemorrhagic areas on skin (ears, chest, abdomen, tail, limbs, perianal area), severe hydropericardium and ascites, non-collapsed lungs with interstitial and alveolar oedema as well as foam in trachea, petechial haemorrhages in lung, heart, kidney and urinary bladder, retroperitoneal oedema, severe hepatic congestion and oedema in gallbladder wall, hyperaemic splenomegaly and haemorrhagic lymphadenitis affecting submandibular, retropharyngeal, tracheobronchial, gastrohepatic, renal and mesenteric lymph nodes (see Figure 4.6).

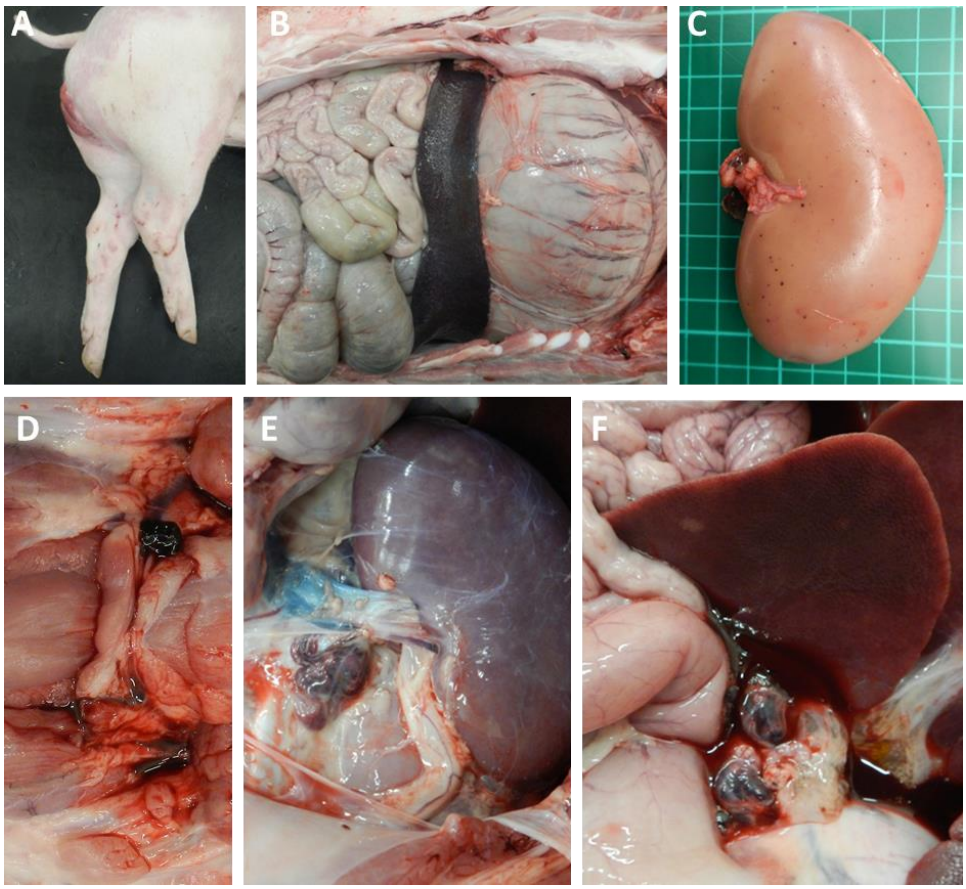

Figure 4.6 Examples of the main lesions observed in both wild-type and RELA-edited pigs post infection with high virulence ASFV isolate Benin 98/1. A. Cyanotic and haemorrhagic areas on skin (limbs and perianal area); B. Enlarged purple/black spleen (hyperemic splenomegaly) C. Petechial haemorrhages in kidney (cortex); D-F. Tracheobronchial, renal and gastrohepatic lymph nodes with various degrees of haemorrhagic lymphadenitis.

Lesions typical of ASF were observed more frequently and/or severely in the final experiment compared to those observed during the pilot experiment, possibly due to euthanasia occurring one day later PI (Fig. 4.7.A). No statistical difference in the total macroscopic lesions were found between the control and RELA trunc pigs. However, a significant difference was identified between gall bladder scoring of control and homozygotes ($p = 0.0345$), with oedema identified in the gallbladder of 5/8 of the homozygous pigs and only in 1/8 of the wild-type control pigs (Figure 4.7.B).

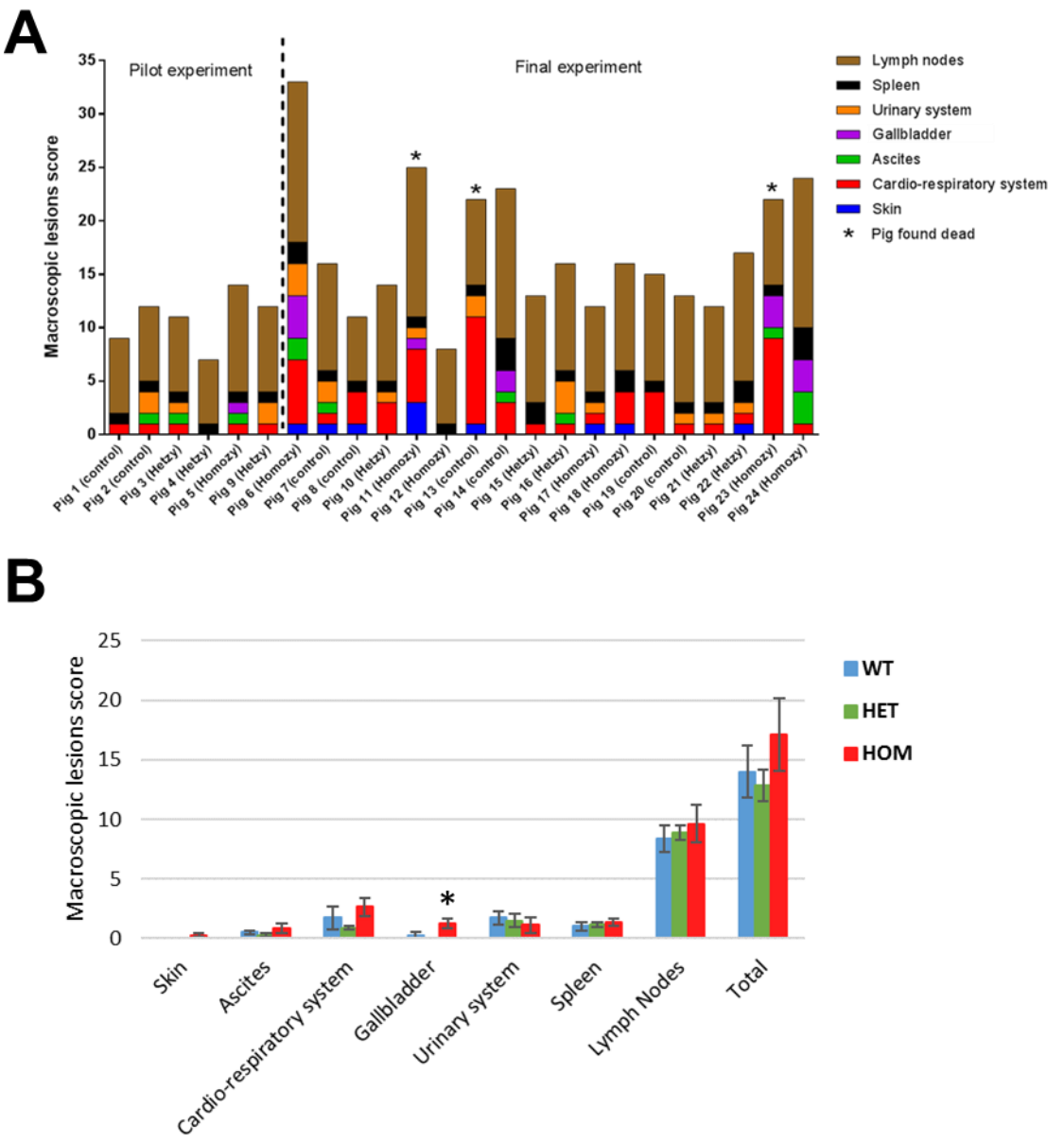

Figure 4.7 Macrolesion scoring. A) Macrolession scoring for individual animals at termination. B) Macrolession scoring for each cohort, wild-type, heterozygous and homozygous for the RELA trunc mutation. Significant difference was calculated between the wild-type controls (n=8) and RelA-edited (heterozygous (n=8) and homozygous (n=8)) at each category using a Student's paired t-test. Significant difference is indicated with black symbol *($p<0.05$). Error bars represent the S.E.M.

Analysis of cytokine expression in whole blood during ASFV infection

During the experiment, blood samples were collected from each pig at day 0, day 3 or 4 (day 3 for pilot study and day 4 for final study) and at termination. Due to difficulties in bleeding pigs, blood samples were not obtained from some animals. RNA extraction, approximately 3 ml of whole blood was collected into Tempus™ blood RNA tubes containing 6 ml of Stabilizing reagent (Applied Biosystems). RNA was extracted from whole blood and reverse transcribed to cDNA. The cDNA was heated at 56°C for 2 hours to ensure inactivation of any contaminating virus before transporting to the Roslin Institute. The same panel of 10 cytokines analysed in the *in vitro* experiment were assessed again in the blood samples by qRT-PCR (see Section 2.7.3). The expression level of each gene was normalised to the mean of cyclophilin A (PPIA) and beta-2-microglobulin (B2M) expression and the expression levels were calculated relative to the uninfected control for each animal. Comparisons between groups were made at day 4 PI and at day 6 PI (i.e. termination). The total number of bloods analysed at day 4 PI included 6 wild-type controls, 5 heterozygotes and 6 homozygotes; and analysis at day 6 PI included 6 wild-type controls, 6 heterozygotes and 4 homozygotes. The results show that the relative mRNAs levels for chemokines CXCL10, CCL2 and CXCL2 were significantly lower induced at least one time-point following infection in the RELA-edited animals compared to the wild-type controls (Figure 4.8). It is also worth noting that the induction of TNF, IL1B, IL6, CXCL2, CSF2 and IFNA in the homozygote animals was lower with low variability compared to the other genotypes at day 6 PI, although this difference was not statistically significantly based on a Students paired t-test.

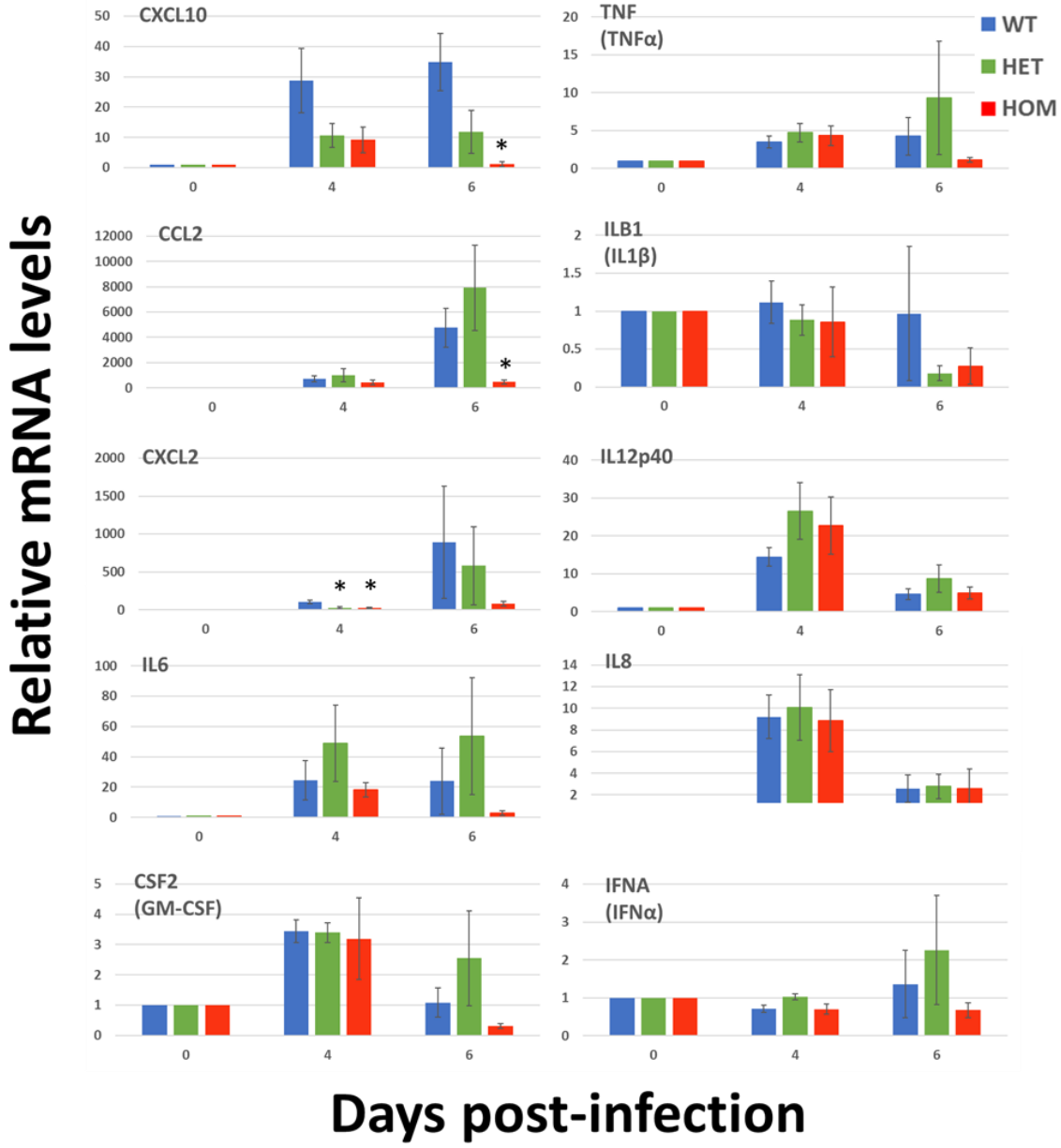

Figure 4.8 Blood transcript levels over time of animals from final study. qRT-PCR analysis of ASF-associated cytokine genes (CXCL10, IL1B, CCL2, CSF2, CXCL2, IL6, IL8, IL12p40, TNF, IFNA) in whole blood of wild-type and RELA-edited pigs after infection with pathogenic Benin 97/1 ASFV isolate. Relative expression was calculated by normalising to the corresponding uninfected animal (blood taken at day 0). Significant difference was calculated between the wild-type controls ($n \geq 6$) and RelA-edited (heterozygous ($n \geq 6$) and homozygous ($n \geq 4$)) at each time post-infection or stimulation using a Student's paired t-test. Significant difference is indicated with black symbol *($p<0.05$). Error bars represent the S.E.M.

4.3 Discussion

The ASF virus is likely to have evolved to carefully manipulate its natural hosts, including soft ticks, bushpig and warthog, in a persistent sylvatic cycle of infection. ASFV and *Sus scrofa* have not co-evolved, and ASFV infection generally leads to a rapid haemorrhagic disease with an extremely high mortality rate; fatal pathologies may occur before infected animals can mount an adaptive immune response. Elevated production of pro-inflammatory cytokines by infected macrophages are speculated to cause the rapid onset of ASF pathogenesis that leads to death in the domestic pig (Gómez del Moral et al., 1999, Gil et al., 2008).

The overall aim of the Whitelaw group is to genetically engineer an immune response in the domestic pig for tolerance of ASFV infection, similar to that of the warthog. To achieve this an understanding of the genetics underlying the tolerance of the natural hosts to infection with ASFV is required. A previous study identified variation within porcine RELA as a likely candidate (Palgrave et al., 2011). The three functional changes identified in warthog RELA results in the loss of three possible phosphorylation sites present in the TAD domain of domestic pig RelA. This is hypothesised to cause an altered transcriptional response to infection with ASFV. RelA is a prominent regulator of cytokines associated with ASF pathogenesis. It is also worth noting that RelA is a known regulator of both pro- and anti-apoptotic genes (Baldwin et al., 2001, Barkett and Gilmore., 1999, Kasibhatla et al., 1998, Pahl., 1999, Campbell et al., 2004). Virulent ASFV isolates are known to repress the apoptotic response of infected macrophages, likely promoting the survival and dissemination of the virus (Sierra et al., 1991, Sánchez-Cordón et al., 2008). Conversely, apoptosis of uninfected bystander lymphocytes is induced by ASFV infected macrophages, which is thought to play a major role in ASF pathogenesis (Oura et al., 1998).

It has been proposed that a reduced NF-κB activation may subdue the rapid onset of ASF pathogenesis allowing time for an adaptive immune response to the virus to initiate immunity (Palgrave et al., 2011). We hypothesised that ASFV infected macrophages would retain a similar delay in transcription response to TNFα observed in fibroblast cells containing the RELA trunc mutation (see Chapter 3). An altered cytokine response to infection with virulent isolate Benin 97/1 was identified in

homozygous and heterozygous macrophages *in vitro* compared to wild-type controls (see Section 4.2.1).

4.3.1 Examination of *in vitro* results

Macrophages were infected with either a high virulence isolate, Benin 97/1, or low virulence isolate, OURT 88/3. The clinical outcome varies depending on the ASFV viral isolate. Most ASFV isolates are considered highly virulent, like Benin 97/1, with infection resulting in a highly acute disease with 100% mortality. However, some isolates are of moderate virulence with 50% mortality or low virulence with no fatalities. Low virulence isolate, OURT 88/3 is naturally attenuated and can provide infected pigs with protection against subsequent challenge with related virulent isolates (Oura et al., 2005, King et al., 2011). However, OURT 88/3 infection often induces mild clinical symptoms with an extremely low mortality rate (Boinas et al., 2004., Oura et al., 2005., King et al., 2011). Previous reports focus on comparing the cytokine responses of host macrophages to infection with either low virulence and high virulence ASFV isolates (Gil et al., 2003, Zhang et al., 2006, Gil et al., 2008, Fishbourne et al., 2013a). Understanding of the different cytokine responses of macrophages infected with isolates of differing virulence could indicate which responses are necessary for developing sufficient immune response or for inducing the ASF pathogenesis.

In previous studies, mRNA levels of the pro-inflammatory cytokine TNFα were significantly increased in macrophages infected with a low virulence isolate (NH/P68) compared to infection with high virulent isolate (L60; Gil et al., 2003., Gil et al., 2008). In contrast, in this study we observed significantly enhanced TNFα mRNA levels in wild-type macrophages infected with high virulent isolate (Benin 97/1) compared to infection with low virulence isolate (OURT 88/3). These conflicting results may be due to the effect of the different isolates used and/or the time-points examined PI. In our analysis comparing the induced mRNA levels of the RELA trunc macrophages to wild-type control macrophages, the TNFα transcript level was significantly lower at the 4 hours PI with Benin 97/1 in the RELA trunc macrophages. Conversely, the TNFα protein levels in the supernatants of ASFV-infected macrophages quantified by ELISA analysis found no significant difference between the RELA cohorts. The levels of

proteins detected by the ELISA analysis are influenced not only by the mRNA levels but also by the protein translation, processing, stability and secretion during infection. Thus, it is possible that the increased mRNA levels of TNFα observed in the wild-type macrophages will not translate to increased levels of secreted TNFα protein levels. Alternatively, this change in mRNA level could be translated to levels of secreted protein however it was not detected at the time-points examined. Another pro-inflammatory cytokine, IL-1β, was previously been found to be differentially expressed in wild-type macrophages infected with high virulence isolate Malawi LIL20/1 ASFV compared with un-infected cells (Zhang et al., 2008). Furthermore, high virulence isolate induced higher levels of secreted IL-1β compared to the low virulence isolate OURT 88/3 (Zhang et al., 2008). In our study, differential expression of IL-1β was not observed in wild-type macrophages after infection with either isolate. Again, this may be the result of different isolates and time-points PI used in this study. However, homozygous macrophages were found to be have enhanced IL-1β mRNA and secreted protein levels after infection with virulent isolate Benin 97/1. The release of cytokines TNFα, IL-1β, IL-6 and IL-8 from ASFV infected macrophages is pro-inflammatory, pro-apoptotic and pro-coagulant, and thought to be the primary inducers of lymphocyte depletion, disseminated intravascular coagulation and haemorrhagic lesions observed in acute ASF (Gómez-Villamandos et al., 2013).

An immunoregulatory cytokine identified previously to be upregulated early in ASFV infection of host macrophages response is IL-12p40 (Gil et al 2008). This cytokine is important for the promotion of proliferation and survival of NK and T cells and the differentiation of the $CD4^+$ and $CD8^+$ T cells populations (Kim et al., 2008). The Gil et al., (2008) study identified that IL-12p40 mRNA levels were significantly increased in macrophages infected with a low virulence ASFV isolate NH/P68 (NHV). IL-12p40 is speculated to favour the host by promoting activation of T-cells vital for the formation of an adaptive immune response that is lacking in highly virulent infections. Once again, our study did not concur with the previous report, as ASFV infected wild-type macrophages upregulate expression of IL-12p40 when infected with either OURT or Benin. However, ASFV infected homozygous macrophages did display significantly increased IL-12p40 mRNA levels, with both high and low virulence

isolates. It is worth noting that IL-12p40 also acts as a chemoattractant for macrophages (Cooper & Khader., 2007). Recruiting macrophages to infection sites could be of benefit to the virus, concentrating macrophages for further cycles of infection.

A study carried out by Fishbourne et al., (2013a) of the chemokine response of *in vitro* ASFV infected macrophages found that CXCL10, CCL2 and CXCL2 amongst others where differentially expressed. Chemokines are chemotactic cytokines which promote recruitment and activation of leukocytes. CXCL10 is a chemoattractant for $CD4^+$ T-cells and was found to be upregulated in response in macrophages infected with ASFV. In accordance with the study by Fishbourne et al., (2013a), the upregulation of CXCL10 was higher in cells infected with low virulence isolate, OURT 88/3, compared to high virulence isolate, Benin 97/1. Increased levels CXCL10 were speculated to contribute to induction of adaptive immune response providing effective protection against ASFV in low virulence infections. However, CXCL10 has also been reported, together with either IL-2 or IFNα to induce apoptosis of bystander T-cells (Sidahmed et al., 2012). Chemokines CCL2 and CXCL2 were previously found to be down-regulated in macrophages infected with ASFV at 16 hours PI. In our study, analysing earlier time-points PI, the mRNA levels of CCL2 and CXCL2 were down-regulated in OURT 88/3 infected wild-type macrophages but not in Benin 97/1 in infected wild-type macrophages. In fact, CCL2 was upregulated in wild-type macrophages at 8 hours PI with both OURT 88/3 and Benin 97/1. This upregulation was significantly higher in cells infected with Benin 97/1 compared to OURT 88/3. CCL2 is involved in the recruitment of monocytes to sites of active infection, and as such could possibly act to concentrate susceptible cells for infection (Deshmane et al., 2009). CXCL2 is a chemoattract of neutrophils and elevated expression is often associated with autoimmune and inflammatory disorders (Kobayashi., 2008).

Increased IFNA expression was previously in identified in macrophages infected with the low virulence ASFV NH/P68 isolate compared to high virulence ASFV L60 isolate (Gil et al., 2008). Our results of IFNA expression are in accordance with this study, however no difference was observed between RELA genotypes. IFNA, encodes interferon-alpha (IFNα), a member of the type I interferons (IFNs). The type I

interferons are a multi-gene family of cytokines which are best known for their involvement in early antiviral responses (McNab et al., 2015). Furthermore, preincubation of porcine macrophages with either IFNα or IFNγ inhibits ASFV replication *in vitro* (Esparza et al., 1988). The ASFV multigene families 350 and 505 are involved in inhibition of host type I IFN expression and recent studies have found that deletion of these regions from the genomes of highly virulent ASFV isolates attenuates them (Afonso et al., 2004, O'Donnell et al., 2015, Reis et al.; 2016). NF-κB is known to regulate expression of both IFNβ (Hiscott et al., 1989) and IFNγ (Sica et al., 1997). Thus, inclusion of these genes in future analysis of RELA-edited animal's response to ASFV infection would be of interest due to their potential importance in the clinical outcome of ASFV infection.

It is generally accepted that ASF is caused primarily by the factors secreted by the infected macrophages. From our *in vitro* analysis, we have identified that several cytokines previously associated with ASF are dysregulated in ASFV infected homozygous macrophages compared to control cells, these include TNFα, IL-1β, IL-12p40, CXCL10, CCL2 and CXCL2. Although some studies have analysed the cytokine responses of infected macrophages *in vitro*, they often have conflicting results, likely due to differences in both the ASFV isolates used and the time-points PI analysed. It is difficult to decipher the downstream impact of these early cytokine responses on the *in vivo* disease pathogenesis. The *in vivo* response adds multiple layers of complexity influenced by the site and dose of ASFV infection along with environmental differences including factors secreted by other cells and tissues, and the downstream effects of the secreted cytokines on the surrounding uninfected cells. However, predictions can be made based on known functions of specific cytokines. It has been proposed that higher levels of IL12p40 and CXCL10 expression in response to ASFV infection may contribute to an effective immune response to low virulence isolates. As these two genes are upregulated more in macrophages homozygous for the RELA trunc mutation we could expect this to be beneficial to the host. Conversely, higher expression of both CCL2 and CXCL2 were observed in the infected homozygous cells compared to wild-type cells, potentially contributing to increased viral replication and spread.

4.3.2 Examination of *in vivo* results

An *in vivo* study was carried out to see if these changes in the ASFV induced cytokine response identified in RELA-edited macrophages translated to an altered clinical outcome to infection with Benin 97/1.

During the infection with Benin 97/1 blood samples were taken from each animal for cytokine expression analysis. Significantly lower mRNA levels of chemokines CXCL10, CXCL2 and CCL2 were identified in infected homozygous animals compared to infected wild-type controls. In an animal challenge study carried out by Fishbourne et al (2013b) a significantly higher expression of these three chemokines was observed in the whole blood of pigs infected with high virulence ASFV isolate Benin 97/1 compared to the low virulence ASFV isolate OURT 88/3, suggesting that lower mRNA levels may result in less severe clinical outcome. However, unfortunately all RELA-edited animals went on to develop acute ASF with no significant difference in their clinical outcomes to ASFV infection compared with controls.

Our *in vivo* results contrast with findings from *in vitro* analysis of infected macrophages, where mRNA levels of CXCL10, CXCL2 and CCL2 were found to be significantly higher in Benin 97/1 infected homozygous cells compared to infected wild-type cells. The *in vivo* study analysed mRNA levels in whole blood days after infection. Moreover, the cytokine response *in vivo* may be influenced by the various different cell types and the local cytokine environment present in the blood.

Acute ASF is characterised by multiple haemorrhages, lymphopenia associated with intense destruction of lymphoid tissue and disseminated intravascular coagulation, leading to death, usually within less than 10 days. In this study, clinical signs and characteristic macroscopic lesions of acute ASF were recorded. However, no analysis was made on the levels of lymphopenia, a hallmark of the disease. Lymphocyte depletion has been observed in the peripheral blood, bone marrow, spleen and lymph nodes of ASFV infected animals (Zakaryan et al., 2015). As NF-κB is a regulator of apoptosis it may have been interesting to compare the levels of lymphopenia between infected RELA trunc and control animals.

Two homozygotes and one control died before their clinical signs met the moderate severity end-point set. In retrospect, these sudden deaths make us question the design of the animal experiment. The highly virulent Benin 97/1 isolate was initially selected for this study as cytokine expression data from previous publications existed providing comparative data (Fishbourne et al., 2013a, Fishbourne et al., 2013b). It is possible that the sudden deaths occurred due to the viral dose. It has been suggested that for future experiments, testing of viral doses be carried out before initiating the main study. This would involve inoculating control pigs with different viral titres and evaluation disease progression to select optimum dose for the experiment. It may be that inoculating RELA-edited animals for slow disease progression would permit time to develop an effective immune response. In this study, we use intramuscular injection to administer ASFV however intranasal administration also exists, which may offer a more 'natural' route of infection (Sánchez-Cordón et al., 2017). Alternatively, one or two animals could be inoculated and co-housed with un-infected animals. However, this method is particularly difficult to control compared to administered inoculations.

In conclusion, our results show that live pigs carrying the RELA trunc mutation are not resilient to ASFV despite the altered RelA activity *in vitro.*

Chapter 5 Using CRISPR/Cas9 gene editing system to introduce S531P into the domestic pig RELA locus

5.1 Introduction

Polymorphisms within porcine RELA have been hypothesised to underlie resilience to African swine fever (ASF; Palgrave et al, 2011. ASF is a highly contagious lethal disease of domestic and feral pigs, caused by infection with African swine fever virus (ASFV). Domestic pigs infected with virulent ASFV isolates undergo a rapid-onset lethal haemorrhagic fever. In contrast, porcine species indigenous to Sub-Saharan Africa, such as warthogs and bushpigs, display no clinical signs post-infection with virulent ASFV isolates (Anderson et al, 1998; Oura et al, 1998; Thomson et al, 1980; Thomson et al, 1985). To date, no genetic variation is known to exist within the domestic pig populations that confers resilience to ASF. A previous study in the Whitelaw group sought out to identify genetic variation between two pig species, the highly susceptible domesitic pig (*Sus scrofa*), and the ASF resilient warthog (*Phacochoerus africanus*), that could underlie the difference in host response to ASFV infection. This lead to the discovery an intriguing candidate, after identifying functional polymorphisms in porcine RELA (Palgrave, et al, 2011).

RELA encodes for a subunit of NF-κB, which is a key transcription factor involved in, amongst other roles, activating immune and inflammatory responses. The NF-κB subunits, including RelA, are known to be evolutionary and structurally conserved across mammalian species (O'Shea & Perkins, 2008). Moreover, the NF-κB transcription factor family is suggested to have originated as far back as the beginning of the metazoan lineage (Gauthier & Degnan, 2008; Sulivan et al, 2007). Three amino acid differences were identified between the warthog and the domestic pig RelA, T448A, S485P, and S531P, which are displayed in Figure 5.1. It was demonstrated that these changes, in particular S531P, impacted on the activity of NF-κB *in vitro*; the warthog RELA displays reduced NF-κB activity in basal and induced conditions compared to the domestic pig RELA (Palgrave et al, 2011).

It was hypothesised that the warthog variant RELA had the potential to underlie the warthog's apparent tolerance to ASFV infection. In order to test this hypothesis, genetic engineering tools have been employed to introduce the warthog RELA changes into the domestic pig RELA locus. This has been achieved by members of the Whitelaw group using ZFNs (Lillico at el, 2016). ZFN encoding mRNA alongside a plasmid donor template, containing the desired warthog SNP flanked by sequence homologous to the DNA target, were delivered directly into zygotes by microinjection, before subsequent transfer into recipient sows. Three piglets born from this procedure were either heterozygous or homozygous for the desired changes. Two piglets contained all three desired warthog SNPs and one piglet was homozygous for SNPs encoding only the first two amino acid modifications (i.e. T448A and S485P).

As previously mentioned, it was observed that one SNP, causing a serine to proline change at position 531, was responsible for significantly reducing the NF-κB activity of warthog RelA (Palgrave et al, 2011). This serine site a well-characterised phosphorylation site in human RelA, which when phosphorylated increases activity of NF-κB (Wang et al., 2000). It was hypothesised that this single amino acid change between the warthog and the domestic pig caused by one SNP, may be responsible for warthog's resilience to African Swine Fever.

The following results chapter will describe the utilisation of the CRISPR-Cas9 editing system to introduce one warthog SNP, causing the serine to proline amino acid change, in the domestic pig RELA locus for the production of live edited animals.

```
SS --DLFPLIFP SEPAPASGPY VEIIEQPKQR GMRFRYKCEG RSAGSIPGER STDTTKTHPT IKINGYTGPG  [ 70]
PA --........ .......... .......... .......... .......... .......... ..........  [ 70]
BB --........ .......... .......... .......... .......... .......... ..........  [ 70]
HS MDE....... A...Q..... .......... .......... .......... .......... ..........  [ 70]

SS TVRISLVTKD PPHRPHPHEL VGKDCRDGFY EAELCPDRCI HSFQNLGIQC VKKRDLEQAI NQRIQTNNNP  [140]
PA .......... .......... .......... .......... .......... .......... ..........  [140]
BB .......... .......... .......... .......... .......... .......... S.........  [140]
HS .......... .......... .......... .......... .......... .......... S.........  [140]

SS FQVPIEEQRG DYDLNAVRLC FQVTVRDPAG RPLRLPPVLS HPIFDNRAPN TAELKICRVN RNSGSCLGGD  [210]
PA .......... .......... .......... .......... .......... .......... ..........  [210]
BB .......... .......... .......... .......... .......... .......... ..........  [210]
HS .......... .......... ........S. .........P .......... .......... ..........  [210]

SS EIFLLCDKVQ KEDIEVYFTG PGWEARGSFS QADVHRQVAI VFRTPPYADP SLQAPVRVSM QLRRPSDREL  [280]
PA .......... .......... .......... .......... .......... .......... ..........  [280]
BB .......... E......... .......... .......... .......S.. .......... ..........  [280]
HS .......... .......... .......... .......... .......... .......... ..........  [280]

SS SEPMEFQYLP DTDDRHRIEE KRKRTYETFK SIMKKSPFNG PTDPRPATRR IAVPSRSSAS VPKPAPQPYP  [350]
PA .......... .......... .......... .......... .......... .......... ..........  [350]
BB .......... .......... .......... .......... .......... .......... ..........  [350]
HS .......... .......... .......... ........S. ......PP.. .......... ..........  [350]

SS FTPSLSTINF DEFTPMAFAS GQIPGQTSAL APAPAPVLVQ APAPAPAPAM ASALAQAPAP VPVLAPGLAQ  [420]
PA .......... .......... .......... .......... .......... .......... ..........  [420]
BB .......... .......... .......A.. V......... .......--. .......... ..........  [418]
HS ..S......Y ...PT.V.P. ...-S.A... ....PQ..P. .......... V......... .......PP.  [419]

SS AVAPPAPKTN QAGEGTLTEA LLQLQFDTDE DLGALLGNNT DPTVFTDLAS VDNSEFQQLL NQGVSMPPHT  [490]
PA .......... .......... .......A.. .......... .......... .......... ....P.....  [490]
BB .......... .......... .......A.. .......... .......... .....S.... ....P.....  [488]
HS ........PT .......S.. .......-.. ........S. ..A....... .......... ...IPVA...  [488]

SS AEPMLMEYPE AITRLVTGSQ RPPDPAPTPL GASGLTNGLL SGDEDFSSIA DMDFSALLSQ ISS* [554]
PA .......... .......... .......... .......... P......... .......... .... [554]
BB .......... .......... .......... .......... .......... .......... .... [552]
HS T......... ........A. .......A.. ..P..P.... .......... .......... .... [552]
```

Figure 5.1 RelA protein alignment. The domestic pig (SS) amino acid sequence is displayed, with sequence variation in the warthog (PA), Babyrousa (BB) and human (HS) indicated underneath. The three amino acid differences, T448A, S485P, and S531P, between the warthog and domestic pig are highlighted in black. The Rel homology domain (RHD) is indicated with a single underline, the transactivation domain 2 (TA2) is dashed underlined and the transactivation domain 1 (TA1) is double underlined. The nuclear localisation signal (NLS), KRKR, is dotted underlined. Figure reproduced from Palgrave et al, (2011).

5.2 Aims

The main aims of this chapter are:

- To investigate if the serine at position 531 in porcine RelA is conserved across mammalian species.
- To use the CRISPR-Cas9 editing system to produce domestic pigs that contain the 'warthog' proline substitution at position 531 in their porcine RelA.

5.3 Results

5.3.1 Comparison of the RelA 531 site between mammalian species

In order to investigate whether the S531 of domestic pig RelA is evolutionarily conserved in mammals, an alignment was carried out, using all known mammalian RelA protein sequences present in the NCBI databases.

Out of the 88 mammalian species screened, only six did not contain the serine at the equivalent domestic pig 531 site, these include; two species of bat, the little brown bat and Brandt's bat; two species of shrew, the common shrew and the cape elephant shrew; one species of lagomorph, the American pika, and one species of swine, the warthog (Figure 5.2). Two of these species, Brant's bat and the cape elephant shrew, contain a threonine at the equivalent domestic pig 531 site. Threonine, along with serine and tyrosine residues have the potential to receive a covalently bound phosphate group (i.e. be phosphorylated). Casein kinase II (CKII) controls the phosphorylation of the equivalent pig 531 serine in humans (S529), which phosphorylates both threonine and serine residues (Wang et al, 2000; Litchfield, 2003). Thus, the threonine amino acid substitution would likely preserve the phosphorylation status of RelA. The remaining four species, the common shrew, little brown bat, pika and warthog, with an amino acid substitution at position 531 contain either a proline or an alanine residue in place of the serine, thus absolutely abolishing this phosphorylation site.

This protein alignment has revealed that the serine at 531 in the domestic pig sequence is conserved across the majority of mammalian species with a few exceptions, one of which is the warthog, which is the only swine species identified that does not contain serine at position 531. To further investigate if this amino acid substitution plays a role in the differing response to African Swine Fever virus infection between the domestic pig and the warthog, we set out engineer domestic pigs to contain the warthog proline residue at position 531.

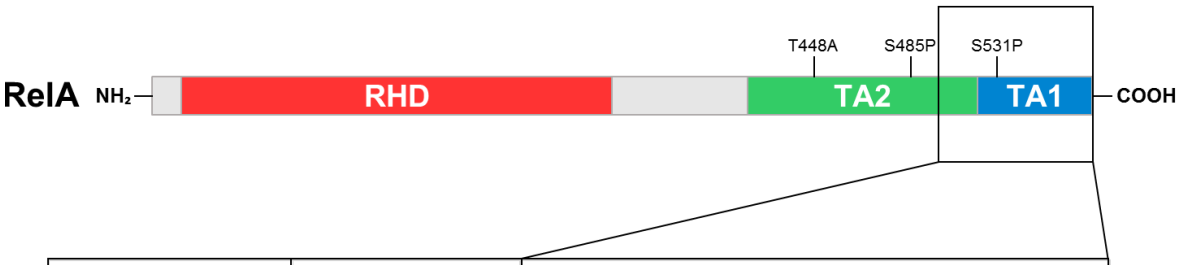

Latin name	Name	The final 60 amino acid sequence of RelA
Sus scrofa	Domestic Pig	MLMEYPEAITRLVTGSQRPPDPAPTPLGASGLTNGLLSGDEDFSSIADMDFSALLSQISS
Potamochoerus larvatus	Bushpig	MLMEYPEAITRLVTGSQRPPDPAPTPLGASGLTNGLLSGDEDFSSIADMDFSALLSQISS
Babyrousa babyrussa	Babirusa	MLMEYPEAITRLVTGSQRPPDPAPTPLGASGLTNGLLSGDEDFSSIADMDFSALLSQISS
Physeter catodon	Sperm Whale	MLMEYPEAITRLVTGSQRPPDPAPTPLGASGLTNGLLSGDEDFSSIADMDFSALLSQISS
Tursiops truncates	Bottle-nosed Dolphin	MLMEYPEAITRLVTGSQRPPDPAPTPLGASGLTNGLLSGDEDFSSIADMDFSALLSQISS
Phacochoerus africanus	Warthog	MLMEYPEAITRLVTGSQRPPDPAPTPLGASGLTNGLLPGDEDFSSIADMDFSALLSQISS
Orcinus orca	Killer Whale	MLMEYPEAITRLVTGSQRPPDPVPTPLGASGLTNGLLSGDEDFSSIADMDFSALLSQISS
Vicugna pacos	Alpaca	MLMEYPEAITRLVTGSQRPPDPAPTPLGASGLTNGLLSGDEDFSSIADMDFSALLSQIGS
Camelus bactrianus	Bactrian Camel	MLMEYPEAITRLVTGSQRPPDPAPTPLGASGLTNGLLSGDEDFSSIADMDFSALLSQIGS
Orycteropus afer afer	Aardvark	MLMEYPEAITRLVTGSQRPPDPAPTPLGASGLPNGLLSGDEDFSSIADMDFSALLSQISS
Bos Taurus	Cow	MLMEYPEAITRLVTGSQRPPDPAPTPLPPSGLTNGLLSGDEDFSSIADMDFSALLSQISS
Trichechus manatus latirostris	West Indian Manatee	MLMEYPEAITRLVTGSQRPPDPAPAPLGASGLANGLLSGDEDFSSIADMDFSALLSQISS
Leptonychotes weddellii	Weddell Seal	MLMEYPEAITRLVTGSQRPPDPAPAPLGASGLPNGLLSGDEDFSSIADMDFSALLSQISS
Odobenus rosmarus divergens	Walrus	MLMEYPEAITRLVTGSQRPPDPAPAPLGASGLPNGLLSGDEDFSSIADMDFSALLSQISS
Felis catus	Cat	MLMEYPEAITRLVTGSQRPPDPAPAPLGASGLPNGLLSGDEDFSSIADMDFSALLSQISS
Acinonyx jubatus	Cheetah	MLMEYPEAITRLVTGSQRPPDPAPAPLGASGLPNGLLSGDEDFSSIADMDFSALLSQISS
Panthera tigris altaica	Siberian Tiger	MLMEYPEAITRLVTGSQRPPDPAPAPLGASGLPNGLLSGDEDFSSIADMDFSALLSQISS
Mustela putorius furo	Ferret	MLMEYPEAITRLVTGSQRPPDPAPAPLGASGLPNGLLSGDEDFSSIADMDFSALLSQISS
Ailuropoda melanoleuca	Giant Panda	MLMEYPEAITRLVTGSQRPPDPAPAPLGASGLPNGLLSGDEDFSSIADMDFSALLSQISS
Carlito syrichta	Philippine Tarsier	MLMEYPEAITRLVTGSQRPPDPAPNPLGASGLANGLLSGDEDFSSIADMDFSALLSQISS
Pteropus vampyrus	Large Fruit Bat	MLMEYPESITRLVTGSQRPPDPAPTPLGASGLPNGLLSGDEDFSSIADMDFSALLSQISS
Chrysochloris asiatica	Golden Mole	MLMEYPEAITRLVSGSQRPPDPAPTPLGASGLPNGLLSGDEDFSSIADMDFSALLSQISS
Mus musculus	Mouse	MLMEYPEAITRLVTGSQRPPDPAPTPLGTSGLPNGL-SGDEDFSSIADMDFSALLSQISS
Manis javanica	Malayan Pangolin	MLMEYPEAITRLVTGSQRPPDPAPTPLGASGLTNGLISGDEDFSSVADMDFSALLNQISS
Ochotona princeps	American Pika	MLMEYPEAITRLVTGSQRPPDPAPAPLGASGLSNGLLAGDEDFSSIADMDFSALLSQISS
Macaca nemestrina	Southern Pig-tailed Macaque	MLMEYPEAITRLVTGAQRPPDPAPAPLGAPGLTNGLLSGDEDFSSIADMDFSALLSQISS
Saguinus labiatus	Red-bellied Tamarin	MLMEYPEAITRLVTGAQRPPDPAPAPLGAPGLPNGLLSGDEDFSSIADMDFSALLSQISS
Myotis brandtii	Brandt's Bat	MLMEYPEAITRLVTGSQNPPDPAPTPLGAAGLANGLLTGDEDFSSIADMDFSALLSQISS
Canis lupus	Grey Wolf	MLMEYPEAITRLVTGSQRPPDPVPAPVGASGLPNGLLSGDEDFSSIADMDFSALLSQISS
Sorex araneus	Common Shrew	MLMEYPESITRLVTGSQRPPDPAPAPLGAPGLSNGLLPGDEDFSSIADMDFSALLSQISS
Pan paniscus	Bonobo	MLMEYPEAITRLVTGAQRPPDPAPAPLGAPGLPNGLLSGDEDFSSIADMDFSALLSQISS
Homo sapiens	Human	MLMEYPEAITRLVTGAQRPPDPAPAPLGAPGLPNGLLSGDEDFSSIADMDFSALLSQISS
Myotis lucifugus	Little brown bat	MLMEYPEAITRLVTGSQNPPDPAPAPLGAAGLANGLLAGDEDFSSIADMDFSALLSQISS
Elephantulus edwardii	Cape elephant shrew	MLMEYPEAITRLVTGSQRPPDPAPAPLGVSGLSNGLLTGDEDFSSIADMDFTALLNQISS

Figure 5.2 The final 60 amino acid of RelA protein alignment in mammalian species. This figure displays an alignment of the final 60 C-terminal amino acids of the RelA protein in a range of mammalian species. All amino acids changes from the domestic pig are represented in red and the vertical red line indicates the position of the relevant serine residue.

5.3.2 Design and validation of short guide RNAs (sgRNAs) in fibroblasts

The CRISPR-Cas9 system derived from *Streptococcus pyogenes* was selected for the HDR-mediated allele exchange from the domestic pig S531 to the warthog P531 RELA allele. Four sgRNAs were designed to target a DSB in close proximity to the codon encoding S531 in the domestic pig. The target binding site sequences, shown in Figure 5.3, were cloned into a plasmid containing a U6 driven sgRNA and CAG driven

Cas9-2A-GFP (further details can be found in Section 2.8.2). Each of the four CRISPR plasmids were transfected into porcine embryonic fibroblasts (PEFs) using the neon electroporation system. The transfected cells were cultured for 48 hours before extracting genomic DNA for analysis. A PCR was carried out on the genomic DNA to amplify a ~300bp region spanning CRISPR target site, using RELA primers. A T7 endonuclease assay was performed on the PCR product to detect on-target cutting events (Figure 5.4). Editing was observed with all four CRISPR transfections, however it was difficult to determine which CRISPR appeared to be most active due to variation in transfection efficiencies. In all subsequent experiments, fluorescence-activated cell sorting (FACS) was used to positively select transfected cells. A GFP sort was performed on the cells following 48 hours in culture before subsequent analysis was carried out. As shown previously, editing was observed in all four CRISPRs (Figure 5.5). Quantification of the T7 gel image was carried out using ImageJ software as described in Guschin et al, 2010. CRISPR #4 was estimated to be the most efficient, so was taken forward to introduce the S531P change in HDR experiments (see following results sections). It is important to note that T7 endonuclease efficiently cleaves mis-matches of ≥2 bases long, however single nucleotide editing events are not always detected, potentially resulting in an underestimation of editing efficiency (Vouillot et al, 2015).

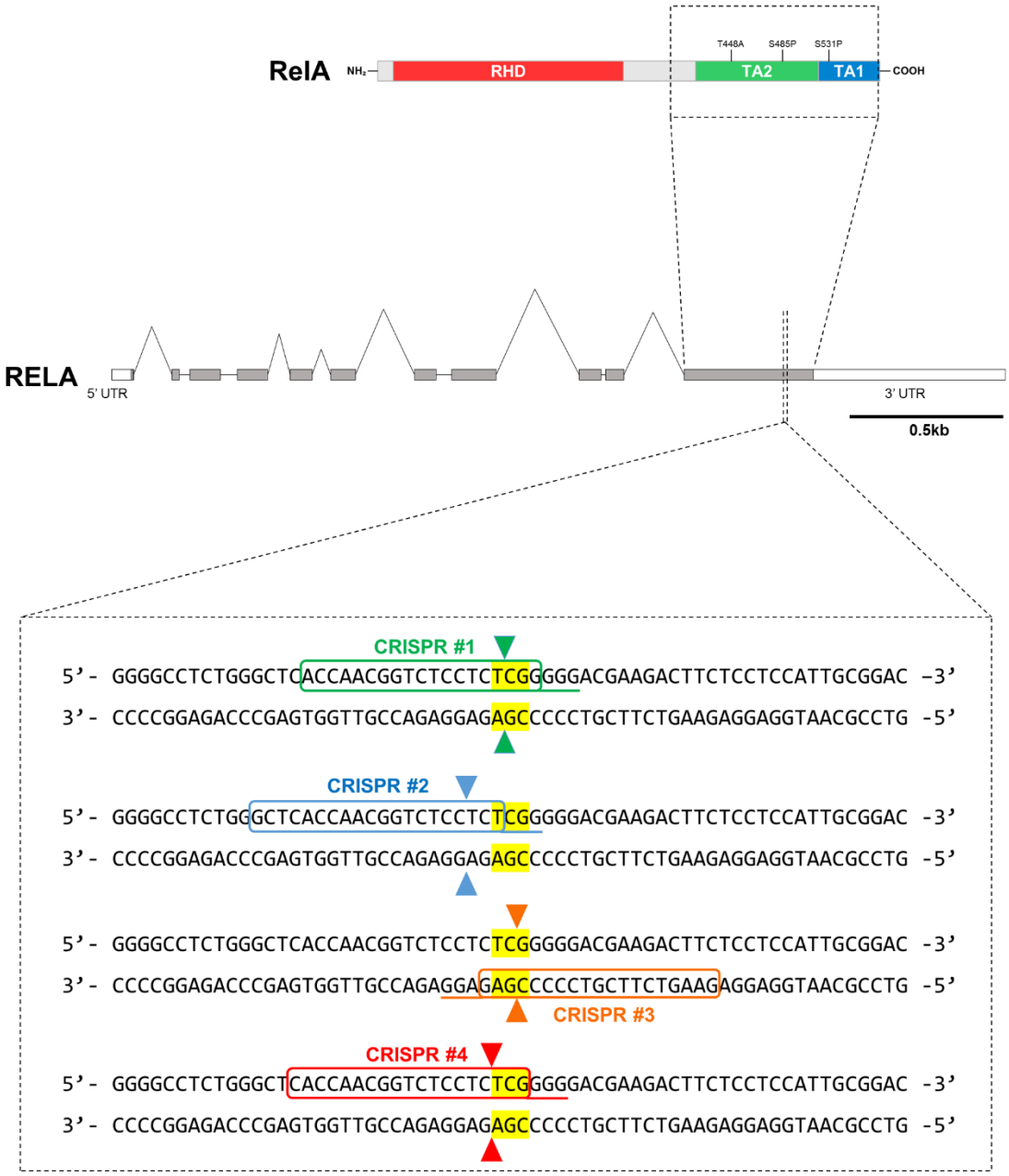

Figure 5.3 Positions of sgRNA binding site on porcine RELA. Schematic diagram showing RelA protein domains, highlighting the protein region that is encoded by the final exon of porcine RELA gene. The porcine RELA gene contains 11 exons that produce a 2.53 kb mRNA transcript. The sgRNA target region in the final exon is highlighted and target DNA sequence is displayed in the lower panel. Each sgRNA binding site is shown individually circled with the corresponding to PAM site underlined in a representative colour. All CRISPRs were designed to induce double strand breaks close to the target codon, highlighted in yellow. DSB sites are indicated with arrows.

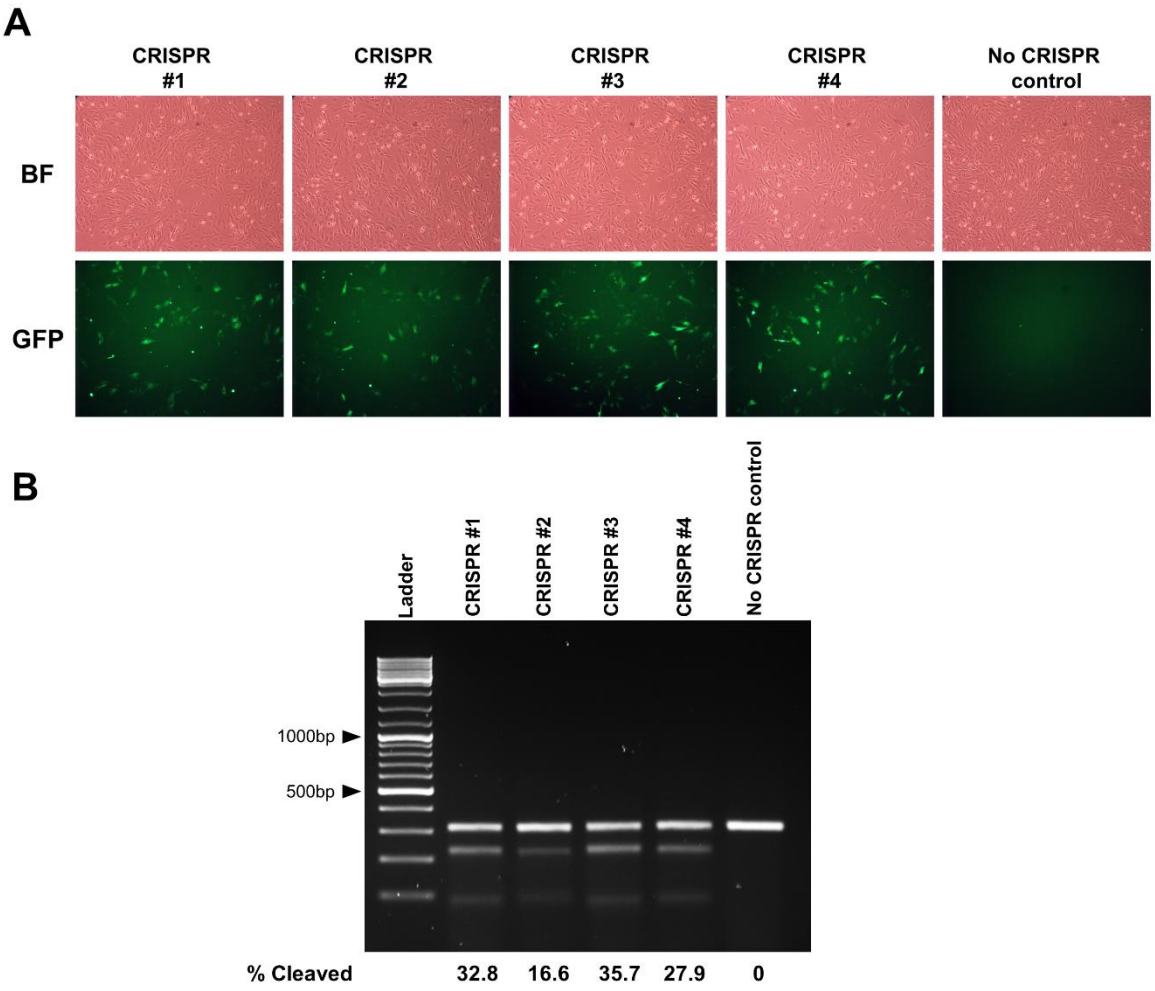

Figure 5.4 Transfection of PEFs with four CRISPRs targeted against porcine RELA. A) Brightfield (BF) and GFP images of transfection of CRISPR plasmid containing Cas9-GFP giving an indication of the transfection efficiency. B) Gel image of the T7 endonuclease assay conducted on transfected fibroblasts. Estimates for editor cutting efficiency are displayed underneath the appropriate lane.

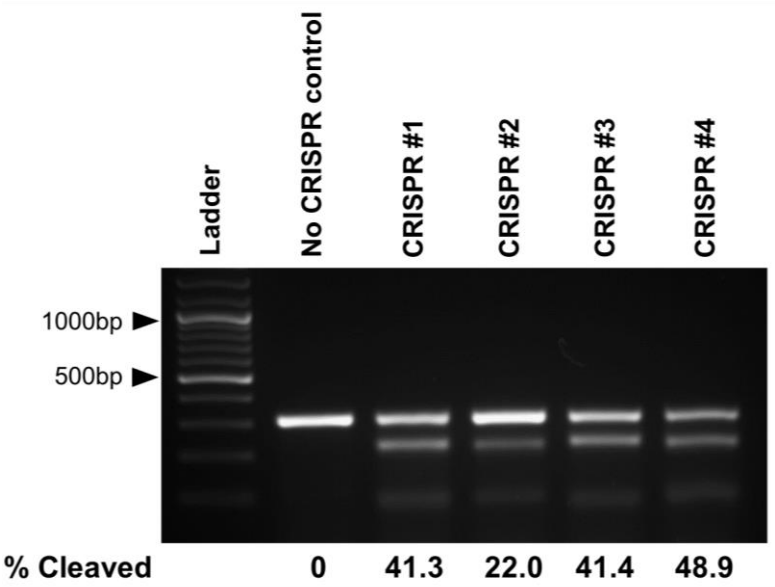

Figure 5.5 Repeat transfections of PEFs with CRISPRs targeted against porcine RELA. Transfected cells were positively selected with GFP cell sorting prior to performing a T7 endonuclease assay. The T7 endonuclease results are displayed with estimations for editor cutting efficiency underneath the appropriate lane.

5.3.3 HDR oligo design and validation in fibroblasts

For all HDR experiments in fibroblasts, CRISPR plasmid #4 was used combined with a series of single stranded oligodeoxynucleotide (ssODN) donor templates designed to introduce codon conversion (TCG to CCG) for desired serine (domestic pig) to proline (warthog) change. All donor templates contain a single nucleotide change (T to C) which introduces both the desired codon change and a novel restriction site (Xma1), enabling RFLP analysis, and a single silent nucleotide change (G to T) to disrupt the PAM site, to block further Cas9 targeting. The four ssODNs were oriented in either sense or anti-sense directions with varying homology arm designs (Figure 5.6, A-B). The 70-mer ssODNs were designed using our laboratory's standard method, in which homology arms are equal lengths with the insert sequence in the centre. The 127-mer anti-sense ssODN was designed based on findings from Richardson et al, 2016 that show an asymmetrical ssODN donor design, comprised of a 35bp homologous sequence that is complementary to the DNA fragment that is released by the Cas9 immediately after cleavage, with insert sequence on the other side of the cut followed by 86bp of homologous sequence, this was found to increase HDR efficiency in human cells by up to 60%.

Each of the four ssODNs were transfected into PEFs alongside the CRISPR #4 plasmid using the neon electroporation system. The PEFs were cultured for 48 hours before selecting GFP positive cells for extraction of genomic DNA for analysis. A PCR was carried out on the genomic DNA to amplify a ~300bp region spanning CRISPR target site, using RELA primers(see Table 2.3 for primer sequences). A T7 endonuclease assay was subsequently performed on the PCR product to confirm on-target cutting events. To estimate the HDR efficiency, RFLP analysis with Xma1 was performed on the same PCR product. HDR was detected in all cells transfected with CRISPR #4 plus each of the donor ssODNs, however the efficiency was too low for image quantification (Figure 5.6, C). This experiment was repeated resulting in the same outcome.

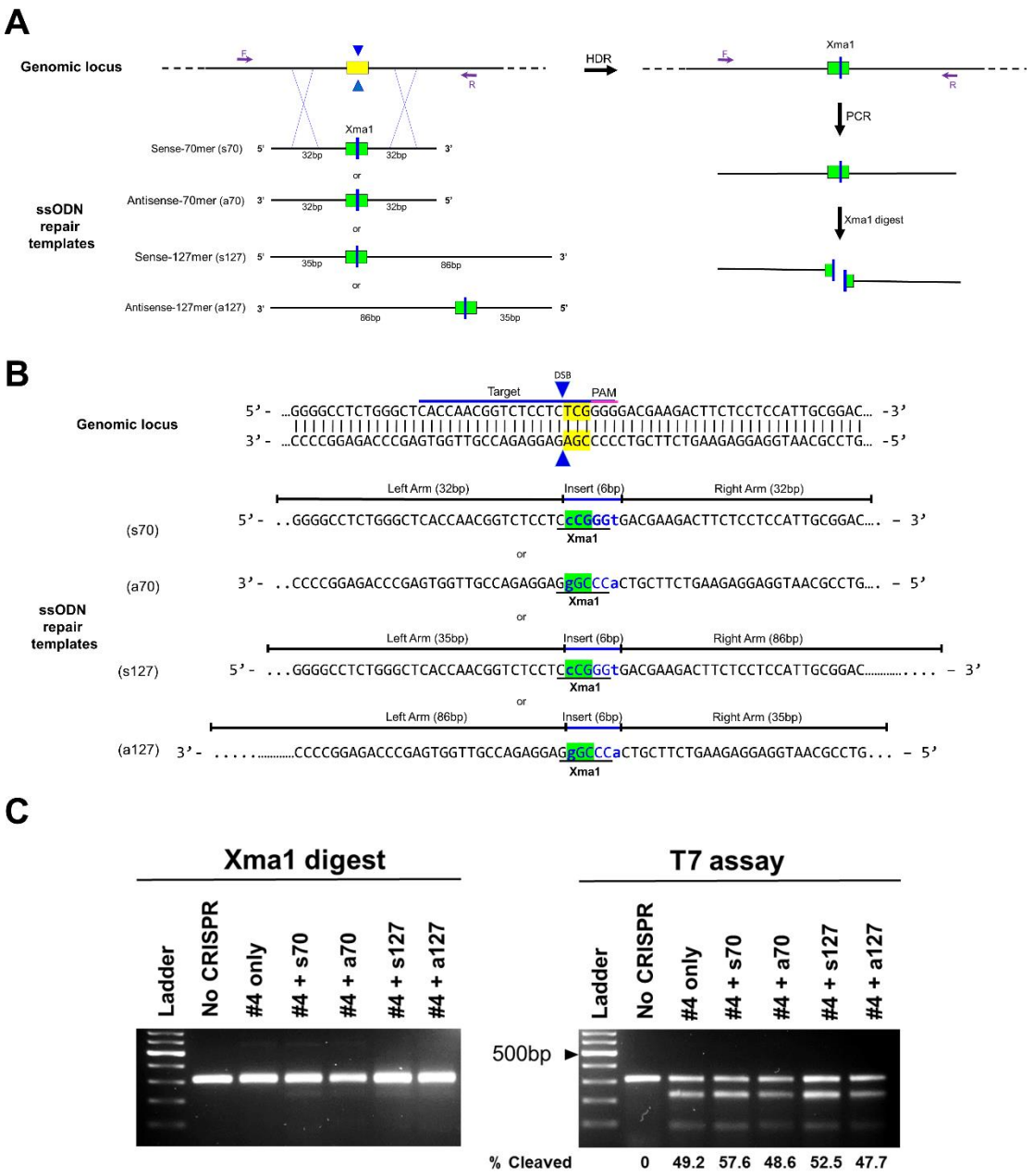

Figure 5.6 Co-transfection of ssODNs and CRISPR#4 to incorporate mutations into the RELA locus. A) The schematic shows the four ssODNs donor DNAs. Each ssODN was designed to introduce a precise change (green box) which also introduces an XmaI site into the RELA genomic locus (yellow box) following cleavage by Cas9 (blue triangle). B) ssODN donor DNAs used to incorporate mutations into the porcine RELA locus; a single nucleotide change (T→C) converts, TCG to CCG, encoding the desired S531P conversion. This same base change also introduces an XmaI site (underlined) which can be utilised to assess HDR efficiency. A second proximal single nucleotide change disrupts the PAM site to block re-cutting. The four ssODNs are oriented in either the sense or the antisense direction with varying left and right homology arm lengths. C) Agarose gel analysis of PCR products from genomic DNA of PEFs transfected with CRISPR#4 plus the ssODN indicated. RFLP with XmaI or a T7 endonuclease assay were used to assess HDR and NHEJ frequency respectively.

5.3.4 Improving HDR efficiencies

Due to the low frequency of HDR observed in the experiments described previously, it was hypothesised that the introduction of compounds known to inhibit NHEJ could be used to bias the cells repair system to HDR. The HDR experiments were repeated with the addition of NHEJ inhibitors SCR7 or L755507 in the post-transfection cell culture media at a final concentration of 1 μM and 5 μM respectively. SCR7 and L75507 were found to increase the HDR frequency in studies using mammalian cell lines and embryos (Maruyama et al, 2015; Chen et al, 2015). However, in this study the RFLP analysis clearly shows that these inhibitors did not work, neither of the NHEJ inhibitors increased the levels of HDR (Figure 5.7).

All data thus far suggested that the ssODNs were unlikely to work with a high efficiency. However, other members of the Whitelaw group have reported that the frequency of HDR is significantly higher in embryos compared to somatic cells. It is often the case that HDR is lower in somatic cell types compared to stem cell types, due to the lower fraction of cells that will be in S phase, where HDR is the primary DSB repair mechanism (Kass et al, 2012). As these editor reagents have been developed for the production of genetically engineered animals they were taken forward into the embryo despite poor frequency of HDR in fibroblasts.

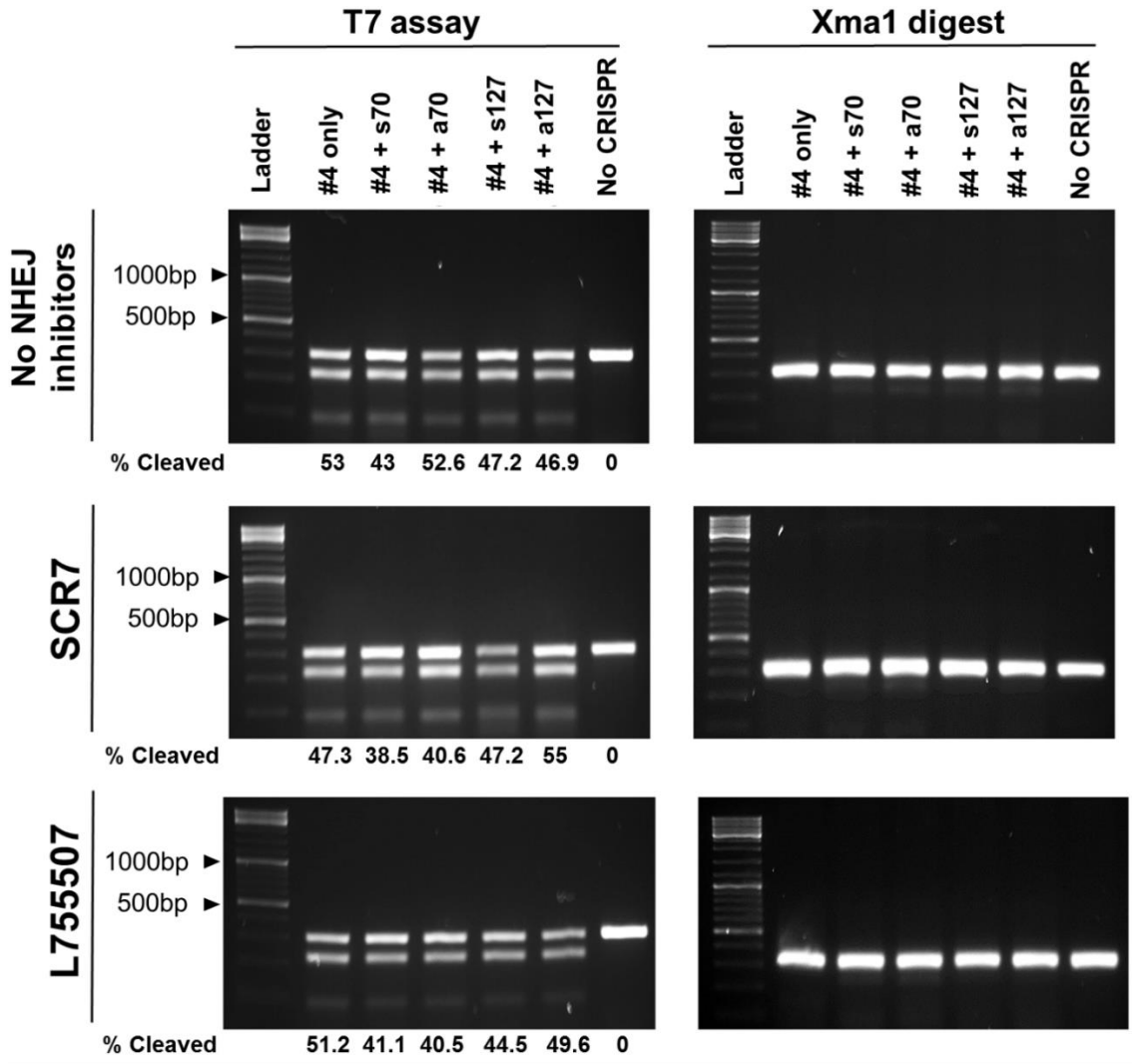

Figure 5.7 HDR results with NHEJ inhibitors. Agarose gel analysis of PCR products from genomic DNA of PEFs transfected with CRISPR#4 plus the ssODN indicated, that were subsequently cultured with or without the indicated NHEJ inhibitor. RFLP with Xma1 or a T7 endonuclease assay were used to assess HDR and NHEJ frequency respectively.

5.3.5 Porcine embryo injections

To produce genome edited pigs with the desired changes, the CRISPR-Cas9 editors and donor template were delivered into the fertilised porcine oocytes by cytoplasmic micro-injection carried out by Dr Simon Lillico. It has been reported that CRISPR-Cas9 editors are most efficient when delivered into the cell in a combination of crRNA, tracrRNA, Cas9 protein, pre-complexed before delivery, so this method was selected for this study (Aida et al., 2015). CRISPR #4 crRNA was used for all zygote injections based on the high on-target cutting efficiency the CRISPR#4 sgRNA identified in fibroblasts (see Section 2.1.2). It was not possible to quantify which ssODN was optimal based on the HDR experiments in fibroblasts (see Section 2.1.3) thus the 127-mer anti-sense ssODN was selected based on previous success reported in Richardson et al, 2016.

Each zygote was subjected to a single 2-5 pl cytoplasmic injection of a mix containing CRISPR #4 and 127-mer anti-sense ssODN. Approximately 40 injected zygotes where transferred into each of 4 recipient sows, the remaining zygotes were cultured to blastocyst stage (day 6-7) before harvesting to carry out further analysis. Blastocysts were analysed by PCR and sequencing to detect any on-target editing events.

In the first round of injections the injection mixture, referred to as Mix 1, contained CRISPR #4 crRNA and tracrRNA both at a concentration of 0.5 pmol/µl, Cas9 protein at a concentration of 0.24 pmol/µl and 127-mer anti-sense ssODN at a concentration of 100 ng/µl. The *in vitro* development of zygotes injected with Mix 1 to blastocyst stage was observed by Dr Simon Lillico to be poor compared with previous work carried out by the Whitelaw group. In contrast with Mix 1, the injection components previously used by the Whitelaw group all contained sgRNA and NEB Cas9 protein, which were both resuspended and stored in Embyromax buffer before use (see Section 2.12.3 for buffer details). Our injection mixes all contain IDT Cas9 protein, synthesised crRNA and tracrRNA, which were resuspended and stored in IDT Duplex Buffer according the manufacturer's guidelines. In preparation of Mix 1, these components were subsequently diluted in Embyromax to the desired concentration (see Section 2.8.8 for details). For the second round of injections, referred to as Mix

2, the concentration of each component was reduced by half in Embyromax buffer in attempt to reduce any toxicity effects. The development of zygotes injected with Mix 2 to blastocysts was higher compared to Mix 1 injected zygotes (microinjection mixes are summarised in Table 5.1 and *in vitro* culture results are summarised in Table 5.2).

Sequencing of the RELA locus revealed that three of the six blastocysts analysed were edited. Editing events included HDR and NHEJ events, indicated by the indel mutations identified, see Figure 5.8 for sequence traces. For one of the edited embryos, mix 1 blastocyst 2, the NHEJ editing event was identified in a lower signal intensity trace from the wild-type trace, suggesting that this embryo is mosaic for this editing event i.e. the editing event occurred in a single cell after the zygote had gone through cell division, thus not all cells contain the edited allele. The remaining two edited blastocysts, contain a wild-type trace and edited trace in their chromatogram with similar signal intensities indicating that they are heterozygotes i.e. the editing event occurred in the one cell zygote before cell division. Due to the low number of injected zygotes that developed to blastocyst stage, it was unexpected that any would contain the desired HDR editing event. However, a HDR event was identified in a single blastocyst, mix 1 blastocyst 1, confirming that the CRISPR-Cas9 reagents plus 127-mer ssODN donor template are effective in zygotes. The predicted protein changes for each of the identified editing events are displayed in Figure 5.9.

Out of the four recipient sows, two were confirmed as pregnant (embryo transfers and recipient pregnancies are summarised in Table 5.3). Despite the lower blastocyst development observed *in vitro*, the two pregnant sows were both recipients of zygotes that had been injected with Mix 1. Analysis of these animals will be carried out once they are born.

Injection mix	Conc. of CRISPR RNA (pmol/µl)	Conc. of tracrRNA (pmol/µl)	Conc. of Cas9 protein (pmol/µl)	Conc. of ssODN template (ng/ul)
Mix 1	0.5	0.5	0.24	100
Mix 2	0.25	0.25	0.12	50

Table 5.1 Injection mixes. Details of concentration of reagents used in each injection mix. All components were ordered from IDT.

Injection mix	No. of embryos cultured	No. developed to blastocyst	No. of blastocysts edited
Mix 1	30	2 of 30	2 of 2
Mix 2	23	4 of 23	1 of 4
Uninjected controls	20	7 of 20	N/A

Table 5.2 *In vitro* embryo culture results.

Injection mix	No. of embyros injected	No. embyros transfered	No. of recipients	No. of pregnancies
Mix 1	110	80	2	2 of 2
Mix 2	105	77	2	0 of 2

Table 5.3 Embryo injections and transfers.

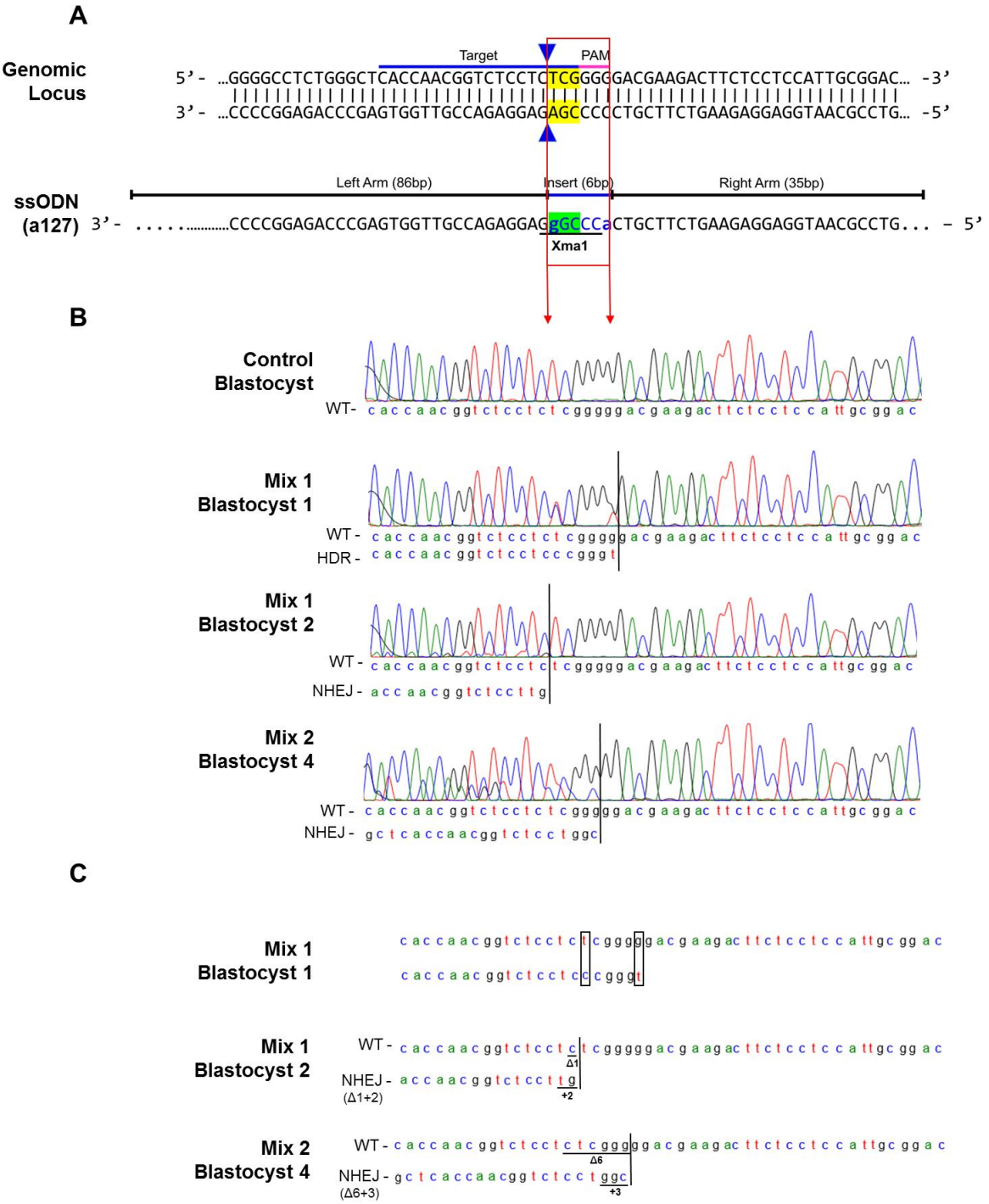

Figure 5.8 *In vitro* blastocyst sequencing analysis. A) Diagram displaying the sequence of both the genomic locus targeted for double strand break (site indicated with triangles) and the ssODN donor template. B) Sequence chromatograms from wild-type control and edited blastocysts. Note sequencing was performed using the RELA reverse primer and that the reverse complement of the chromatogram is displayed. The black line on each chromatogram indicates the start of the deviations from wild-type sequence. C) Displays the sequence reading for each trace from edited blastocysts chromatogram with HDR induced changes indicated with box and NHEJ induced mutations underlined and annotated.

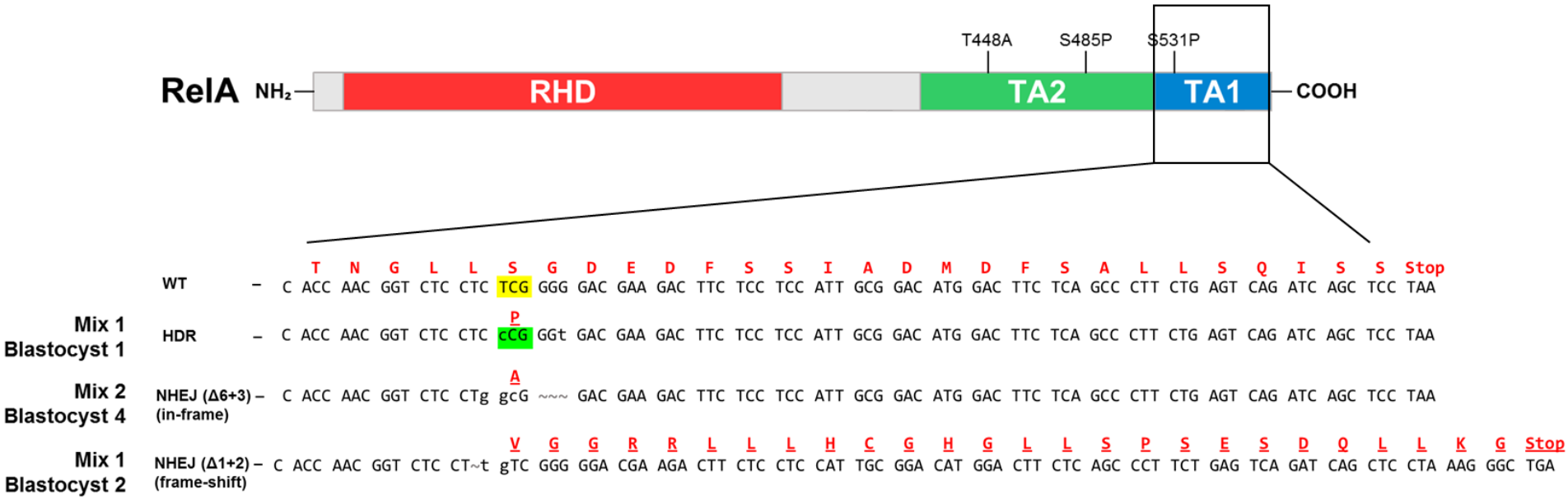

Figure 5.9 Protein coding changes based on editing events identified in blastocysts. Schematic diagram showing RelA's protein domains, highlighting the TA1 domain, which is expanded to show the amino acid sequence predicted from the blastocyst editing events identified in the final exon of porcine RELA. The DNA sequence is displayed in black with base pair changes from wild-type sequence in lower case. Above the encoding DNA sequence is the predicted amino acid sequence in red with the amino acid changes from wild-type underlined.

5.4 Discussion

Programmable nucleases have given us the capabilities to induce targeted genomic modification into virtually any organism with relative ease and success. Traditional breeding has been blindly manipulating the genomes of livestock and crops for thousands of years. With the use of genome editors, we can modify the genomes precisely to improve or alter any trait in which the underlying genetics is understood.

In this chapter I have demonstrated how CRISPRs can be used to generate a precise change into the porcine RELA locus, ultimately for the production of genetically engineered domestic pigs that are resilient to African Swine Fever.

5.4.1 Interpretation of conservation of S531 in porcine RelA across Mammalian species

Immune-related genes usually undergo rapid evolutionary change due to selective pressures induced by aggressive pathogens present within different environments. However, many of the identified putative phosphorylation sites located in the transactivation domain in RelA are highly conserved across species (O'Shea & Perkins, 2008). The equivalent 531 domestic pig serine site in humans (S529) is one of the characterised phosphorylation sites that is reportedly conserved across species. When phosphorylated by CKII, the NF-κB transcriptional activity is upregulated (Wang et al, 2000). We chose to further investigate how conserved this serine residue is in mammals by aligning all the predicted RelA protein sequences currently in the NCBI database. The equivalent domestic pig 531 serine was present in the majority of species screened, with exception of 6 species including the warthog. This has been previously hypothesised to underlie the difference in response to infection with ASFV between the domestic pig and the warthog, all other swine were found to retain this serine site. We identified that this serine site is not completely conserved across all mammalian species as five other species where identified to contain an amino acid substitution at this position. However, two of these species contained a threonine residue at this site which can also phosphorylated by CKII. The remaining three other species contain an alternative amino acid that cannot be phosphorylated, thus they will most likely display a lower NF-κB activity in response to some NF-κB signal inductions. It is conceivable that these species have obtained this change due to

evolutionary adaptation against a pathogen, as hypothesised in the warthog against ASFV.

5.4.2 HDR efficiency in fibroblasts

All CRISPRs generated in this study were found to be efficiently active in primary porcine embryonic fibroblasts (Figure 5.5). However, when donor ssODN templates were introduced, only a low level of HDR editing events were detected via RFLP analysis. The HDR efficiency was even too low for accurate quantification, as the uncut band is oversaturated on the gel image (Figure 5.6). In general, NHEJ is the predominant mechanism of double strand break (DSB) repair in somatic cells, even in the presence of homologous donor templates (Fattah et al, 2010). Thus, low levels of HDR were to be expected, yet, many other studies have reported much greater frequencies of HDR in somatic cells than that observed in this study (Tan et al, 2013; He et al, 2016; Abu-Bonsrah et al, 2016). It is difficult to interpret why such a low HDR frequency was observed in this study without direct comparisons, however it is possible that the cell type and the target locus could be restrictive factors. Miyaoka et al, 2016, identified that the frequency of HDR-mediated editing events, when using the CRISPR-Cas9 system, is highly dependent on the target locus, nuclease and cell type.

There are a few strategies used to stimulate HDR-mediated editing events in CRISPR-Cas9 experiments, one is to suppress the NHEJ by inhibiting key molecules in the pathway. This method has been successful, increasing the efficiency of HDR editing events up to 19-fold in mammalian cells (Chu et al, 2015; Vartak et al, 2015; Yu et al., 2015). In attempt to increase the frequency of HDR in this study, two small NHEJ inhibitor compounds, SCR7 and L755507, were employed, however neither were found to improve levels of DNA template introgression (Figure 5.7). It is possible that these treatments were not used at the appropriate concentrations as no optimisation was carried out prior to use. Concentrations were selected based on data from treated mouse embryonic fibroblasts (Maruyama et al, 2015). This result was disappointing, however, as the HDR frequency is highly dependent on cell type, and we generate transgenic animals by embryo microinjection, the developed reagents were taken forward to test in embryos.

If higher a HDR frequency was required in fibroblast cells, there are alternative strategies that could have been tested. These involve synchronising the cells to a HDR permissive phase (i.e. late S and G2 phases) of the cell cycle and delivering the CRISPR/Cas9 and donor template in a time-dependant manner (Lin et al, 2014).

5.4.3 Embryos injections and *in vitro* culture

Low numbers of zygotes injected with the CRISPR-Cas9 mix 1 developed to blastocyst *in vitro*. The poor blastocyst development *in vitro* suggests that the concentration of CRISPR-Cas9 and/or the ssODN may be toxic to the embryo. Thus, the concentration of each reagent i.e. crRNA, tracrRNA, ssODN and Cas9 protein was reduced by half in the subsequent CRISPR-Cas9 microinjections (mix 2), which improved the *in vitro* development to blastocyst (see Table 5.2). The observed toxicity may also be accountable to the Duplex buffer, which had not previously been used in any embryo injections carried out by the Whitelaw group, it was recommended by supplier for storage of the Cas9 protein and synthesised crRNA and tracrRNA. The Duplex buffer concentration was also diluted in half for the final round of CRISPR-Cas9 injections (mix 2).

In general, the development of porcine zygotes to blastocyst stage *in vitro* is low compared to other mammals, such as sheep, cattle and mice (Dang-Nguyen et al, 2011). Moreover, the microinjection procedure reduces this embryo viability further due to inflicted physical damage to the zygote. Despite, the lower *in vitro* porcine embryo development of zygotes injected with Mix 1, these injected zygotes resulted in maintained pregnancies in both recipient sows. Pregnancy in pigs is only maintained when a minimum of 4-5 embryos implant at day 14, this suggests that embryo development of injected zygotes was significantly higher *in vivo* than *in vitro* (King et al, 2006).

5.4.4 Mosaicism caused by CRISPR-Cas9

A mosaic mutation was identified one of the injected blastocysts (Figure 5.8). This most likely due to the CRISPR-Cas9 systems ability to repeatedly target genes past the one cell stage in embryonic development, often leading to mosaicism of the introduced mutation. Mosaicism a common issue when using direct injection of CRISPR-Cas9

editors for the production of genetically engineered organisms, particularly when targeting in zebrafish and Xenopus. Mosaicism is high in these vertebrates, likely due to their very rapid early development. The zygotes of zebrafish and Xenopus go through their first cell division at approximately 45 and 90 minutes respectfully (Zhang & Masui., 1999, Fuentes & Fernandez., 2010). In contrast, the pig zygote takes approximately 16 hours before reaching the two-cell stage. Prolonged expression of the Cas9 in the embryo is a likely cause of mosaicism. Thus, in attempt to reduce the frequency of mosaics in this study, Cas9 protein was directly injected into zygotes instead of more frequently used Cas9 mRNA. As we observed in this study, mosaicism can also occur when using Cas9 protein. If any of the founder animals are born for this study are mosaic for the desired editing event, they can be checked for germline transmission to determine if they should be used to produce first generation edited animals.

An alternative method to generate transgenic animals, instead of embryo microinjection, is to perform editing in somatic cells followed by somatic cell nuclear transfer (SCNT). This route avoids mosaicism and, as the editing events can be identified in cells before use, it can guarantee that any animals born from this procedure would contain the selected editing event. However, SCNT has many limitations, it is very expensive as it requires a high level of technical expertise and the efficiency of producing live animals from cloning is low meaning that large numbers of animals are required to supply oocytes and to act as recipients.

5.4.5 Off-target effects of CRISPR-Cas9

In this study, we identified the on-target editing events in the injected blastocysts by sequencing across the target locus. However, many studies have demonstrated that off-target DNA cleavage is common in the CRISPR-Cas system, as mismatches are often tolerated between the crRNA and the target DNA, particularly in the sequence furthest away from the PAM site (Cong et al, 2013; Jiang et al, 2013; Pattanayak et al, 2013; Fu et al, 2013). Some of these studies observed that the mutagenesis frequency of off-site targets was occasionally higher than the intended target site (Jiang et al, 2013; Fu et al, 2013). This lack of complete specificity required for the Cas9 nuclease cleavage is believed to be important in the adaptive prokaryotic defence mechanism. As viral

genomes evolve rapidly, the CRISPR-Cas systems allowance of DNA cleavage at sites containing mismatches may permit host defence against the next genetically similar invading genome. However, in applications of genetic engineering, off-target mutagenesis is undesirable. In this study, we utilised web-based tools (see Section 2.10 for details) that improve the sgRNA design to minimise the off-target effects. Previous studies have shown that when rational sgRNA design strategies are employed, off-target effects are significantly reduced, although often still detectable, they are rare enough to be accepted for use in biological studies (Doench et al, 2016). However, for applications in human therapeutics the CRISPR-Cas9 off-target phenomena is considered a major safety issue. In the case of genetically engineered livestock species, a low off-targeting effect is unlikely to create major safety issues however it does have the potential to confound the phenotype of founder animals, if required a breeding program may be performed to remove any unwanted mutations. Recently, *Streptocococcus pyogenes* Cas9 (spCas9) has been modified to reduce its ability to make to non-specific DNA contacts, this version of spCas9 has proven to diminish any detectable off-targeting effects (Kleinstiver et al, 2016). This alternative Cas9 will likely be wide-spread in all future applications of the CRISPR-Cas system.

Despite the low frequency of HDR-mediated editing events observed when testing the developed CRISPRs in fibroblasts, the desired HDR editing event was present in one of six analysed blastocysts. Making it more plausible that some of the piglets born from the two pregnant recipients may contain this desired editing event, bringing us closer to having animals with the desired warthog polymorphism that is hypothesised to underlie the tolerant host response to infection with ASFV.

Chapter 6 General Discussion

6.1 Background and aims

Animal disease imposes a huge burden on the livestock industry, impacting both welfare and production. Major outbreaks of transboundary diseases, such as foot and mouth disease, rinderpest, classical swine disease and African swine fever (ASF), have resulted in devastating global economic losses. As a result, scientific research is engaged in lowering this impact by generating effective preventative measures and treatments. One way to reduce livestock disease is to select animals that are genetically resistant, traditionally carried out through selective animal breeding programs; however, this is a time-consuming process and requires that appropriate genetic variation exists within the population. Advances in genome engineering technologies offer us an alternative approach, with the capability to make genetic improvements in livestock within a single generation.

ASF is a re-emerging global threat to the swine industry. At present, there is no vaccine or treatment for ASF, and disease control relies on rapid diagnosis, quarantine and the mass slaughter of animals. Unlike the domestic pig, swine indigenous to Sub-Saharan Africa, such as the warthog, show no clinical signs of disease following infection with ASFV. A comparative study identified three functional polymorphisms in the porcine RELA hypothesised to underlie the difference in host response to ASFV. RELA encodes for NF-κB subunit, RelA. NF-κB, is an evolutionary conserved transcription factor family evolutionary which plays a vital role in upregulating immune and inflammatory responses, including many of the pro-inflammatory cytokines indicated in ASF pathology (Zhang et al., 2006, Gómez del Moral et al., 1999, Gómez-Villamandos et al., 2013). The specific RELA polymorphisms identified alter potential phosphorylation sites within the C-terminal transactivation domain of RelA which have been found to modulate NF-κB transcriptional activity *in vitro*. In order to test this hypothesis, the Whitelaw group set out to investigate whether genome editing tools could be employed to engineer the RELA sequence of domestic pigs. When this project was initiated it was unknown whether the direct injection of editor mRNAs into livestock zygotes would work. TALEN editors were developed to target the

polymorphic region of porcine RELA and directly injected into pig zygotes for the production of RELA-edited animals

The original aims of this thesis were to genotype pigs born following zygote injection with mRNAs encoding genome editors targeting RELA, to carry out phenotypic characterisation, and to subsequently define their response to African swine fever virus infection.

6.2 Progress

In Chapter 3, initial genotyping was completed and a specific set of editing events were selected for further characterisation. These editing events encoded for a RelA protein that lacked the final 60 amino acids of wild-type RelA. These missing residues encode the C-terminal region of the transactivation domain encompassing the entire TA1, which is conserved between mammalian species and thought to be responsible for mediating most of RelA's transcriptional activity (O'Shea & Perkin., 2008, Mukherjee et al., 2013). To investigate the impact of altered RELA *in vitro* I used TNFα, a potent inducer of NF-κB, to stimulate fibroblasts isolated from skin biopsies and assessed their resultant transcriptional activity by quantifying the expression of several RelA-dependent genes. As anticipated, fibroblasts containing only truncated RelA displayed a delay in upregulation of the genes examined, suggesting a reduced transcriptional activity. This included a gene that encodes for IκBα, which is known to be important for termination of TNFα induced NF-κB activation, providing a NF-κB negative feedback loop (Arenzana-Seisdedos et al., 1997, Chen et al., 2001, Huang & Miyamoto., 2001). I also observed higher induced expression levels of RelA-dependent genes at later time-points in cells containing only truncated RelA, which may indicate a prolonged NF-κB activation as a consequence of delayed IκBα production. To investigate further, a RelA nuclear translocation assay was carried out which demonstrated that truncated RelA had an extended presence in the nucleus post-induction compared to wild-type, again implying a prolonged period of NF-κB activation. During these experiments, I unexpectedly discovered that truncated RelA translocated to the nucleus with both delayed kinetics and at reduced total level at all time-points analysed post-TNFα stimulation. This work provides the first evidence that the C-terminal region of RelA is important for its nuclear translocation. The lower

transcriptional activity of the truncated form may in part be due to its reduced nuclear translocation. However, the current data are difficult to interpret as we observe the confounding effects of altered translocation kinetics with the truncated transcription activation domain – the altered rate at which the truncated protein shuttles within the cell is likely to be influenced by its prior influence on basal cellular levels of a range of proteins which are regulated by NF-κB, including many which encode other NF-κB pathway components, such as TRAF2, A20, REL, NFKBIA, NFKBIE, NFKBIZ, NFKB1, NFKB2, RELB. Lower basal levels of in IκBα and C-Rel proteins were identified in fibroblasts homozygous for the RelA truncation compared to wild-type. In conclusion, I found that this truncation did alter the NF-κB signalling although clear understanding of the mechanisms was complicated by the complexity of the biological network. Gross phenotypic analysis of individuals revealed no defects associated with the modified animals, including histological analysis of the lymphoid tissues. Interestingly and unexpectedly, pigs homozygous for the RelA truncation were found to have significantly lower body weights compared to wild-type controls.

In Chapter 4, I investigated how the altered NF-κB signalling identified in the edited animals would impact on their cytokine response when macrophages were challenged with ASFV *in vitro*. The dysregulation of gene transcription in ASFV infected macrophages has been demonstrated by many studies and is thought to be a major factor underlying the disease state (Powell et al., 1996, Gómez del Moral et al., 1999, Gil et al., 2008). I isolated macrophages from both edited and control pigs, carried out an ASFV infection *in vitro*, and observed whether there was any change in the expression profile of cytokines reported to be perturbed during ASFV infection. Differences were observed in the upregulation of ASF-associated cytokines in response to infection in RELA-edited cells. However, it was difficult to predict how these would impact on disease pathogenesis *in vivo* due to the complex nature of the immune response. An *in vivo* study was carried out to see if the changes identified *in vitro* translated to an altered clinical outcome for the RELA-edited pigs. Unfortunately, these pigs displayed similar clinical outcome to that of the wild-type controls.

At the start of this study, genome editing in livestock was in its infancy, in fact the founder animals characterised in this thesis were the first live pigs born from genome

editing directly in zygotes (Lillico et al., 2013). Subsequent application of genetic engineering tools has allowed the introduction of these warthog RELA changes into the domestic pig RELA locus, producing live pigs with all three warthog SNPs (Lillico at el, 2016). In Chapter 5 of this thesis, I designed, tested and applied reagents to demonstrate how CRISPRs can be used to generate a precise change into the porcine RELA locus. I successfully introduced a single warthog SNP into *Sus scrofa* RELA locus. This SNP was previously found to be responsible for significantly reducing the NF-κB activity of warthog RelA compared to wild-type (Palgrave et al, 2011).

Once made, interpreting the potential downstream effects of this change to the RelA protein will be complicated. The RelA subunit is the most abundant of the transcriptionally active subunit of the NF-κB transcription factor family, regulating expression of a plethora of genes in the majority of cell types (Schmitz & Baeuerle, 1991). Moreover, the activation of NF-κB is typically the cell's first response to potentially harmful stimuli and it in turn upregulates genes that mediate the activation of many other signalling pathways involved in immune and inflammatory response, cell survival response and cell proliferation. Thus, altering the NF-κB pathway will likely impacts on many intra- and inter-cellular biological networks. Furthermore, translating observations made *in vitro* to predict an outcome in tissues or at the level of the entire organism *in vivo* is extremely challenging due to the complexity of interactions within these biological systems.

6.3 Alternative approaches with the aim of creating an ASF resilient domestic pig

Variation between warthog and domestic pig RELA was identified by Palgrave et al (2011), using a candidate approach which aimed to identify genetic variation between these species that could potentially underlie their differing responses to ASFV infection. Since this initial study, significant progress has been made in identifying ASFV genes important in inducing pathogenesis in the domestic pig. Deletion of viral multigene families MGF360 and MGF530 has been shown to attenuate highly virulent isolates in the domestic pig (O'Donnell et al., 2015, Reis et al., 2016). The MGF360 and MGF530. genes are known to be involved in inhibiting induction of IFNs in host cells (Afonso et al., 2004, Golding et al., 2016). However, the mechanistic roles of the

encoding proteins are yet to be uncovered. Further research into understanding the targets and functions of the viral proteins encoded by MGF360/MGF530, may provide us with novel candidate genes to compare between the ASFV-tolerant-warthog and the highly susceptible domestic pig. Interestingly, RelA is also a known regulator of several IFNs (Hiscott et al., 1989, Sica et al., 1997).

The majority of traits are polygenic, so it may be that the warthog's apparent tolerance to ASFV infection is mediated by a composite of genetic differences between the immune system of the domestic pig and the warthog. In a recent genomic study, differences in the repertoire of immune-related genes in the domestic pig were identified in comparison with other mammals (Dawson et al., 2016). It would be interesting to extend this study to include the warthog genome, which may reveal differences in the immune systems genes and therefore the basis of their resistance to ASFV.

A recent study has shown that genome editors can be successfully used to engineer pigs to be resistant to PRRSV (Whitworth et al., 2016, Burkard et al., 2017). This was achieved through CRISPR/Cas9 editing to delete part of the viral receptor, CD163, required for PRRSV entry. ASFV enters cells by either receptor-mediated endocytosis or through macropinocytosis (non-specific mechanism; Alcamí et al., 1990, Hernáez et al., 2016). Cellular receptors that mediate ASFV entry have not yet been identified. ASFV is known to be able enter numerous different cells types from a variety of species, but only swine monocytes/macrophages demonstrate robust viral replication (Alcamí et al., 1989, Alcamí et al., 1990, Carrascosa et al., 1999). This suggests that specific host factors in these cells are required for the ASFV production process. Recently, libraries of sgRNAs have been designed to efficiently generate loss-of-function mutations in every protein-coding gene in the genomes of mice and humans (Koike-Yusa et al., 2014; Wang et al., 2014), enabling genome wide CRISPR-Cas9 knockout (GeCKO) screens. This approach is proving to be an effective systematic approach to identify novel genes essential for various biological processes (Shalem et al., 2014, Koike-Yusa et al., 2014). A domestic pig GeCKO library is currently being constructed at the Roslin Institute which would enable genome wide screening for

genes that facilitate ASFV replication in swine monocyte/macrophage cells via positive and negative selection using a recombinant ASFV expressing GFP.

Further investigation into the warthog RELA will continue with a planned challenge of the genome edited pigs reported by Lillico et al (2016) with ASFV.

6.4 Obstacles to overcome with genetic engineering for livestock purposes

Genome editing technologies have the potential to revolutionise agriculture. There is tremendous pressure on the livestock industry to increase the sustainability of production, while also enhancing animal welfare. Genetic improvement of livestock using editors has many benefits over selective breeding methods, as it permits; the fixation of alleles without any deleterious inbreeding effects; the introduction alleles that are not present in the population and; the desired genetic change can be implemented within one generation. Editors can be used to introduce genetic changes to remove alleles associated with deleterious traits and increase desirable alleles associated with favourable traits. However, the majority of traits are polygenic meaning that they are controlled by variation in multiple genes. Several studies have shown that CRISPR/Cas9 can be employed in a multiplex format (i.e. to simultaneously edit multiple genetic loci in the same cell) by co-introduction of multiple site-specific sgRNAs with or without repair templates, into zygotes of mice and pig (Wang et al., 2013., Wang et al., 2016). Other technical issues to overcome are off-targeting effects, genetic mosaicism and low HDR efficiency in using the CRISPR/Cas9 system in zygotes (see Section 5.4.2,4-5 for further discussion on these technical obstacles).

Aside from the practical issues associated with the technical delivery and function of genome editors *in vivo*, an important component for the success of engineering of livestock genomes will be the discovery of genetic variants that underlie beneficial traits. Currently, many livestock breeding companies are collecting genomic data which when combined with advances in genomic analysis of allelic sequence variation may lead to an increased understanding of the genetics underlying desirable traits. However, many genomic analyses identify large genomic regions, known as

quantitative trait loci, or haplotypes of SNPs that are associated with a specific trait. To date the largest region knocked in using CRISPR/Cas9 is a 200 kb region performed in mouse zygotes (Yoshimi et al., 2016). It may be possible to knock-in larger regions utilising editors alongside large templates delivered in either lentivirus or artificial chromosomes such as BACs and YAC.

Another major obstacle for genome engineering in livestock is the acceptance of technology by society, regulators and breeding industries. Current regulations on the use of gene-editing (GE) technologies in food animal production are unclear. At present, the majority of legislation on GMOs for food consumption relates to crops rather than animals. In general, GM and GE plants are widely grown and accepted for human consumption. However, regulation varies internationally. Europe currently has one of the most restrictive regulations in place, with only a few GM crops authorised to be grown. In contrast with crops, the number of GMO animals that approved for human consumption is lagging. In 2015, AquAdvantage salmon, produced by insertion of a transgene, were the first GMO to be approved for human consumption by the FDA in the United States. However, the assessment process on this application lasted nearly 10 years from first submission. The level of regulation on genome edited livestock has yet to be set in most countries. Uncertainties surrounding these regulations are restricting investment and thus development of GE technologies for commercial use. Less restrictive regulations on GMOs for food would encourage novel applications, potentially increasing the sustainability in livestock production that is demanded worldwide.

APPENDICES

Appendix A: PX458 vector map

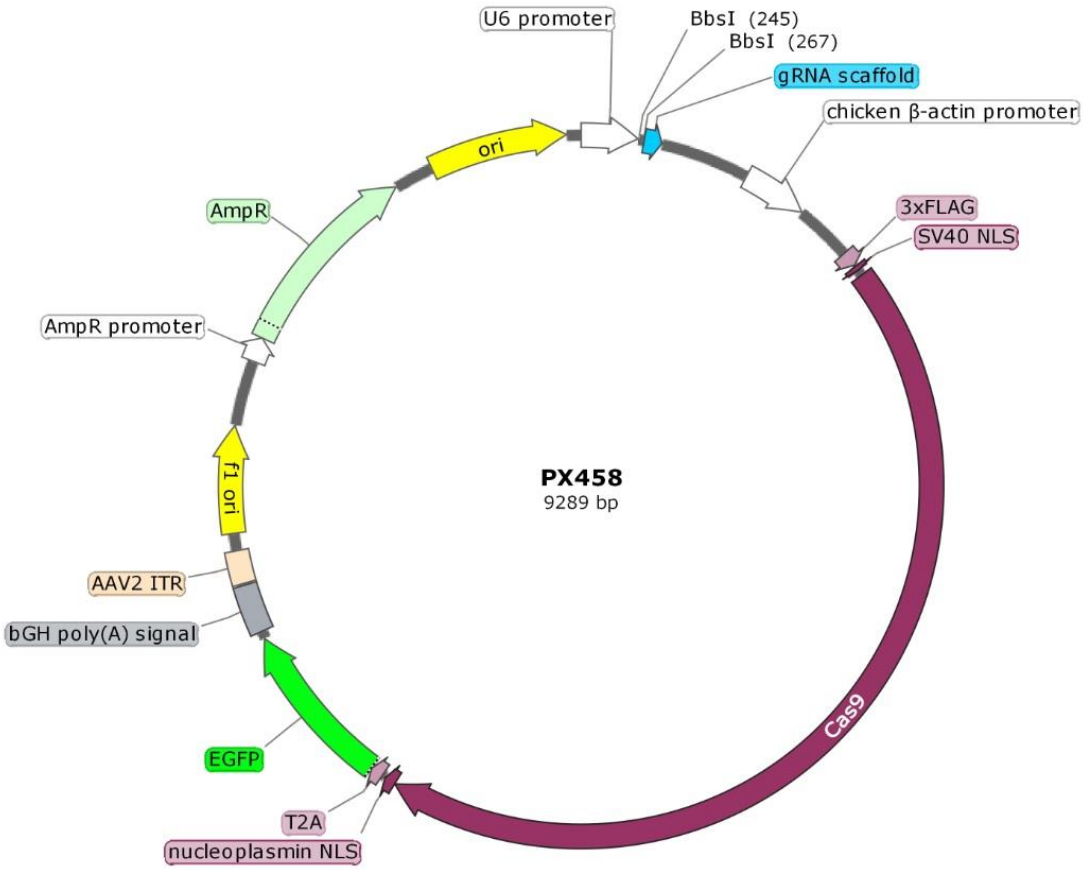

Appendix B: List of tissues collected in fixative from RELA-edited pigs at post-mortem

Tissue samples:
Submandibular lymph node
Prescapular lymph node
Popliteal lymph node
Mesenteric lymph node
Mediastinal lymph node
Thyroid gland
Thymus
Trachea
Lung
Heart (right ventricle)
Heart (left ventricle)
Heart (septum)
Aorta
Duodenum
Jejunum
Ileum
Caecum
Pancreas
Liver
Spleen
Kidney
Skeletal muscle (biceps femoris)
Bone marrow

Appendix C: Lymph node scoring

H&E stained sections of lymph nodes were examined by pathologist, Dr Pip Beard. Scores were assigned for the following; 1) whether the lymphoid nodules were distinctly demarcated from the surrounding parenchyma (catergoriesed into either distinct, indistinct or variable), 2) whether there were apoptotic cells in the lymphoid nodule (either yes or no) and 3) an estimate of the percentage of the lymph node cross section which consisted of cortical tissue. No significant difference was found in any of the scoring categories.

		Submandibular lymph node		
Pig ID	**RELA Genotype**	**lymphoid nodules**	**apoptosis**	**% cortical tissue**
258	Wild-type			
261	Wild-type	indistinct	yes	40
262	Wild-type	distinct	yes	70
268	Wild-type			
269	Wild-type			
271	Bi-allelic	indistinct	no	50
275	Bi-allelic	distinct	yes	70
276	Bi-allelic			
278	Bi-allelic	distinct	yes	70
274	Heterozygous	distinct	yes	90
223	Heterozygous	variable	yes	90
214	Heterozygous	distinct	yes	70

		Prescapular lymph node		
Pig ID	**RELA Genotype**	**lymphoid nodules**	**apoptosis**	**% cortical tissue**
258	Wild-type	distinct	yes	80
261	Wild-type			
262	Wild-type	indistinct	no	60
268	Wild-type			
269	Wild-type	distinct	yes	20
271	Bi-allelic			
275	Bi-allelic		yes	20
276	Bi-allelic			
278	Bi-allelic	indistinct	no	50
274	Heterozygous			
223	Heterozygous	distinct	yes	80
214	Heterozygous	indistinct	no	80

		Mediastinal lymph node		
Pig ID	**RELA Genotype**	**lymphoid nodules**	**apoptosis**	**% cortical tissue**
258	Wild-type	variable	no	90
261	Wild-type			
262	Wild-type			
268	Wild-type	indistinct	no	60
269	Wild-type	indistinct	yes	80
271	Bi-allelic			
275	Bi-allelic	distinct	yes	70
276	Bi-allelic			
278	Bi-allelic	distinct	yes	70
274	Heterozygous	variable	yes	60
223	Heterozygous	distinct	yes	50
214	Heterozygous	indistinct	no	50

		Mesenteric lymph node		
Pig ID	**RELA Genotype**	**lymphoid nodules**	**apoptosis**	**% cortical tissue**
258	Wild-type			
261	Wild-type	indistinct	no	90
262	Wild-type			
268	Wild-type	indistinct	yes	90
269	Wild-type	indistinct	yes	90
271	Bi-allelic	distinct	yes	80
275	Bi-allelic			
276	Bi-allelic	variable	yes	70
278	Bi-allelic	distinct	yes	60
274	Heterozygous	distinct	yes	80
223	Heterozygous	indistinct	no	50
214	Heterozygous	indistinct	no	70

		Popliteal lymph node		
Pig ID	**RELA Genotype**	**lymphoid nodules**	**apoptosis**	**% cortical tissue**
258	Wild-type	indistinct	yes	70
261	Wild-type			
262	Wild-type	indistinct	yes	30
268	Wild-type			
269	Wild-type	distinct	no	40
271	Bi-allelic	indistinct	no	50
275	Bi-allelic	indistinct	yes	60
276	Bi-allelic			
278	Bi-allelic			
274	Heterozygous			
223	Heterozygous			
214	Heterozygous			

Appendix D: Clinical scoring guidelines

ITEM	Score	Description
Inappetence	0-6	0: No abnormality 1: MILD (reduced eating) 4: MODERATE (only picking at food) 6: SEVERE (not eating)
Recumbence	0-6	0: No abnormality 1: MILD (lethargic) 2: MODERATE (get up only when touched) 4: MODERATE/SEVERE (slow to get up when touched) 6: SEVERE (remain recumbent when touched)
Skin hemorrhage/cyanosis	0-3	0: No abnormality 1: MILD (hemorrhagic areas on ears and body) 3: MODERATE/SEVERE (generalised hemorrhage all over body)
Joint swelling	0-4	0: No abnormality 1: MILD (joint swelling) 4: SEVERE (joint swelling with difficulty walking)
Laboured breathing and coughing	0-3	0: No abnormality 1: MILD 3: SEVERE
Ocular discharge	0-1	0: No abnormality 1: MILD (gummed up eyes)
Diarrhoea	0-3	0: No abnormality 1: MILD 3: SEVERE (bloody diarrhoea)
Blood in Urine	0-4	0: No abnormality 4: Blood in Urine
Vomiting	0-4	0: No abnormality 4: Vomiting
Rectal temperature (°C)	0-5	0: < 39 1: 39.0 < to 39.5 2: 39.5 ≤ to < 40 3: 40.0 to ≤ 40.5 4: 40.6 ≤ 41 5: > 41

Appendix E: Macroscopic lesion scoring guidelines

ITEM	Score	Description/Lesion
External examination		
Body condition	0-4	0: Normal → 4: Cachectic
Eyes/conjunctiva	0-3	1: Slight hyperaemia 2: Hyperaemia, swelling of eyelids and clear ocular discharge 3: Congested ocular mucosa with haemorrhages, inflamed eyelids and intense cloudy ocular discharge (gummed up eyes)
Nostrils	0-3	1: Moderate nasal discharge 2: Intense mucosal nasal discharge 3: Foam material in nostrils 3: Nasal haemorrhages (epistaxis)/blood traces around nostrils
Tonsils	0-3	2: Erythema in tonsils 3: Necrotic areas in tonsils
Oral cavity	0-3	3: Necrotic areas in tongue 3: Foamy material in mouth
Skin	0-6	1: Areas with skin erythema (ears, flanks, abdomen) 1: Cyanotic areas (tip of the ears or tail, distal limbs, chest and abdomen) 3: Generalized reddening of the skin with haemorrhages all over body 4: Varioliform skin eruptions 4: Abscess 5: Necrotic areas on skin/chronic skin ulcers 6: Necrotic areas/chronic skin ulcers all over the body
Subcutis	0-3	2: Areas with subcutaneous oedema, haemorrhages and haematomas 3: Generalized subcutaneous oedema, haemorrhages and haematomas all over the body
Musculoskeletal system		
Skeletal muscle	0-3	2: Areas with oedema/haemorrhages within the fascial planes 3: Generalized oedema/haemorrhages within the fascial planes all over the body
Joints	0-4	3: Moderate joint swelling due to serofibrinous periarthritis/arthritis 4: Severe joint swelling with difficulty walking due to purulent periarthritis/arthritis
Thoracic cavity		
Exudates	0-3	1: Moderate hydrothorax (with reddish fluid) 2: Severe hydrothorax (with deep red fluid) 3: Haemothorax
Pericardium	0-3	1: Moderate hydropericardium (with reddish fluid) 2: Severe hydropericardium (with reddish fluid) 3: Haemopericardium 3: Fibrinous pericarditis
Heart	0-3	1: Petechial haemorrhages on epicardium 2: Variable presence of petechial haemorrhages/ecchymoses on epicardium, myocardium and endocardium 3: Haemorrhagic heart with extensive coalescent haemorrh (ecchymoses) on epicardium, myocardium and endocardium
Lung (lack of) collapse	0-3	1: Mild lack of collapse with no ribs impressions 2: Moderate lack of collapse with mild or scarce ribs impressions 3: Moderate to severe lack of collapse with apparent ribs impressions
Congestion/haemorrhage	0-3	1: Mild congestion or active hyperaemia, diffuse or patchy distributed in parenchyma. No haemorrhages 2: Variable degree of congest. or active hyperaemia. Multifocal to coalescent randomly distributed petechiae and purpurae

		3: Variable degree of congest/hyper. Multifocal to coalescent random and interlobul. distributed haemorrh (ecchymoses)
Oedema (foam in trachea)	0-3	1: Scarce or no presence of foamy material in trachea/bronchus (alveolar oedema) and minimal (interstitial oedema) 2: Mild to moderate presence of foamy material in trachea/bronchus and moderate distension of interlobular walls 3: Marked presence of foamy material in trachea/brochus and intense distension of interlobular walls
Consolidation of pulmonar parenchyma	0-4	1: Minimal to mild cranio-ventral (uni/bilateral) consolidation (bronchopneumonia) 2: Moderate cranio-ventral (uni/bilateral) consolidation (bronchopneumonia) 3: Marked-extended cranio-ventral (uni/bilateral) consolidation bronchopneum.(with red and grey hepatization of lobules) 4: Necrotic pneumonia 4: Purulent lesions
Pleura	0-3	3: Fibrinous pleuritis/pleural adhesions
Abdominal cavity		
Ascites	0-4	1: Slight 2: Moderate 3: Intense 4: Hemoabdomen
Stomach	0-4	1: Petechiae on serosa surface 2: Petechiae/ecchymoses on serosa surface 3: Petechiae/ecchymoses on serosa & haemorrhages on mucosa surface 4: Necrotic areas/ulcers
Duodenum	0-4	1: Petechiae on serosa surface 2: Petechiae/ecchymoses on serosa surface 4: Petechiae/ecchymoses on serosa & haemorrhages on mucosa surface 4: Necrotic areas/ulcers
Jejunum	0-4	
Ileum	0-4	
Ileoceal valve	0-4	
Cecum	0-4	
Colon	0-4	
Rectum	0-4	
Liver	0-3	1: Mild multifocal parenchymatous colour changes with slight hepatomegaly 2: Hepatomegaly, moderate congestion and presence multifocal punctiform redness areas/haemorrhages 3: Hepatomegaly, intense congestion and presence of coalescent punctiform redness areas/ haemorrhages
Gallbladder	0-4	1: Mild to moderate oedema affecting gallbladder wall/cystic duct 2: Oedema affecting gallbladder wall/cystic duct with haemorrhages on serosa/submucosa surface 3: Intense oedema affecting gallbladder wall/cystic duct with severe haemorrhages on ser/subm surface and blood clots 4: Necrotic areas/ulcers
Urinary system		
Kidney	0-1	1: Perirrenal oedema
Parenchymal kidney hemmorhages (cortico-medular)	0-3	1: Mild multifocal cortical and medullar petechiae with multifocal vascular angiectasia 2: Moderate multifocal cortical (petechiae) and medullar (purpurae) haemorrhages with moderate pelvic dilation 3: Marked diffuse cor-med haemo. with diffuse general renal darkness, marked pelvic dilation and extens. subcapsul haemo
Parenchymal kidney hemmorhages (medulo-cortical)	0-3	1: Minimal to mild multifocal cortical and medullar petechiae 2: Moderate multifocal cortical and medullar haemorrhages (petechiae) with preponderance of cortical affectation 3: Marked multif. cor-med petechiae with preponder. of cortical affectation with/without multif. moderate pelvic purpurae
Urinary Bladder	0-3	1: Mild multifocal petechiae on mucosa surface without/with mild colour changes in urinary bladder wall 2: Multifocal petechiae and ecchymoses on mucosa, submucosa and serosa with oedema in urinary bladder wall 3: Coalescent haemo. on muc. Subm. and ser. with intense oedem. in urin. bladd. wall and presence of clots on muc. surface
Lymphoid system		

Spleen	0-4	1: Mild hyperemic splenomegaly (minimal to mild bleeding after sectioning) 2: Moderate/partial hyperemic splenomegaly (moderate bleeding after sectioning) 3: Intense hyperemic splenomegaly (marked bleeding after sectioning) 3: Focal necrosis/infarcts 4: Hyperplasic splenomegaly (no bleeding after sectioning)/cicatrization of partial hyperemic splenomegaly
Submandibular lymph node	0-3	1: Increased size and edematous with moderate colour changes 2: Increased size, edematous and haemorrhagic 3: Increased size, edematous and completely haemorrhagic similar to a blood clot 4: Hyperplasia without haemorrhagic changes/with occasional peripheral haemorrhages
Retropharingeal lymph node	0-3	
Tracheobronchial lymph node	0-3	
Gastrohepatic lymph node	0-3	
Renal lymph node	0-3	
Mesenteric lymph node	0-3	
Thymus	0-2	1: Moderate colour changes with occasional petechiae 2: Petechiae and ecchymoses
Endochrine system		
Thyroid gland	0-1	1: Increased size/haemorrhages
Adrenal gland	0-1	
Pancreas	0-1	

Bibliography

Abu-Bonsrah, K.D., Zhang, D., and Newgreen, D.F. (2016). CRISPR/Cas9 Targets Chicken Embryonic Somatic Cells In Vitro and In Vivo and generates Phenotypic Abnormalities. Sci Rep 6, 34524.

Adhikari, A., Xu, M., and Chen, Z.J. (2007). Ubiquitin-mediated activation of TAK1 and IKK. Oncogene 26, 3214-3226.

Afonso, C.L., Piccone, M.E., Zaffuto, K.M., Neilan, J., Kutish, G.F., Lu, Z., Balinsky, C.A., Gibb, T.R., Bean, T.J., Zsak, L., et al. (2004). African swine fever virus multigene family 360 and 530 genes affect host interferon response. J Virol 78, 1858-1864.

Aigner, B., Renner, S., Kessler, B., Klymiuk, N., Kurome, M., Wünsch, A., and Wolf, E. (2010). Transgenic pigs as models for translational biomedical research. J Mol Med (Berl) 88, 653-664.

Alcamo, E., Hacohen, N., Schulte, L.C., Rennert, P.D., Hynes, R.O., and Baltimore, D. (2002). Requirement for the NF-kappaB family member RelA in the development of secondary lymphoid organs. J Exp Med 195, 233-244.

Alcamo, E., Mizgerd, J.P., Horwitz, B.H., Bronson, R., Beg, A.A., Scott, M., Doerschuk, C.M., Hynes, R.O., and Baltimore, D. (2001). Targeted mutation of TNF receptor I rescues the RelA-deficient mouse and reveals a critical role for NF-kappa B in leukocyte recruitment. J Immunol 167, 1592-1600.

Alcamí, A., Carrascosa, A.L., and Viñuela, E. (1989). Saturable binding sites mediate the entry of African swine fever virus into Vero cells. Virology 168, 393-398.

Alcamí, A., Carrascosa, A.L., and Viñuela, E. (1990). Interaction of African swine fever virus with macrophages. Virus Res 17, 93-104.

Anders, C., Bargsten, K., and Jinek, M. (2016). Structural Plasticity of PAM Recognition by Engineered Variants of the RNA-Guided Endonuclease Cas9. Mol Cell 61, 895-902.

Anderson, E.C., Hutchings, G.H., Mukarati, N., and Wilkinson, P.J. (1998). African swine fever virus infection of the bushpig (Potamochoerus porcus) and its significance in the epidemiology of the disease. Vet Microbiol 62, 1-15.

Andrés, G., García-Escudero, R., Simón-Mateo, C., and Viñuela, E. (1998). African swine fever virus is enveloped by a two-membraned collapsed cisterna derived from the endoplasmic reticulum. J Virol 72, 8988-9001.

Arenzana-Seisdedos, F., Thompson, J., Rodriguez, M.S., Bachelerie, F., Thomas, D., and Hay, R.T. (1995). Inducible nuclear expression of newly synthesized I kappa B alpha negatively regulates DNA-binding and transcriptional activities of NF-kappa B. Mol Cell Biol 15, 2689-2696.

Arenzana-Seisdedos, F., Turpin, P., Rodriguez, M., Thomas, D., Hay, R.T., Virelizier, J.L., and Dargemont, C. (1997). Nuclear localization of I kappa B alpha promotes active transport of NF-kappa B from the nucleus to the cytoplasm. J Cell Sci 110 (Pt 3), 369-378.

Ashall, L., Horton, C.A., Nelson, D.E., Paszek, P., Harper, C.V., Sillitoe, K., Ryan, S., Spiller, D.G., Unitt, J.F., Broomhead, D.S., et al. (2009). Pulsatile stimulation determines timing and specificity of NF-kappaB-dependent transcription. Science 324, 242-246.

Baldwin, A.S. (1996). The NF-kappa B and I kappa B proteins: new discoveries and insights. Annu Rev Immunol 14, 649-683.

Baldwin, A.S. (2001). Control of oncogenesis and cancer therapy resistance by the transcription factor NF-kappaB. J Clin Invest 107, 241-246.

Barkett, M., and Gilmore, T.D. (1999). Control of apoptosis by Rel/NF-kappaB transcription factors. Oncogene 18, 6910-6924.

Barrangou, R., and Marraffini, L.A. (2014). CRISPR-Cas systems: Prokaryotes upgrade to adaptive immunity. Mol Cell 54, 234-244.

Beg, A.A., Sha, W.C., Bronson, R.T., Ghosh, S., and Baltimore, D. (1995). Embryonic lethality and liver degeneration in mice lacking the RelA component of NF-kappa B. Nature 376, 167-170.

Beg, A.A., and Baltimore, D. (1996). An essential role for NF-kappaB in preventing TNF-alpha-induced cell death. Science 274, 782-784.

Beg, A.A., Sha, W.C., Bronson, R.T., and Baltimore, D. (1995). Constitutive NF-kappa B activation, enhanced granulopoiesis, and neonatal lethality in I kappa B alpha-deficient mice. Genes Dev 9, 2736-2746.

Bevan, M.W., Flavell, R.B., and Chilton, M.D. (1992). A chimaeric antibiotic resistance gene as a selectable marker for plant cell transformation. 1983. Biotechnology 24, 367-370.

Bevan, M.W., Flavell, R.B., and Chilton, M.D. (1983). A chimaeric antibiotic resistance gene as a selectable marker for plant cell transformation. Biotechnology 24, 367-370.

Bibikova, M., Golic, M., Golic, K.G., and Carroll, D. (2002). Targeted chromosomal cleavage and mutagenesis in Drosophila using zinc-finger nucleases. Genetics 161, 1169-1175.

Binns, R.M. (1982). Organisation of the lymphoreticular system and lymphocyte markers in the pig. Vet Immunol Immunopathol 3, 95-146.

Bishop, R.P., Fleischauer, C., de Villiers, E.P., Okoth, E.A., Arias, M., Gallardo, C., and Upton, C. (2015). Comparative analysis of the complete genome sequences of Kenyan African swine fever virus isolates within p72 genotypes IX and X. Virus Genes 50, 303-309.

Bitar, R., Beauparlant, P., Lin, R., Pitha, P., and Hiscott, J. (1995). Retrovirus-mediated transfer of nuclear factor-kappa B subunit genes modulates I kappa B alpha and interferon beta expression. Cell Growth Differ 6, 965-976.

Bitinaite, J., Wah, D.A., Aggarwal, A.K., and Schildkraut, I. (1998). FokI dimerization is required for DNA cleavage. Proc Natl Acad Sci U S A 95, 10570-10575.

Blome, S., Gabriel, C., and Beer, M. (2013). Pathogenesis of African swine fever in domestic pigs and European wild boar. Virus Res 173, 122-130.

Boch, J., and Bonas, U. (2010). Xanthomonas AvrBs3 family-type III effectors: discovery and function. Annu Rev Phytopathol 48, 419-436.

Boch, J., Scholze, H., Schornack, S., Landgraf, A., Hahn, S., Kay, S., Lahaye, T., Nickstadt, A., and Bonas, U. (2009). Breaking the code of DNA binding specificity of TAL-type III effectors. Science 326, 1509-1512.

Bogdanove, A.J., and Voytas, D.F. (2011). TAL effectors: customizable proteins for DNA targeting. Science 333, 1843-1846.

Bohuslav, J., Kravchenko, V.V., Parry, G.C., Erlich, J.H., Gerondakis, S., Mackman, N., and Ulevitch, R.J. (1998). Regulation of an essential innate immune response by the p50 subunit of NF-kappaB. J Clin Invest 102, 1645-1652.

Boinas, F.S., Hutchings, G.H., Dixon, L.K., and Wilkinson, P.J. (2004). Characterization of pathogenic and non-pathogenic African swine fever virus isolates from Ornithodoros erraticus inhabiting pig premises in Portugal. J Gen Virol 85, 2177-2187.

Bolotin, A., Quinquis, B., Sorokin, A., and Ehrlich, S.D. (2005). Clustered regularly interspaced short palindrome repeats (CRISPRs) have spacers of extrachromosomal origin. Microbiology 151, 2551-2561.

Bonas, U., Stall, R.E., and Staskawicz, B. (1989). Genetic and structural characterization of the avirulence gene avrBs3 from Xanthomonas campestris pv. vesicatoria. Mol Gen Genet 218, 127-136.

Borca, M.V., Carrillo, C., Zsak, L., Laegreid, W.W., Kutish, G.F., Neilan, J.G., Burrage, T.G., and Rock, D.L. (1998). Deletion of a CD2-like gene, 8-DR, from African swine fever virus affects viral infection in domestic swine. J Virol 72, 2881-2889.

Bosselman, R.A., Hsu, R.Y., Boggs, T., Hu, S., Bruszewski, J., Ou, S., Kozar, L., Martin, F., Green, C., and Jacobsen, F. (1989). Germline transmission of exogenous genes in the chicken. Science 243, 533-535.

Bouquet, A., and Juga, J. (2013). Integrating genomic selection into dairy cattle breeding programmes: a review. Animal 7, 705-713.

Bowes, M.A., and Kenny, A.J. (1986). Endopeptidase-24.11 in pig lymph nodes. Purification and immunocytochemical localization in reticular cells. Biochem J 236, 801-810.

Bradford, M.M. (1976). A rapid and sensitive method for the quantitation of microgram quantities of protein utilizing the principle of protein-dye binding. Anal Biochem 72, 248-254.

Breese, S.S., and DeBoer, C.J. (1966). Electron microscope observations of African swine fever virus in tissue culture cells. Virology 28, 420-428.

Bren, G.D., Solan, N.J., Miyoshi, H., Pennington, K.N., Pobst, L.J., and Paya, C.V. (2001). Transcription of the RelB gene is regulated by NF-kappaB. Oncogene 20, 7722-7733.

Briggs, A.W., Rios, X., Chari, R., Yang, L., Zhang, F., Mali, P., and Church, G.M. (2012). Iterative capped assembly: rapid and scalable synthesis of repeat-module DNA such as TAL effectors from individual monomers. Nucleic Acids Res 40, e117.

Brinster, R.L., Chen, H.Y., Trumbauer, M., Senear, A.W., Warren, R., and Palmiter, R.D. (1981). Somatic expression of herpes thymidine kinase in mice following injection of a fusion gene into eggs. Cell 27, 223-231.

Burkard, C., Lillico, S.G., Reid, E., Jackson, B., Mileham, A.J., Ait-Ali, T., Whitelaw, C.B., and Archibald, A.L. (2017). Precision engineering for PRRSV resistance in pigs: Macrophages from genome edited pigs lacking CD163 SRCR5 domain are fully resistant to both PRRSV genotypes while maintaining biological function. PLoS Pathog 13, e1006206.

Burkly, L., Hession, C., Ogata, L., Reilly, C., Marconi, L.A., Olson, D., Tizard, R., Cate, R., and Lo, D. (1995). Expression of relB is required for the development of thymic medulla and dendritic cells. Nature 373, 531-536.

Burrage, T.G., Lu, Z., Neilan, J.G., Rock, D.L., and Zsak, L. (2004). African swine fever virus multigene family 360 genes affect virus replication and generalization of infection in Ornithodoros porcinus ticks. J Virol 78, 2445-2453.

Caamaño, J.H., Rizzo, C.A., Durham, S.K., Barton, D.S., Raventós-Suárez, C., Snapper, C.M., and Bravo, R. (1998). Nuclear factor (NF)-kappa B2 (p100/p52) is required for normal splenic microarchitecture and B cell-mediated immune responses. J Exp Med *187*, 185-196.

Campbell, K.J., Rocha, S., and Perkins, N.D. (2004). Active repression of antiapoptotic gene expression by RelA(p65) NF-kappa B. Mol Cell 13, 853-865.

Campbell, K.J., Witty, J.M., Rocha, S., and Perkins, N.D. (2006). Cisplatin mimics ARF tumor suppressor regulation of RelA (p65) nuclear factor-kappaB transactivation. Cancer Res 66, 929-935.

Carlson, D.F., Tan, W., Lillico, S.G., Stverakova, D., Proudfoot, C., Christian, M., Voytas, D.F., Long, C.R., Whitelaw, C.B., and Fahrenkrug, S.C. (2012). Efficient TALEN-mediated gene knockout in livestock. Proc Natl Acad Sci U S A 109, 17382-17387.

Carlson, D.F., Lancto, C.A., Zang, B., Kim, E.S., Walton, M., Oldeschulte, D., Seabury, C., Sonstegard, T.S., and Fahrenkrug, S.C. (2016). Production of hornless dairy cattle from genome-edited cell lines. Nat Biotechnol 34, 479-481.

Carrasco, L., Bautista, M.J., Gómez-Villamandos, J.C., Martin de las Mulas, J., Chacón-M de Lara, F., Wilkinson, P.J., and Sierra, M.A. (1997a). Development of microscopic lesions in splenic cords of pigs infected with African swine fever virus. Vet Res 28, 93-99.

Carrasco, L., Chàcón-M de Lara, F., Martín de Las Mulas, J., Gómez-Villamandos, J.C., Sierra, M.A., Villeda, C.J., and Wilkinson, P.J. (1997b). Ultrastructural changes related to the lymph node haemorrhages in acute African swine fever. Res Vet Sci 62, 199-204.

Carrasco, L., Núñez, A., Salguero, F.J., Díaz San Segundo, F., Sánchez-Cordón, P., Gómez-Villamandos, J.C., and Sierra, M.A. (2002). African swine fever: Expression of interleukin-1 alpha and tumour necrosis factor-alpha by pulmonary intravascular macrophages. J Comp Pathol 126, 194-201.

Carrascosa, A.L., Bustos, M.J., Galindo, I., and Viñuela, E. (1999). Virus-specific cell receptors are necessary, but not sufficient, to confer cell susceptibility to African swine fever virus. Arch Virol 144, 1309-1321.

Carrascosa, J.L., Carazo, J.M., Carrascosa, A.L., García, N., Santisteban, A., and Viñuela, E. (1984). General morphology and capsid fine structure of African swine fever virus particles. Virology 132, 160-172.

Carrascosa, J.L., González, P., Carrascosa, A.L., Garciá-Barreno, B., Enjuanes, L., and Viñuela, E. (1986). Localization of structural proteins in African swine fever virus particles by immunoelectron microscopy. J Virol 58, 377-384.

Carrillo, C., Borca, M.V., Afonso, C.L., Onisk, D.V., and Rock, D.L. (1994). Long-term persistent infection of swine monocytes/macrophages with African swine fever virus. J Virol 68, 580-583.

Cermak, T., Doyle, E.L., Christian, M., Wang, L., Zhang, Y., Schmidt, C., Baller, J.A., Somia, N.V., Bogdanove, A.J., and Voytas, D.F. (2011). Efficient design and assembly of custom TALEN and other TAL effector-based constructs for DNA targeting. Nucleic Acids Res 39, e82.

Chan, A.W., Chong, K.Y., Martinovich, C., Simerly, C., and Schatten, G. (2001). Transgenic monkeys produced by retroviral gene transfer into mature oocytes. Science 291, 309-312.

Chapman, D.A., Tcherepanov, V., Upton, C., and Dixon, L.K. (2008). Comparison of the genome sequences of non-pathogenic and pathogenic African swine fever virus isolates. J Gen Virol 89, 397-408.

Chen Lf, Fischle, W., Verdin, E., and Greene, W.C. (2001). Duration of nuclear NF-kappaB action regulated by reversible acetylation. Science 293, 1653-1657.

Chernikova, D., Motamedi, S., Csürös, M., Koonin, E.V., and Rogozin, I.B. (2011). A late origin of the extant eukaryotic diversity: divergence time estimates using rare genomic changes. Biol Direct 6, 26.

Christian, M., Cermak, T., Doyle, E.L., Schmidt, C., Zhang, F., Hummel, A., Bogdanove, A.J., and Voytas, D.F. (2010). Targeting DNA double-strand breaks with TAL effector nucleases. Genetics 186, 757-761.

Chu, V.T., Weber, T., Wefers, B., Wurst, W., Sander, S., Rajewsky, K., and Kühn, R. (2015). Increasing the efficiency of homology-directed repair for CRISPR-Cas9-induced precise gene editing in mammalian cells. Nat Biotechnol 33, 543-548.

Clark, A.J. (1998). Gene expression in the mammary glands of transgenic animals. Biochem Soc Symp 63, 133-140.

Clark, S.A., Kinghorn, B.P., Hickey, J.M., and van der Werf, J.H. (2013). The effect of genomic information on optimal contribution selection in livestock breeding programs. Genet Sel Evol 45, 44.

Cobbold, C., Windsor, M., and Wileman, T. (2001). A virally encoded chaperone specialized for folding of the major capsid protein of African swine fever virus. J Virol 75, 7221-7229.

Cogswell, P.C., Scheinman, R.I., and Baldwin, A.S. (1993). Promoter of the human NF-kappa B p50/p105 gene. Regulation by NF-kappa B subunits and by c-REL. J Immunol 150, 2794-2804.

Cohen, S.N., Chang, A.C., and Hsu, L. (1972). Nonchromosomal antibiotic resistance in bacteria: genetic transformation of Escherichia coli by R-factor DNA. Proc Natl Acad Sci U S A 69, 2110-2114.

Collart, M.A., Baeuerle, P., and Vassalli, P. (1990). Regulation of tumor necrosis factor alpha transcription in macrophages: involvement of four kappa B-like motifs and of constitutive and inducible forms of NF-kappa B. Mol Cell Biol 10, 1498-1506.

Cong, L., Ran, F.A., Cox, D., Lin, S., Barretto, R., Habib, N., Hsu, P.D., Wu, X., Jiang, W., Marraffini, L.A., et al. (2013). Multiplex genome engineering using CRISPR/Cas systems. Science 339, 819-823.

Cooper, A.M., and Khader, S.A. (2007). IL-12p40: an inherently agonistic cytokine. Trends Immunol 28, 33-38.

Costard, S., Wieland, B., de Glanville, W., Jori, F., Rowlands, R., Vosloo, W., Roger, F., Pfeiffer, D.U., and Dixon, L.K. (2009). African swine fever: how can global spread be prevented? Philos Trans R Soc Lond B Biol Sci 364, 2683-2696.

Croquet, C., Mayeres, P., Gillon, A., Vanderick, S., and Gengler, N. (2006). Inbreeding depression for global and partial economic indexes, production, type, and functional traits. J Dairy Sci 89, 2257-2267.

Cyranoski, D. (2016). Chinese scientists to pioneer first human CRISPR trial. Nature 535, 476-477.

Daetwyler, H.D., Villanueva, B., Bijma, P., and Woolliams, J.A. (2007). Inbreeding in genome-wide selection. J Anim Breed Genet 124, 369-376.

Davis, A.J., Chi, L., So, S., Lee, K.J., Mori, E., Fattah, K., Yang, J., and Chen, D.J. (2014). BRCA1 modulates the autophosphorylation status of DNA-PKcs in S phase of the cell cycle. Nucleic Acids Res 42, 11487-11501.

Dawson, H.D., Smith, A.D., Chen, C., and Urban, J.F. (2016). An in-depth comparison of the porcine, murine and human inflammasomes; lessons from the porcine genome and transcriptome. Vet Microbiol.

de Villiers, E.P., Gallardo, C., Arias, M., da Silva, M., Upton, C., Martin, R., and Bishop, R.P. (2010). Phylogenomic analysis of 11 complete African swine fever virus genome sequences. Virology 400, 128-136.

Dejardin, E. (2006). The alternative NF-kappaB pathway from biochemistry to biology: pitfalls and promises for future drug development. Biochem Pharmacol 72, 1161-1179.

Dejardin, E., Deregowski, V., Chapelier, M., Jacobs, N., Gielen, J., Merville, M.P., and Bours, V. (1999). Regulation of NF-kappaB activity by I kappaB-related proteins in adenocarcinoma cells. Oncogene 18, 2567-2577.

Deng, D., Yan, C., Pan, X., Mahfouz, M., Wang, J., Zhu, J.K., Shi, Y., and Yan, N. (2012). Structural basis for sequence-specific recognition of DNA by TAL effectors. Science 335, 720-723.

Denning, C., Burl, S., Ainslie, A., Bracken, J., Dinnyes, A., Fletcher, J., King, T., Ritchie, M., Ritchie, W.A., Rollo, M., et al. (2001). Deletion of the alpha(1,3)galactosyl transferase (GGTA1) gene and the prion protein (PrP) gene in sheep. Nat Biotechnol 19, 559-562.

Deshmane, S.L., Kremlev, S., Amini, S., and Sawaya, B.E. (2009). Monocyte chemoattractant protein-1 (MCP-1): an overview. J Interferon Cytokine Res 29, 313-326.

Detray, D.E. (1957). African swine fever in wart hogs (Phacochoerus aethiopicus). J Am Vet Med Assoc 130, 537-540.

Devin, A., Cook, A., Lin, Y., Rodriguez, Y., Kelliher, M., and Liu, Z. (2000). The distinct roles of TRAF2 and RIP in IKK activation by TNF-R1: TRAF2 recruits IKK to TNF-R1 while RIP mediates IKK activation. Immunity 12, 419-429.

Diaz Montilla, R., and Sanchez Botija, C. (1966). [The evolution of African swine pest in Spain during the period of May 1965 to April 1966]. Bull Off Int Epizoot 66, 707-709.

DiDonato, J.A., Hayakawa, M., Rothwarf, D.M., Zandi, E., and Karin, M. (1997). A cytokine-responsive IkappaB kinase that activates the transcription factor NF-kappaB. Nature 388, 548-554.

Dixon, L.K., Chapman, D.A., Netherton, C.L., and Upton, C. (2013). African swine fever virus replication and genomics. Virus Res 173, 3-14.

Dixon, L.K., Abrams, C.C., Bowick, G., Goatley, L.C., Kay-Jackson, P.C., Chapman, D., Liverani, E., Nix, R., Silk, R., and Zhang, F. (2004). African swine fever virus proteins involved in evading host defence systems. Vet Immunol Immunopathol *100*, 117-134.

Doench, J.G., Fusi, N., Sullender, M., Hegde, M., Vaimberg, E.W., Donovan, K.F., Smith, I., Tothova, Z., Wilen, C., Orchard, R., et al. (2016). Optimized sgRNA design to maximize activity and minimize off-target effects of CRISPR-Cas9. Nat Biotechnol 34, 184-191.

Doetschman, T., Gregg, R.G., Maeda, N., Hooper, M.L., Melton, D.W., Thompson, S., and Smithies, O. (1987). Targetted correction of a mutant HPRT gene in mouse embryonic stem cells. Nature 330, 576-578.

Doi, T.S., Takahashi, T., Taguchi, O., Azuma, T., and Obata, Y. (1997). NF-kappa B RelA-deficient lymphocytes: normal development of T cells and B cells, impaired production of IgA and IgG1 and reduced proliferative responses. J Exp Med 185, 953-961.

Doi, T.S., Marino, M.W., Takahashi, T., Yoshida, T., Sakakura, T., Old, L.J., and Obata, Y. (1999). Absence of tumor necrosis factor rescues RelA-deficient mice from embryonic lethality. Proc Natl Acad Sci U S A 96, 2994-2999.

Dong, J., Jimi, E., Zhong, H., Hayden, M.S., and Ghosh, S. (2008). Repression of gene expression by unphosphorylated NF-kappaB p65 through epigenetic mechanisms. Genes Dev 22, 1159-1173.

Dreier, B., Beerli, R.R., Segal, D.J., Flippin, J.D., and Barbas, C.F. (2001). Development of zinc finger domains for recognition of the 5'-ANN-3' family of DNA sequences and their use in the construction of artificial transcription factors. J Biol Chem 276, 29466-29478.

Dreier, B., Fuller, R.P., Segal, D.J., Lund, C.V., Blancafort, P., Huber, A., Koksch, B., and Barbas, C.F. (2005). Development of zinc finger domains for recognition of the 5'-CNN-3' family DNA sequences and their use in the construction of artificial transcription factors. J Biol Chem 280, 35588-35597.

Dreier, B., Segal, D.J., and Barbas, C.F. (2000). Insights into the molecular recognition of the 5'-GNN-3' family of DNA sequences by zinc finger domains. J Mol Biol 303, 489-502.

Dreyer, A.K., Hoffmann, D., Lachmann, N., Ackermann, M., Steinemann, D., Timm, B., Siler, U., Reichenbach, J., Grez, M., Moritz, T., et al. (2015). TALEN-mediated functional correction of X-linked chronic granulomatous disease in patient-derived induced pluripotent stem cells. Biomaterials 69, 191-200.

Elrod-Erickson, M., Benson, T.E., and Pabo, C.O. (1998). High-resolution structures of variant Zif268-DNA complexes: implications for understanding zinc finger-DNA recognition. Structure 6, 451-464.

Esparza, I., González, J.C., and Viñuela, E. (1988). Effect of interferon-alpha, interferon-gamma and tumour necrosis factor on African swine fever virus replication in porcine monocytes and macrophages. J Gen Virol 69 (Pt 12), 2973-2980.

Eteqadi, B., Ghavi Hossein-Zadeh, N., and Shadparvar, A.A. (2015). Inbreeding effects on reproductive traits in Iranian Guilan sheep. Trop Anim Health Prod 47, 533-539.

Fan, C.M., and Maniatis, T. (1991). Generation of p50 subunit of NF-kappa B by processing of p105 through an ATP-dependent pathway. Nature 354, 395-398.

Fattah, F., Lee, E.H., Weisensel, N., Wang, Y., Lichter, N., and Hendrickson, E.A. (2010). Ku regulates the non-homologous end joining pathway choice of DNA double-strand break repair in human somatic cells. PLoS Genet 6, e1000855.

Fishbourne, E., Abrams, C.C., Takamatsu, H.H., and Dixon, L.K. (2013a). Modulation of chemokine and chemokine receptor expression following infection of porcine macrophages with African swine fever virus. Vet Microbiol 162, 937-943.

Fishbourne, E., Hutet, E., Abrams, C., Cariolet, R., Le Potier, M.F., Takamatsu, H.H., and Dixon, L.K. (2013b). Increase in chemokines CXCL10 and CCL2 in blood from pigs infected with high compared to low virulence African swine fever virus isolates. Vet Res 44, 87.

Frantz, L.A., Schraiber, J.G., Madsen, O., Megens, H.J., Cagan, A., Bosse, M., Paudel, Y., Crooijmans, R.P., Larson, G., and Groenen, M.A. (2015). Evidence of long-term gene flow and selection during domestication from analyses of Eurasian wild and domestic pig genomes. Nat Genet 47, 1141-1148.

Franzoni, G., Graham, S.P., Giudici, S.D., Bonelli, P., Pilo, G., Anfossi, A.G., Pittau, M., Nicolussi, P.S., Laddomada, A., and Oggiano, A. (2017). Characterization of the interaction of African swine fever virus with monocytes and derived macrophage subsets. Vet Microbiol 198, 88-98.

Franzoso, G., Carlson, L., Poljak, L., Shores, E.W., Epstein, S., Leonardi, A., Grinberg, A., Tran, T., Scharton-Kersten, T., Anver, M., et al. (1998). Mice deficient in nuclear factor (NF)-kappa B/p52 present with defects in humoral responses, germinal center reactions, and splenic microarchitecture. J Exp Med 187, 147-159.

Franzoso, G., Carlson, L., Scharton-Kersten, T., Shores, E.W., Epstein, S., Grinberg, A., Tran, T., Shacter, E., Leonardi, A., Anver, M., et al. (1997). Critical roles for the Bcl-3 oncoprotein in T cell-mediated immunity, splenic microarchitecture, and germinal center reactions. Immunity 6, 479-490.

Fu, Y., Foden, J.A., Khayter, C., Maeder, M.L., Reyon, D., Joung, J.K., and Sander, J.D. (2013). High-frequency off-target mutagenesis induced by CRISPR-Cas nucleases in human cells. Nat Biotechnol 31, 822-826.

Gaj, T., Guo, J., Kato, Y., Sirk, S.J., and Barbas, C.F. (2012). Targeted gene knockout by direct delivery of zinc-finger nuclease proteins. Nat Methods 9, 805-807.

Garrick, D.J. (2011). The nature, scope and impact of genomic prediction in beef cattle in the United States. Genet Sel Evol 43, 17.

Gasiunas, G., Barrangou, R., Horvath, P., and Siksnys, V. (2012). Cas9-crRNA ribonucleoprotein complex mediates specific DNA cleavage for adaptive immunity in bacteria. Proc Natl Acad Sci U S A 109, E2579-2586.

Gauthier, M., and Degnan, B.M. (2008). The transcription factor NF-kappaB in the demosponge Amphimedon queenslandica: insights on the evolutionary origin of the Rel homology domain. Dev Genes Evol 218, 23-32.

Gerber, P.J., Steinfeld, H., Henderson, B., Mottet, A., Opio, C., Dijkman, J., Falcucci, A. and Tempio, G. (2013). Tackling climate change through livestock – A global assessment of emissions and mitigation opportunities. Food and Agriculture Organization of the United Nations (FAO), Rome.

Gerritsen, M.E., Williams, A.J., Neish, A.S., Moore, S., Shi, Y., and Collins, T. (1997). CREB-binding protein/p300 are transcriptional coactivators of p65. Proc Natl Acad Sci U S A 94, 2927-2932.

Gil, S., Spagnuolo-Weaver, M., Canals, A., Sepúlveda, N., Oliveira, J., Aleixo, A., Allan, G., Leitão, A., and Martins, C.L. (2003). Expression at mRNA level of cytokines and A238L gene in porcine blood-derived macrophages infected in vitro

with African swine fever virus (ASFV) isolates of different virulence. Arch Virol 148, 2077-2097.

Gil, S., Sepúlveda, N., Albina, E., Leitão, A., and Martins, C. (2008). The low-virulent African swine fever virus (ASFV/NH/P68) induces enhanced expression and production of relevant regulatory cytokines (IFNalpha, TNFalpha and IL12p40) on porcine macrophages in comparison to the highly virulent ASFV/L60. Arch Virol 153, 1845-1854.

Gilbert, L.A., Horlbeck, M.A., Adamson, B., Villalta, J.E., Chen, Y., Whitehead, E.H., Guimaraes, C., Panning, B., Ploegh, H.L., Bassik, M.C., et al. (2014). Genome-Scale CRISPR-Mediated Control of Gene Repression and Activation. Cell 159, 647-661.

Golding, J.P., Goatley, L., Goodbourn, S., Dixon, L.K., Taylor, G., and Netherton, C.L. (2016). Sensitivity of African swine fever virus to type I interferon is linked to genes within multigene families 360 and 505. Virology 493, 154-161.

Golovan, S.P., Meidinger, R.G., Ajakaiye, A., Cottrill, M., Wiederkehr, M.Z., Barney, D.J., Plante, C., Pollard, J.W., Fan, M.Z., Hayes, M.A., et al. (2001). Pigs expressing salivary phytase produce low-phosphorus manure. Nat Biotechnol 19, 741-745.

González, A., Talavera, A., Almendral, J.M., and Viñuela, E. (1986). Hairpin loop structure of African swine fever virus DNA. Nucleic Acids Res 14, 6835-6844.

Goodarzi, A.A., Jeggo, P., and Lobrich, M. (2010). The influence of heterochromatin on DNA double strand break repair: Getting the strong, silent type to relax. DNA Repair (Amst) 9, 1273-1282.

Gordon, J.W., and Ruddle, F.H. (1981). Integration and stable germ line transmission of genes injected into mouse pronuclei. Science 214, 1244-1246.

Groenen, M.A. (2016). A decade of pig genome sequencing: a window on pig domestication and evolution. Genet Sel Evol 48, 23.

Grumont, R.J., Richardson, I.B., Gaff, C., and Gerondakis, S. (1993). rel/NF-kappa B nuclear complexes that bind kB sites in the murine c-rel promoter are required for constitutive c-rel transcription in B-cells. Cell Growth Differ 4, 731-743.

Guo, J., Gaj, T., and Barbas, C.F. (2010). Directed evolution of an enhanced and highly efficient FokI cleavage domain for zinc finger nucleases. J Mol Biol 400, 96-107.

Gupta, N., Delrow, J., Drawid, A., Sengupta, A.M., Fan, G., and Gélinas, C. (2008). Repression of B-cell linker (BLNK) and B-cell adaptor for phosphoinositide 3-kinase (BCAP) is important for lymphocyte transformation by rel proteins. Cancer Res 68, 808-814.

Gómez-Puertas, P., Rodríguez, F., Oviedo, J.M., Ramiro-Ibáñez, F., Ruiz-Gonzalvo, F., Alonso, C., and Escribano, J.M. (1996). Neutralizing antibodies to different proteins of African swine fever virus inhibit both virus attachment and internalization. J Virol 70, 5689-5694.

Gómez del Moral, M., Ortuño, E., Fernández-Zapatero, P., Alonso, F., Alonso, C., Ezquerra, A., and Domínguez, J. (1999). African swine fever virus infection induces tumor necrosis factor alpha production: implications in pathogenesis. J Virol 73, 2173-2180.

Gómez-Villamandos, J.C., Hervás, J., Moreno, C., Carrasco, L., Bautista, M.J., Caballero, J.M., Wilkinson, P.J., and Sierra, M.A. (1997). Subcellular changes in the tonsils of pigs infected with acute African swine fever virus. Vet Res 28, 179-189.

Gómez-Villamandos, J.C., Bautista, M.J., Sánchez-Cordón, P.J., and Carrasco, L. (2013). Pathology of African swine fever: the role of monocyte-macrophage. Virus Res 173, 140-149.

Hamilton, D.L., and Abremski, K. (1984). Site-specific recombination by the bacteriophage P1 lox-Cre system. Cre-mediated synapsis of two lox sites. J Mol Biol 178, 481-486.

Hammer, R.E., Pursel, V.G., Rexroad, C.E., Wall, R.J., Bolt, D.J., Ebert, K.M., Palmiter, R.D., and Brinster, R.L. (1985). Production of transgenic rabbits, sheep and pigs by microinjection. Nature 315, 680-683.

Han, Z.S., and Ip, Y.T. (1999). Interaction and specificity of Rel-related proteins in regulating Drosophila immunity gene expression. J Biol Chem 274, 21355-21361.

Hannink, M., and Temin, H.M. (1990). Structure and autoregulation of the c-rel promoter. Oncogene 5, 1843-1850.

Hauschild, J., Petersen, B., Santiago, Y., Queisser, A.L., Carnwath, J.W., Lucas-Hahn, A., Zhang, L., Meng, X., Gregory, P.D., Schwinzer, R., et al. (2011). Efficient generation of a biallelic knockout in pigs using zinc-finger nucleases. Proc Natl Acad Sci U S A 108, 12013-12017.

Hayden, M.S., and Ghosh, S. (2004). Signaling to NF-kappaB. Genes Dev 18, 2195-2224.

He, Z., Proudfoot, C., Whitelaw, C.B., and Lillico, S.G. (2016). Comparison of CRISPR/Cas9 and TALENs on editing an integrated EGFP gene in the genome of HEK293FT cells. Springerplus 5, 814.

Heath, C.M., Windsor, M., and Wileman, T. (2001). Aggresomes resemble sites specialized for virus assembly. J Cell Biol 153, 449-455.

Hein, H., Schlüter, C., Kulke, R., Christophers, E., Schröder, J.M., and Bartels, J. (1997). Genomic organization, sequence, and transcriptional regulation of the human eotaxin gene. Biochem Biophys Res Commun 237, 537-542.

Hernáez, B., Guerra, M., Salas, M.L., and Andrés, G. (2016). African Swine Fever Virus Undergoes Outer Envelope Disruption, Capsid Disassembly and Inner Envelope Fusion before Core Release from Multivesicular Endosomes. PLoS Pathog 12, e1005595.

Herrero, M., Grace, D., Njuki, J., Johnson, N., Enahoro, D., Silvestri, S. (2013). The roles of livestock in developing countries. Animal 7, 3-18.

Hervás, J., Gómez-Villamandos, J.C., Méndez, A., Carrasco, L., and Sierra, M.A. (1996). The lesional changes and pathogenesis in the kidney in African swine fever. Vet Res Commun 20, 285-299.

Hess, W.R., Endris, R.G., Lousa, A., and Caiado, J.M. (1989). Clearance of African swine fever virus from infected tick (Acari) colonies. J Med Entomol 26, 314-317.

Heusch, M., Lin, L., Geleziunas, R., and Greene, W.C. (1999). The generation of nfkb2 p52: mechanism and efficiency. Oncogene 18, 6201-6208.

Heuschele, W.P., and Coggins, L. (1965). Isolation of African swine fever virus from a giant forest hog. Bull Epizoot Dis Afr 13, 255-256.

Heuschele, W.P., and Coggins, L. (1969). Epizootiology of African swine fever virus in warthogs. Bull Epizoot Dis Afr 17, 179-183.

Hinz, M., Arslan, S., and Scheidereit, C. (2012). It takes two to tango: IκBs, the multifunctional partners of NF-κB. Immunol Rev 246, 59-76.

Hiscott, J., Alper, D., Cohen, L., Leblanc, J.F., Sportza, L., Wong, A., and Xanthoudakis, S. (1989). Induction of human interferon gene expression is associated with a nuclear factor that interacts with the NF-kappa B site of the human immunodeficiency virus enhancer. J Virol 63, 2557-2566.

Hiscott, J., Marois, J., Garoufalis, J., D'Addario, M., Roulston, A., Kwan, I., Pepin, N., Lacoste, J., Nguyen, H., and Bensi, G. (1993). Characterization of a functional NF-kappa B site in the human interleukin 1 beta promoter: evidence for a positive autoregulatory loop. Mol Cell Biol 13, 6231-6240.

Hiscott, J., Kwon, H., and Génin, P. (2001). Hostile takeovers: viral appropriation of the NF-kappaB pathway. J Clin Invest 107, 143-151.

Hoffmann, A., Levchenko, A., Scott, M.L., and Baltimore, D. (2002). The IkappaB-NF-kappaB signaling module: temporal control and selective gene activation. Science 298, 1241-1245.

Holkers, M., Maggio, I., Liu, J., Janssen, J.M., Miselli, F., Mussolino, C., Recchia, A., Cathomen, T., and Gonçalves, M.A. (2013). Differential integrity of TALE nuclease genes following adenoviral and lentiviral vector gene transfer into human cells. Nucleic Acids Res 41, e63.

Horwitz, B.H., Scott, M.L., Cherry, S.R., Bronson, R.T., and Baltimore, D. (1997). Failure of lymphopoiesis after adoptive transfer of NF-kappaB-deficient fetal liver cells. Immunity 6, 765-772.

Hsu, H., Shu, H.B., Pan, M.G., and Goeddel, D.V. (1996). TRADD-TRAF2 and TRADD-FADD interactions define two distinct TNF receptor 1 signal transduction pathways. Cell 84, 299-308.

Hu, Y., Baud, V., Delhase, M., Zhang, P., Deerinck, T., Ellisman, M., Johnson, R., and Karin, M. (1999). Abnormal morphogenesis but intact IKK activation in mice lacking the IKKalpha subunit of IkappaB kinase. Science 284, 316-320.

Huang, T.T., Kudo, N., Yoshida, M., and Miyamoto, S. (2000). A nuclear export signal in the N-terminal regulatory domain of IkappaBalpha controls cytoplasmic localization of inactive NF-kappaB/IkappaBalpha complexes. Proc Natl Acad Sci U S A 97, 1014-1019.

Huang, T.T., and Miyamoto, S. (2001). Postrepression activation of NF-kappaB requires the amino-terminal nuclear export signal specific to IkappaBalpha. Mol Cell Biol 21, 4737-4747.

Huang, B., Yang, X.D., Lamb, A., and Chen, L.F. (2010). Posttranslational modifications of NF-kappaB: another layer of regulation for NF-kappaB signaling pathway. Cell Signal 22, 1282-1290.

Huang, P., Xiao, A., Zhou, M., Zhu, Z., Lin, S., and Zhang, B. (2011). Heritable gene targeting in zebrafish using customized TALENs. Nat Biotechnol 29, 699-700.

Huxford, T., Huang, D.B., Malek, S., and Ghosh, G. (1998). The crystal structure of the IkappaBalpha/NF-kappaB complex reveals mechanisms of NF-kappaB inactivation. Cell 95, 759-770.

Iotsova, V., Caamaño, J., Loy, J., Yang, Y., Lewin, A., and Bravo, R. (1997). Osteopetrosis in mice lacking NF-kappaB1 and NF-kappaB2. Nat Med 3, 1285-1289.

Ishino, Y., Shinagawa, H., Makino, K., Amemura, M., and Nakata, A. (1987). Nucleotide sequence of the iap gene, responsible for alkaline phosphatase isozyme conversion in Escherichia coli, and identification of the gene product. J Bacteriol 169, 5429-5433.

Iwai, K. (2012). Diverse ubiquitin signaling in NF-κB activation. Trends Cell Biol 22, 355-364.

Iyer, L.M., Aravind, L., and Koonin, E.V. (2001). Common origin of four diverse families of large eukaryotic DNA viruses. J Virol 75, 11720-11734.

Iyer, L.M., Balaji, S., Koonin, E.V., and Aravind, L. (2006). Evolutionary genomics of nucleo-cytoplasmic large DNA viruses. Virus Res 117, 156-184.

Jackson, D.A., Symons, R.H., and Berg, P. (1972). Biochemical method for inserting new genetic information into DNA of Simian Virus 40: circular SV40 DNA molecules containing lambda phage genes and the galactose operon of Escherichia coli. Proc Natl Acad Sci U S A 69, 2904-2909.

Jaenisch, R., and Mintz, B. (1974). Simian virus 40 DNA sequences in DNA of healthy adult mice derived from preimplantation blastocysts injected with viral DNA. Proc Natl Acad Sci U S A 71, 1250-1254.

Jenko, J., Gorjanc, G., Cleveland, M.A., Varshney, R.K., Whitelaw, C.B., Woolliams, J.A., and Hickey, J.M. (2015). Potential of promotion of alleles by genome editing to improve quantitative traits in livestock breeding programs. Genet Sel Evol 47, 55.

Jiang, W., Bikard, D., Cox, D., Zhang, F., and Marraffini, L.A. (2013). RNA-guided editing of bacterial genomes using CRISPR-Cas systems. Nat Biotechnol 31, 233-239.

Jinek, M., Chylinski, K., Fonfara, I., Hauer, M., Doudna, J.A., and Charpentier, E. (2012). A programmable dual-RNA-guided DNA endonuclease in adaptive bacterial immunity. Science 337, 816-821.

Johnson, C., Van Antwerp, D., and Hope, T.J. (1999). An N-terminal nuclear export signal is required for the nucleocytoplasmic shuttling of IkappaBalpha. EMBO J 18, 6682-6693.

Jori, F., et al. (2007). The role of wild hosts (wild pigs and ticks) in the epidemiology of African swine fever in West Africa and Madagascar. In Proc. 12th Int. Conf. Assoc. Inst. Trop. Vet. Med, 8–22. Montpellier, France: CIRAD.

Jori, F., and Bastos, A.D. (2009). Role of wild suids in the epidemiology of African swine fever. Ecohealth 6, 296-310.

Jori, F., Vial, L., Penrith, M.L., Pérez-Sánchez, R., Etter, E., Albina, E., Michaud, V., and Roger, F. (2013). Review of the sylvatic cycle of African swine fever in sub-Saharan Africa and the Indian ocean. Virus Res 173, 212-227.

Jost, P.J., and Ruland, J. (2007). Aberrant NF-kappaB signaling in lymphoma: mechanisms, consequences, and therapeutic implications. Blood 109, 2700-2707.

Jouvenet, N., Monaghan, P., Way, M., and Wileman, T. (2004). Transport of African swine fever virus from assembly sites to the plasma membrane is dependent on microtubules and conventional kinesin. J Virol 78, 7990-8001.

Jouvenet, N., Windsor, M., Rietdorf, J., Hawes, P., Monaghan, P., Way, M., and Wileman, T. (2006). African swine fever virus induces filopodia-like projections at the plasma membrane. Cell Microbiol 8, 1803-1811.

Karin, M., and Greten, F.R. (2005). NF-kappaB: linking inflammation and immunity to cancer development and progression. Nat Rev Immunol 5, 749-759.

Kasibhatla, S., Brunner, T., Genestier, L., Echeverri, F., Mahboubi, A., and Green, D.R. (1998). DNA damaging agents induce expression of Fas ligand and subsequent apoptosis in T lymphocytes via the activation of NF-kappa B and AP-1. Mol Cell 1, 543-551.

Kato, T., Delhase, M., Hoffmann, A., and Karin, M. (2003). CK2 Is a C-Terminal IkappaB Kinase Responsible for NF-kappaB Activation during the UV Response. Mol Cell 12, 829-839.

Kearns, J.D., Basak, S., Werner, S.L., Huang, C.S., and Hoffmann, A. (2006). IkappaBepsilon provides negative feedback to control NF-kappaB oscillations, signaling dynamics, and inflammatory gene expression. J Cell Biol 173, 659-664.

Kiernan, R., Brès, V., Ng, R.W., Coudart, M.P., El Messaoudi, S., Sardet, C., Jin, D.Y., Emiliani, S., and Benkirane, M. (2003). Post-activation turn-off of NF-kappa B-dependent transcription is regulated by acetylation of p65. J Biol Chem 278, 2758-2766.

Kim, D.J., Youn, J.I., Seo, S.H., Jin, H.T., and Sung, Y.C. (2008). Differential regulation of antigen-specific CD8+ T cell responses by IL-12p40 in a dose-dependent manner. J Immunol 180, 7167-7174.

Kim, H., and Kim, J.S. (2014). A guide to genome engineering with programmable nucleases. Nat Rev Genet 15, 321-334.

King, K., Chapman, D., Argilaguet, J.M., Fishbourne, E., Hutet, E., Cariolet, R., Hutchings, G., Oura, C.A., Netherton, C.L., Moffat, K., et al. (2011). Protection of European domestic pigs from virulent African isolates of African swine fever virus by experimental immunisation. Vaccine 29, 4593-4600.

King, T., and De Sousa, P.A. (2006). Maintenance of pregnancy in pigs with limited viable embryos. Methods Mol Biol 348, 79-90.

Kleinstiver, B.P., Pattanayak, V., Prew, M.S., Tsai, S.Q., Nguyen, N.T., Zheng, Z., and Joung, J.K. (2016). High-fidelity CRISPR-Cas9 nucleases with no detectable genome-wide off-target effects. Nature 529, 490-495.

Kleinstiver, B.P., Prew, M.S., Tsai, S.Q., Topkar, V.V., Nguyen, N.T., Zheng, Z., Gonzales, A.P., Li, Z., Peterson, R.T., Yeh, J.R., et al. (2015). Engineered CRISPR-Cas9 nucleases with altered PAM specificities. Nature 523, 481-485.

Klement, J.F., Rice, N.R., Car, B.D., Abbondanzo, S.J., Powers, G.D., Bhatt, P.H., Chen, C.H., Rosen, C.A., and Stewart, C.L. (1996). IkappaBalpha deficiency results in a sustained NF-kappaB response and severe widespread dermatitis in mice. Mol Cell Biol 16, 2341-2349.

Klug, A., and Rhodes, D. (1987). Zinc fingers: a novel protein fold for nucleic acid recognition. Cold Spring Harb Symp Quant Biol 52, 473-482.

Kobayashi, Y. (2008). The role of chemokines in neutrophil biology. Front Biosci 13, 2400-2407.

Koike-Yusa, H., Li, Y., Tan, E.P., Velasco-Herrera, M.e.C., and Yusa, K. (2014). Genome-wide recessive genetic screening in mammalian cells with a lentiviral CRISPR-guide RNA library. Nat Biotechnol 32, 267-273.

Konermann, S., Brigham, M.D., Trevino, A.E., Hsu, P.D., Heidenreich, M., Cong, L., Platt, R.J., Scott, D.A., Church, G.M., and Zhang, F. (2013). Optical control of mammalian endogenous transcription and epigenetic states. Nature 500, 472-476.

Konermann, S., Brigham, M.D., Trevino, A.E., Joung, J., Abudayyeh, O.O., Barcena, C., Hsu, P.D., Habib, N., Gootenberg, J.S., Nishimasu, H., et al. (2015). Genome-scale transcriptional activation by an engineered CRISPR-Cas9 complex. Nature 517, 583-588.

Köntgen, F., Grumont, R.J., Strasser, A., Metcalf, D., Li, R., Tarlinton, D., and Gerondakis, S. (1995). Mice lacking the c-rel proto-oncogene exhibit defects in lymphocyte proliferation, humoral immunity, and interleukin-2 expression. Genes Dev 9, 1965-1977.

Krappmann, D., and Scheidereit, C. (2005). A pervasive role of ubiquitin conjugation in activation and termination of IkappaB kinase pathways. EMBO Rep 6, 321-326.

Kunsch, C., and Rosen, C.A. (1993). NF-kappa B subunit-specific regulation of the interleukin-8 promoter. Mol Cell Biol 13, 6137-6146.

Lammerding, J., Schulze, P.C., Takahashi, T., Kozlov, S., Sullivan, T., Kamm, R.D., Stewart, C.L., and Lee, R.T. (2004). Lamin A/C deficiency causes defective nuclear mechanics and mechanotransduction. J Clin Invest 113, 370-378.

Lange, C., Hemmrich, G., Klostermeier, U.C., López-Quintero, J.A., Miller, D.J., Rahn, T., Weiss, Y., Bosch, T.C., and Rosenstiel, P. (2011). Defining the origins of the NOD-like receptor system at the base of animal evolution. Mol Biol Evol 28, 1687-1702.

Lei, Y., Guo, X., Liu, Y., Cao, Y., Deng, Y., Chen, X., Cheng, C.H., Dawid, I.B., Chen, Y., and Zhao, H. (2012). Efficient targeted gene disruption in Xenopus embryos using engineered transcription activator-like effector nucleases (TALENs). Proc Natl Acad Sci U S A 109, 17484-17489.

Leitão, A., Cartaxeiro, C., Coelho, R., Cruz, B., Parkhouse, R.M., Portugal, F., Vigário, J.D., and Martins, C.L. (2001). The non-haemadsorbing African swine fever virus isolate ASFV/NH/P68 provides a model for defining the protective anti-virus immune response. J Gen Virol 82, 513-523.

Lernbecher, T., Kistler, B., and Wirth, T. (1994). Two distinct mechanisms contribute to the constitutive activation of RelB in lymphoid cells. EMBO J 13, 4060-4069.

Li, T., Liu, B., Spalding, M.H., Weeks, D.P., and Yang, B. (2012). High-efficiency TALEN-based gene editing produces disease-resistant rice. Nat Biotechnol 30, 390-392.

Li, Z., and Nabel, G.J. (1997). A new member of the I kappaB protein family, I kappaB epsilon, inhibits RelA (p65)-mediated NF-kappaB transcription. Mol Cell Biol 17, 6184-6190.

Li, Z.W., Chu, W., Hu, Y., Delhase, M., Deerinck, T., Ellisman, M., Johnson, R., and Karin, M. (1999). The IKKbeta subunit of IkappaB kinase (IKK) is essential for

nuclear factor kappaB activation and prevention of apoptosis. J Exp Med 189, 1839-1845.

Li, P., Estrada, J.L., Burlak, C., Montgomery, J., Butler, J.R., Santos, R.M., Wang, Z.Y., Paris, L.L., Blankenship, R.L., Downey, S.M., et al. (2015). Efficient generation of genetically distinct pigs in a single pregnancy using multiplexed single-guide RNA and carbohydrate selection. Xenotransplantation 22, 20-31.

Li, Q., Estepa, G., Memet, S., Israel, A., and Verma, I.M. (2000). Complete lack of NF-kappaB activity in IKK1 and IKK2 double-deficient mice: additional defect in neurulation. Genes Dev 14, 1729-1733.

Li, Q., Van Antwerp, D., Mercurio, F., Lee, K.F., and Verma, I.M. (1999a). Severe liver degeneration in mice lacking the IkappaB kinase 2 gene. Science 284, 321-325.

Li, Z.W., Chu, W., Hu, Y., Delhase, M., Deerinck, T., Ellisman, M., Johnson, R., and Karin, M. (1999b). The IKKbeta subunit of IkappaB kinase (IKK) is essential for nuclear factor kappaB activation and prevention of apoptosis. J Exp Med 189, 1839-1845.

Liao, G., Zhang, M., Harhaj, E.W., and Sun, S.C. (2004). Regulation of the NF-kappaB-inducing kinase by tumor necrosis factor receptor-associated factor 3-induced degradation. J Biol Chem 279, 26243-26250.

Libermann, T.A., and Baltimore, D. (1990). Activation of interleukin-6 gene expression through the NF-kappa B transcription factor. Mol Cell Biol 10, 2327-2334.

Lieber, M.R. (2010). The mechanism of double-strand DNA break repair by the nonhomologous DNA end-joining pathway. Annu Rev Biochem 79, 181-211.

Lillico, S.G., Proudfoot, C., Carlson, D.F., Stverakova, D., Neil, C., Blain, C., King, T.J., Ritchie, W.A., Tan, W., Mileham, A.J., et al. (2013). Live pigs produced from genome edited zygotes. Sci Rep 3, 2847.

Lillico, S.G., Proudfoot, C., King, T.J., Tan, W., Zhang, L., Mardjuki, R., Paschon, D.E., Rebar, E.J., Urnov, F.D., Mileham, A.J., et al. (2016). Mammalian interspecies substitution of immune modulatory alleles by genome editing. Sci Rep 6, 21645.

Lin, L., DeMartino, G.N., and Greene, W.C. (1998). Cotranslational biogenesis of NF-kappaB p50 by the 26S proteasome. Cell 92, 819-828.

Lin, S., Staahl, B.T., Alla, R.K., and Doudna, J.A. (2014). Enhanced homology-directed human genome engineering by controlled timing of CRISPR/Cas9 delivery. Elife 3, e04766.

Liu, J., Li, C., Yu, Z., Huang, P., Wu, H., Wei, C., Zhu, N., Shen, Y., Chen, Y., Zhang, B., et al. (2012). Efficient and specific modifications of the Drosophila genome by means of an easy TALEN strategy. J Genet Genomics 39, 209-215.

Liu, S.F., and Malik, A.B. (2006). NF-kappa B activation as a pathological mechanism of septic shock and inflammation. Am J Physiol Lung Cell Mol Physiol 290, L622-L645.

Liu, X., Wang, Y., Tian, Y., Yu, Y., Gao, M., Hu, G., Su, F., Pan, S., Luo, Y., Guo, Z., et al. (2014). Generation of mastitis resistance in cows by targeting human lysozyme gene to β-casein locus using zinc-finger nucleases. Proc Biol Sci 281, 20133368.

Lo, D., Pursel, V., Linton, P.J., Sandgren, E., Behringer, R., Rexroad, C., Palmiter, R.D., and Brinster, R.L. (1991). Expression of mouse IgA by transgenic mice, pigs and sheep. Eur J Immunol 21, 1001-1006.

Lombardi, L., Ciana, P., Cappellini, C., Trecca, D., Guerrini, L., Migliazza, A., Maiolo, A.T., and Neri, A. (1995). Structural and functional characterization of the promoter regions of the NFKB2 gene. Nucleic Acids Res 23, 2328-2336.

Luo, J., Song, Z., Yu, S., Cui, D., Wang, B., Ding, F., Li, S., Dai, Y., and Li, N. (2014). Efficient generation of myostatin (MSTN) biallelic mutations in cattle using zinc finger nucleases. PLoS One 9, e95225.

Luther, N.J., Majiyagbe, K.A., Shamaki, D., Lombin, L.H., Antiabong, J.F., Antiagbong, J.F., Bitrus, Y., and Owolodun, O. (2007). Detection of African swine fever virus genomic DNA in a Nigerian red river hog (Potamochoerus porcus). Vet Rec 160, 58-59.

Maclean, N., Woodall, C., and Crossley, F. (1987). Injection of the mouse MT-1 gene into rainbow trout eggs and assay of trout fry for resistance to cadmium and zinc toxicity. Experientia Suppl 52, 471-475.

Maeder, M.L., Thibodeau-Beganny, S., Osiak, A., Wright, D.A., Anthony, R.M., Eichtinger, M., Jiang, T., Foley, J.E., Winfrey, R.J., Townsend, J.A., et al. (2008). Rapid "open-source" engineering of customized zinc-finger nucleases for highly efficient gene modification. Mol Cell 31, 294-301.

Mak, A.N., Bradley, P., Cernadas, R.A., Bogdanove, A.J., and Stoddard, B.L. (2012). The crystal structure of TAL effector PthXo1 bound to its DNA target. Science 335, 716-719.

Makarova, K.S., Haft, D.H., Barrangou, R., Brouns, S.J., Charpentier, E., Horvath, P., Moineau, S., Mojica, F.J., Wolf, Y.I., Yakunin, A.F., et al. (2011). Evolution and classification of the CRISPR-Cas systems. Nat Rev Microbiol 9, 467-477.

Makris, C., Godfrey, V.L., Krähn-Senftleben, G., Takahashi, T., Roberts, J.L., Schwarz, T., Feng, L., Johnson, R.S., and Karin, M. (2000). Female mice heterozygous for IKK gamma/NEMO deficiencies develop a dermatopathy similar to the human X-linked disorder incontinentia pigmenti. Mol Cell 5, 969-979.

Malek, S., Chen, Y., Huxford, T., and Ghosh, G. (2001). IkappaBbeta, but not IkappaBalpha, functions as a classical cytoplasmic inhibitor of NF-kappaB dimers by masking both NF-kappaB nuclear localization sequences in resting cells. J Biol Chem 276, 45225-45235.

Manso Ribeiro, J. J., and J. A. Azevedo. (1961). La peste porcine africaine au Portugal. Bull Off Int Epizoot 55, 88-108.

Mantovani, A., Sozzani, S., and Introna, M. (1997). Endothelial activation by cytokines. Ann N Y Acad Sci 832, 93-116.

Marchant, J.N., Rudd, A.R., Mendl, M.T., Broom, D.M., Meredith, M.J., Corning, S., and Simmins, P.H. (2000). Timing and causes of piglet mortality in alternative and conventional farrowing systems. Vet Rec 147, 209-214.

Maruyama, T., Dougan, S.K., Truttmann, M.C., Bilate, A.M., Ingram, J.R., and Ploegh, H.L. (2015). Increasing the efficiency of precise genome editing with CRISPR-Cas9 by inhibition of nonhomologous end joining. Nat Biotechnol 33, 538-542.

Mathes, E., O'Dea, E.L., Hoffmann, A., and Ghosh, G. (2008). NF-kappaB dictates the degradation pathway of IkappaBalpha. EMBO J 27, 1357-1367.

Mattioli, I., Sebald, A., Bucher, C., Charles, R.P., Nakano, H., Doi, T., Kracht, M., and Schmitz, M.L. (2004). Transient and selective NF-kappa B p65 serine 536 phosphorylation induced by T cell costimulation is mediated by I kappa B kinase beta and controls the kinetics of p65 nuclear import. J Immunol 172, 6336-6344.

Mattson, M.P., and Camandola, S. (2001). NF-kappaB in neuronal plasticity and neurodegenerative disorders. J Clin Invest 107, 247-254.

Mebus, C.A., and Dardiri, A.H. (1980). Western hemisphere isolates of African swine fever virus: asymptomatic carriers and resistance to challenge inoculation. Am J Vet Res 41, 1867-1869.

Mémet, S., Laouini, D., Epinat, J.C., Whiteside, S.T., Goudeau, B., Philpott, D., Kayal, S., Sansonetti, P.J., Berche, P., Kanellopoulos, J., et al. (1999). IkappaBepsilon-deficient mice: reduction of one T cell precursor subspecies and enhanced Ig isotype switching and cytokine synthesis. J Immunol 163, 5994-6005.

Mc Guire, C., Prinz, M., Beyaert, R., and van Loo, G. (2013). Nuclear factor kappa B (NF-κB) in multiple sclerosis pathology. Trends Mol Med 19, 604-613.

McGranahan, N., Furness, A.J., Rosenthal, R., Ramskov, S., Lyngaa, R., Saini, S.K., Jamal-Hanjani, M., Wilson, G.A., Birkbak, N.J., Hiley, C.T., et al. (2016). Clonal neoantigens elicit T cell immunoreactivity and sensitivity to immune checkpoint blockade. Science 351, 1463-1469.

McNab, F., Mayer-Barber, K., Sher, A., Wack, A., and O'Garra, A. (2015). Type I interferons in infectious disease. Nat Rev Immunol 15, 87-103.

McVey, M., and Lee, S.E. (2008). MMEJ repair of double-strand breaks (director's cut): deleted sequences and alternative endings. Trends Genet 24, 529-538.

Mendenhall, E.M., Williamson, K.E., Reyon, D., Zou, J.Y., Ram, O., Joung, J.K., and Bernstein, B.E. (2013). Locus-specific editing of histone modifications at endogenous enhancers. Nat Biotechnol 31, 1133-1136.

Meng, X., Noyes, M.B., Zhu, L.J., Lawson, N.D., and Wolfe, S.A. (2008). Targeted gene inactivation in zebrafish using engineered zinc-finger nucleases. Nat Biotechnol 26, 695-701.

Merika, M., Williams, A.J., Chen, G., Collins, T., and Thanos, D. (1998). Recruitment of CBP/p300 by the IFN beta enhanceosome is required for synergistic activation of transcription. Mol Cell 1, 277-287.

Meyer, E., Aglyamova, G.V., Wang, S., Buchanan-Carter, J., Abrego, D., Colbourne, J.K., Willis, B.L., and Matz, M.V. (2009). Sequencing and de novo analysis of a coral larval transcriptome using 454 GSFlx. BMC Genomics 10, 219.

Meyer, M., de Angelis, M.H., Wurst, W., and Kühn, R. (2010). Gene targeting by homologous recombination in mouse zygotes mediated by zinc-finger nucleases. Proc Natl Acad Sci U S A 107, 15022-15026.

Micheau, O., and Tschopp, J. (2003). Induction of TNF receptor I-mediated apoptosis via two sequential signaling complexes. Cell 114, 181-190.

Miller, J., McLachlan, A.D., and Klug, A. (1985). Repetitive zinc-binding domains in the protein transcription factor IIIA from Xenopus oocytes. EMBO J 4, 1609-1614.

Miskin, J.E., Abrams, C.C., Goatley, L.C., and Dixon, L.K. (1998). A viral mechanism for inhibition of the cellular phosphatase calcineurin. Science 281, 562-565.

Miyaoka, Y., Berman, J.R., Cooper, S.B., Mayerl, S.J., Chan, A.H., Zhang, B., Karlin-Neumann, G.A., and Conklin, B.R. (2016). Systematic quantification of HDR and NHEJ reveals effects of locus, nuclease, and cell type on genome-editing. Sci Rep 6, 23549.

Mogi, M., Kondo, T., Mizuno, Y., and Nagatsu, T. (2007). p53 protein, interferon-gamma, and NF-kappaB levels are elevated in the parkinsonian brain. Neurosci Lett 414, 94-97.

Mojica, F.J., Díez-Villaseñor, C., García-Martínez, J., and Soria, E. (2005). Intervening sequences of regularly spaced prokaryotic repeats derive from foreign genetic elements. J Mol Evol 60, 174-182.

Mojica, F.J., Díez-Villaseñor, C., Soria, E., and Juez, G. (2000). Biological significance of a family of regularly spaced repeats in the genomes of Archaea, Bacteria and mitochondria. Mol Microbiol 36, 244-246.

Montgomery, R. (1921). On a form of swine fever occurring in British East Africa (Kenya Colony). J Comp Pathol 34, 159-191.

Moorthy, A.K., Savinova, O.V., Ho, J.Q., Wang, V.Y., Vu, D., and Ghosh, G. (2006). The 20S proteasome processes NF-kappaB1 p105 into p50 in a translation-independent manner. EMBO J 25, 1945-1956.

Morton, J., Davis, M.W., Jorgensen, E.M., and Carroll, D. (2006). Induction and repair of zinc-finger nuclease-targeted double-strand breaks in Caenorhabditis elegans somatic cells. Proc Natl Acad Sci U S A 103, 16370-16375.

Moscou, M.J., and Bogdanove, A.J. (2009). A simple cipher governs DNA recognition by TAL effectors. Science 326, 1501.

Msaki, A., Sánchez, A.M., Koh, L.F., Barré, B., Rocha, S., Perkins, N.D., and Johnson, R.F. (2011). The role of RelA (p65) threonine 505 phosphorylation in the regulation of cell growth, survival, and migration. Mol Biol Cell 22, 3032-3040.

Mukherjee, S.P., Behar, M., Birnbaum, H.A., Hoffmann, A., Wright, P.E., and Ghosh, G. (2013). Analysis of the RelA:CBP/p300 interaction reveals its involvement in NF-κB-driven transcription. PLoS Biol 11, e1001647.

Mur, L., Atzeni, M., Martínez-López, B., Feliziani, F., Rolesu, S., and Sanchez-Vizcaino, J.M. (2016). Thirty-Five-Year Presence of African Swine Fever in Sardinia: History, Evolution and Risk Factors for Disease Maintenance. Transbound Emerg Dis 63, e165-177.

Murphy, T.L., Cleveland, M.G., Kulesza, P., Magram, J., and Murphy, K.M. (1995). Regulation of interleukin 12 p40 expression through an NF-kappa B half-site. Mol Cell Biol 15, 5258-5267.

Mussolino, C., Alzubi, J., Fine, E.J., Morbitzer, R., Cradick, T.J., Lahaye, T., Bao, G., and Cathomen, T. (2014). TALENs facilitate targeted genome editing in human cells with high specificity and low cytotoxicity. Nucleic Acids Res 42, 6762-6773.

Muñoz-Moreno, R., Galindo, I., Cuesta-Geijo, M., Barrado-Gil, L., and Alonso, C. (2015). Host cell targets for African swine fever virus. Virus Res 209, 118-127.

Nakaseko, Y., Neuhaus, D., Klug, A., and Rhodes, D. (1992). Adjacent zinc-finger motifs in multiple zinc-finger peptides from SWI5 form structurally independent, flexibly linked domains. J Mol Biol 228, 619-636.

Nakata, A., Amemura, M., and Makino, K. (1989). Unusual nucleotide arrangement with repeated sequences in the Escherichia coli K-12 chromosome. J Bacteriol 171, 3553-3556.

Nakshatri, H., Bhat-Nakshatri, P., Martin, D.A., Goulet, R.J., and Sledge, G.W. (1997). Constitutive activation of NF-kappaB during progression of breast cancer to hormone-independent growth. Mol Cell Biol 17, 3629-3639.

Neilan, J.G., Lu, Z., Kutish, G.F., Zsak, L., Lewis, T.L., and Rock, D.L. (1997). A conserved African swine fever virus IkappaB homolog, 5EL, is nonessential for growth in vitro and virulence in domestic swine. Virology 235, 377-385.

Neilan, J.G., Zsak, L., Lu, Z., Burrage, T.G., Kutish, G.F., and Rock, D.L. (2004). Neutralizing antibodies to African swine fever virus proteins p30, p54, and p72 are not sufficient for antibody-mediated protection. Virology 319, 337-342.

Nelson, D.E., Ihekwaba, A.E., Elliott, M., Johnson, J.R., Gibney, C.A., Foreman, B.E., Nelson, G., See, V., Horton, C.A., Spiller, D.G., et al. (2004). Oscillations in NF-kappaB signaling control the dynamics of gene expression. Science 306, 704-708.

Neuhaus, D., Nakaseko, Y., Schwabe, J.W., and Klug, A. (1992). Solution structures of two zinc-finger domains from SWI5 obtained using two-dimensional 1H nuclear magnetic resonance spectroscopy. A zinc-finger structure with a third strand of beta-sheet. J Mol Biol 228, 637-651.

Nogal, M.L., González de Buitrago, G., Rodríguez, C., Cubelos, B., Carrascosa, A.L., Salas, M.L., and Revilla, Y. (2001). African swine fever virus IAP homologue inhibits caspase activation and promotes cell survival in mammalian cells. J Virol 75, 2535-2543.

Norberg, E.; Sørensen, A. C. (2006) Inbreeding in Danish meat sheep breeds. Proceedings of the 8th World Congress on Genetics Applied to Livestock Production, Belo Horizonte, Minas Gerais, Brazil, 13-18 August, 2006 2006 pp.04-14 ref.11

O'Donnell, V., Holinka, L.G., Gladue, D.P., Sanford, B., Krug, P.W., Lu, X., Arzt, J., Reese, B., Carrillo, C., Risatti, G.R., et al. (2015). African Swine Fever Virus Georgia Isolate Harboring Deletions of MGF360 and MGF505 Genes Is Attenuated

in Swine and Confers Protection against Challenge with Virulent Parental Virus. J Virol 89, 6048-6056.

O'Shea, J.M., and Perkins, N.D. (2008). Regulation of the RelA (p65) transactivation domain. Biochem Soc Trans 36, 603-608.

Okamoto, T. (2006). NF-kappaB and rheumatic diseases. Endocr Metab Immune Disord Drug Targets 6, 359-372.

Okita, K., Ichisaka, T., and Yamanaka, S. (2007). Generation of germline-competent induced pluripotent stem cells. Nature 448, 313-317.

Oltjen, J.W. and Beckett, J.L. (1996). Role of ruminant livestock in sustainable agricultural systems. J Anim Sci 74, 1406-1409.

Ouaaz, F., Li, M., and Beg, A.A. (1999). A critical role for the RelA subunit of nuclear factor kappaB in regulation of multiple immune-response genes and in Fas-induced cell death. J Exp Med 189, 999-1004.

Oura, C.A., Denyer, M.S., Takamatsu, H., and Parkhouse, R.M. (2005). In vivo depletion of CD8+ T lymphocytes abrogates protective immunity to African swine fever virus. J Gen Virol 86, 2445-2450.

Oura, C.A., Powell, P.P., Anderson, E., and Parkhouse, R.M. (1998). The pathogenesis of African swine fever in the resistant bushpig. J Gen Virol 79 (Pt 6), 1439-1443.

Pacifico, F., and Leonardi, A. (2006). NF-kappaB in solid tumors. Biochem Pharmacol 72, 1142-1152.

Pahl, A., and Szelenyi, I. (2002). Asthma therapy in the new millennium. Inflamm Res 51, 273-282.

Pahl, H.L. (1999). Activators and target genes of Rel/NF-kappaB transcription factors. Oncogene 18, 6853-6866.

Palgrave, C.J., Gilmour, L., Lowden, C.S., Lillico, S.G., Mellencamp, M.A., and Whitelaw, C.B. (2011). Species-specific variation in RELA underlies differences in NF-κB activity: a potential role in African swine fever pathogenesis. J Virol 85, 6008-6014.

Pattanayak, V., Lin, S., Guilinger, J.P., Ma, E., Doudna, J.A., and Liu, D.R. (2013). High-throughput profiling of off-target DNA cleavage reveals RNA-programmed Cas9 nuclease specificity. Nat Biotechnol 31, 839-843.

Pavletich, N.P., and Pabo, C.O. (1991). Zinc finger-DNA recognition: crystal structure of a Zif268-DNA complex at 2.1 A. Science 252, 809-817.

Penrith, M.L., Lopes Pereira, C., Lopes da Silva, M.M., Quembo, C., Nhamusso, A., and Banze, J. (2007). African swine fever in Mozambique: review, risk factors and considerations for control. Onderstepoort J Vet Res 74, 149-160.

Perkins, N.D. (2006). Post-translational modifications regulating the activity and function of the nuclear factor kappa B pathway. Oncogene 25, 6717-6730.

Phelps, C.B., Sengchanthalangsy, L.L., Huxford, T., and Ghosh, G. (2000). Mechanism of I kappa B alpha binding to NF-kappa B dimers. J Biol Chem 275, 29840-29846.

Plowright, W., Parker, J., and Peirce, M.A. (1969). African swine fever virus in ticks (Ornithodoros moubata, murray) collected from animal burrows in Tanzania. Nature 221, 1071-1073.

Plowright, W., Perry, C.T., and Peirce, M.A. (1970). Transovarial infection with African swine fever virus in the argasid tick, Ornithodoros moubata porcinus, Walton. Res Vet Sci 11, 582-584.

Plowright, W., Perry, C.T., and Greig, A. (1974). Sexual transmission of African swine fever virus in the tick, Ornithodoros moubata porcinus, Walton. Res Vet Sci 17, 106-113.

Plowright W. (1981). African swine fever. In: Davis, J.W., Karstad L.H., Trainer, D.O. (Eds.), Diseases of Wild Animals, 2nd edn., Iowa State University Press. Ames, IA. 178-190.

Plowright W., Thomson G. R., Neser J. A. (1994). African swine fever. In Infectious diseases of livestock, with special reference to southern Africa, vol 1. 1st edn Cape Town, South Africa: Oxford University Press, 567–599.

Pohl, T., Gugasyan, R., Grumont, R.J., Strasser, A., Metcalf, D., Tarlinton, D., Sha, W., Baltimore, D., and Gerondakis, S. (2002). The combined absence of NF-kappa B1 and c-Rel reveals that overlapping roles for these transcription factors in the B cell lineage are restricted to the activation and function of mature cells. Proc Natl Acad Sci U S A 99, 4514-4519.

Porteus, M.H., and Baltimore, D. (2003). Chimeric nucleases stimulate gene targeting in human cells. Science 300, 763.

Portugal, R., Leitão, A., and Martins, C. (2009). Apoptosis in porcine macrophages infected in vitro with African swine fever virus (ASFV) strains with different virulence. Arch Virol 154, 1441-1450.

Pourcel, C., Salvignol, G., and Vergnaud, G. (2005). CRISPR elements in Yersinia pestis acquire new repeats by preferential uptake of bacteriophage DNA, and provide additional tools for evolutionary studies. Microbiology 151, 653-663.

Powell, P.P., Dixon, L.K., and Parkhouse, R.M. (1996). An IkappaB homolog encoded by African swine fever virus provides a novel mechanism for downregulation of proinflammatory cytokine responses in host macrophages. J Virol 70, 8527-8533.

Proudfoot, C., Carlson, D.F., Huddart, R., Long, C.R., Pryor, J.H., King, T.J., Lillico, S.G., Mileham, A.J., McLaren, D.G., Whitelaw, C.B., et al. (2015). Genome edited sheep and cattle. Transgenic Res 24, 147-153.

Ramakrishnan, M.A. (2016). Determination of 50% endpoint titer using a simple formula. World J Virol 5, 85-86.

Ramirez, C.L., Foley, J.E., Wright, D.A., Müller-Lerch, F., Rahman, S.H., Cornu, T.I., Winfrey, R.J., Sander, J.D., Fu, F., Townsend, J.A., et al. (2008). Unexpected failure rates for modular assembly of engineered zinc fingers. Nat Methods 5, 374-375.

Randall, R.E., and Goodbourn, S. (2008). Interferons and viruses: an interplay between induction, signalling, antiviral responses and virus countermeasures. J Gen Virol 89, 1-47.

Raoult, D., Audic, S., Robert, C., Abergel, C., Renesto, P., Ogata, H., La Scola, B., Suzan, M., and Claverie, J.M. (2004). The 1.2-megabase genome sequence of Mimivirus. Science 306, 1344-1350.

Razani, B., Zarnegar, B., Ytterberg, A.J., Shiba, T., Dempsey, P.W., Ware, C.F., Loo, J.A., and Cheng, G. (2010). Negative feedback in noncanonical NF-kappaB signaling modulates NIK stability through IKKalpha-mediated phosphorylation. Sci Signal 3, ra41.

Reber, L., Vermeulen, L., Haegeman, G., and Frossard, N. (2009). Ser276 phosphorylation of NF-kB p65 by MSK1 controls SCF expression in inflammation. PLoS One 4, e4393.

Reis, A.L., Abrams, C.C., Goatley, L.C., Netherton, C., Chapman, D.G., Sanchez-Cordon, P., and Dixon, L.K. (2016). Deletion of African swine fever virus interferon inhibitors from the genome of a virulent isolate reduces virulence in domestic pigs and induces a protective response. Vaccine 34, 4698-4705.

Reis, A.L., Netherton, C., and Dixon, L.K. (2017). Unraveling the Armor of a Killer: Evasion of Host Defenses by African Swine Fever Virus. J Virol 91.

Richardson, C.D., Ray, G.J., DeWitt, M.A., Curie, G.L., and Corn, J.E. (2016). Enhancing homology-directed genome editing by catalytically active and inactive CRISPR-Cas9 using asymmetric donor DNA. Nat Biotechnol 34, 339-344.

Richt, J.A., Kasinathan, P., Hamir, A.N., Castilla, J., Sathiyaseelan, T., Vargas, F., Sathiyaseelan, J., Wu, H., Matsushita, H., Koster, J., et al. (2007). Production of cattle lacking prion protein. Nat Biotechnol 25, 132-138.

Rubin, G.M., and Spradling, A.C. (1982). Genetic transformation of Drosophila with transposable element vectors. Science 218, 348-353.

Ruland, J. (2011). Return to homeostasis: downregulation of NF-κB responses. Nat Immunol 12, 709-714.

Robinson, T. (2014) Mapping the global distribution of livestock. PLoS ONE 9 e96084.

Römer, P., Hahn, S., Jordan, T., Strauss, T., Bonas, U., and Lahaye, T. (2007). Plant pathogen recognition mediated by promoter activation of the pepper Bs3 resistance gene. Science 318, 645-648.

Rowlands, R.J., Duarte, M.M., Boinas, F., Hutchings, G., and Dixon, L.K. (2009). The CD2v protein enhances African swine fever virus replication in the tick vector, Ornithodoros erraticus. Virology 393, 319-328.

Rudolph, D., Yeh, W.C., Wakeham, A., Rudolph, B., Nallainathan, D., Potter, J., Elia, A.J., and Mak, T.W. (2000). Severe liver degeneration and lack of NF-kappaB activation in NEMO/IKKgamma-deficient mice. Genes Dev 14, 854-862.

Ruiz Gonzalvo, F., Caballero, C., Martinez, J., and Carnero, M.E. (1986). Neutralization of African swine fever virus by sera from African swine fever-resistant pigs. Am J Vet Res 47, 1858-1862.

Salguero, F.J., Ruiz-Villamor, E., Bautista, M.J., Sánchez-Cordón, P.J., Carrasco, L., and Gómez-Villamandos, J.C. (2002). Changes in macrophages in spleen and lymph nodes during acute African swine fever: expression of cytokines. Vet Immunol Immunopathol 90, 11-22.

Salguero, F.J., Sánchez-Cordón, P.J., Núñez, A., Fernández de Marco, M., and Gómez-Villamandos, J.C. (2005). Proinflammatory cytokines induce lymphocyte apoptosis in acute African swine fever infection. J Comp Pathol 132, 289-302.

Schmitz, M.L., and Baeuerle, P.A. (1991). The p65 subunit is responsible for the strong transcription activating potential of NF-kappa B. EMBO J 10, 3805-3817.

Schmitz, M.L., dos Santos Silva, M.A., and Baeuerle, P.A. (1995). Transactivation domain 2 (TA2) of p65 NF-kappa B. Similarity to TA1 and phorbol ester-stimulated activity and phosphorylation in intact cells. J Biol Chem 270, 15576-15584.

Schomberg, D.T., Tellez, A., Meudt, J.J., Brady, D.A., Dillon, K.N., Arowolo, F.K., Wicks, J., Rousselle, S.D., and Shanmuganayagam, D. (2016). Miniature Swine for Preclinical Modeling of Complexities of Human Disease for Translational Scientific Discovery and Accelerated Development of Therapies and Medical Devices. Toxicol Pathol 44, 299-314.

Schoonbroodt, S., Ferreira, V., Best-Belpomme, M., Boelaert, J.R., Legrand-Poels, S., Korner, M., and Piette, J. (2000). Crucial role of the amino-terminal tyrosine residue 42 and the carboxyl-terminal PEST domain of I kappa B alpha in NF-kappa B activation by an oxidative stress. J Immunol 164, 4292-4300.

Schreck, R., and Baeuerle, P.A. (1990). NF-kappa B as inducible transcriptional activator of the granulocyte-macrophage colony-stimulating factor gene. Mol Cell Biol 10, 1281-1286.

Schreiber, K.H., and Kennedy, B.K. (2013). When lamins go bad: nuclear structure and disease. Cell 152, 1365-1375.

Schreiber, S., Nikolaus, S., and Hampe, J. (1998). Activation of nuclear factor kappa B inflammatory bowel disease. Gut 42, 477-484.

Schröfelbauer, B., Polley, S., Behar, M., Ghosh, G., and Hoffmann, A. (2012). NEMO ensures signaling specificity of the pleiotropic IKKβ by directing its kinase activity toward IκBα. Mol Cell 47, 111-121.

Scott, C.T. (2005). The zinc finger nuclease monopoly. Nat Biotechnol 23, 915-918.

Scott, M.L., Fujita, T., Liou, H.C., Nolan, G.P., and Baltimore, D. (1993). The p65 subunit of NF-kappa B regulates I kappa B by two distinct mechanisms. Genes Dev 7, 1266-1276.

Sebban, H., Yamaoka, S., and Courtois, G. (2006). Posttranslational modifications of NEMO and its partners in NF-kappaB signaling. Trends Cell Biol 16, 569-577.

Sebé-Pedrós, A., de Mendoza, A., Lang, B.F., Degnan, B.M., and Ruiz-Trillo, I. (2011). Unexpected repertoire of metazoan transcription factors in the unicellular holozoan Capsaspora owczarzaki. Mol Biol Evol 28, 1241-1254.

Segal, D.J., Dreier, B., Beerli, R.R., and Barbas, C.F. (1999). Toward controlling gene expression at will: selection and design of zinc finger domains recognizing each of the 5'-GNN-3' DNA target sequences. Proc Natl Acad Sci U S A 96, 2758-2763.

Sen, R., and Baltimore, D. (1986). Multiple nuclear factors interact with the immunoglobulin enhancer sequences. Cell 46, 705-716.

Senftleben, U., Cao, Y., Xiao, G., Greten, F.R., Krähn, G., Bonizzi, G., Chen, Y., Hu, Y., Fong, A., Sun, S.C., et al. (2001). Activation by IKKalpha of a second, evolutionary conserved, NF-kappa B signaling pathway. Science 293, 1495-1499.

Sha, W.C., Liou, H.C., Tuomanen, E.I., and Baltimore, D. (1995). Targeted disruption of the p50 subunit of NF-kappa B leads to multifocal defects in immune responses. Cell 80, 321-330.

Shalem, O., Sanjana, N.E., Hartenian, E., Shi, X., Scott, D.A., Mikkelsen, T.S., Heckl, D., Ebert, B.L., Root, D.E., Doench, J.G., et al. (2014). Genome-scale CRISPR-Cas9 knockout screening in human cells. Science 343, 84-87.

Shih, V.F., Davis-Turak, J., Macal, M., Huang, J.Q., Ponomarenko, J., Kearns, J.D., Yu, T., Fagerlund, R., Asagiri, M., Zuniga, E.I., et al. (2012). Control of RelB during dendritic cell activation integrates canonical and noncanonical NF-κB pathways. Nat Immunol 13, 1162-1170.

Shih, V.F., Kearns, J.D., Basak, S., Savinova, O.V., Ghosh, G., and Hoffmann, A. (2009). Kinetic control of negative feedback regulators of NF-kappaB/RelA determines their pathogen- and cytokine-receptor signaling specificity. Proc Natl Acad Sci U S A 106, 9619-9624.

Shipley, G.D., Keeble, W.W., Hendrickson, J.E., Coffey, R.J., and Pittelkow, M.R. (1989). Growth of normal human keratinocytes and fibroblasts in serum-free medium is stimulated by acidic and basic fibroblast growth factor. J Cell Physiol 138, 511-518.

Sica, A., Dorman, L., Viggiano, V., Cippitelli, M., Ghosh, P., Rice, N., and Young, H.A. (1997). Interaction of NF-kappaB and NFAT with the interferon-gamma promoter. J Biol Chem 272, 30412-30420.

Simons, J.P., McClenaghan, M., and Clark, A.J. (1987). Alteration of the quality of milk by expression of sheep beta-lactoglobulin in transgenic mice. Nature 328, 530-532.

Smith, J., Bibikova, M., Whitby, F.G., Reddy, A.R., Chandrasegaran, S., and Carroll, D. (2000). Requirements for double-strand cleavage by chimeric restriction enzymes with zinc finger DNA-recognition domains. Nucleic Acids Res 28, 3361-3369.

Solan, N.J., Miyoshi, H., Carmona, E.M., Bren, G.D., and Paya, C.V. (2002). RelB cellular regulation and transcriptional activity are regulated by p100. J Biol Chem 277, 1405-1418.

Stein, S.J., and Baldwin, A.S. (2013). Deletion of the NF-κB subunit p65/RelA in the hematopoietic compartment leads to defects in hematopoietic stem cell function. Blood 121, 5015-5024.

Stehlik, C., de Martin, R., Binder, B.R., and Lipp, J. (1998). Cytokine induced expression of porcine inhibitor of apoptosis protein (iap) family member is regulated by NF-kappa B. Biochem Biophys Res Commun 243, 827-832.

Stinchcomb, D.T., Shaw, J.E., Carr, S.H., and Hirsh, D. (1985). Extrachromosomal DNA transformation of Caenorhabditis elegans. Mol Cell Biol 5, 3484-3496.

Sullivan, J.C., Kalaitzidis, D., Gilmore, T.D., and Finnerty, J.R. (2007). Rel homology domain-containing transcription factors in the cnidarian Nematostella vectensis. Dev Genes Evol 217, 63-72.

Sun, S.C. (2011). Non-canonical NF-κB signaling pathway. Cell Res 21, 71-85.

Sun, S.C., Ganchi, P.A., Ballard, D.W., and Greene, W.C. (1993). NF-kappa B controls expression of inhibitor I kappa B alpha: evidence for an inducible autoregulatory pathway. Science 259, 1912-1915.

Symington, L.S. (2016). Mechanism and regulation of DNA end resection in eukaryotes. Crit Rev Biochem Mol Biol 51, 195-212.

Sánchez-Cordón, P.J., Chapman, D., Jabbar, T., Reis, A.L., Goatley, L., Netherton, C.L., Taylor, G., Montoya, M., and Dixon, L. (2017). Different routes and doses influence protection in pigs immunised with the naturally attenuated African swine fever virus isolate OURT88/3. Antiviral Res 138, 1-8.

Sánchez-Cordón, P.J., Romero-Trevejo, J.L., Pedrera, M., Sánchez-Vizcaíno, J.M., Bautista, M.J., and Gómez-Villamandos, J.C. (2008). Role of hepatic macrophages during the viral haemorrhagic fever induced by African Swine Fever Virus. Histol Histopathol 23, 683-691.

Takeda, K., Takeuchi, O., Tsujimura, T., Itami, S., Adachi, O., Kawai, T., Sanjo, H., Yoshikawa, K., Terada, N., and Akira, S. (1999). Limb and skin abnormalities in mice lacking IKKalpha. Science 284, 313-316.

Tam, W.F., Lee, L.H., Davis, L., and Sen, R. (2000). Cytoplasmic sequestration of rel proteins by IkappaBalpha requires CRM1-dependent nuclear export. Mol Cell Biol 20, 2269-2284.

Tan, W., Carlson, D.F., Lancto, C.A., Garbe, J.R., Webster, D.A., Hackett, P.B., and Fahrenkrug, S.C. (2013). Efficient nonmeiotic allele introgression in livestock using custom endonucleases. Proc Natl Acad Sci U S A 110, 16526-16531.

Tebas, P., Stein, D., Tang, W.W., Frank, I., Wang, S.Q., Lee, G., Spratt, S.K., Surosky, R.T., Giedlin, M.A., Nichol, G., et al. (2014). Gene editing of CCR5 in autologous CD4 T cells of persons infected with HIV. N Engl J Med 370, 901-910.

Ten, R.M., Paya, C.V., Israël, N., Le Bail, O., Mattei, M.G., Virelizier, J.L., Kourilsky, P., and Israël, A. (1992). The characterization of the promoter of the gene encoding the p50 subunit of NF-kappa B indicates that it participates in its own regulation. EMBO J 11, 195-203.

Tesson, L., Usal, C., Ménoret, S., Leung, E., Niles, B.J., Remy, S., Santiago, Y., Vincent, A.I., Meng, X., Zhang, L., et al. (2011). Knockout rats generated by embryo microinjection of TALENs. Nat Biotechnol 29, 695-696.

Thomas, K.R., and Capecchi, M.R. (1987). Site-directed mutagenesis by gene targeting in mouse embryo-derived stem cells. Cell 51, 503-512.

Thompson, J.E., Phillips, R.J., Erdjument-Bromage, H., Tempst, P., and Ghosh, S. (1995). I kappa B-beta regulates the persistent response in a biphasic activation of NF-kappa B. Cell 80, 573-582.

Thomson, G.R. (1985). The epidemiology of African swine fever: the role of free-living hosts in Africa. Onderstepoort J Vet Res 52, 201-209.

Thomson, G.R., Gainaru, M.D., and Van Dellen, A.F. (1980). Experimental infection of warthos (Phacochoerus aethiopicus) with African swine fever virus. Onderstepoort J Vet Res 47, 19-22.

Tian, B., Nowak, D.E., Jamaluddin, M., Wang, S., and Brasier, A.R. (2005). Identification of direct genomic targets downstream of the nuclear factor-kappaB transcription factor mediating tumor necrosis factor signaling. J Biol Chem 280, 17435-17448.

Tong, C., Li, P., Wu, N.L., Yan, Y., and Ying, Q.L. (2010). Production of p53 gene knockout rats by homologous recombination in embryonic stem cells. Nature 467, 211-213.

Trelle, M.B., Ramsey, K.M., Lee, T.C., Zheng, W., Lamboy, J., Wolynes, P.G., Deniz, A., and Komives, E.A. (2016). Binding of NFκB Appears to Twist the Ankyrin Repeat Domain of IκBα. Biophys J 110, 887-895.

Tulman, E.R., Delhon, G.A., Ku, B.K., and Rock, D.L. (2009). African swine fever virus. Curr Top Microbiol Immunol 328, 43-87.

Ueda, A., Ishigatsubo, Y., Okubo, T., and Yoshimura, T. (1997). Transcriptional regulation of the human monocyte chemoattractant protein-1 gene. Cooperation of two NF-kappaB sites and NF-kappaB/Rel subunit specificity. J Biol Chem 272, 31092-31099.

Valen, G., Yan, Z.Q., and Hansson, G.K. (2001). Nuclear factor kappa-B and the heart. J Am Coll Cardiol 38, 307-314.

van Berkel, P.H., Welling, M.M., Geerts, M., van Veen, H.A., Ravensbergen, B., Salaheddine, M., Pauwels, E.K., Pieper, F., Nuijens, J.H., and Nibbering, P.H. (2002). Large scale production of recombinant human lactoferrin in the milk of transgenic cows. Nat Biotechnol 20, 484-487.

van Essen, D., Engist, B., Natoli, G., and Saccani, S. (2009). Two modes of transcriptional activation at native promoters by NF-kappaB p65. PLoS Biol 7, e73.

Vartak, S.V., and Raghavan, S.C. (2015). Inhibition of nonhomologous end joining to increase the specificity of CRISPR/Cas9 genome editing. FEBS J 282, 4289-4294.

Vermeulen, L., De Wilde, G., Van Damme, P., Vanden Berghe, W., and Haegeman, G. (2003). Transcriptional activation of the NF-kappaB p65 subunit by mitogen- and stress-activated protein kinase-1 (MSK1). EMBO J 22, 1313-1324.

Viatour, P., Merville, M.P., Bours, V., and Chariot, A. (2005). Phosphorylation of NF-kappaB and IkappaB proteins: implications in cancer and inflammation. Trends Biochem Sci 30, 43-52.

Vodicka, P., Smetana, K., Dvoránková, B., Emerick, T., Xu, Y.Z., Ourednik, J., Ourednik, V., and Motlík, J. (2005). The miniature pig as an animal model in biomedical research. Ann N Y Acad Sci 1049, 161-171.

Vojta, A., Dobrinić, P., Tadić, V., Bočkor, L., Korać, P., Julg, B., Klasić, M., and Zoldoš, V. (2016). Repurposing the CRISPR-Cas9 system for targeted DNA methylation. Nucleic Acids Res 44, 5615-5628.

Wang, D., Westerheide, S.D., Hanson, J.L., and Baldwin, A.S. (2000). Tumor necrosis factor alpha-induced phosphorylation of RelA/p65 on Ser529 is controlled by casein kinase II. J Biol Chem 275, 32592-32597.

Wang, V.Y., Huang, W., Asagiri, M., Spann, N., Hoffmann, A., Glass, C., and Ghosh, G. (2012). The transcriptional specificity of NF-κB dimers is coded within the κB DNA response elements. Cell Rep 2, 824-839.

Wang, H., Yang, H., Shivalila, C.S., Dawlaty, M.M., Cheng, A.W., Zhang, F., and Jaenisch, R. (2013). One-step generation of mice carrying mutations in multiple genes by CRISPR/Cas-mediated genome engineering. Cell 153, 910-918.

Wang, T., Wei, J.J., Sabatini, D.M., and Lander, E.S. (2014). Genetic screens in human cells using the CRISPR-Cas9 system. Science 343, 80-84.

Wang, X., Cao, C., Huang, J., Yao, J., Hai, T., Zheng, Q., Zhang, H., Qin, G., Cheng, J., Wang, Y., et al. (2016). One-step generation of triple gene-targeted pigs using CRISPR/Cas9 system. Sci Rep 6, 20620.

Wardley, R.C., de M Andrade, C., Black, D.N., de Castro Portugal, F.L., Enjuanes, L., Hess, W.R., Mebus, C., Ordas, A., Rutili, D., Sanchez Vizcaino, J., et al. (1983). African Swine Fever virus. Brief review. Arch Virol 76, 73-90.

Wefers, B., Panda, S.K., Ortiz, O., Brandl, C., Hensler, S., Hansen, J., Wurst, W., and Kühn, R. (2013). Generation of targeted mouse mutants by embryo microinjection of TALEN mRNA. Nat Protoc 8, 2355-2379.

Weih, F., Carrasco, D., Durham, S.K., Barton, D.S., Rizzo, C.A., Ryseck, R.P., Lira, S.A., and Bravo, R. (1995). Multiorgan inflammation and hematopoietic abnormalities in mice with a targeted disruption of RelB, a member of the NF-kappa B/Rel family. Cell 80, 331-340.

Weih, F., Durham, S.K., Barton, D.S., Sha, W.C., Baltimore, D., and Bravo, R. (1997). p50-NF-kappaB complexes partially compensate for the absence of RelB: severely increased pathology in p50(-/-)relB(-/-) double-knockout mice. J Exp Med 185, 1359-1370.

Werner, S.L., Kearns, J.D., Zadorozhnaya, V., Lynch, C., O'Dea, E., Boldin, M.P., Ma, A., Baltimore, D., and Hoffmann, A. (2008). Encoding NF-kappaB temporal control in response to TNF: distinct roles for the negative regulators IkappaBalpha and A20. Genes Dev 22, 2093-2101.

Whiteside, S.T., Epinat, J.C., Rice, N.R., and Israël, A. (1997). I kappa B epsilon, a novel member of the I kappa B family, controls RelA and cRel NF-kappa B activity. EMBO J 16, 1413-1426.

Whitworth, K.M., Rowland, R.R., Ewen, C.L., Trible, B.R., Kerrigan, M.A., Cino-Ozuna, A.G., Samuel, M.S., Lightner, J.E., McLaren, D.G., Mileham, A.J., et al. (2016). Gene-edited pigs are protected from porcine reproductive and respiratory syndrome virus. Nat Biotechnol 34, 20-22.

Wilmut, I., Schnieke, A.E., McWhir, J., Kind, A.J., and Campbell, K.H. (1997). Viable offspring derived from fetal and adult mammalian cells. Nature 385, 810-813.

Wu, C.J., Conze, D.B., Li, T., Srinivasula, S.M., and Ashwell, J.D. (2006). Sensing of Lys 63-linked polyubiquitination by NEMO is a key event in NF-kappaB activation [corrected]. Nat Cell Biol 8, 398-406.

Wu, H., Wang, Y., Zhang, Y., Yang, M., Lv, J., and Liu, J. (2015). TALE nickase-mediated SP110 knockin endows cattle with increased resistance to tuberculosis. Proc Natl Acad Sci U S A 112, E1530-1539.

Xiao, G., Harhaj, E.W., and Sun, S.C. (2001). NF-kappaB-inducing kinase regulates the processing of NF-kappaB2 p100. Mol Cell 7, 401-409.

Yavarifard, R., Ghavi Hossein-Zadeh, N., and Shadparvar, A.A. (2014). Population genetic structure analysis and effect of inbreeding on body weights at different ages in Iranian Mehraban sheep. J Anim Sci Technol 56, 34.

Yoshimi, K., Kunihiro, Y., Kaneko, T., Nagahora, H., Voigt, B., and Mashimo, T. (2016). ssODN-mediated knock-in with CRISPR-Cas for large genomic regions in zygotes. Nat Commun 7, 10431.

Yu, C., Liu, Y., Ma, T., Liu, K., Xu, S., Zhang, Y., Liu, H., La Russa, M., Xie, M., Ding, S., et al. (2015). Small molecules enhance CRISPR genome editing in pluripotent stem cells. Cell Stem Cell 16, 142-147.

Yu, G., Chen, J., Yu, H., Liu, S., Xu, X., Sha, H., Zhang, X., Wu, G., Xu, S., and Cheng, G. (2006). Functional disruption of the prion protein gene in cloned goats. J Gen Virol 87, 1019-1027.

Yáñez, R.J., Rodríguez, J.M., Nogal, M.L., Yuste, L., Enríquez, C., Rodriguez, J.F., and Viñuela, E. (1995). Analysis of the complete nucleotide sequence of African swine fever virus. Virology 208, 249-278.

Zabel, U., and Baeuerle, P.A. (1990). Purified human I kappa B can rapidly dissociate the complex of the NF-kappa B transcription factor with its cognate DNA. Cell 61, 255-265.

Zakaryan, H., and Revilla, Y. (2016). African swine fever virus: current state and future perspectives in vaccine and antiviral research. Vet Microbiol 185, 15-19.

Zakaryan, H., Cholakyans, V., Simonyan, L., Misakyan, A., Karalova, E., Chavushyan, A., and Karalyan, Z. (2015). A study of lymphoid organs and serum proinflammatory cytokines in pigs infected with African swine fever virus genotype II. Arch Virol 160, 1407-1414.

Zhang, F., Hopwood, P., Abrams, C.C., Downing, A., Murray, F., Talbot, R., Archibald, A., Lowden, S., and Dixon, L.K. (2006). Macrophage transcriptional responses following in vitro infection with a highly virulent African swine fever virus isolate. J Virol 80, 10514-10521.

Zhang, Y., Shim, E.Y., Davis, M., and Lee, S.E. (2009). Regulation of repair choice: Cdk1 suppresses recruitment of end joining factors at DNA breaks. DNA Repair (Amst) 8, 1235-1241.

Zhang, F., Moon, A., Childs, K., Goodbourn, S., and Dixon, L.K. (2010). The African swine fever virus DP71L protein recruits the protein phosphatase 1 catalytic subunit to dephosphorylate eIF2alpha and inhibits CHOP induction but is dispensable for these activities during virus infection. J Virol 84, 10681-10689.

Zhang, C., Wang, L., Ren, G., Li, Z., Ren, C., Zhang, T., Xu, K., and Zhang, Z. (2014). Targeted disruption of the sheep MSTN gene by engineered zinc-finger nucleases. Mol Biol Rep 41, 209-215.

Zhong, H., May, M.J., Jimi, E., and Ghosh, S. (2002). The phosphorylation status of nuclear NF-kappa B determines its association with CBP/p300 or HDAC-1. Mol Cell 9, 625-636.

Zhong, H., Voll, R.E., and Ghosh, S. (1998). Phosphorylation of NF-kappa B p65 by PKA stimulates transcriptional activity by promoting a novel bivalent interaction with the coactivator CBP/p300. Mol Cell 1, 661-671.

Ziegler-Heitbrock, H.W., Sternsdorf, T., Liese, J., Belohradsky, B., Weber, C., Wedel, A., Schreck, R., Bäuerle, P., and Ströbel, M. (1993). Pyrrolidine dithiocarbamate inhibits NF-kappa B mobilization and TNF production in human monocytes. J Immunol 151, 6986-6993.

Zsak, L., Lu, Z., Burrage, T.G., Neilan, J.G., Kutish, G.F., Moore, D.M., and Rock, D.L. (2001). African swine fever virus multigene family 360 and 530 genes are novel macrophage host range determinants. J Virol 75, 3066-3076.

Zsak, L., Onisk, D.V., Afonso, C.L., and Rock, D.L. (1993). Virulent African swine fever virus isolates are neutralized by swine immune serum and by monoclonal antibodies recognizing a 72-kDa viral protein. Virology 196, 596-602.